Title

A pooled CRISPRi screen to probe Pseudomonas aeruginosa gene vulnerability during murine lung infection and phage predation

Author

Prasad, Neha Kalanadhabhatla

Publication Date

2022

Peer reviewed|Thesis/dissertation

A pooled CRISPRi screen to probe Pseudomonas aeruginosa gene vulnerability during murine lung infection and phage predation

by

Neha Prasad

DISSERTATION

Submitted in partial satisfaction of the requirements for degree of

DOCTOR OF PHILOSOPHY

in

Chemistry and Chemical Biology

in the

GRADUATE DIVISION

of the

UNIVERSITY OF CALIFORNIA, SAN FRANCISCO

Approved:

DocuSigned by:
Carol Gross
7AFBE9046E0744C...

Carol Gross

Chair

DocuSigned by:
Ian Seiple
DocuSigned by:
Danica Fujimori
DocuSigned by:
Oren Rosenberg
9727D020CAED4ED...

Ian Seiple

Danica Fujimori

Oren Rosenberg

Committee Members

Dedication and Acknowledgements

This dissertation is in dedication to my mentors over the years: those who took a chance on me, taught me with patience and meticulousness, gave me the freedom and flexibility to learn multi-dimensionally, celebrated my successes and helped me grow from my failures, and motivated me to develop my own passions and ambitions. During my eight years in the Antimicrobial Resistance space, I have found that this research community is especially passionate, resilient, visionary, and altruistic. I am humbled and continually inspired by the people who have dedicated their careers and lives to tackling the complicated, interdisciplinary problems associated with AMR.

Contributions

Chapter 1 of this thesis is a reprint of the material as it appears in:

> Prasad NK, Seiple IB, Cirz RT, Rosenberg OS. Leaks in the Pipeline: a Failure Analysis of Gram-Negative Antibiotic Development from 2010 to 2020. *Antimicrob Agents Chemother*. 2022;66(5):e0005422

Chapter 2 of this thesis was completed in collaboration with Dr. Jiuxin Qu, PhD and is a reprint of the material as it appears in:

> Qu J, Prasad NK, Yu MA, et al. Modulating Pathogenesis with Mobile-CRISPRi. *J Bacteriol*. 2019;201(22):e00304-19.

Chapter 3 of this thesis is in preparation for manuscript submission and was completed in collaboration with Dr. Michelle Yu, MD, PhD, Dr. Jason Peters, PhD, Ryan Ward, and Michael Kwon.

Chapter 4 of this thesis contains data that was collected in collaboration with Dr. Adolfo Cuesta, PhD, Dr. Andrea Fossati, PhD, Dr. Shweta Karambelkar, PhD, and Natalie Whitis under the additional guidance of Dr. Joseph Bondy-Denomy, PhD, and Dr. Danielle Swaney, PhD.

A pooled CRISPRi screen to probe *Pseudomonas aeruginosa* gene vulnerability during murine lung infection and phage predation

Neha Prasad

Abstract

Despite their extraordinary ability to cure infectious diseases, most antibiotics have dose-limiting, off-target toxicities that impede the clinical development of novel small molecule candidates targeting multi-drug resistant pathogens. For existing antibiotic targets, large dosages of antibiotics are needed to achieve the requisite cellular potency to clear the bacterial burden during infection. In this work we explore strategies to lower the required dosage by identifying genetic vulnerabilities of the pathogen *Pseudomonas aeruginosa* during lung infection and antibacterial therapy administration. We probe these genetic vulnerabilities with Mobile-CRISPRi, a genetic tool that enables partial genetic inhibition and detection of hypersensitivity to clearance by the immune system or predation by bacteriophage. Designing chemical inhibitors that mimic the genetic inhibition leading to loss of bacterial fitness during lung infection or phage therapy may provide an avenue for future antibacterial development efforts.

Chapter 1 profiles antibiotics with Gram-negative activity that have been discontinued during clinical development over the last decade, largely due to toxicity issues in phase 1 clinical trials;

Chapter 2 details the construction of a Mobile-CRISPRi system in Pseudomonas aeruginosa with constitutive promoters driving dCas9 activity and its implementation in a murine pneumonia model to recapitulate the attenuation of virulence through inhibition of the transcriptional activator *exsA*;

Chapter 3 entails the construction of a pooled Mobile-CRISPRi library in *Pseudomonas aeruginosa*, where each strain has a distinct essential gene knocked down, and the implementation of this library in a murine pneumonia model to detect *in vivo* genetic vulnerabilities;

Chapter 4 features genetic and proteomic efforts to identify *Pseudomonas aeruginosa* determinants of hypersensitization to killing by DMS bacteriophage.

Table of Contents

CHAPTER 3

CHAPTER 4

List of Figures

CHAPTER 1:

CHAPTER 2:

CHAPTER 3

CHAPTER 4

List of Tables

CHAPTER 1:

CHAPTER 2:

CHAPTER 3

List of Abbreviations

Acr- Anti-CRISPR

ALT- Alanine Aminotransferase enzyme, a measure of liver injury

BLI- Beta-Lactamase Inhibitor

CDC- Centers for Disease Control and Prevention

CABP- Community-Acquired Bacterial Pneumonia

CE- Conditionally Essential

CFU- Colony-Forming Units

CRISPRi- Clustered Regularly Interspaced Short Palindromic Repeats- Interference

c/u UTI- complicated/uncomplicated Urinary Tract Infection

c/u IAI- complicated/uncomplicated Intra-Abdominal Infection

FDA- United States Food and Drug Administration

GNB- Gram-Negative Bacteria

HABP- Hospital-Acquired Bacterial Pneumonia

IV- Intravenous

MAD- Multiple Ascending Dose

MIC- Minimum Inhibitory Concentration

NGS- Next-generation Sequencing

OM- outer membrane

PD- Pharmacodynamics

PK- Pharmacokinetics

PMB- Polymyxin B

SAD- Single Ascending Dose

SOC- standard of care

TQT- Thorough QT, in reference to QT intervals measured by an electrocardiogram

VABP- Ventilator-Associated Bacterial Pneumonia

WHO- World Health Organization

X/MDR- Extensively/Multiple Drug Resistant

Chapter 1

Shortcomings of antibiotic clinical development

Abstract

The WHO has warned that our current arsenal of antibiotics is not innovative enough to face impending infectious diseases, especially those caused by multi-drug resistant Gram-negative pathogens. Though the current preclinical pipeline is well-stocked with novel candidates, the last FDA-approved antibiotic with a novel mechanism of action against Gram-negative bacteria was discovered nearly 60 years ago. Of all the antibiotic candidates that initiated INDs in the 2000s, 17% earned FDA approval within 12 years, while an overwhelming 62% were discontinued in that time frame. These "leaks" in the clinical pipeline, where compounds with clinical potential are abandoned during clinical development, indicate that scientific innovations are not reaching the clinic and providing benefits to patients. This is true for not only novel candidates, but also for candidates from existing antibiotic classes with clinically validated targets. By identifying the sources of the leaks in the clinical pipeline, future developmental efforts can be directed towards strategies that are more likely to flow into clinical use. In this review, we conduct a detailed failure analysis of clinical candidates with Gram-negative activity that have fallen out of the clinical pipeline over the past decade. Though limited by incomplete data disclosure from companies engaging in antibiotic development, we

attempt to distill the developmental challenges faced by each discontinued candidate. It is our hope that this insight can help de-risk antibiotic development and bring new, effective antibiotics to the clinic.

Introduction

Bacterial resistance to antibiotics is a growing public health crisis: 1.27 million global deaths were attributed to multidrug resistance (MDR) in 2019. (1) Left unchecked, MDR could lead to 10 million global annual deaths in 2050. (2, 3) Modern medicine relies on antibiotics to control secondary bacterial infections from routine procedures like surgery and chemotherapy. These secondary infections may become untreatable due to antibiotic-resistant bacteria, escalating the risk of common medical procedures.

Of the most threatening MDR pathogens identified by the CDC (4) and WHO (2), Gram-negative bacteria (GNB), including *Klebsiella pneumoniae* (of the *Enterobacteriaceae* family), *Acinetobacter baumannii*, and *Pseudomonas aeruginosa,* stand out as urgent unmet needs. In addition to their general intrinsic resistance to antibiotics, all three have developed critical resistance to the carbapenem class of antibiotics, leaving limited alternative treatment options. (5, 6) Despite the growing threat of untreatable infections, the 2020 global antibiotic clinical pipeline contained only 23 candidates with GNB activity, none of which belonged to a new class. (7) The high incidence of cross-resistance with existing antibiotics implies that resistance development to these new agents is closely trailing. (8) While the success rate from phase 1 trials to FDA approval for

all antibacterial therapeutics between 2011–2020 was 16.3%, (9) the last FDA-approved antibiotic with a novel mechanism of action against GNB was discovered nearly 60 years ago.

Clinical studies initiated in the 1980s and 1990s (largely cephalosporins, fluoroquinolones, and macrolides) had high success rates, with 40% of candidates obtaining market approval in a median time of 6 years. However, of the 61 antibiotics approved for use between 1980–2009, 43% have been withdrawn by the FDA, and the 6 antibiotics withdrawn due to safety issues were all fluoroquinolones. Moreover, the number of antibacterial Investigational New Drug (IND) applications filed with the FDA between 2010–2019 is the lowest it has been in the past 4 decades. (10) In spite of the unique challenges of antibiotic discovery, (11–14) 72% of candidates in the current global preclinical pipeline represent novel classes, with overlapping cellular targets and mechanisms of action that are distinct from those of antibiotics used in the clinic today. (7, 15) The consequences of failure are unbearable for the small companies that drive antibiotic development and for the future of a society that so heavily depends on efficacious antibiotics.

Here we profile antibiotic candidates with GNB activity that have fallen out of the clinical pipeline over the last decade and identify trends in their development. These vignettes are limited by the extent of information disclosure by the companies pursuing these candidates, but we hope to inform future discovery and development efforts by

highlighting patterns in these failures. Stronger predictors of success may enable more diverse candidates from the preclinical pipeline to enter a de-risked clinical pipeline and emerge as FDA-approved therapeutics.

Results

Overview of the clinical development pipeline for GNB-active antibiotics (2010–2020)

The clinical development pipeline for systemic GNB-active candidates over the past decade is detailed in **Table 1.1**. Despite the desperate need for antibiotics with novel targets and high target diversity in the preclinical pipeline, most candidates in clinical development are from clinically validated classes (**Figure 1.1**)—presumably due to the higher perceived risk of pursuing a non-clinically validated target. While half of all classes in development contain an antibiotic that has been approved in the past 10 years, the other half comprises unexploited antibiotic targets: MurA, tRNA synthetases, LpxC, and LptD.

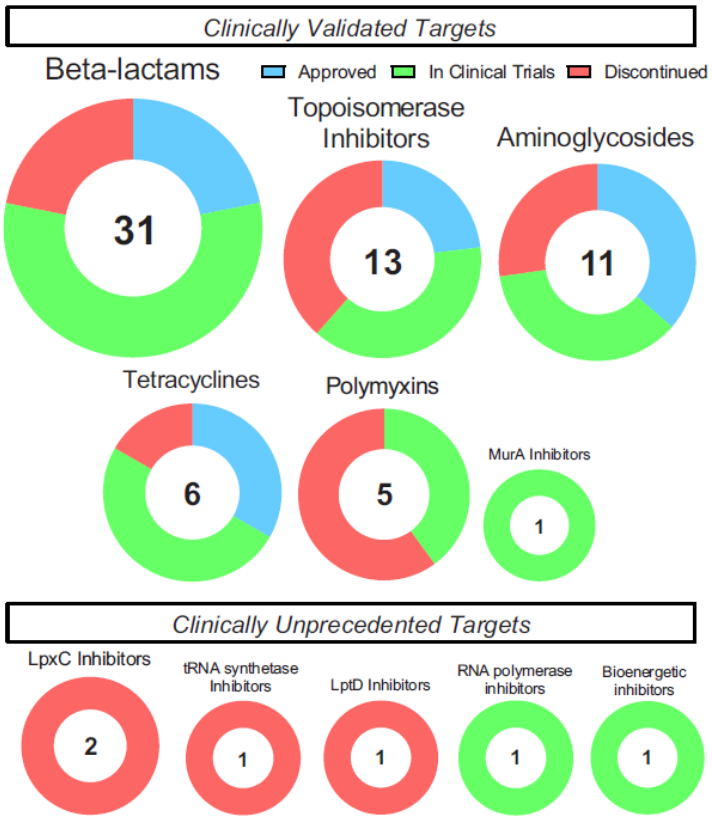

Figure 1.1: GNB-active clinical candidates by class and clinical trial status
Antibiotic classes that have undergone clinical development between 2010–2020 are represented as circles. Segments are colored according to proportions of candidates in that class that have been approved (blue), are currently in clinical development (green), or have been discontinued (red).

Table 1.1: Clinical development details of GNB-active antibiotic candidates between 2010–2020

List of abbreviations used in table: BLI- beta-lactamase inhibitor; Breakthrough therapy- FDA designation to expedite development and review of drugs; CF- cystic fibrosis; DBO- diazabicyclooctane class of beta-lactamase inhibitors with PBP-binding properties; DCGI- Drugs Controller General of India; EMA-European Medicines Agency; FDA- U.S. Food & Drug Administration; LPAD- Limited Population Pathway for Antibacterial and Antifungal Drugs designation given by FDA to indicate limited usage recommendation; NCFB- non-Cystic Fibrosis Bronchiectasis; NDA- New Drug Application, filed after clinical trials; NMPA- Chinese National Medical Products Administration; NTAP- New Technology Add-On Payment designation given by Centers for Medicare & Medicaid Services as incentive for hospitals; NTM- non-tubercular mycobacterium; Orphan Drug- FDA designation given as incentive; PBP- penicillin binding protein; QIDP- Qualified Infectious Disease Product designation given by FDA as incentive; Reserve- classification by World Health Organization to indicate "last-resort" option; Watch- classification by World Health Organization to indicate limited usage recommendation

Candidate	Sponsors and Developers	Phase	Approval or Discontinuation Date / Last Status Update	Approved or Intended Indications							Approved or Expected Activity Spectrum				Formulation			Regulatory Designations	Comments
				UTI	HABP / VABP	CABP	cIAI	ABSSSI	CF pulmonary infection / NCFB	bacteremia	*Enterobacteriaceae*	*P. aeruginosa*	*A. baumannii*	Notable for Gram-positive coverage	IV	oral	Inhalation		
MurA inhibitors																			
Contepo / IV Fosfomycin	Nabriva Therapeutics / Zavante	NDA stage	Nov 2020									limited						QIDP / NTAP	fosfomycin is approved by FDA as oral treatment for uUTIs; IV fosfomycin has been used for over 45 years outside the U.S. to treat cUTIs; FDA rejected in June 2020 due to manufacturing concerns that are currently unresolvable due to travel restrictions; the first QIDP to be granted conditional NTAP approval prior to receiving FDA approval
tRNA Synthetase Inhibitors																			
Epetraborole / GSK2251052 / AN3365	Anacor / GlaxoSmithKline	Discontinued after Phase 2	Oct 2012																
LpxC Inhibitors																			
ACHN-975	Achaogen	Discontinued after Phase 1	July 2013																
RC-01	Recida Therapeutics	Discontinued after Phase 1	May 2019	unannounced															
LptD Inhibitors																			
Murepavadin	Polyphor/ Roche AG	Discontinued IV formulation after Phase 3 ; oral formulation to start Phase 1	July 2019 ; Dec 2020															QIDP	clinical trial authorization was granted by the UK Medicines and Healthcare products Regulatory Agency for inhaled murepavadin in Dec 2020
RNA polymerase Inhibitors																			
BV100 / Rifabutin	BioVersys AG	Phase 1	Nov 2020															QIDP	rifabutin (Mycobutin) was approved by the FDA in 1992 as an oral formulation for the prevention of disseminated NTM disease in patients with advanced HIV infection; from ansamycin class of antibiotics
Bioenergetic inhibitors																			
Pravibismane / MBN-101	Microbion Corp.	Phase 2- topical; preclinical- inhalation	June 2020															QIDP / Orphan Drug	broad-spectrum; clinical trials have been conducted for topical formulations for diabetic foot ulcer infection and orthopedic implant infection indications. Inhalation formulation is in preclinical stage.

Candidate	Sponsors and Developers	Phase	Approval or Discontinuation Date / Last Status Update	Approved or Intended Indications							Approved or Expected Activity Spectrum				Formulation			Regulatory Designations	Comments
				UTI	HABP / VABP	CABP	cIAI	ABSSSI	CF pulmonary infection / NCFB	bacteremia	*Enterobacteriaceae*	*P. aeruginosa*	*A. baumannii*	Notable for Gram-positive coverage	IV	oral	Inhalation		
Tetracyclines																			
Xerava / Eravacycline	Tetraphase Pharmaceuticals/ La Jolla Pharmaceutical Co.	Approved by FDA	Aug 2018				■				■		■		■			QIDP	oral formulation and cUTI indication were tested in clinical trials but ultimately not approved (IGNITE2, IGNITE3)
Nuzyra / Omadacycline	Paratek Pharmaceuticals	Approved by FDA	Oct 2018			■		■			■		limited	■	■	■		QIDP / NTAP	first-in-class aminomethylcycline; phase 2 oral and IV formulations for cUTI completed in Oct 2019
TP-6076	Tetraphase Pharmaceuticals/ La Jolla Pharmaceutical Co.	Phase 2- ready for licensing	March 2020	unannounced							■		■		■				
TP-271	Tetraphase Pharmaceuticals/ La Jolla Pharmaceutical Co.	Phase 2- ready for licensing	March 2020			■							■	■	■	■		QIDP	omadacycline derivative, optimized for Gram-positive respiratory pathogens
KBP-7072	KBP BioSciences Pharmaceutical Technical Co.	Phase 1	Aug 2020		■	■							■	■		■		QIDP	
TP-2758	Tetraphase Pharmaceuticals/ La Jolla Pharmaceutical Co.	Discontinued after Phase 1	2013	■	■		■				■		■		■	■			
Polymyxins																			
SPR206	Spero Therapeutics / Everest Medicines	Phase 1	Nov 2020	■	■						■	■	■		■			QIDP	replaced SPR741 as lead from potentiator platform for further clinical development; has independent in vitro activity in addition to potentiation effect
MRX-8	MicuRX	Phase 1	Aug 2020	unannounced							■	■	■		■				CARB-X funding for phase 1 trial announced Aug 2020
SPR741	Spero Therapeutics	Discontinued after Phase 1	Jan 2020	■	■						■	■	■		■				
Colobreathe / Colistimethate Dry Powder Inhalation (Colistin)	Forest Laboratories	Rejected by FDA	Feb 2012						■		■	■	■				■		approved by EMA in Feb 2012
CB-182,804	Cubist Pharmaceuticals	Discontinued after Phase 1	Sept 2010	■	■		■			■	■	■	■		■				
Topoisomerase Inhibitors																			
Aeroquin / Quinsair / Levofloxacin Inhalation Solution (MP-376)	Chiesi Pharmaceuticals / Mpex Pharmaceuticals / Horizon Pharmaceuticals/ Raptor Pharmaceuticals / Forest Laboratories	Approved by FDA	Aug 2015						■			■		■			■	QIDP	marketed in Canada and Latin America as Quinsair; in this formulation, levofloxacin is complexed with $Mg2+$ and aerosolized by a nebulizer
Lascufloxacin	Kyorin Pharmaceutical Co., Ltd	Approved by PMDA & EMA	PMDA: Sept 2019, Nov 2020 / EMA: July 2020			■					■			■	■	■			oral formulation approved Sept 2019 in Japan and July 2020 in Europe; IV formulation approved Nov 2020 in Japan
Baxdela/ Delafloxacin	Melinta Therapeutics	Approved by FDA	June 2017 / June 2019			■		■			limited		limited		■	■		QIDP	anionic character allows for better accumulation in cell; approved for ABSSSI in 2017, CABP in 2019
Levonadifloxacin (WCK 771) / prodrug Alalevonadifloxacin (WCK 2349)	Wockhardt Ltd.	Approved by DCGI; NDA stage at FDA	Jan 2020					■		■	limited	limited	limited		■	■		QIDP	WCK 771 is IV, WCK 2349 is oral
Gepotidacin / GSK2140944	GlaxoSmithKline	Phase 3	July 2020	■				■			limited			for *N. gonorrhoeae* infections		■			first-in-class triazaacenaphthylene
Finafloxacin	MerLion Pharmaceuticals Pte Ltd.	Phase 3-ready	March 2018	■			■	■			■	■	■	■	■	■		QIDP	otic suspension was approved by FDA in 2015, but systemic formulation has not yet been approved; unlike other quinolones, it is active in acidic conditions and has higher potency against ESBL-producing *Enterobacteriaceae*
Taigexyn / Nemonoxacin	TaiGen Biotechnology Co.	Phase 3-ready	Sept 2020			■		■			limited	limited	limited		■	■		QIDP	marketed in Russia, Taiwan, China, as Taigexyn
Zabofloxacin	Dong Wha Pharmaceuticals / Pacific Beach BioSciences	Phase 3- stalled	March 2015	■		■					limited			■	■	■			approved for treating acute exacerbations of chronic obstructive pulmonary disease in South Korea with name "Zabolante" in 2015; Phase 2 trial for oral formulation in CABP was discontinued in 2012 due to financial considerations but obtained approval for Phase 3 trials; company website still lists candidate under development
Apulmiq / Linhaliq / Pulmaquin / inhalation ciprofloxacin	Savara Pharmaceuticals / Grifols / Aradigm	Rejected by FDA & EMA	Dec 2020						■			■					■	Orphan Drug / QIDP	QIDP designation in 2014, rejected by FDA in 2018 & 2019, rejected by EMA in 2019
Ciprofloxacin Dry Powder Inhalation	Bayer / Nektar Therapeutics	Rejected by FDA	Nov 2017						■			■					■	Breakthrough Therapy / Orphan Drug / QIDP	uses T-326 inhaler developed by Novartis; rejected due to safety, efficacy, and resistance concerns
Avarofloxacin	Furiex Pharmaceuticals / Allergan	Discontinued after Phase 2	Feb 2013			■		■				limited		■	■	■		QIDP	
DS-8587	Daiichi- Sankyo	Discontinued after Phase 1	April 2013	■		■					■		■	■	■				
KPI-10	Wakunaga Pharmaceutical / Kaldex Pharmaceuticals	Discontinued after Phase 1	Sept 2012	■		■					■		■	■		■			

Candidate	Sponsors and Developers	Phase	Approval or Discontinuation Date / Last Status Update	Approved or Intended Indications							Approved or Expected Activity Spectrum				Formulation			Regulatory Designations	Comments
				UTI	HABP / VABP	CABP	cIAI	ABSSSI	CF pulmonary infection / NCFB	bacteremia	*Enterobacteriaceae*	*P. aeruginosa*	*A. baumannii*	Notable for Gram-positive coverage	IV	oral	Inhalation		
β-lactam + β-lactamase inhibitor (BLI)																			
Teflaro / Ceftaroline Fosamil	AbbVie / Allergan / Forest Laboratories / Cerexa Inc.	Approved by FDA	Oct 2010 / Dec 2016															QIDP	approved for pediatric use in 2016
Cayston / Aztreonam Lysine	Gilead Sciences	Approved by FDA	Feb 2010																
Zerbaxa: Tazobactam + Ceftolozane	Cubist Pharmaceuticals / Merck & Co. / Astellas Pharma	Approved by FDA	Dec 2014 / June 2019															QIDP / NTAP	approved for cIAI in 2014 and HABP/VABP in 2019
Avycaz: Ceftazidime + Avibactam	Abbvie / Allergan / Pfizer / Forest Laboratories / Cerexa Inc.	Approved by FDA	Feb 2015 / March 2019															QIDP	first-in-class DBO BLI avibactam; approved for cUTI and cIAI in 2015 and HABP/VABP label expansion in 2018; approved for pediatric cIAI and cUTI in 2019
Vabomere / Carbavance: Meropenem + Vaborbactam	Melinta Therapeutics / The Medicines Company / Rempex Pharmaceuticals	Approved by FDA	Aug 2017															QIDP / NTAP	first-in-class boronate BLI varobactam; Phase 3 study of HABP/VABP, bacteremia, and UTI due to CRE completed in July 2017 (TANGO-II); Phase 3 study of HABP/VABP was withdrawn in Jan 2019 with no patient enrollment
Recarbrio: Imipenem + Cilastatin + Relebactam	Merck & Co.	Approved by FDA	July 2019 / June 2020															QIDP / NTAP	cilastatin prevents degradation of imipenem in the kidneys; approved for HABP/VABP in 2020
Fetroja / Cefiderocol	Shionogi & Co. Ltd.	Approved by FDA	Nov 2019 / Sept 2020															QIDP / NTAP	first approved siderophore-antibiotic conjugate; approved for cUTI in 2019, HABP/VABP in 2020; carbapenem-resistant pathogen focus study for EMA approval was published in 2020
Exblifep: Cefepime + enmetazobactam / AAI101	Allecra Therapeutics / Orchid Pharma	NDA stage (FDA and EMA)	Feb 2020															QIDP	sulfone BLI enmetazobactam is structurally similar to tazobactam, but has neutral charge
Sulopenem	Iterum Therapeutics PLC / Pfizer Inc.	NDA stage	Dec 2020															QIDP	was in clinical development in mid-1990s but was discontinued until 2003
Tebipenem Pivoxil Hydrobromide / SPR994	Spero Therapeutics / Meiji Seika / Wyeth	NDA stage	Sept 2020									limited	limited					QIDP	prodrug with HBr salt for stability; non-salt form approved in Japan
Cefepime + Taniborbactam / VNX5133	VenatoRx Pharmaceuticals	Phase 3	Aug 2020															QIDP	boronate BLI taniborbactam
Aztreonam + Avibactam	Pfizer Inc. / AbbVie / Allergan / AstraZeneca	Phase 3	Aug 2020															QIDP	DBO BLI avibactam
WCK 5222 / Cefepime + Zidebactam	Wockhardt Ltd	Phase 3	April 2020															QIDP	DBO BLI zidebactam; seeking approval by FDA, EMA, and NMPA
Sulbactam + Durlobactam / ETX-2514	Entasis Therapeutics / Zai Lab Ltd.	Phase 3	May 2020															QIDP	DBO BLI durlobactam; Sulbactam is traditionally known as a BLI but has a strong affinity for PBP3 in *Acinetobacter*; durlobactam can inhibit PBP2 and restore activity of sulbactam in resistant organisms
WCK 4282: Cefepime + Tazobactam	Wockhardt Ltd	Phase 3	April 2020															QIDP	sulfone BLI tazobactam; seeking approval by FDA, EMA, and NMPA
Zevtera / Ceftobiprole	Basilea Pharmaceutica Ltd. / Johnson & Johnson	Phase 3	July 2020		only HABP					*S. aureus* only								QIDP	has been approved in outside markets; FDA did not approve in 2008
Benapenem	Sihuan Pharmaceutical	Phase 3	Aug 2020				only IAI												clinical development only for NMPA
Mecillinam / Pivmecillinam	Utility Therapeutics Ltd. / Leo Pharma																	QIDP	oral formulation is prodrug pivmecillinam HCl; IV formulation contains the active drug mecillinam; approved for uUTI in Europe, and some African and Asian countries
BOS 228 / LYS228	Boston Pharmaceuticals	Phase 2	May 2020															QIDP	phase 2 trials were terminated as part of the out-licensure of the agent to Boston Pharmaceuticals; scalable synthesis for commerical manufacturing published May 2020
Ceftibuten + VNRX-7145	VenatoRx Pharmaceuticals	Phase 1	July 2020	unannounced															boronate BLI VNRX-7145; ceftibuten is 3rd gen cephalosporin approved 1995
ORAvance / OMNIvance: QPX-7728	Qpex Biopharma / Brii Biosciences	Phase 1	Dec 2020	unannounced															QPX-7728 is a BLI to be paired with other beta-lactams for ORAvance and OMNIvance
WCK 6777	Wockhardt Ltd	Phase 1	April 2020															QIDP	
ARX-1796	Pfizer / Arixa Pharmaceuticals	Phase 1	Oct 2020																oral prodrug form of avibactam
Cefpodoxime Proxetil + ETX0282	Entasis Therapeutics Inc.	Phase 1	Nov 2020																DBO BLI ETX0282; both ETX0282 and cefpodoxime proxetil are prodrugs
Meropenem + Nacubactam / QP0595	NacuGen Therapeutics / Roche	Phase 1	Nov 2020															QIDP	DBO BLI nacubactam
Ceftaroline + Avibactam	AbbVie / Allergan / AstraZeneca / Forest Laboratories	Discontinued after Phase 2	May 2017																ceftaroline approved in 2010 for Gram-positive infections; combination with avibactam BLI was pursued to cover resistant isolates
GT-1 + GT-055	Geom Therapeutics / LegoChem Biosciences	Discontinued after Phase 1	April 2019	unannounced															GT-1 is a siderophore-cephalosporin conjugate; DBO BLI GT-055
AIC499 + BLI	AiCuris	Discontinued after Phase 1	2019								limited	limited	limited						
C-Scape: Ceftibuten + Clavulanate	Cipla / Achaogen	Discontinued after Phase 1	June 2019															QIDP	ceftibuten was approved by FDA in 1995; clavulanate has been approved as BLI adjuvant since 1984
GSK3342830	GlaxoSmithKline	Discontinued after Phase 1	Nov 2017	unannounced															
BAL30072	Basilea Pharmaceutica	Discontinued after Phase 1	Aug 2016																
Biapenem / RPX-2003 + Vaborbactam / RPX7009	The Medicines Company / Rempex Pharmaceuticals	Discontinued after Phase 1	2014																developed by Lederle Laboratories in 1990s but abandoned; approved in Japan and China; this was the original Carbavance combination, but biapenem was later replaced by meropenem for regulatory reasons

Candidate	Sponsors and Developers	Phase	Approval or Discontinuation Date / Last Status Update	Approved or Intended Indications							Approved or Expected Activity Spectrum				Formulation			Regulatory Designations	Comments
				UTI	HABP / VABP	CABP	cIAI	ABSSSI	CF pulmonary infection / NCFB	bacteremia	*Enterobacteriaceae*	*P. aeruginosa*	*A. baumannii*	Notable for Gram-positive coverage	IV	oral	Inhalation		
MurA inhibitors																			
Contepo / IV Fosfomycin	Nabriva Therapeutics / Zavante	NDA stage	Nov 2020									limited						QIDP / NTAP	fosfomycin is approved by FDA as oral treatment for uUTIs; IV fosfomycin has been used for over 45 years outside the U.S. to treat cUTIs; FDA rejected in June 2020 due to manufacturing concerns that are currently unresolvable due to travel restrictions; the first QIDP to be granted conditional NTAP approval prior to receiving FDA approval
tRNA Synthetase Inhibitors																			
Epetraborole / GSK2251052 / AN3365	Anacor / GlaxoSmithKline	Discontinued after Phase 2	Oct 2012																
LpxC Inhibitors																			
ACHN-975	Achaogen	Discontinued after Phase 1	July 2013																
RC-01	Recida Therapeutics	Discontinued after Phase 1	May 2019	unannounced															
LptD Inhibitors																			
Murepavadin	Polyphor/ Roche AG	Discontinued IV formulation after Phase 3 ; oral formulation to start Phase 1	July 2019 ; Dec 2020															QIDP	clinical trial authorization was granted by the UK Medicines and Healthcare products Regulatory Agency for inhaled murepavadin in Dec 2020
RNA polymerase Inhibitors																			
BV100 / Rifabutin	BioVersys AG	Phase 1	Nov 2020															QIDP	rifabutin (Mycobutin) was approved by the FDA in 1992 as an oral formulation for the prevention of disseminated NTM disease in patients with advanced HIV infection; from ansamycin class of antibiotics
Bioenergetic inhibitors																			
Pravibismane / MBN-101	Microbion Corp.	Phase 2- topical; preclinical- inhalation	June 2020															QIDP / Orphan Drug	broad-spectrum; clinical trials have been conducted for topical formulations for diabetic foot ulcer infection and orthopedic implant infection indications. Inhalation formulation is in preclinical stage.

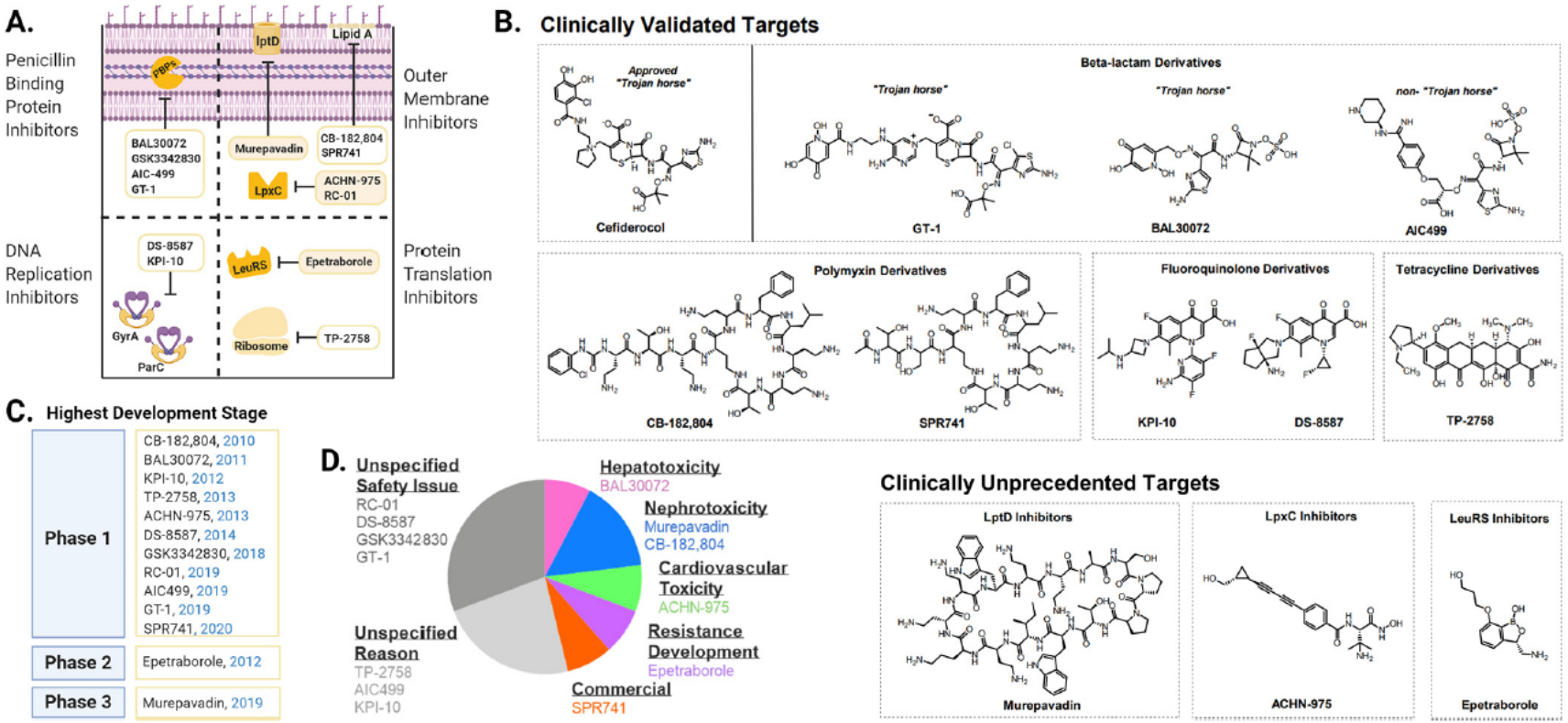

Figure 1.2: Profile of GNB-active clinical candidates discontinued between 2010–2020.

A) Cellular localization of targets of discontinued candidates. Yellow boxes represent inhibitors of clinically unprecedented targets. B) Chemical structures of discontinued candidates. Structures were retrieved from the following PubChem IDs: Murepavadin: 91824766, ACHN-975: 71466517, CB-182,804: 405560444, SPR740: 53323381, BAL30072: 135905457, DS-8587: 56640741, KPI-10: 11676981, Epetraborole: 46836890, Cefiderocol: 77843966. TP-2758 structure was not found on Pubchem and was instead replicated from Sun, 2018. AIC499 structure was not found on Pubchem and was instead replicated from Frieschem, 2021. Structures of RC-01 and GSK3342830 are not disclosed. C) Year and clinical trial stage at time of discontinuation. Candidates appear in chronological order for each trial stage. D) Reasons for discontinuation. Limited information gathered from public press releases and published literature. Created with Biorender.com.

Although most discontinued candidates are first-time entrants into the clinical development pipeline, some candidates have traversed the pipeline as a different formulation (for example, inhalation therapies) or purposed for other indications (for example, label expansions). The remainder of this review profiles the journey of the 13 first-time entrants that have fallen out of the clinical pipeline. These select candidates target components of the outer membrane (OM), DNA replication, protein translation, and PBPs (**Figure 1.2A**). The structural diversity (**Figure 1.2B**) reflects the variety of mechanisms of action employed to inhibit GNB growth. Most of these candidates were discontinued after phase 1 (**Figure 1.2C**) due to safety concerns (**Figure 1.2D**).

Discontinued candidates with clinically validated targets

B-lactam derivatives

Degradation of β-lactams by β-lactamases is a common resistance mechanism that has been partially addressed by structural optimization of the β-lactam scaffold, adjunctive administration of β-lactamase inhibitors (BLIs), and attachment of a siderophore for improved cellular uptake. (16) Among the many attempts since 1980 to overcome resistance by attaching an iron-chelating group to a β-lactam, (17, 18) cefiderocol was the first siderophore-antibiotic conjugate to gain FDA approval in 2019. No other clinical-stage siderophore-β-lactam conjugate (cefetecol, BAL30072, GSK3342830, GT-1) has progressed past phase 1 trials.

BAL30072

BAL30072 is a siderophore-monobactam conjugate developed by Basilea Pharmaceutica (Basel, Switzerland) derived from tigemonam, with an appended dihydroxypyridinone moiety for iron chelation. Portions of the structure resemble aztreonam and avibactam. BAL30072 exhibits bactericidal activity against *P. aeruginosa*, *Acinetobacter* species, and *Enterobacteriaceae* and is stable to metallo-β-lactamases. (19, 20) While most monobactams singularly inhibit PBP3, BAL30072 also engages the bifunctional PBPs 1a and 1b in *E. coli*. (19) Accordingly, while filamentation is usually observed in *E. coli* cells treated with monobactams targeting PBP3, (21) BAL30072 triggers spheroplasting prior to lysis. (19) This spheroplasting phenotype is also elicited by some bicyclic β-lactams (22) and β-lactamase enhancers that target PBP2. (23)

Several *in vitro* studies indicate the synergy of BAL30072 in combination with meropenem or colistin against various MDR GNB clinical isolates. (24–26) *In vivo* synergy was evaluated in soft-tissue infection models of rats challenged with *A. baumannii*. While BAL30072 showed statistically significant activity, the addition of meropenem was not additive, synergistic, or antagonistic. (24) This finding may be rationalized: BAL30072 and carbapenems both inhibit PBP2 in *A. baumannii*, limiting the pair's success to mere additive effects. The synergy of these antibiotics might be exploited against *Enterobacteriaceae* or *P. aeruginosa*, where they have complementary PBP-binding profiles. (26) In murine septicemia, the combination therapy offered protection against

carbapenem-resistant *P. aeruginosa* and MDR *A. baumannii*—the former due to complementary PBP binding profiles, and the latter possibly due to complementary β-lactamase binding profiles. (26)

A 2010 phase 1 SAD study reported no serious adverse events at doses up to 8 g. The MAD study established a maximum tolerated dose, limited by elevated ALT levels. In 2014, Basilia initiated another phase 1 MAD study of BAL30072, both alone and in combination with meropenem. When 2 g BAL30072 was administered as 1-h IV infusions every 8 h (6 g/day), or when 4 g of BAL30072 administered as continuous 22-h infusions for 6 days, abnormally high ALT levels were observed in almost all healthy study subjects as early as 3 days post-treatment, and development of the IV formulation was ceased. (27) *In vitro* studies revealed that BAL30072 inhibits the mitochondrial electron transport chain, β-oxidation, and glycolysis in HepG2 liver cells at concentrations of 100–200 μM, which is clinically relevant only after long-term exposure. (27, 28) These findings were unexpected given positive toxicity studies in rats and marmosets dosed with BAL30072 for 4 weeks. (27)

To assess utility for UTI, urinary concentrations of BAL30072 were analyzed in MAD study subjects. (26, 28) Bactericidal activity against *P. aeruginosa* was weak in urine, presumably due to low concentration of iron and consequent competition with native siderophores. (28) Basilea also began preclinical studies of an inhalation formulation for treatment of

pulmonary infections in CF patients, which was stopped in 2016 due to lack of confidence in the candidate's success. (29)

GSK3342830

GlaxoSmithKline (London, UK) and Shionogi (Osama, Japan) initiated a collaboration in 2010 to discover novel cephem antibiotics with GNB activity, yielding two promising cephalosporin-siderophore conjugates. In 2015, Shionogi retained rights to cefiderocol, which became the first siderophore-antibiotic conjugate to gain FDA approval, (30) and GlaxoSmithKline retained rights to the catechol-cephem GSK3342830.

Phase 1 GSK3342830 trials began in 2017. (31) In the SAD component, PK properties consistent with other cephalosporins, including cefiderocol, and no severe adverse events were detected at doses up to 6 g. (32) In the MAD study, 11 subjects received 1 g GSK3342830 as a single IV infusion on day 1, 3-times-a-day IV infusions on days 2 through 14, and a single IV infusion on day 15. 4 participants discontinued the treatment due to headache, malaise, and/or fever, and 1 had high ALT levels leading to automatic discontinuation. The 6 subjects remaining in the study experienced malaise, headache, and fever with an onset between 9–10 days, and a general decrease in platelet counts (32) While symptoms could be related to known off-target binding to the 5HT-3 serotonin receptor, this interaction seemed physiologically unlikely. (32) GSK3342830 was discontinued following these results in 2018.

GT-1 & GT-055

GT-1 (LCB10-0200) is a siderophore-cephalosporin conjugate developed by LegoChem Biosciences (Daejeon, Korea) in a joint venture with Geom Therapeutics (San Francisco, CA, USA). The candidate features the same dihydroxypyridinone siderophore appendage present in BAL30072 and a similar side chain to ceftazidime. GT-1 demonstrated efficacy against *P. aeruginosa* in murine models of systemic, thigh, respiratory tract, and urinary tract infections. (33) Its activity spectrum also covers MDR *Enterobacteriaceae* and *A. baumannii*. (34) The candidate was paired with GT-055 (LCB18-055), a diazabicyclooctane BLI with intrinsic activity against PBP2. (35, 36)

A phase 1 study was registered in Australia in 2019. (37) Only 8 participants were enrolled in this trial when it was terminated due to unspecified safety reasons, presumably hepatotoxicity.

AIC499

AIC499 is a monobactam bearing high resemblance to aztreonam with notable activity against MDR *A. baumannii* and *P. aeruginosa*. Structural analysis shows hydrophobic interactions between the phenyl portion of the head group with PBP3, while the piperidine portion has a dynamic configuration with lesser impact on binding yet beneficial PK/PD properties. (38) The candidate was noted to have potent antibacterial activity when co-administered with a BLI, though the combination that AiCuris Anti-

infective Cures GmbH (Wuppertal, Germany) pursued in clinical trials was unspecified. Phase 1 began in Austria in 2017, with phase 2 planned for cIAI and cUTI. These results are unpublished, and the candidate was removed from the company's pipeline in 2019 for undisclosed reasons.

Fluoroquinolone derivatives

Fluoroquinolones began receiving FDA approval in the late 1960s for treating UTIs and respiratory tract infections, but the FDA has issued many side effect warnings for these antibiotics since 2008. Reports of these adverse events during post-marketing surveillance led to the withdrawal of several fluoroquinolones. Second- and third-generation fluoroquinolones like ciprofloxacin, levofloxacin, and moxifloxacin are still used to treat GNB infections.

DS-8587

DS-8587 is a broad-spectrum fluoroquinolone synthesized by Daiichi Sankyo (Tokyo, Japan) with enhanced bactericidal activity against *Acinetobacter baumannii*. The candidate retains the core structure of post-second-generation fluoroquinolones, most closely resembling moxifloxacin; however, the fluorination of the cyclopropyl group, the C7 octahydrocyclopentapyrrole, and the methylated C8 distinguish the candidate from the newer generation candidates that have other fused pyrrolidines at C7 and an ether or no functionality at C8. The dual-targeting compound has micromolar IC_{50} values for *A. baumannii* ParC and GyrA enzymes, high potency against clinical isolates of *A. baumannii*

with mutated ParC and GyrA domains, and low resistance frequency and efflux pump susceptibility. (39) In a murine calf muscle infection, efficacy was correlated with AUC/MIC values, like other quinolones. (40)

Daiichi Sankyo previously marketed three fluoroquinolones (ofloxacin, levofloxacin, and sitafloxacin), but DS-8587 development was discontinued in 2014 after phase 1 for unexplained reasons. 2017 studies revealed the *in vivo* efficacy of DS-8587 against *Fusobacterium necrophorum*, a pathogenic obligate GNB anaerobe, in murine liver abscess. (41)

KPI-10

KPI-10 (WQ3813) is a synthetic fluoroquinolone, bearing similarity to 4th-generation trovafloxacin, discovered by Wakunaga Pharmaceutical (Osaka, Japan). The broad-spectrum activity against *Enterobacteriaceae*, MDR *Acinetobacter species, N. gonorrhoeae*, and notable Gram-positive organisms including methicillin resistant *Staphylococcus aureus* (MRSA) and *S. pneumoniae*. (42–44) pointed towards the candidate's utility in treating both CABP and UTI infections.

Kalidex Pharmaceuticals (Menlo Park, CA, USA) licensed the global development and commercialization rights to the candidate. Phase 1 of the oral formulation began in 2012. The SAD study demonstrated a favorable safety and PK profile, supporting a daily oral

dosing regimen. (45) Clinical development was discontinued for undisclosed reasons, and Kalidex reportedly ceased operation in 2016.

Tetracycline derivatives

TP-2758

Tetraphase (Watertown, MA, USA) optimized the convergent total synthesis of tetracycline to access analogs that are inaccessible by semi-synthesis. (46) This approach produced one clinically approved antibiotic (eravacycline) and two other phase-1 candidates (TP-271 and TP-6076). TP-2758, with a chiral 8-pyrrodinyl substitution, was discovered while generating a series of novel 7-methoxy-8-heterocyclyl tetracycline analogs. (47) Derivatives of tetracyclines, called glycylcyclines, were developed to combat the rise of tetracycline resistance. While most tetracyclines are orally dosed, glycylcyclines like tigecycline are restricted to IV dosing. TP-2758 was projected to become the first orally bioavailable glycycline.

TP-2758 was more potent than tigecycline against *A. baumannii* and *Enterobacteriaceae*, and both oral and IV dosing of TP-2758 significantly reduced the burden of infection in murine pyelonephritis induced by *E. coli* or MDR *K. pneumoniae.* (48) Oral bioavailability values vary between animal species: while tetracycline has oral bioavailabilities of only 14.9% in rats and 6.7% in monkeys, it is greater than 70% in humans. (48) TP-2758 had oral bioavailabilities of 8.62% in rats and 30.4% in monkeys, implying higher oral bioavailability

in humans than tetracycline. (48) Phase 1 studies (49) for oral formulation began in 2011, but results are unavailable. TP-2758 was removed from the company's pipeline in 2013, and Tetraphase was acquired by La Jolla Pharmaceutical Company in 2020.

Polymyxin derivatives

Polymyxins are cationic cyclic peptides (net charge of +5) thought to selectively disrupt and permeabilize the GNB OM to result in bactericidality, though evidence suggests that they may have more than one target. (50) When polymyxins were first introduced to the clinic, they were quickly abandoned due to high incidences of dose-limiting nephrotoxicity and neurotoxicity. (51) However, with the rise of MDR Gram-negative pathogens, this class has resurged in the clinic as a last-resort therapy. (52) The two clinically administered polymyxins, polymyxin B (PMB) and colistin, are manufactured by fermentation as an impure, heterogeneous mix of related compounds. CB-182,804 was the first polymyxin to undergo clinical trials under the FDA's oversight.

CB-182,804

BioSource Pharmaceuticals (Spring Valley, NY, USA) developed a semi-synthetic route to substitute the N-terminal fatty acyl group that contributes to the toxicity of PMB utilizing a deacylase enzyme from the microorganism *Actinoplanes utahensis*. (53) After screening many urea-linked halophenyl functionalities for antimicrobial activity, the 2-chlorophenylurea derivative, CB-182,804, emerged as a lead candidate. The candidate had bactericidal activity against *E. coli*, *K. pneumoniae*, *P. aeruginosa*, and *A. baumannii.*

Cubist Pharmaceuticals (Lexington, MA, USA) obtained a provisional license for the candidate, and subsequent patents were filed jointly to further develop the strategy. (54)

The MICs of CB-182,804 against 5,000 clinical isolates were only two-fold higher than PMB, with observable cross-resistance. (55) Similarly, *in vivo* efficacy in murine *P. aeruginosa* lung and *A. baumannii* thigh infection models were comparable for the two. (56) However, the EC_{50} values against a rat renal tubule cell line were >1000 mg/L for CB-182,804 and 318 mg/L for PMB. (56) In Cynomolgus monkeys dosed 6.6 mg/kg/day 3-times-a-day for 7 days, CB-182,804 showed limited renal tubular histological changes, whereas PMB exhibited renal tubular degeneration; at a higher dose of 9.9 mg/kg/day, CB-182,804 elicited only a slight increase in blood urea nitrogen and serum creatinine, whereas PMB elicited severe signs of nephrotoxicity. (57) CB-182,804 also demonstrated more favorable PK/PD parameters than PMB, including decreased serum protein binding, increased plasma clearance, increased volume of distribution, and less systemic exposure—as well as a lower C_{max}. (57) Clinical trials began in February 2009, but development of this molecule ceased in 2010, presumably due to nephrotoxicity issues. (58) Cubist was acquired by Merck Pharmaceuticals in 2015.

SPR741

SPR741 (NAB741) is a fully synthetic PMB derivative that was designed to curtail nephrotoxicity issues associated with this class through reduced positive charge (3+) and removal of the highly lipophilic fatty-acid side chain in PMB. (59) In a rat model, renal

clearance of SPR741 was 400-fold higher than colistin, suggesting improved safety-related PK properties. (59) Despite having weak antibacterial activity, sub-MIC dosing of SPR741 enhances the permeation of other antibiotics through the OM. (60) *In vivo* studies confirm this potentiation with expanded azithromycin coverage against MDR *Enterobacteriaceae*, (61) and synergy with rifampicin against XDR *A. baumannii*. (62)

In a phase 1 drug-drug interaction study, IV dosing of other antibiotics (1.0 g of ceftazidime, 4.5 g of piperacillin-tazobactam, or 1.0 g of aztreonam) with 400 mg SPR741 did not significantly affect concentration-versus-time profile, clearance, or half-life of either drug. (63) In the MAD study, 25% of subjects experienced decreased creatinine clearance across all drug-dosage cohorts: 3 in 600-mg, 1 in 400-mg, 1 in 150-mg, 1 in 50-mg. (63) Of these 6 subjects, 5 had normal creatinine levels at day 16, while one from the 600-mg cohort had a moderate increase in serum creatinine level above baseline level that began on day 14. SPR741 was discontinued in January 2020 and replaced by SPR206, a different polymyxin analog from the potentiator platform. While SPR741 was developed as an antibiotic adjuvant, SPR206 has antibacterial activity as a standalone therapy and boasts a potentially superior safety and efficacy profile than SPR741.

Discontinued candidates with clinically unprecedented targets

Murepavadin (LptD inhibitor)

Inspired by the antimicrobial host defense peptide protegrin I, Polyphor Ltd. (Allschwil, Switzerland) synthesized and screened a library of β-hairpin-shaped macrocyclic protein epitope mimetics for antimicrobial activity. (64–67) While initial leads exhibited hemolysis of red blood cells and degradation by serum enzymes, optimization towards antibacterial activity yielded the clinical candidate murepavadin (POL-7080). (67, 68) Murepavadin reportedly targets the β-barrel protein LptD, (68–70) an essential (71) surface-exposed OM protein that acts in a complex (72–74) to incorporate LPS into the OM of GNB. The differential N-terminal lengths of LptD among GNB is thought to confer the specificity of murepavadin to the *P. aeruginosa* protein. (68) In preclinical studies, murepavadin outperformed comparator antibiotics, including colistin, against even XDR *P. aeruginosa* clinical isolates. (75, 76) Though oral bioavailability was low in rats, subcutaneous administration in humans yielded a bioavailability of 67–79% and a half-life of 5–8 h. The discovery and development of murepavadin has previously been reviewed. (77)

Roche (Basel, Switzerland) obtained a license to develop and commercialize murepavadin in 2013. Six phase 1 studies explored the safety, tolerability, and PK of murepavadin: a combined SAD and MAD study in healthy male subjects; (78) a multiple-dose study evaluating the penetration of murepavadin into the lungs; (79) a drug-drug interaction investigation of murepavadin with colistin, (80) and with amikacin; (81) a TQT study with

SAD; (82) and a SAD study of murepavadin in subjects with renal function impairment. (83) Systemic exposure to murepavadin increased in subjects with renal function impairment, indicating a need for dose-adjustment based on creatinine clearance rate. (84) Despite Roche returning the murepavadin development license to Polyphor in 2015, two phase 2 studies were successfully completed: a 14-day dosage of murepavadin in subjects with acute exacerbation of non-cystic fibrosis bronchiectasis due to *P. aeruginosa* infection (85) and a MAD study of murepavadin co-administered with SOC in subjects with VABP due to *P. aeruginosa* infection. (86) In the latter study, clinical cure was achieved in 10 out of 12 (83%) patients with confirmed *P. aeruginosa,* and the 28-day all-cause mortality rate in this population was 9%. (87)

Though murepavadin's narrow spectrum of activity provides advantages as a treatment option, it complicated the phase 3 clinical trial design. (88) While phase 1 and 2 tested murepavadin as a monotherapy, the ethics of phase 3 trials in pneumonia patients necessitated the coadministration of murepavadin with a broad-spectrum drug. (88) The co-administered antibiotic needed to have no pseudomonal activity, to avoid confounding the results of the trial. Ertapenem, a first-line therapy for CABP, was ultimately chosen for coadministration, and the appropriate dosing for HABP/VABP was determined. (88)

Murepavadin underwent two separate phase 3 trials to test its efficacy in HABP/VABP infection due to *P. aeruginosa.* (89, 90) The FDA-approved non-inferiority study (PRISM-

UDR) (89) compared murepavadin + ertapenem to 1 β-lactam antibiotic to treat HABP/VABP driven by *P. aeruginosa* in clinical centers with low incidence of MDR. The EMA-approved study (PRISM-MDR), (90) in contrast, compared murepavadin + 1 anti-pseudomonal antibiotic to 2 anti-pseudomonal antibiotics in clinical centers with high incidence of MDR to assess murepavadin efficacy over SOC. Though 25–40% incidence of kidney injury was anticipated based on the comparator arm, 56% of patients treated with murepavadin in the VABP study showed evidence of acute kidney injury. (91) Polyphor terminated IV formulation development as of July 2019 due to nephrotoxicity concerns. Murepavadin was the only GNB-active clinical candidate in this decade to be discontinued after phase 3. Polyphor continued pre-clinical development of an inhalation formulation of murepavadin, and clinical trial authorization was granted in the United Kingdom in December 2020.

ACHN-975 (LpxC inhibitor)

LpxC is a cytosolic zinc-dependent metalloenzyme that catalyzes the first committed step of lipid A biosynthesis. While many antibiotic discovery programs have pursued LpxC inhibitors, (92) Achaogen's (South San Francisco, CA, USA) structure-based discovery effort yielded the first LpxC inhibitor to advance into clinical trials. Like other previously patented LpxC inhibitors, (93, 94) this synthetic compound contains a hydroxamic acid moiety that coordinates the catalytic Zn^{2+} and a long hydrophobic tail that interacts with the active site tunnel.

While the genetic sequence of LpxC is highly conserved across GNB, the subtle structural differences in LpxC influence the potency and dynamics of inhibition. (95) ACHN-975 exhibited optimal efficacy when the dose was administered once-daily for *P. aeruginosa,* but administered multiple times a day for *E. coli* and *K. pneumoniae*, so an intermittent high-dose regimen was established to treat respiratory *P. aeruginosa* infections. (96) The possibility of resistance emergence set the minimum required dose: at concentrations 4-fold higher than the MIC, the frequency of resistance ranged from 10^{-7}–10^{-10} in *P. aeruginosa* clinical isolates. (96) However, ACHN-975 induces bradycardia in preclinical animal models, (97) setting a maximum tolerated dose.

In 2012, a phase 1 SAD study to assess the candidate's safety, tolerability, and PK in 50 healthy volunteers (98) was completed. The therapeutic window was deemed insufficient due to concentration-driven dose-limiting cardiovascular toxicity (transient hypotension without tachycardia), which occurred in the first subject who received an 18 mg/kg infusion. (99) A 2013 MAD study (100) was prematurely terminated after enrolling four subjects. Participants encountered inflammation at the infusion site after repeat dosing of 4 mg/kg, three-times-a-day for 3–4 days.

In 2015, Achaogen began an optimization program focusing on *P. aeruginosa.* (99) This pathogen was more sensitive to LpxC inhibition in *in vivo* models than *Enterobacteriaceae* species, and the structural features of *P. aeruginosa* LpxC seemed more amenable for curtailing drug toxicity. (99) To investigate structure-toxicity

relationships, a high content assay in anesthetized rats was developed to assess maximum tolerated concentrations. (99) Cardiovascular toxicity was attributed to a nonspecific effect of basic amines so a new candidate was identified with a wider therapeutic window. With the removal of the amine, this new candidate was non-solubilizable at 10–100 mg/mL concentrations using acidic pH. (99) To overcome solubility issues and accommodate the anticipated dose of >1 g per day, the hydroxyl tail was converted to a phosphate prodrug. Surprisingly, this new prodrug, dosed in a simple aqueous formulation, demonstrated cardiovascular toxicity in the anesthetized rat model, even though the parent molecule, dosed in a pH-adjusted hydroxypropyl-cyclodextrin, did not. (99) Compounds and insights from these studies were passed on to Forge Therapeutics (San Diego, CA, USA) after Achaogen filed for bankruptcy in 2019.

RC-01 (LpxC inhibitor)

FUJIFILM Toyama Chemical Co. Ltd. (Toyoma, Japan) screened compounds with malonamide, a derivative of the zinc-chelating hydroxamic acid, for LpxC activity. RC-01 (T-1228) was identified as a lead compound, exhibiting sub-nanomolar IC_{50} against LpxC and bactericidal activity against *P. aeruginosa* and *Enterobacteriaceae*. (101) *In vitro* exposure of RC-01 to GNB reduces the release of LPS, (102) corroborating *in vivo* data from other LpxC inhibitors that decrease LPS-dependent stimulation of the host immune system, thereby attenuating bacterial virulence. (103) In mouse models of *P. aeruginosa*-induced pneumonia and *E. coli*-induced UTI, the most highly correlated PK/PD parameter

with efficacy was fAUC/MIC. (104) The frequency of resistance to RC-01 at 4x MIC was 10^{-7}–10^{-8}. (105)

In 2019, Recida Therapeutics (Menlo Park, CA, USA) licensed the development and commercialization rights for RC-01 outside of Japan. LpxC-associated cardiovascular toxicity was unapparent with RC-01: atleast 400 mg/kg/day was tolerated in 2-week repeated IV dosing in rats and dogs, with unreported fAUC and C_{max}. (106) Two formulations of RC-01 were pursued: an inhalation therapy for respiratory infections and IV therapy for systemic infections. The programs were prematurely terminated after enrolling 8 subjects in a phase 1 SAD study (107) for unspecified safety reasons. Recida soon after surrendered its business rights in California, and MicuRx was granted rights for investigational treatment with RC-01 in China.

Epetraborole (LeuRS inhibitor)

Epetraborole (GSK2251052, AN3365) is a bacteriostatic oxaborole-containing inhibitor (108) of leucyl-tRNA synthetase (LeuRS) that was discovered in a structure-based rational design screen led by Anacor Pharmaceuticals (Palo Alto, CA, USA). The only FDA-approved aminoacyl-tRNA synthetase inhibitor is mupirocin, which targets isoleucyl-tRNA synthetase for treatment of Gram-positive infections. (109–111) Mupirocin is restricted to topical use due to rapid metabolism of its ester moiety and resistance emergence. (112)

The mechanism of a benzoxaborole antifungal agent trapping the active conformation of the editing site of LeuRS inspired the rational design of epetraborole. (113) Guided by crystallography, benzoxaborole analogs with extended coverage against *A. baumannii* were synthesized. (113, 114) Screening against MDR clinical isolates demonstrated a 10^{-7} one-step resistance frequency at 4x MIC, (114) coverage of anaerobic microorganisms (115, 116), and low MIC_{90}s against *P. aeruginosa.* (117) Mouse thigh infections highlighted the candidate's efficacy against MDR GNB *in vivo.* (114)

In 2009, Anacor initiated phase 1 trials for the IV formulation and reported favorable safety and PK properties in 72 subjects. (118) In accordance with a 2007 alliance forged with Glaxosmith-Kline (London, UK), GSK obtained an exclusive license for epetraborole in 2010. Phase 1 trials included SAD and MAD studies of oral formulations, (119) small cohort mass balance study of the IV formulation, (120) and serum and pulmonary PK of the IV formulation. (121) Like mupirocin, epetraborole is highly metabolized in monkeys and humans: oxidation of the propanol side chain by the polymorphic alcohol dehydrogenase generates an inactive carboxylic acid metabolite. (122) Following a 1,500 mg IV infusion of the candidate in 6 human subjects, the candidate was found in systemic circulation and urinary excretion in its original form and, to a great extent, its oxidized form.

GSK initiated phase 2 trials for cUTI (123) and cIAI. (124) In 3 of the 14 patients receiving epetraborole in the cUTI study, resistant isolates were recovered after only 1 day of

treatment. (125) Whole-genome sequencing revealed target-specific mutations in the LeuRS editing domain that conferred a low fitness cost. (125) The emergence of these fit mutants suggests that either this specific mode of binding to LeuRS or general inhibition of LeuRS is unproductive for impeding bacterial growth. Due to resistance concerns, the cUTI study was terminated in 2012, and the cIAI study was terminated as a precaution, even though isolates from 3 of the 9 patients who received epetraborole in this study maintained baseline susceptibility to the drug candidate. (125) GSK also assessed drug distribution in epithelial lining fluid and alveolar macrophages, which showed promise for efficacy under a pneumonia indication. (126) GSK soon after returned licensing rights to Anacor, which was acquired by Pfizer in 2016.

Discussion

A decade of leakiness in the GNB-active antibiotic clinical development pipeline is apparent from this review. The most prominent crack in the pipeline is the transition between phase 1 and phase 2. Data from AntibioticDB, (127) a growing repository for antibiotics in global preclinical and clinical development from the 1960s to the present, shows similar termination frequencies by clinical stage of development. In contrast, drugs from other therapeutic areas (including the "infectious disease" category) have the lowest success rate in the transition from phase 2 to phase 3 trials. (128)

Both AntibioticsDB and Hay et al. cite toxicology concerns (observable in phase 1) and lack of efficacy (post-phase 1) as equally large determinants of failure for clinical

candidates with disclosed discontinuation reasons. For the GNB-active candidates of this decade, however, halts over the past ten years are largely attributable to safety issues in phase 1 trials; besides safety, three candidates were discontinued for unknown reasons, only one encountered resistance, one was replaced officially for commercial reasons, and none cited efficacy concerns (**Fig 1.2C**).

Of the 13 discontinued candidates, 4 could have been first-in-class inhibitors, representing 3 novel targets: LptD, LpxC, LeuRS. CB-182,804 was the first polymyxin to undergo clinical trials. 3 of the 4 discontinued β-lactams attempted to follow the siderophore-antibiotic conjugation strategy successfully employed by cefiderocol. Overall, it is unclear whether novel targets are exceptionally failure-prone given their small sample size. The poor safety profiles of these novel candidates may be due to the modalities of inhibiting new targets and/or the unanticipated toxicities of the novel chemical scaffolds. In the search for new antibiotics, the termination of first-in-class antibiotics is especially painful, as these new drugs provide hope for evading MDR.

Some of these discontinued clinical candidates do not strictly follow empirical guidelines for antibiotic design. (129, 130) For example, while epetraborole was the only candidate terminated due to emergence of resistance, LpxC inhibitors ACHN-975 and RC-01 posed the same concerns for resistance due to their requisite high exposure and single-copy-single-enzyme targeting mechanism. (96) Additionally, ACHN-975 chelates the catalytic zinc of LpxC with hydroxamic acid, which is associated with the release of toxic metabolic

byproducts and off-target inhibition. (99, 131–133) However, replacing the moiety impairs inhibitory potency and antibacterial activity with persisting toxicity, (134, 135) underscoring the need for probing structure-toxicity relationships in new antibiotic classes. Conceivably, *in vivo* preclinical models are good predictors of antibacterial efficacy but poor predictors of safety, and alternate methods for assessing structure-toxicity relationships in *vitro* and *in vivo* should be developed.

The termination of some candidates was surprising considering the published toxicity data. Though hepatotoxicity was unapparent in preclinical models, BAL30072 treatment caused elevated ALT levels after only 3 days. *In vitro* nephrotoxicity is an unreliable predictor of clinical nephrotoxicity, (136) which is especially problematic for polymyxins like CB-182,804. (137, 138) Despite decades of polymyxin use, structure-toxicity relationships of this class are still understudied; this gap in understanding coupled with the characteristic toxicity of this class may account for the dearth of analog development. (139) Likewise, the long history of the β-lactam class, the similarity of siderophore-conjugated candidates to approved antibiotics, and the prior approval of one siderophore-conjugated antibiotic were insufficient to bring more siderophore-conjugated antibiotics to the clinic, and a better understanding of structure-toxicity relationships of the linker and iron-chelator components may de-risk future development. The case of murepavadin highlights a latent nephrotoxicity concern that only surfaced in phase 3: phase 1 and 2 trials comprised of 8 studies, in which 257

subjects received at least a single dose of murepavadin for up to 15 days, and the only 3 SAEs reported were fully reversible after discontinuation. (77) As patients in phase 3 trials are typically sicker than the healthy subjects in phase 1, antibiotic toxicology must account for higher acuity settings.

Can discontinued candidates be revived in the clinical pipeline? Polyphor has already initiated murepavadin clinical development by reformulating from IV to oral. An inhalation formulation could benefit pneumonia treatment candidates with dose-limiting toxicity by decreasing systemic exposure and increasing concentration in lung tissues, (140) and all approved inhaled antibiotics are reformulations of compounds initially dosed through IV or oral route.

Another strategy for candidates with dose-limiting toxicity is coadministration in a synergistic combination therapy to expand their therapeutic window. While this strategy invites challenges pertaining to matching PK properties, it has been employed for several antibiotics: Novel BLIs have successfully extended the spectrum of β-lactams to MDR GNB. (141) In addition to binding β-lactamases, some potentiators inhibit cell growth in PBP-binding dependent and independent mechanisms. (142, 143) Discontinued PBP-binding candidates could be explored further in combination with a BLI or as an adjuvant for other β-lactams of complementary PBP-binding and β-lactamase-binding properties. For example, synergy of BAL30072 with meropenem compelled Basilea to pursue

combination therapy in phase 1 trials, despite the dose-limiting hepatotoxicity encountered in the previous MAD study of BAL30072 alone.

Similarly, antibiotic potency and/or spectrum of activity can be potentiated with polymyxins. Polymyxins have been investigated as potentiators for other classes of antibiotics without conclusive evidence of synergy in clinical treatments. (144, 145) *In vitro* studies show evidence of polymyxin synergy with many antibiotics, (146) including the addition of rifampicin to CB-182804 to improve potency and MDR coverage. (55) SPR741 employed this potentiation strategy, though it was discontinued after phase 1 trials for commercial reasons.

Additionally, LpxC inhibitors have demonstrated synergy with antibiotics for which GNB activity is limited by the OM, like rifampin and tetracycline. (92) LpxC inhibition may contribute to *A. baumannii* clearance *in vivo* by enhancing bacterial opsonophagocytosis and reducing inflammation, (103) despite the non-essentiality of LPS biosynthesis in this species and resultant *in vitro* inefficacy of LpxC inhibitors. This anti-virulence-based mechanism of action may reduce its likelihood of encountering resistance and extend the co-administered antibiotic's spectrum of activity.

Finally, there is a critical yet latent misalignment of the antibiotic discovery pipeline with the clinical development pipeline. (147) While antibiotic discovery typically focuses on identifying candidates corresponding to a particular MDR pathogen, cellular target, or chemical structure, late-stage clinical trials primarily test the candidate's efficacy in the

context of clinical indications. Even if a candidate fills an unmet need by targeting a critical MDR pathogen or demonstrating low cross-resistance, that coverage may be moot when tested at clinical trial sites with low incidence of MDR and compared to SOCs with high efficacy against susceptible pathogens. (148) Since rapid determination of an infection's causative organism is usually infeasible, empiric treatment based on infection site is common. Recently, the FDA required an infection site-specific indication while the EMA preferred a resistant pathogen-specific indication for phase 3 trials of cefiderocol. (30, 149) Such innovations in clinical trial design may enable the alignment of approved antibiotics with the unmet needs associated with antimicrobial resistance.

Structural, preclinical, and clinical data was inaccessible for several candidates. Considering that some public funding was critical to the early success of many candidates, we echo the call for broader data sharing. (150) Although some public databases have compiled data, including clinicaltrials.gov, the Pew Charitable Trusts, SPARK, and AntibioticsDB, we should strive for completeness in archiving. As Achaogen, after declaring bankruptcy, shared its LpxC platform data with Forge Therapeutics, other abandoned data and learned lessons should be passed on.

In conclusion, the critical leak in the GNB-active antibiotic clinical development pipeline is between phase 1 and phase 2 and is largely attributable to safety issues. By sealing this rupture, we can increase the likelihood of FDA approval and de-risk investment in the antibiotic space. Given the complexities of antibiotic design from target validation and

permeability to evasion of resistance mechanisms and non-conventional pharmacological properties, the low diversity of clinical trial termination reasons is notable. While safety presents a major challenge of antibiotic clinical development in this decade, solving this phase 1 issue may expose other issues in later clinical trials or post-approval, like resistance or efficacy. Without innovations in preclinical predictive studies and clinical trial designs, (147) the novel candidates in today's preclinical pipeline that transition to clinical development in the next decade may face the same complications and consequences as those of the last. Alternatively, novel candidates with favorable *in vivo* profiles may be abandoned in the preclinical stage if the false positive rate of preclinical toxicity assays is too high. Lastly, with many candidates withdrawn without public explanation for why, it is challenging to learn from previous mistakes. Increased data sharing through existing mechanisms could reduce redundancy and accelerate future antibiotic development.

Acknowledgements

I thank my co-authors, Dr. Ryan T. Cirz, Dr. Ian B. Seiple, and Dr. Oren S. Rosenberg, for productive discussions, and Dr. John H. Rex for sharing this publication widely with his audience. Beyond research articles, information from virtual conferences and webinars, such as the REVIVE series created by GARDP, informed the narrative around antibiotic development.

References

1. Antimicrobial Resistance Collaborators. 2022. Global burden of bacterial antimicrobial resistance in 2019: a systematic analysis. Lancet 399:629–655.

2. 2017. WHO | Global priority list of antibiotic-resistant bacteria to guide research, discovery, and development of new antibiotics.

3. Review on Antimicrobial Resistance. 2014. Antimicrobial Resistance: Tackling a Crisis for the Health and Wealth of Nations.

4. (u.s.) CFDCAP, Centers for Disease Control and Prevention (U.S.). 2019. Antibiotic resistance threats in the United States, 2019 https://doi.org/10.15620/cdc:82532.

5. Bassetti M, Peghin M, Vena A, Giacobbe DR. 2019. Treatment of Infections Due to MDR Gram-Negative Bacteria. Frontiers in Medicine https://doi.org/10.3389/fmed.2019.00074.

6. Isler B, Doi Y, Bonomo RA, Paterson DL. 2019. New Treatment Options against Carbapenem-Resistant Infections. Antimicrob Agents Chemother 63.

7. Butler MS, Paterson DL. 2020. Antibiotics in the clinical pipeline in October 2019. J Antibiot 73:329–364.

8. Theuretzbacher U, Bush K, Harbarth S, Paul M, Rex JH, Tacconelli E, Thwaites GE. 2020. Critical analysis of antibacterial agents in clinical development. Nat Rev Microbiol 18:286–298.

9. New BIO report examines the State of antibacterial innovation. https://www.bio.org/press-release/new-bio-report-examines-state-antibacterial-innovation. Retrieved 4 March 2022.

10. Dheman N, Mahoney N, Cox EM, Farley JJ, Amini T, Lanthier ML. 2020. An Analysis of Antibacterial Drug Development Trends in the US, 1980 - 2019. Clin Infect Dis https://doi.org/10.1093/cid/ciaa859.

11. Silver LL. 2011. Challenges of antibacterial discovery. Clin Microbiol Rev 24:71–109.

12. McDowell LL, Quinn CL, Leeds JA, Silverman JA, Silver LL. 2019. Perspective on Antibacterial Lead Identification Challenges and the Role of Hypothesis-Driven Strategies. SLAS Discov 24:440–456.

13. O'Shea R, Moser HE. 2008. Physicochemical properties of antibacterial compounds: implications for drug discovery. J Med Chem 51:2871–2878.

14. Hughes D, Karlén A. 2014. Discovery and preclinical development of new antibiotics. Ups J Med Sci 119:162–169.

15. Theuretzbacher U, Outterson K, Engel A, Karlén A. 2020. The global preclinical antibacterial pipeline. Nat Rev Microbiol 18:275–285.

16. Bush K. 2018. Past and Present Perspectives on β-Lactamases. Antimicrob Agents Chemother 62.

17. Möllmann U, Heinisch L, Bauernfeind A, Köhler T, Ankel-Fuchs D. 2009. Siderophores as drug delivery agents: application of the "Trojan Horse" strategy. BioMetals https://doi.org/10.1007/s10534-009-9219-2.

18. Page MGP. 2013. Siderophore conjugates. Annals of the New York Academy of Sciences https://doi.org/10.1111/nyas.12024.

19. Page MGP, Dantier C, Desarbre E. 2010. In vitro properties of BAL30072, a novel siderophore sulfactam with activity against multiresistant gram-negative bacilli. Antimicrob Agents Chemother 54:2291–2302.

20. Higgins PG, Stefanik D, Page MGP, Hackel M, Seifert H. 2012. In vitro activity of the siderophore monosulfactam BAL30072 against meropenem-non-susceptible Acinetobacter baumannii. J Antimicrob Chemother 67:1167–1169.

21. Curtis NA, Eisenstadt RL, Turner KA, White AJ. 1985. Inhibition of penicillin-binding protein 3 of Escherichia coli K-12. Effects upon growth, viability and outer membrane barrier function. J Antimicrob Chemother 16:287–296.

22. Hanberger H, Nilsson LE, Kihlström E, Maller R. 1990. Postantibiotic effect of beta-lactam antibiotics on Escherichia coli evaluated by bioluminescence assay of bacterial ATP. Antimicrob Agents Chemother 34:102–106.

23. Gutmann L, Vincent S, Billot-Klein D, Acar JF, Mrèna E, Williamson R. 1986. Involvement of penicillin-binding protein 2 with other penicillin-binding proteins in lysis of Escherichia coli by some beta-lactam antibiotics alone and in synergistic lytic effect of amdinocillin (mecillinam). Antimicrob Agents Chemother 30:906–912.

24. Russo TA, Page MGP, Beanan JM, Olson R, Hujer AM, Hujer KM, Jacobs M, Bajaksouzian S, Endimiani A, Bonomo RA. 2011. In vivo and in vitro activity of the siderophore monosulfactam BAL30072 against Acinetobacter baumannii. J Antimicrob Chemother 66:867–873.

25. Hornsey M, Phee L, Stubbings W, Wareham DW. 2013. In vitro activity of the novel monosulfactam BAL30072 alone and in combination with meropenem versus a diverse collection of important Gram-negative pathogens. Int J Antimicrob Agents 42:343–346.

26. Hofer B, Dantier C, Gebhardt K, Desarbre E, Schmitt-Hoffmann A, Page MGP. 2013. Combined effects of the siderophore monosulfactam BAL30072 and carbapenems on multidrug-resistant Gram-negative bacilli. J Antimicrob Chemother 68:1120–1129.

27. Paech F, Messner S, Spickermann J, Wind M, Schmitt-Hoffmann A-H, Witschi AT, Howell BA, Church RJ, Woodhead J, Engelhardt M, Krähenbühl S, Maurer M. 2017. Mechanisms of hepatotoxicity associated with the monocyclic β-lactam antibiotic BAL30072. Arch Toxicol 91:3647–3662.

28. Straubinger M, Blenk H, Naber KG, Wagenlehner FME. 2016. Urinary Concentrations and Antibacterial Activity of BAL30072, a Novel Siderophore Monosulfactam, against Uropathogens after Intravenous Administration in Healthy Subjects. Antimicrob Agents Chemother 60:3309–3315.

29. Taylor NP. 2016. Basilea drops inhaled antibiotic, expands cancer program in early-stage rejig. Fierce Biotech. https://www.fiercebiotech.com/biotech/basilea-drops-inhaled-antibiotic-expands-cancer-program-early-stage-rejig. Retrieved 4 March 2022.

30. Echols R, Ariyasu M, Nagata TD. 2019. Pathogen-focused Clinical Development to Address Unmet Medical Need: Cefiderocol Targeting Carbapenem Resistance. Clin Infect Dis 69:S559–S564.

31. A Study to Evaluate Safety, Tolerability and Pharmacokinetics of Ascending Intravenous Single Dose and Repeat Dose of GSK3342830. https://clinicaltrials.gov/ct2/show/NCT02751424. Retrieved 4 February 2021.

32. Tenero D, Farinola N, Berkowitz EM, Tiffany CA, Qian Y, Xue Z, Raychaudhuri A, Gardiner DF. 2019. Pharmacokinetics, Safety, and Tolerability Evaluation of Single and Multiple Doses of GSK3342830 in Healthy Volunteers. Clin Pharmacol Drug Dev 8:754–764.

33. Oh S-H, Park H-S, Kim H-S, Yun J-Y, Oh K, Cho Y-L, Kwak J-H. 2017. Antimicrobial activities of LCB10-0200, a novel siderophore cephalosporin, against the clinical isolates of Pseudomonas aeruginosa and other pathogens. Int J Antimicrob Agents 50:700–706.

34. Nguyen LP, Pinto NA, Vu TN, Lee H, Cho YL, Byun J-H, D'Souza R, Yong D. 2020. In Vitro Activity of a Novel Siderophore-Cephalosporin, GT-1 and Serine-Type β-Lactamase Inhibitor, GT-055, against Escherichia coli, Klebsiella pneumoniae and Acinetobacter spp. Panel Strains. Antibiotics (Basel) 9.

35. Lee J, Cho Y-L, Shin S, Biek D. 2019. Penicillin binding protein (PBP) activity of beta-lactamase inhibitor GT-055.

36. Sader HS. 2018. Antimicrobial Activity of the Novel Siderophore Cephalosporin GT-1 Tested Alone and Combined with the β-Lactamase Inhibitor GT-055 against Molecularly Characterized Enterobacteriaceae Clinical Isolates.

37. ANZCTR - Registration. https://anzctr.org.au/Trial/Registration/TrialReview.aspx?ACTRN=12618001980224. Retrieved 3 February 2021.

38. Freischem S, Grimm I, López-Pérez A, Willbold D, Klenke B, Vuong C, Dingley AJ, Weiergräber OH. 2021. Interaction Mode of the Novel Monobactam AIC499 Targeting Penicillin Binding Protein 3 of Gram-Negative Bacteria. Biomolecules 11.

39. Higuchi S, Onodera Y, Chiba M, Hoshino K, Gotoh N. 2013. PotentIn VitroAntibacterial Activity of DS-8587, a Novel Broad-Spectrum Quinolone, against Acinetobacter baumannii. Antimicrobial Agents and Chemotherapy https://doi.org/10.1128/aac.02374-12.

40. Higuchi S, Kurosaka Y, Uoyama S, Yoshida K, Chiba M, Ishii C, Fujikawa K, Karibe Y, Hoshino K. 2014. Anti-multidrug-resistant Acinetobacter baumannii activity of DS-8587: In vitro activity and in vivo efficacy in a murine calf muscle infection model. J Infect Chemother 20:312–316.

41. Nagaoka K, Yanagihara K, Morinaga Y, Kurosaka Y, Hoshino K, Kohno S. 2017. In vivo antianaerobe activity of DS-8587, a new fluoroquinolone, against Fusobacterium necrophorum in a mouse model. J Infect Chemother 23:131–135.

42. Suzuki H, Hayashi N, Amago T, Takenaka H, Amano H, Itoh K, Kuramoto Y, Yazaki A. 2008. WQ-3810, a next generation respiratory fluoroquinolone with outstanding activity against QRSP.

43. Flamm, R. K., Biedenbach, D. J., Sader, H. S., Konrardy, M. L. & Jones, R. N. 2009. KPI-10 In Vitro Activity Tested Against Pathogens Commonly Associated with Community-Acquired Bacterial Pneumonia Infections.

44. Kazamori D, Suzuki H, Amago T, Itoh K, Yazaki A. 2009. In vitro activity of WQ-3813 against nosocomial pathogens.

45. Eckburg PB, Ge Y, Jiang V, Kilfoil T, Talbot GH. 2012. Safety & pharmacokinetics of KPI-10, a novel fluoroquinolone, in healthy adults receiving single-dose oral administrations.

46. Sun C, Xiao X-Y. 2017. Fully Synthetic Tetracyclines: Increasing Chemical Diversity to Combat Multidrug-Resistant Bacterial Infections. Topics in Medicinal Chemistry https://doi.org/10.1007/7355_2017_11.

47. Zhang W-Y, Sun C, Hunt D, He M, Deng Y, Zhu Z, Chen C-L, Katz CE, Niu J, Hogan PC, Xiao X-Y, Dunwoody N, Ronn M. 2016. Process Development and Scale-up of Fully Synthetic Tetracycline TP-2758: A Potent Antibacterial Agent with Excellent Oral Bioavailability. Organic Process Research & Development https://doi.org/10.1021/acs.oprd.5b00404.

48. Sun C, Deng Y, Hunt DK, Fyfe C, Chen C-L, Clark RB, Grossman TH, Sutcliffe JA, Xiao X-Y. 2018. Heterocyclyl tetracyclines. 2. 7-Methoxy-8-pyrrolidinyltetracyclines: discovery of TP-2758, a potent, orally efficacious antimicrobial against Gram-negative pathogens. The Journal of Antibiotics https://doi.org/10.1038/ja.2017.86.

49. A Phase 1, Randomized, Placebo-Controlled, Single-Blind, Multiple-Dose, Dose-Escalation Clinical Study to Assess the Safety and Pharmacokinetics of TP-2758 in Normal Healthy Volunteers. EudraCT.

50. Trimble MJ, Mlynárčik P, Kolář M, Hancock REW. 2016. Polymyxin: Alternative Mechanisms of Action and Resistance. Cold Spring Harb Perspect Med 6.

51. Koch-Weser J, Sidel VW, Federman EB, Kanarek P, Finer DC, Eaton AE. 1970. Adverse effects of sodium colistimethate. Manifestations and specific reaction rates during 317 courses of therapy. Ann Intern Med 72:857–868.

52. Evans ME, Feola DJ, Rapp RP. 1999. Polymyxin B sulfate and colistin: old antibiotics for emerging multiresistant gram-negative bacteria. Ann Pharmacother 33:960–967.

53. A. LR. January 2010. Antibiotic compositions for the treatment of gram negative infections. /2010/075416. World Patent.

54. Curran WV, Liu CM, Bombardier ACD, Leese RA, Hwang YS, Lippa BS, Zhang Y. April 2013. Antibiotic compositions for the treatment of gram negative infections. 8415307B1. US Patent.

55. Quale J, Shah N, Kelly P, Babu E, Backer M, Rosas-Garcia G, Salamera J, George A, Bratu S, Landman D. 2012. Activity of polymyxin B and the novel polymyxin analogue CB-182,804 against contemporary Gram-negative pathogens in New York City. Microb Drug Resist 18:132–136.

56. Arya A, Li T, Zhang S, et al. 2010. Efficacy of CB-182,804, a Novel Polymyxin Analog, in Rat and Mouse Models of Gram-Negative Bacterial Infections.

57. Coleman S, Deats T, Pawliuk R, et al. 2010. CB-182,804 is Less Nephrotoxic as Compared to Polymyxin B in Monkeys Following Seven Days of Repeated Intravenous Dosing.

58. Blaskovich MAT, Pitt ME, Elliott AG, Cooper MA. 2018. Can octapeptin antibiotics combat extensively drug-resistant (XDR) bacteria? Expert Rev Anti Infect Ther 16:485–499.

59. Vaara M, Siikanen O, Apajalahti J, Fox J, Frimodt-Møller N, He H, Poudyal A, Li J, Nation RL, Vaara T. 2010. A novel polymyxin derivative that lacks the fatty acid tail and carries only three positive charges has strong synergism with agents excluded by the intact outer membrane. Antimicrob Agents Chemother 54:3341–3346.

60. Corbett D, Wise A, Langley T, Skinner K, Trimby E, Birchall S, Dorali A, Sandiford S, Williams J, Warn P, Vaara M, Lister T. 2017. Potentiation of Antibiotic Activity by a Novel Cationic Peptide: Potency and Spectrum of Activity of SPR741. Antimicrob Agents Chemother 61.

61. Stainton SM, Abdelraouf K, Utley L, Pucci MJ, Lister T, Nicolau DP. 2018. Assessment of the In Vivo Activity of SPR741 in Combination with Azithromycin against Multidrug-Resistant Enterobacteriaceae Isolates in the Neutropenic Murine Thigh Infection Model. Antimicrob Agents Chemother 62.

62. Zurawski DV, Reinhart AA, Alamneh YA, Pucci MJ, Si Y, Abu-Taleb R, Shearer JP, Demons ST, Tyner SD, Lister T. 2017. SPR741, an Antibiotic Adjuvant, Potentiates the In Vitro and In Vivo Activity of Rifampin against Clinically Relevant Extensively Drug-Resistant Acinetobacter baumannii. Antimicrob Agents Chemother 61.

63. Eckburg PB, Lister T, Walpole S, Keutzer T, Utley L, Tomayko J, Kopp E, Farinola N, Coleman S. 2019. Safety, Tolerability, Pharmacokinetics, and Drug Interaction Potential of SPR741, an Intravenous Potentiator, after Single and Multiple Ascending Doses and When Combined with β-Lactam Antibiotics in Healthy Subjects. Antimicrob Agents Chemother 63.

64. Robinson JA, Shankaramma SC, Jetter P, Kienzl U, Schwendener RA, Vrijbloed JW, Obrecht D. 2005. Properties and structure–activity studies of cyclic β-hairpin peptidomimetics based on the cationic antimicrobial peptide protegrin I. Bioorganic & Medicinal Chemistry https://doi.org/10.1016/j.bmc.2005.01.009.

65. Zerbe K, Moehle K, Robinson JA. 2017. Protein Epitope Mimetics: From New Antibiotics to Supramolecular Synthetic Vaccines. Acc Chem Res 50:1323–1331.

66. Schmidt J, Patora-Komisarska K, Moehle K, Obrecht D, Robinson JA. 2013. Structural studies of β-hairpin peptidomimetic antibiotics that target LptD in Pseudomonas sp. Bioorg Med Chem 21:5806–5810.

67. Shankaramma SC, Athanassiou Z, Zerbe O, Moehle K, Mouton C, Bernardini F, Vrijbloed JW, Obrecht D, Robinson JA. 2002. Macrocyclic hairpin mimetics of the cationic antimicrobial peptide protegrin I: a new family of broad-spectrum antibiotics. Chembiochem 3:1126–1133.

68. Srinivas N, Jetter P, Ueberbacher BJ, Werneburg M, Zerbe K, Steinmann J, Van der Meijden B, Bernardini F, Lederer A, Dias RLA, Misson PE, Henze H, Zumbrunn J, Gombert FO, Obrecht D, Hunziker P, Schauer S, Ziegler U, Käch A, Eberl L, Riedel K, DeMarco SJ, Robinson JA. 2010. Peptidomimetic antibiotics target outer-membrane biogenesis in Pseudomonas aeruginosa. Science 327:1010–1013.

69. Andolina G, Bencze L-C, Zerbe K, Müller M, Steinmann J, Kocherla H, Mondal M, Sobek J, Moehle K, Malojčić G, Wollscheid B, Robinson JA. 2018. A Peptidomimetic Antibiotic Interacts with the Periplasmic Domain of LptD from Pseudomonas aeruginosa. ACS Chem Biol 13:666–675.

70. Werneburg M, Zerbe K, Juhas M, Bigler L, Stalder U, Kaech A, Ziegler U, Obrecht D, Eberl L, Robinson JA. 2012. Inhibition of lipopolysaccharide transport to the outer membrane in Pseudomonas aeruginosa by peptidomimetic antibiotics. Chembiochem 13:1767–1775.

71. Braun M, Silhavy TJ. 2002. Imp/OstA is required for cell envelope biogenesis in Escherichia coli. Molecular Microbiology https://doi.org/10.1046/j.1365-2958.2002.03091.x.

72. Qiao S, Luo Q, Zhao Y, Zhang XC, Huang Y. 2014. Structural basis for lipopolysaccharide insertion in the bacterial outer membrane. Nature 511:108–111.

73. Dong H, Xiang Q, Gu Y, Wang Z, Paterson NG, Stansfeld PJ, He C, Zhang Y, Wang W, Dong C. 2014. Structural basis for outer membrane lipopolysaccharide insertion. Nature 511:52–56.

74. Wu T, McCandlish AC, Gronenberg LS, Chng S-S, Silhavy TJ, Kahne D. 2006. Identification of a protein complex that assembles lipopolysaccharide in the outer membrane of Escherichia coli. Proc Natl Acad Sci U S A 103:11754–11759.

75. Sader HS, Dale GE, Rhomberg PR, Flamm RK. 2018. Antimicrobial Activity of Murepavadin Tested against Clinical Isolates of Pseudomonas aeruginosa from the United States, Europe, and China. Antimicrob Agents Chemother 62.

76. Sader HS, Flamm RK, Dale GE, Rhomberg PR, Castanheira M. 2018. Murepavadin activity tested against contemporary (2016–17) clinical isolates of XDR Pseudomonas aeruginosa. Journal of Antimicrobial Chemotherapy https://doi.org/10.1093/jac/dky227.

77. Martin-Loeches I, Dale GE, Torres A. 2018. Murepavadin: a new antibiotic class in the pipeline. Expert Review of Anti-infective Therapy https://doi.org/10.1080/14787210.2018.1441024.

78. Wach A, Dembowsky K, Dale GE. 2018. Pharmacokinetics and Safety of Intravenous Murepavadin Infusion in Healthy Adult Subjects Administered Single and Multiple Ascending Doses. Antimicrob Agents Chemother 62.

79. A Single Center Study to Evaluate the Penetration of RO7033877 Into the Lung in Healthy Volunteers.

80. A Phase 1 Clinical Study in Healthy Volunteers to Investigate the drug-drug Interaction Between Multiple Doses of RO7033877 and Multiple Doses of Colistin Methanesulfonate Sodium (CMS). https://clinicaltrials.gov/ct2/show/NCT02156323. Retrieved 3 February 2021.

81. DDI Study to Investigate Interaction Between Amikacin and POL7080. https://clinicaltrials.gov/ct2/show/NCT02897869. Retrieved 3 February 2021.

82. A Two-part, Single-dose, Randomized Study to Evaluate the Safety of Supra-therapeutic Doses of RO7033877 and to Investigate the Effect of RO7033877 on the QTc Interval. https://clinicaltrials.gov/ct2/show/NCT02165332. Retrieved 3 February 2021.

83. Pharmacokinetics and Safety of POL7080 in Patients With Renal Impairment. https://clinicaltrials.gov/ct2/show/NCT02110459. Retrieved 4 February 2021.

84. Dale GE, Halabi A, Petersen-Sylla M, Wach A, Zwingelstein C. 2018. Pharmacokinetics, Tolerability, and Safety of Murepavadin, a Novel Antipseudomonal Antibiotic, in Subjects with Mild, Moderate, or Severe Renal Function Impairment. Antimicrobial Agents and Chemotherapy https://doi.org/10.1128/aac.00490-18.

85. Safety, Efficacy and PK/PD of POL7080 in Patients With Exacerbation of Non-cystic Fibrosis Bronchiectasis. https://clinicaltrials.gov/ct2/show/NCT02096315. Retrieved 4 February 2021.

86. Pharmacokinetics, Safety and Efficacy of POL7080 in Patients With Ventilator Associated Pseudomonas Aeruginosa Pneumonia. https://clinicaltrials.gov/ct2/show/NCT02096328. Retrieved 4 February 2021.

87. Armagantis A, Zakynthinos S, Mandragos C, et al. Efficacy of murepavadin coadministered with standard of care in a phase 2 study in patients with ventilator-associated pneumonia due to suspected or documented Pseudomonas aeruginosa infection.

88. Bader JC, Lakota EA, Dale GE, Sader HS, Rex JH, Ambrose PG, Bhavnani SM. 2019. Pharmacokinetic-Pharmacodynamic Evaluation of Ertapenem for Patients with

Hospital-Acquired or Ventilator-Associated Bacterial Pneumonia. Antimicrobial Agents and Chemotherapy https://doi.org/10.1128/aac.00318-19.

89. Pivotal Study in Nosocomial Pneumonia Suspected or Confirmed to be Due to Pseudomonas - Full Text View - ClinicalTrials.Gov. https://clinicaltrials.gov/ct2/show/NCT03582007. Retrieved 4 February 2021.

90. Pivotal Study in VAP Suspected or Confirmed to be Due to Pseudomonas Aeruginosa - Full Text View - ClinicalTrials.Gov. https://clinicaltrials.gov/ct2/show/NCT03409679. Retrieved 4 February 2021.

91. 2019. Polyphor temporarily halts enrollment in the Phase III studies of murepavadin for the treatment of patients with nosocomial pneumonia. Polyphor. https://www.polyphor.com/news/corporate-news-details/?newsid=1775911.

92. Erwin AL. 2016. Antibacterial Drug Discovery Targeting the Lipopolysaccharide Biosynthetic Enzyme LpxC. Cold Spring Harb Perspect Med 6.

93. Kalinin DV, Holl R. 2017. LpxC inhibitors: a patent review (2010-2016). Expert Opin Ther Pat 27:1227–1250.

94. Zhang J, Zhang L, Li X, Xu W. 2012. UDP-3-O-(R-3-hydroxymyristoyl)-N-acetylglucosamine deacetylase (LpxC) inhibitors: a new class of antibacterial agents. Curr Med Chem 19:2038–2050.

95. Mdluli KE, Witte PR, Kline T, Barb AW, Erwin AL, Mansfield BE, McClerren AL, Pirrung MC, Tumey LN, Warrener P, Raetz CRH, Stover CK. 2006. Molecular validation of LpxC as an antibacterial drug target in Pseudomonas aeruginosa. Antimicrob Agents Chemother 50:2178–2184.

96. Krause KM, Haglund CM, Hebner C, Serio AW, Lee G, Nieto V, Cohen F, Kane TR, Machajewski TD, Hildebrandt D, Pillar C, Thwaites M, Hall D, Miesel L, Hackel M, Burek A, Andrews LD, Armstrong E, Swem L, Jubb A, Cirz RT. 2019. Potent LpxC Inhibitors with Activity against Multidrug-Resistant Pseudomonas aeruginosa. Antimicrob Agents Chemother 63.

97. Bornheim L, McKinnell J, Fuchs-Knotts T, Boggs J, Kostrub CF. 2013. Preclinical safety evaluation of the novel LpxC inhibitor ACHN-975 in rat and monkey.

98. A Study to Assess the Safety, Tolerability, and Pharmacokinetics of ACHN-975 in Healthy Volunteers. https://clinicaltrials.gov/ct2/show/NCT01597947. Retrieved 4 February 2021.

99. Cohen F, Aggen JB, Andrews LD, Assar Z, Boggs J, Choi T, Dozzo P, Easterday AN, Haglund CM, Hildebrandt DJ, Holt MC, Joly K, Jubb A, Kamal Z, Kane TR, Konradi AW, Krause KM, Linsell MS, Machajewski TD, Miroshnikova O, Moser HE, Nieto V, Phan T, Plato C, Serio AW, Seroogy J, Shakhmin A, Stein AJ, Sun AD, Sviridov S, Wang Z,

Wlasichuk K, Yang W, Zhou X, Zhu H, Cirz RT. 2019. Optimization of LpxC Inhibitors for Antibacterial Activity and Cardiovascular Safety. ChemMedChem 14:1560–1572.

100. A Multiple Dose Study to Assess the Safety, Tolerability, and Pharmacokinetics of ACHN-975 in Healthy Volunteers. https://clinicaltrials.gov/ct2/show/NCT01870245. Retrieved 4 February 2021.

101. M. Shoji, Y. Suzumura, M. Fujiwara, C. Kurosaki, Y. Nozaki, S. Mizunaga. 2019. T-1228 (RC-01), a New LpxC Inhibitor Exhibiting Potent Activity against Multi-Drug Resistant Gram-Negative Pathogens: Design, Synthesis and Structure-Activity Relationship.

102. M. Fujiwara, S. Nakagawa, S. Mizunaga, M. Eto. 2019. Inhibition of LpxC Activity and Elimination of Lipopolysaccharide (LPS) Release by T-1228 (RC-01).

103. Lin L, Tan B, Pantapalangkoor P, Ho T, Baquir B, Tomaras A, Montgomery JI, Reilly U, Barbacci EG, Hujer K, Bonomo RA, Fernandez L, Hancock REW, Adams MD, French SW, Buslon VS, Spellberg B. 2012. Inhibition of LpxC protects mice from resistant Acinetobacter baumannii by modulating inflammation and enhancing phagocytosis. MBio 3.

104. S. Nakagawa, M. Fujiwara, M. Eto, S. Mizunaga. 2019. PK/PD Analysis of T-1228 (RC-01), a Novel LpxC Inhibitor, Using Murine Pneumonia and Urinary Tract Infection Models.

105. S. Mizunaga, M. Fujiwara, S. Nakagawa, M. Eto. 2019. In Vitro Resistance Development of T-1228 (RC-01), a Novel LpxC Inhibitor, Compared with Other Agents.

106. Y. Ge, Y. Nozaki, S. Mochizuki. 2019. Evaluation of the General Preclinical Toxicological Profile of RC-01, a Novel LpxC Inhibitor.

107. Single and Multiple Dose Escalation Trial of an Intravenous Antibiotic RC-01. https://clinicaltrials.gov/ct2/show/NCT03832517. Retrieved 4 February 2021.

108. Baker SJ, Hernandez VS, Sharma R, Nieman JA, Akama T, Zhang Y-K, Plattner JJ, Alley MRK, Singh R, Rock F. October 2010. Boron-containing small molecules. 7816344B2. US Patent.

109. Hudson IR. 1994. The efficacy of intranasal mupirocin in the prevention of staphylococcal infections: a review of recent experience. J Hosp Infect 27:81–98.

110. Sutherland R, Boon RJ, Griffin KE, Masters PJ, Slocombe B, White AR. 1985. Antibacterial activity of mupirocin (pseudomonic acid), a new antibiotic for topical use. Antimicrob Agents Chemother 27:495–498.

111. Ochsner UA, Sun X, Jarvis T, Critchley I, Janjic N. 2007. Aminoacyl-tRNA synthetases: essential and still promising targets for new anti-infective agents. Expert Opin Investig Drugs 16:573–593.

112. Walker ES, Vasquez JE, Dula R, Bullock H, Sarubbi FA. 2003. Mupirocin-Resistant, Methicillin-Resistant Staphylococcus aureus: Does Mupirocin Remain Effective? Infection Control & Hospital Epidemiology https://doi.org/10.1086/502218.

113. Rock FL, Mao W, Yaremchuk A, Tukalo M, Crépin T, Zhou H, Zhang Y-K, Hernandez V, Akama T, Baker SJ, Plattner JJ, Shapiro L, Martinis SA, Benkovic SJ, Cusack S, Alley MRK. 2007. An antifungal agent inhibits an aminoacyl-tRNA synthetase by trapping tRNA in the editing site. Science 316:1759–1761.

114. Hernandez V, Crépin T, Palencia A, Cusack S, Akama T, Baker SJ, Bu W, Feng L, Freund YR, Liu L, Meewan M, Mohan M, Mao W, Rock FL, Sexton H, Sheoran A, Zhang Y, Zhang Y-K, Zhou Y, Nieman JA, Anugula MR, Keramane EM, Savariraj K, Reddy DS, Sharma R, Subedi R, Singh R, O'Leary A, Simon NL, De Marsh PL, Mushtaq S, Warner M, Livermore DM, Alley MRK, Plattner JJ. 2013. Discovery of a novel class of boron-based antibacterials with activity against gram-negative bacteria. Antimicrob Agents Chemother 57:1394–1403.

115. Mendes RE, Alley MRK, Sader HS, Biedenbach DJ, Jones RN. 2013. Potency and spectrum of activity of AN3365, a novel boron-containing protein synthesis inhibitor, tested against clinical isolates of Enterobacteriaceae and nonfermentative Gram-negative bacilli. Antimicrob Agents Chemother 57:2849–2857.

116. Goldstein EJC, Citron DM, Tyrrell KL, Merriam CV. 2013. Comparative in vitro activities of GSK2251052, a novel boron-containing leucyl-tRNA synthetase inhibitor, against 916 anaerobic organisms. Antimicrob Agents Chemother 57:2401–2404.

117. SK Bouchillon, M Hackel, DJ Hoban, SP Hawser, NE Scangarella-Oman. 2011. GSK2251052, a Novel Boron-containing Protein Synthesis Inhibitor, with Comparative in vitro Activity against Pseudomonas aeruginosa from a Global Population.

118. Safety, Pharmacokinetics (PK) and Tolerability Study of a Novel Drug for Treatment of Bacterial Infections. https://clinicaltrials.gov/ct2/show/NCT01015014. Retrieved 15 February 2021.

119. A Randomized, Single Blind, Placebo Controlled Study to Evaluate Safety, Tolerability, and Pharmacokinetics of Single Oral Doses and Repeat Escalating Oral Doses of GSK2251052 in Healthy Adult Subjects. https://clinicaltrials.gov/ct2/show/NCT01262885. Retrieved 4 February 2021.

120. GSK2251052 Mass Balance in Healthy Adult Subjects. https://clinicaltrials.gov/ct2/show/NCT01475695. Retrieved 4 February 2021.

121. An Open-label, Randomized, Single Period, Parallel-Cohort Study To Evaluate Serum and Pulmonary Pharmacokinetics Following Single and Multiple Dose

Administration of Intravenous GSK2251052 in Healthy Adult Subjects. https://clinicaltrials.gov/ct2/show/NCT01267968. Retrieved 4 February 2021.

122. Bowers GD, Tenero D, Patel P, Huynh P, Sigafoos J, O'Mara K, Young GC, Dumont E, Cunningham E, Kurtinecz M, Stump P, Conde JJ, Chism JP, Reese MJ, Yueh YL, Tomayko JF. 2013. Disposition and metabolism of GSK2251052 in humans: a novel boron-containing antibiotic. Drug Metab Dispos 41:1070–1081.

123. GSK2251052 in Complicated Urinary Tract Infection. https://clinicaltrials.gov/ct2/show/NCT01381549. Retrieved 4 February 2021.

124. GSK2251052 in the Treatment of Complicated Intra-abdominal Infections. https://clinicaltrials.gov/ct2/show/NCT01381562. Retrieved 4 February 2021.

125. O'Dwyer K, Spivak AT, Ingraham K, Min S, Holmes DJ, Jakielaszek C, Rittenhouse S, Kwan AL, Livi GP, Sathe G, Thomas E, Van Horn S, Miller LA, Twynholm M, Tomayko J, Dalessandro M, Caltabiano M, Scangarella-Oman NE, Brown JR. 2015. Bacterial resistance to leucyl-tRNA synthetase inhibitor GSK2251052 develops during treatment of complicated urinary tract infections. Antimicrob Agents Chemother 59:289–298.

126. Tenero D, Bowers G, Rodvold KA, Patel A, Kurtinecz M, Dumont E, Tomayko J, Patel P. 2013. Intrapulmonary pharmacokinetics of GSK2251052 in healthy volunteers. Antimicrob Agents Chemother 57:3334–3339.

127. Farrell LJ, Lo R, Wanford JJ, Jenkins A, Maxwell A, Piddock LJV. 2018. Revitalizing the drug pipeline: AntibioticDB, an open access database to aid antibacterial research and development. J Antimicrob Chemother 73:2284–2297.

128. Hay M, Thomas DW, Craighead JL, Economides C, Rosenthal J. 2014. Clinical development success rates for investigational drugs. Nature Biotechnology https://doi.org/10.1038/nbt.2786.

129. Gajdács M. 2019. The Concept of an Ideal Antibiotic: Implications for Drug Design. Molecules 24.

130. Singh SB, Young K, Silver LL. 2017. What is an "ideal" antibiotic? Discovery challenges and path forward. Biochem Pharmacol 133:63–73.

131. Dalvie D, Cosker T, Boyden T, Zhou S, Schroeder C, Potchoiba MJ. 2008. Metabolism distribution and excretion of a matrix metalloproteinase-13 inhibitor, 4-[4-(4-fluorophenoxy)-benzenesulfonylamino]tetrahydropyran-4-carboxylic acid hydroxyamide (CP-544439), in rats and dogs: assessment of the metabolic profile of CP-544439 in plasma and urine of humans. Drug Metab Dispos 36:1869–1883.

132. Sixto-López Y, Gómez-Vidal JA, de Pedro N, Bello M, Rosales-Hernández MC, Correa-Basurto J. 2020. Hydroxamic acid derivatives as HDAC1, HDAC6 and HDAC8 inhibitors with antiproliferative activity in cancer cell lines. Sci Rep 10:10462.

133. Lee MS, Isobe M. 1990. Metabolic activation of the potent mutagen, 2-naphthohydroxamic acid, in Salmonella typhimurium TA98. Cancer Res 50:4300–4307.

134. Galster M, Löppenberg M, Galla F, Börgel F, Agoglitta O, Kirchmair J, Holl R. 2019. Phenylethylene glycol-derived LpxC inhibitors with diverse Zn2+-binding groups. Tetrahedron 75:486–509.

135. Furuya T, Shapiro AB, Comita-Prevoir J, Kuenstner EJ, Zhang J, Ribe SD, Chen A, Hines D, Moussa SH, Carter NM, Sylvester MA, Romero JAC, Vega CV, Sacco MD, Chen Y, O'Donnell JP, Durand-Reville TF, Miller AA, Tommasi RA. 2020. N-Hydroxyformamide LpxC inhibitors, their in vivo efficacy in a mouse Escherichia coli infection model, and their safety in a rat hemodynamic assay. Bioorg Med Chem 28:115826.

136. Huang JX, Blaskovich MA, Cooper MA. 2014. Cell- and biomarker-based assays for predicting nephrotoxicity. Expert Opin Drug Metab Toxicol 10:1621–1635.

137. Gallardo-Godoy A, Muldoon C, Becker B, Elliott AG, Lash LH, Huang JX, Butler MS, Pelingon R, Kavanagh AM, Ramu S, Phetsang W, Blaskovich MAT, Cooper MA. 2016. Activity and Predicted Nephrotoxicity of Synthetic Antibiotics Based on Polymyxin B. Journal of Medicinal Chemistry https://doi.org/10.1021/acs.jmedchem.5b01593.

138. Roberts KD, Azad MAK, Wang J, Horne AS, Thompson PE, Nation RL, Velkov T, Li J. 2015. Antimicrobial Activity and Toxicity of the Major Lipopeptide Components of Polymyxin B and Colistin: Last-Line Antibiotics against Multidrug-Resistant Gram-Negative Bacteria. ACS Infectious Diseases https://doi.org/10.1021/acsinfecdis.5b00085.

139. Velkov T, Roberts KD, Thompson PE, Li J. 2016. Polymyxins: a new hope in combating Gram-negative superbugs? Future Med Chem 8:1017–1025.

140. Wenzler E, Fraidenburg DR, Scardina T, Danziger LH. 2016. Inhaled Antibiotics for Gram-Negative Respiratory Infections. Clin Microbiol Rev 29:581–632.

141. Papp-Wallace KM. 2019. The latest advances in β-lactam/β-lactamase inhibitor combinations for the treatment of Gram-negative bacterial infections. Expert Opin Pharmacother 20:2169–2184.

142. Verbist L. 1986. In-vitro activity of the combinations of ampicillin with mecillinam or with β-lactamase inhibitors against strains resistant to ampicillin. J Antimicrob Chemother 16:719–725.

143. Morinaka A, Tsutsumi Y, Yamada M, Suzuki K, Watanabe T, Abe T, Furuuchi T, Inamura S, Sakamaki Y, Mitsuhashi N, Ida T, Livermore DM. 2015. OP0595, a new diazabicyclooctane: mode of action as a serine β-lactamase inhibitor, antibiotic and β-lactam "enhancer." J Antimicrob Chemother 70:2779–2786.

144. Zusman O, Avni T, Leibovici L, Adler A, Friberg L, Stergiopoulou T, Carmeli Y, Paul M. 2013. Systematic review and meta-analysis of in vitro synergy of polymyxins and carbapenems. Antimicrob Agents Chemother 57:5104–5111.

145. Lenhard JR, Nation RL, Tsuji BT. 2016. Synergistic combinations of polymyxins. Int J Antimicrob Agents 48:607–613.

146. Rabanal F, Cajal Y. 2017. Recent advances and perspectives in the design and development of polymyxins. Nat Prod Rep 34:886–908.

147. Boucher HW, Ambrose PG, Chambers HF, Ebright RH, Jezek A, Murray BE, Newland JG, Ostrowsky B, Rex JH, Infectious Diseases Society of America. 2017. White Paper: Developing Antimicrobial Drugs for Resistant Pathogens, Narrow-Spectrum Indications, and Unmet Needs. J Infect Dis 216:228–236.

148. Rex JH, Talbot GH, Goldberger MJ, Eisenstein BI, Echols RM, Tomayko JF, Dudley MN, Dane A. 2017. Progress in the Fight Against Multidrug-Resistant Bacteria 2005-2016: Modern Noninferiority Trial Designs Enable Antibiotic Development in Advance of Epidemic Bacterial Resistance. Clin Infect Dis 65:141–146.

149. Bassetti M, Echols R, Matsunaga Y, Ariyasu M, Doi Y, Ferrer R, Lodise TP, Naas T, Niki Y, Paterson DL, Portsmouth S, Torre-Cisneros J, Toyoizumi K, Wunderink RG, Nagata TD. 2020. Efficacy and safety of cefiderocol or best available therapy for the treatment of serious infections caused by carbapenem-resistant Gram-negative

bacteria (CREDIBLE-CR): a randomised, open-label, multicentre, pathogen-focused, descriptive, phase 3 trial. Lancet Infect Dis https://doi.org/10.1016/S1473-3099(20)30796-9.

150. Kim W, Krause K, Zimmerman Z, Outterson K. 2021. Improving data sharing to increase the efficiency of antibiotic R&D. Nat Rev Drug Discov 20:1–2.

Chapter 2

Tool Development: Modulating pathogenicity via partial genetic inhibition

Abstract

Conditionally essential (CE) genes are required by pathogenic bacteria to establish and maintain infections. CE genes encode virulence factors, such as secretion systems and effector proteins, as well as biosynthetic enzymes that produce metabolites not found in the host environment. Due to their outsized importance in pathogenesis, CE gene products are attractive targets for the next generation of antimicrobials. However, the precise manipulation of CE gene expression in the context of infection is technically challenging, limiting our ability to understand the roles of CE genes in pathogenesis and accordingly design effective inhibitors. We previously developed a suite of CRISPR interference-based gene knockdown tools that are transferred by conjugation and stably integrate into bacterial genomes that we call Mobile-CRISPRi. Here, we show the efficacy of Mobile-CRISPRi in controlling CE gene expression in an animal infection model. We optimize Mobile-CRISPRi in *Pseudomonas aeruginosa* for use in a murine model of pneumonia by tuning the expression of CRISPRi components to avoid nonspecific toxicity. As a proof of principle, we demonstrate that knock down of a CE gene encoding the type III secretion system (T3SS) activator ExsA blocks effector protein secretion in

culture and attenuates virulence in mice. We anticipate that Mobile-CRISPRi will be a valuable tool to probe the function of CE genes across many bacterial species and pathogenesis models.

Introduction

All pathogenic bacteria require essential and conditionally essential (CE) genes for survival in the host environment. (1) Essential genes are typically defined as genes that are indispensable for growth in rich culture media, whereas CE genes are required only in specific conditions, such as maintenance in a host niche. (2) Next-generation sequencing of bacterial transposon (Tn)-mutant libraries (e.g., transposon sequencing [Tn-Seq] [3] and insertion sequencing [INSeq] [4]) from infected animals has enabled the comprehensive identification of essential and CE genes in a single experiment, rapidly increasing our knowledge of which genes are required for pathogenesis. (5–16) There are two major limitations of using Tn-Seq to study CE genes, both arising from the complete loss of function usually caused by Tn mutagenesis. First, core essential genes are, by definition, excluded from the analysis of environment-specific essentiality. Second, all-or-nothing mutations preclude our ability to observe the relationship between expression levels of the gene product and fitness in the host environment; this information could be valuable in identifying CE genes for which the organism is highly sensitive to slight perturbations, which would be ideal candidates for inhibitors. Thus, methods that can partially perturb CE gene function in the context of pathogenesis are highly valuable.

Gene repression tools that are currently used to study CE genes during infection have provided numerous insights into gene function but have key technical limitations. Antisense RNAs (17, 18) have variable efficacy, substantial off-target effects, (19–21) and cannot be rationally designed. (22) Methods to trigger protein degradation (i.e., degrons) (23–26) require each gene of interest to be tagged at its native locus and suffer from toxicity due to interference with protein function and stability. (26) Gene depletion from inducible promoters also requires the insertion of the promoter upstream of all genes of interest and is limited by the inability to optimize both the control of noninduced promoter expression (leakiness) and the maximal amount of induced gene product. (27)

In contrast, CRISPR interference (CRISPRi)—the use of a catalytically inactive variant of the Cas9 nuclease (dCas9) to repress transcription (28)—is highly efficacious and specific in bacteria, (29) is easily programmable by substituting the first 20 nucleotides of the guide RNA (sgRNA), (30) does not require modification of the chromosome at each targeted gene and maintains the native regulation of targeted genes. We previously developed Mobile-CRISPRi, (31) a technology that enables the transfer and stable integration of CRISPRi systems into diverse bacteria (**Fig. 1A**). Here, we optimize Mobile-CRISPRi for targeting CE genes in a *Pseudomonas aeruginosa* PA14 murine pneumonia model of infection.

Results

Optimized dCas9 expression eliminates toxicity and allows for graded knockdowns

dCas9 overexpression often causes nonspecific toxicity in bacteria, (32) which would likely complicate the interpretation of our CRISPRi experiments in infection models. Indeed, we found that the full induction of an arabinose-inducible promoter (P_{BAD}) driving the expression of dCas9 variants from *Streptococcus pyogenes* ($dCas9_{Spy}$) (28) or *Streptococcus thermophilus* ($dCas9_{sth}$) (33) resulted in reduced growth of PA14 in rich culture medium, whereas partial induction showed no apparent toxicity (**Fig. 2.1B**). We reasoned that titrating chemical inducers (e.g., arabinose) in a murine infection model could be impractical due to variable tissue penetration. (34–38) Instead, we focused on expressing $dCas9_{Spy}$ from a series of weak constitutive promoters from the BioBrick Registry (http://parts.igem.org/Main_Page) to reduce toxicity (**Supplementary Fig. 2.1**) and achieve partial knock down.

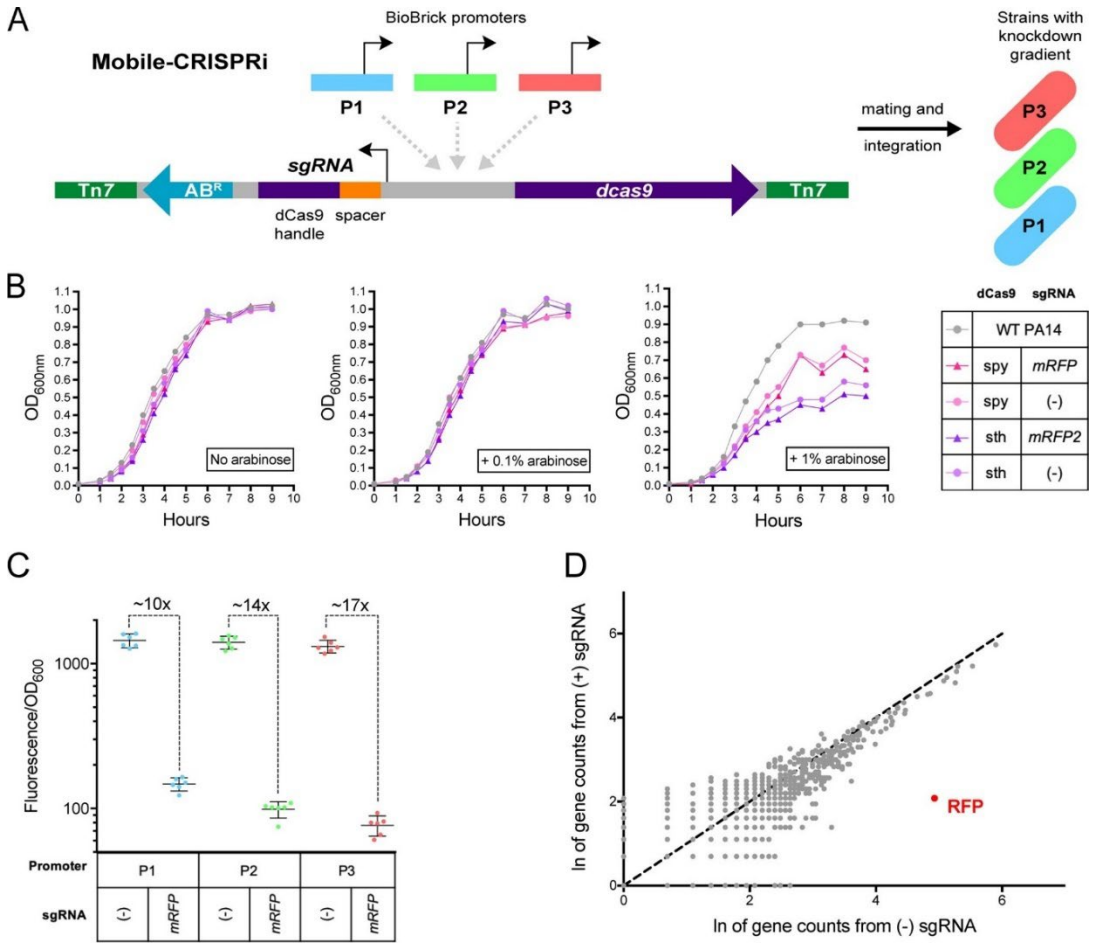

Figure 2.1: Toxicity, efficacy, and specificity of Mobile-CRISPRi in Pseudomonas aeruginosa

(A) Mobile-CRISPRi is comprised of an antibiotic resistance cassette (AB^R), sgRNA spacers specific to the gene of interest, a promoter driving *dcas9* expression, and *dcas9*. These components can be substituted before chromosomal integration into a pathogen to generate a knockdown strain. (B) Wild-type PA14 growth was compared to that of Mobile-CRISPRi PA14 strains featuring arabinose-inducible promoters driving dCas9 activity, two different variants of dCas9 (*S. pyogenes* and *S. thermophilus*), and the presence or absence of *mRFP*-targeting sgRNA. To induce the promoter, these strains were incubated with no arabinose, 0.1% arabinose, or 1% arabinose. (C) *mRFP* was cloned into Mobile-CRISPRi strains with constitutive promoters driving dCas9 expression. The median fluorescence of strains without sgRNA was compared to that of strains with *mRFP*-targeting sgRNA after 14 h of growth. The 10× knockdown associated with P1 is statistically different from the 14× (**, significant *P* value) and 17× knockdown (****, significant *P* value) associated with P2 and P3, respectively. (D) RNA was extracted from mutants featuring P3 with and without *mRFP*-targeting sgRNA. Gene counts from RNA-seq are plotted for each strain with a dashed line of slope = 1 for reference.

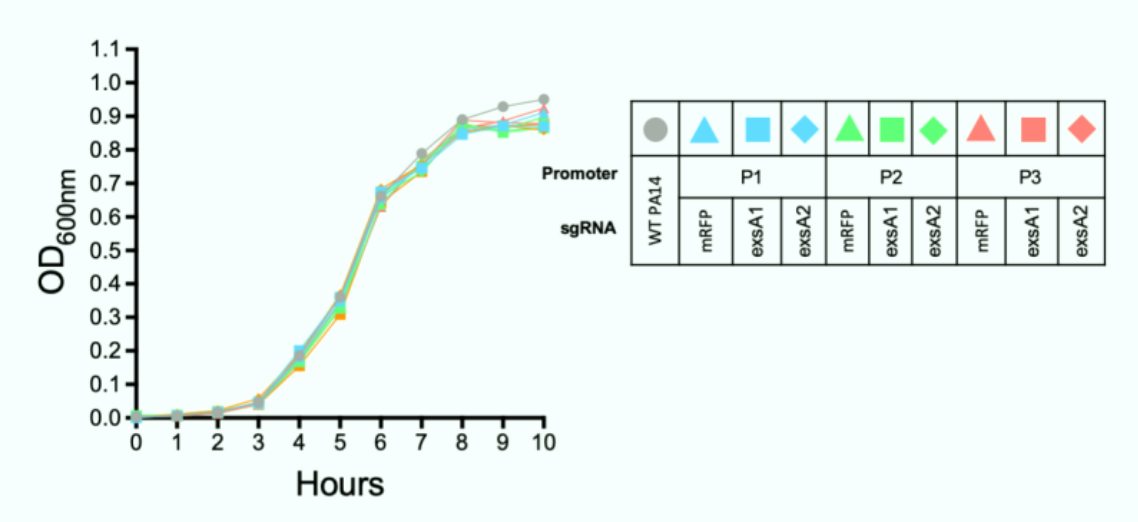

Supplementary Figure 2.1: Growth curves of PA14 strains targeting *exsA*
Indicated strains were incubated for 9–10 hours on a plate shaker, and OD_{600} measurements were taken every hour using a microplate reader.

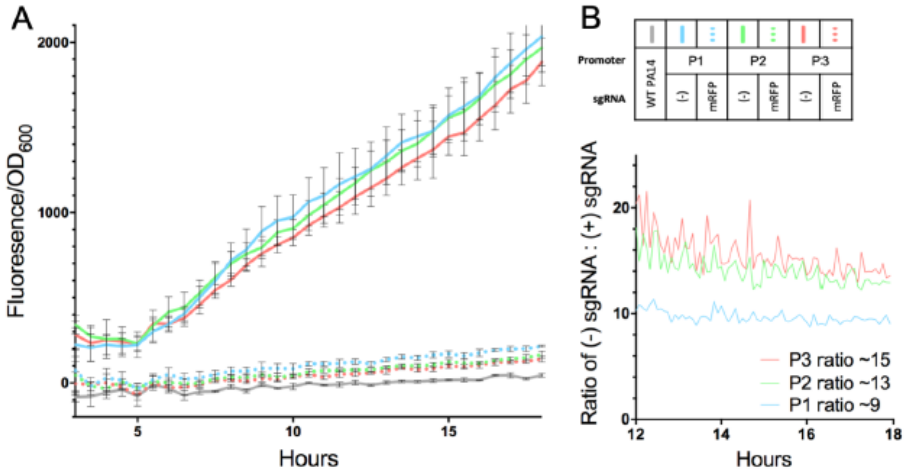

Supplementary Figure 2.2: Constitutive promoter-driven knockdown efficiency over time
The *dcas9* was cloned into Mobile-CRISPRi plasmids under the control of three different constitutive promoters. Strains were incubated in a microplate reader to monitor fluorescence and OD_{600nm} over time. (A) The fluorescence of strains without sgRNA was compared to that of strains with mRFP-targeting sgRNAs after normalization with OD_{600nm}. (B) Ratios of median florescence from strains ((-) sgRNA: (+) sgRNA) were averaged between 12 and 18 hours to calculate knockdown ratios ($p < .0001$ for all three promoters).

To assess Mobile-CRISPRi efficacy using the BioBrick promoter strains, we employed a "test" version of MobileCRISPRi expressing monomeric red fluorescent protein (mRFP) and an sgRNA targeting the *mRFP* gene (31). Knockdown levels were quantified for each promoter through comparing the mutants' fluorescence normalized to growth over time. After 12 hours, we found stable fluorescence ratios between mutants without and with *mRFP*-targeting sgRNA (**Supplementary Fig. 2.2**). The gradient of knockdown ranged from 10- to 17-fold at the 14-hour timepoint, which roughly corresponded to the BioBrick promoter strength used to express dCas9 (**Fig. 2.1C**). We performed RNA sequencing (RNA-seq) on cells expressing dCas9 from the strongest of the three BioBrick promoters in our set and confirmed that CRISPRi retained specificity for RFP (**Fig. 2.1D**). We imaged cells expressing dCas9$_{Spy}$ from all three promoters and found no apparent defects in morphology (**Supplementary Fig. 2.3).** We conclude that Mobile-CRISPRi optimized with BioBrick promoters driving dCas9$_{Spy}$ enables a nontoxic gradient of constitutive knockdowns in *P. aeruginosa* PA14.

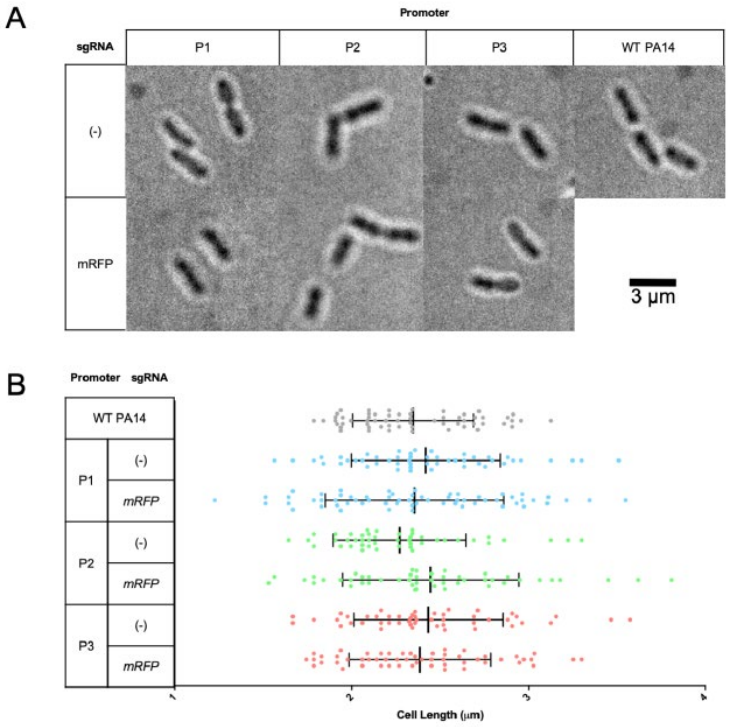

Supplementary Figure 2.3: Phenotypic effects of Mobile-CRISPRi
(A) Mobile-CRISPRi strains containing mRFP-targeting sgRNA or no sgRNA were imaged with a Nikon Ti microscope. No growth defects were observed. (B) The lengths of 45–62 cells for each strain were measured. Differences among means are not significant.

Mobile-CRISPRi targeting of CE genes in a murine pneumonia model

A major goal for developing Mobile-CRISPRi in infection models is to identify CE genes for which a modest perturbation has a substantial impact on pathogenesis. To do so, the system must enable the stable repression of the gene of interest over the course of infection. As a test case, we targeted *exsA*, which encodes the key activator of type III secretion system (T3SS) genes that are required for pathogenesis in *P. aeruginosa*. Because the *exsA* gene is positively autoregulated by the ExsA protein, (39) we reasoned

that modest knockdown would cause a large reduction in the transcription of T3SS genes, resulting in a loss of effector secretion and impaired virulence. Consistent with this, we found that CRISPRi knockdown of *exsA* reduced the expression of T3SS genes by more than 100-fold (**Fig. 2.2A**), similar to the expression levels observed in a strain with an *exsA* disruption (*exsA*::Tn; the Tn insertion position is shown in **Supplementary Fig. 2.4**). (40) We found that all three BioBrick promoters driving dCas9$_{Spy}$ expression were equally effective at reducing *exsA* transcript levels, likely because even modest reductions in ExsA protein levels disrupt positive autoregulation. The *esxA*::Tn transposon mutation is insertional rather than deletional, which may have led to high levels of the nonfunctional *exsA* transcript, as measured by quantitative PCR (qPCR) (**Supplementary Table 2.1**). CRISPRi appeared to be slightly more effective at reducing *exsA* transcript levels than the *exsA*::Tn allele, possibly because CRISPRi can repress both ExsA-dependent transcription from the *exsC* promoter and ExsA-independent transcription from the *exsA* promoter (41). Knock down of *exsA* also eliminated the detectable production of T3SS pilus (PopB/D) and effector (ExoT/U) proteins (**Fig. 2.2B**). Neither the *exsA* knockdown nor the non-targeting control sgRNA strains showed a growth defect in rich culture medium (**Supplementary Fig. 2.1)**.

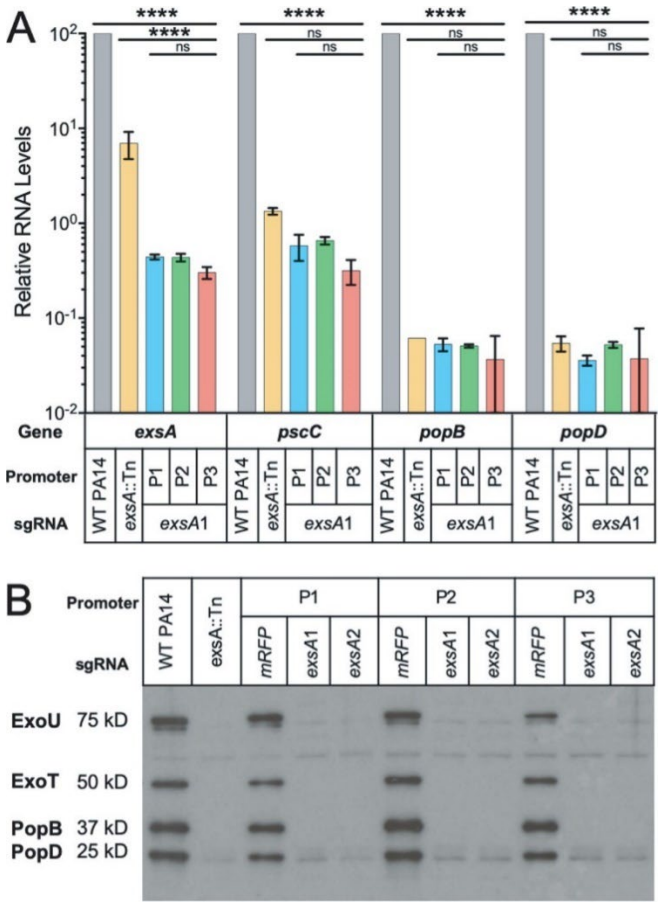

Figure 2.2: T3SS-associated gene transcription and protein secretion profiles
(A) Reverse transcriptase quantitative PCR (RT-qPCR) analysis for T3SS-related genes across PA14 strains, normalized to WT PA14 RNA levels. (B) Immunoblot analysis of exoenzyme U and exoenzyme S secretion for PA14 strains grown in MinS medium (for type III protein secretion induction).

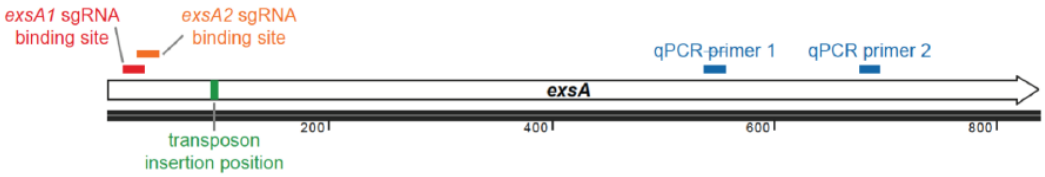

Supplementary Figure 2.4: Map of exsA-related genetic elements
Locations of exsA1 and exsA2 sgRNAs targeting sites on the exsA gene, transposon insertion present in mutant exsA:: Tn, and primers for qRT-PCR.

Supplementary Table 2.1: Sequences of primers used for qRT-PCR

Primers	Sequence 5'-3'
nadB up	CTACCTGGACATCAGCCACA
nadB down	GGTAATGTCGATGCCGAAGT
exsA 159F	AGCACTACCTCAACGAGTGG
exsA 159R	TGTTGAGCAGCAACTGATGG
pscC 63L1	CATTACCTGGCGCTGAACAA
pscC 63R1	CAACTCGTCGACTTCAAGCA
popB 78L1	GCAGAACCTGCAGAAGATGG
popB 78R1	GACTTCTGGGCTTCTTTCGC
popD L1	CGATGAGGATCGCAAGATCG
popD R1	CATCTGGACGAAGGACTGGA

The loss of *exsA* function is known to strongly attenuate virulence in a murine pneumonia model. (42, 43) To test whether Mobile-CRISPRi can be used to probe the functions of CE genes, such as *exsA*, in a host environment, we intratracheally instilled C57BL/6 mice with a range of 10^5 to 10^7 CFU of wild-type (WT) *P. aeruginosa* PA14, an isogenic *exsA*::Tn mutant, or Mobile-CRISPRi strains containing dCas9$_{Spy}$ driven by the P3 BioBrick promoter, and either an *exsA*-targeting sgRNA or a nontargeting control sgRNA. Although CRISPRi using all three BioBrick promoters resulted in similar levels of *exsA* knockdown, we chose P3 because we reasoned that it would serve as the most stringent test of potential dCas9$_{Spy}$ toxicity in the context of a mouse infection. We collected the lungs 18 hours after infection and plated lung homogenates to estimate the number of viable bacteria (44) (**Supplementary Fig. 2.5A**). Strains with the exsA::Tn allele or Mobile-CRISPRi-targeted exsA were highly attenuated for virulence and yielded similar recovery rates (**Fig. 2.3**). This demonstrates that Mobile-CRISPRi is an effective tool to knock down CE genes in PA14 during a mouse infection and implies that Mobile-CRISPRi is as stable during *in vivo* infection as it is during growth in culture. (31) Furthermore, levels of CFU

recovery were similar between WT and nontargeting Mobile-CRISPRi, suggesting that the nonspecific toxicity of dCas9 was mitigated by reduced expression. Other general indicators of infection, including hypothermia and leukopenia, were observed for the nontargeting and WT controls (**Supplementary Fig. 2.5B** and **C**). In contrast, both the exsA::Tn and Mobile-CRISPRi-targeted exsA strains produced similar levels of white blood cell counts (equivalent or higher than those seen in the phosphate-buffered saline [PBS] control) and similar body temperatures, altogether indicative of reduced virulence (**Supplementary Fig. 2.5B** and **C**). Consistent with this, WT and nontargeting strains showed severe lung injury not seen in the exsA::Tn and exsA-targeting strains (**Supplementary Fig. 2.5D**). We conclude that Mobile-CRISPRi can probe CE gene phenotypes in infection models.

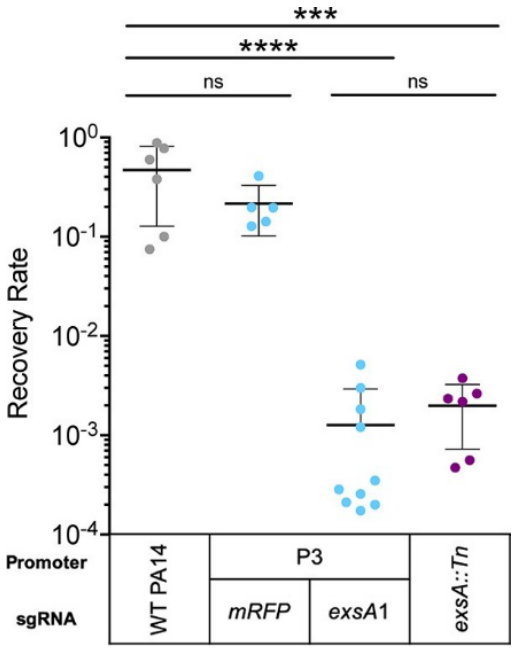

Figure 2.3: Recovery rates following murine lung infection

Following infection, lung homogenate serial dilutions were plated to estimate the CFU of bacteria recovered from the lung. Recovery rate is output CFU relative to input CFU.

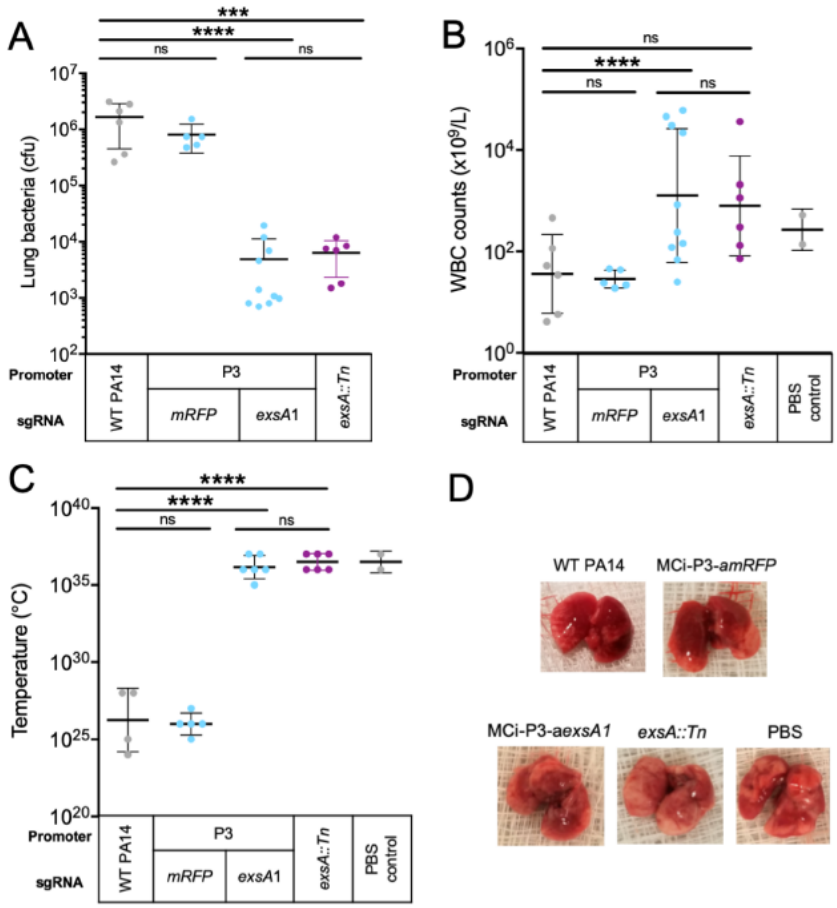

Supplementary Figure 2.5: Phenotypic effects of infection

(A) Recovered CFU counts from plated lung homogenates (B) white blood cell counts (C) rectal temperatures (D) images of qualitative lung injury from mice.

Discussion

A lack of genetic tools that enable facile and precise control over CE and essential gene expression has severely hampered our progress toward understanding bacterial pathogenesis past the point of simply identifying virulence factors. Our work demonstrates that Mobile-CRISPRi is a valuable genetic tool for characterizing CE genes in the context of an animal infection. We establish a synthetic biology approach for generating CRISPRi knockdown gradients and mitigating nonspecific toxicity by using

promoters from the BioBrick Registry to control dCas9 expression. Furthermore, we show that Mobile-CRISPRi repression remains stable despite the stringent fitness constraints imposed during growth in a murine infection model—a key prerequisite to large-scale CRISPRi screens for bacterial gene function in pathogenesis. Finally, as a proof of principle, we successfully use Mobile-CRISPRi to modulate the pathogenesis of *P. aeruginosa* in a mouse pneumonia model by targeting the CE gene *exsA*. Our studies lay the groundwork for future CRISPRi screens that probe the molecular details of pathogenesis.

Mobile-CRISPRi is an excellent complement to established methods of gene function analysis during pathogenesis. Tn-based techniques (e.g., Tn-Seq [3]/INSeq [4]), transposon site hybridization, (45) and signature-tagged mutagenesis (46) have been enormously successful at identifying genes required for growth in mouse models of infection. Mobile-CRISPRi partial knockdowns can be used to further characterize these gene sets by modulating expression to determine the amount of gene product required for virulence. Multiplexed CRISPRi can be used to dissect the genetic pathways by which CE genes operate (29) and will be particularly valuable for characterizing synergies between partially redundant secreted effector proteins. CRISPRi is currently the only method of systematically perturbing essential gene function that can be rationally designed and involves only a single step of strain construction. Thus, a combination of

Mobile-CRISPRi partial knockdowns and Tn libraries will enable a comprehensive characterization of all genes required for pathogenesis—including essential genes.

Both Tn mutagenesis and CRISPRi screens have potential pitfalls that should be considered when interpreting single-gene data. When passaged, Tn-mutagenized strains can accumulate second-site suppressors that distort phenotypic analysis. Relatedly, CRISPRi can be inactivated by mutation; the most frequent type spontaneously occurs in the *dcas9* gene and is enriched in a population of strains when CRISPRi causes a strong fitness defect. (47) To circumvent these fitness defects, the weak P1 version of Mobile-CRISPRi can be used to target "sensitive" genes, for which a modest knock down causes a strong fitness defect. (48) Finally, Tn mutagenesis and CRISPRi can both alter the expression of downstream genes in an operon (i.e., polarity), but the CRISPRi effect is much more predictable because the knock down of downstream genes is generally proportional to that of the targeted gene. (29)

We previously demonstrated that Mobile-CRISPRi could be used to repress gene expression in a number of bacterial pathogens associated with antibiotic resistance (e.g., the *Enterococcus faecium*, *Staphylococcus aureus*, *Klebsiella pneumoniae*, *Acinetobacter baumannii*, *Pseudomonas aeruginosa*, and *Enterobacter* species [ESKAPE] pathogens) (31, 49). Our optimized Mobile-CRISPRi system opens the door to systematic analysis of CE genes in these pathogens during infection, enabling drug-gene interaction studies and, in principle, a screen for new inhibitors that synergize with the host immune system.

Methods

Construction of Mobile-CRISPRi plasmids and strains

Plasmids encoding nuclease-null *Streptococcus pyogenes* and *Streptococcus thermophilus* dCas9s were gifted by Lei Qi and Sarah Fortune, respectively. The vectors containing a Tn7-based Mobile-CRISPRi system were constructed as previously described by Peters. (31) dCas9 was expressed from the arabinose-inducible P_{BAD} promoter and three constitutive promoters, namely, Anderson BBa_J23117 (P1), Anderson BBa_J23114 (P2), and Anderson BBa_J23115 (P3). The chimeric sgRNA was expressed by a constitutive derivative of the P_{trc} promoter with no LacI operator site. In this study, all *Pseudomonas aeruginosa* UCBPP-PA14 Mobile-CRISPRi strains were constructed by tri-parental mating as previously described. (31) Complete lists of plasmids and strains used in the study can be found in **Supplementary Tables 2.2** and **2.3**, respectively, in the supplemental material. The PA14 *exsA*::Tn strain was obtained from a transposon insertion library. (40)

Toxicity measurements

For dCas9 toxicity measurements, WT PA14 and the mutants were streaked onto *Pseudomonas* isolation agar (PIA) plates and incubated for 20 hours at 37°C. On the second day, one colony from each plate was cultured in 2 mL LB and incubated at 37°C with shaking at 350 rpm for 12 hours. Then, cultures were diluted in 100 µL LB medium with no inducer, 0.1% arabinose, or 1% arabinose to yield a mixture with an optical density

at 600 nm (OD_{600nm}) of 0.05 in a 96-well plate (catalog no. 351177; Corning, NY). These cultures were grown with a lid for 9 to 10 hours on a plate shaker (OrbiShaker MP, Benchmark Scientific, NJ) at 37°C and 900 rpm. The OD_{600nm} of the plate cultures was measured every hour using a microplate reader (SpectraMax 340PC; Molecular Devices, CA).

RFP knockdown efficiency

Following triparental mating, two *P. aeruginosa* colonies were picked from each strain to serve as biological replicates and were incubated overnight in 3 mL of LB with 100 µg/mL gentamicin selective medium at 37°C with shaking. These cultures were diluted to 0.01 OD_{600nm} into fresh LB medium, and 200 µL of this culture was added in triplicate to a clear bottom, black, 96-well plate (Corning Costar). This plate was covered with an optically clear seal, and a needle was used to poke holes in each of the wells. Fluorescence (excitation, 557 nm; emission, 592 nm) and OD_{600nm} were monitored during incubation in a microplate reader (Synergy H1; BioTek Instruments, VT) with continuous, fast, double orbital shaking. Samples were blanked with a well containing LB medium. For each replicate, the fluorescence value was divided by OD_{600nm} values at each time point and plotted in 30-minute intervals.

Supplementary Table 2.2: Plasmids used in this study

Name systematic plasmid name
Modules functional components of Mobile-CRISPRi plasmids that are easily exchanged
Origin plasmid replication origin in E. coli donors
E. coli resistance antibiotic resistance used for selection in E. coli donors
Recipient resistance antibiotic resistance used for selection in recipient strains
Reporter reporter gene and promoter inserted into Mobile-CRISPRi
sgRNA promoter promoter driving sgRNA expression; trc promoters with no LacI operator site are constitutive
sgRNA sgRNAs are named after the genes they target
sgRNA sequence sequence defining the sgRNA target
Promoter regulation regulator protein that controls promoters activity
dcas9 promoter promoter driving dcas9 expression
dcas9 variant dCas9 sequence variants; "Sth1" comes from S. thermophilus and works better in *Mycobacterium*. "Has Spy" is human codon optimized and works better in some species (*P. aeruginosa*)
Comment information about the plasmid function or purpose

Plasmid Name	Modules											
	Origin	E. coli resistance	Recipient resistance	Reporter	sgRNA promoter	sgRNA	sgRNA sequence	promoter regulation	dcas9 promoter	dcas9 variant	comment
pJQ3	R6K	carbenicillin	gentamicin	mRFP	PLlacO1	none	NA	Lac operon	PBAD	*S. thermophilus #1*	dCas9 protein toxicity "test" strain
pJQ4	R6K	carbenicillin	gentamicin	mRFP	PLlacO1	none	NA	Lac operon	PBAD	Hsa Spy dcas9::3Xmyc	dCas9 protein toxicity "test" strain
pJQ3_Rock	R6K	carbenicillin	gentamicin	mRFP	trc (no operator)	*amRFP2*	GAAGCCATGGAGATACCTCCTGG	Lac operon	PBAD	*S. thermophilus #1*	dCas9 protein toxicity "test" strain
pJQ4_RR1	R6K	carbenicillin	gentamicin	mRFP	trc (no operator)	*amRFP*	AACTTTCAGTTTAGCGGTCT	Lac operon	PBAD	Hsa Spy dcas9::3Xmyc	dCas9 protein toxicity "test" strain
pJQ11	R6K	carbenicillin	gentamicin	PJ23119-rfp	trc (no operator)	none	NA	none	Anderson BBa_J23117 (0.06 str)	Hsa Spy dcas9::3Xmyc	dCas9 promoter strength "test" strain (no guide)
pJQ12	R6K	carbenicillin	gentamicin	PJ23119-rfp	trc (no operator)	none	NA	none	Anderson BBa_J23114 (0.10 str)	Hsa Spy dcas9::3Xmyc	dCas9 promoter strength "test" strain (no guide)
pJQ13	R6K	carbenicillin	gentamicin	PJ23119-rfp	trc (no operator)	none	NA	none	Anderson BBa_J23115 (0.15 str)	Hsa Spy dcas9::3Xmyc	dCas9 promoter strength "test" strain (no guide)
pJQ15	R6K	carbenicillin	gentamicin	PJ23119-rfp	trc (no operator)	*amRFP*	AACTTTCAGTTTAGCGGTCT	none	Anderson BBa_J23117 (0.06 str)	Hsa Spy dcas9::3Xmyc	dCas9 promoter strength "test" strain (with guide)
pJQ16	R6K	carbenicillin	gentamicin	PJ23119-rfp	trc (no operator)	*amRFP*	AACTTTCAGTTTAGCGGTCT	none	Anderson BBa_J23114 (0.10 str)	Hsa Spy dcas9::3Xmyc	dCas9 promoter strength "test" strain (with guide)
pJQ17	R6K	carbenicillin	gentamicin	PJ23119-rfp	trc (no operator)	*amRFP*	AACTTTCAGTTTAGCGGTCT	none	Anderson BBa_J23115 (0.15 str)	Hsa Spy dcas9::3Xmyc	dCas9 promoter strength "test" strain (with guide)
pJQ23	R6K	carbenicillin	gentamicin	none	trc (no operator)	exsA1	CTGCTTTCGGCCAAGAGATT	none	Anderson BBa_J23117 (0.06 str)	Hsa Spy dcas9::3Xmyc	exsA knockdown strain
pJQ24	R6K	carbenicillin	gentamicin	none	trc (no operator)	exsA2	GACAAGACGTTATCTGCTTT	none	Anderson BBa_J23117 (0.06 str)	Hsa Spy dcas9::3Xmyc	exsA knockdown strain
pJQ25	R6K	carbenicillin	gentamicin	none	trc (no operator)	exsA1	CTGCTTTCGGCCAAGAGATT	none	Anderson BBa_J23114 (0.10 str)	Hsa Spy dcas9::3Xmyc	exsA knockdown strain
pJQ26	R6K	carbenicillin	gentamicin	none	trc (no operator)	exsA2	GACAAGACGTTATCTGCTTT	none	Anderson BBa_J23114 (0.10 str)	Hsa Spy dcas9::3Xmyc	exsA knockdown strain
pJQ27	R6K	carbenicillin	gentamicin	none	trc (no operator)	exsA1	CTGCTTTCGGCCAAGAGATT	none	Anderson BBa_J23115 (0.15 str)	Hsa Spy dcas9::3Xmyc	exsA knockdown strain
pJQ28	R6K	carbenicillin	gentamicin	none	trc (no operator)	exsA2	GACAAGACGTTATCTGCTTT	none	Anderson BBa_J23115 (0.15 str)	Hsa Spy dcas9::3Xmyc	exsA knockdown strain
pJQ31	R6K	carbenicillin	gentamicin	none	trc (no operator)	none	NA	araC	PBAD	Hsa Spy dcas9::3Xmyc	exsA knockdown control strain
pJQ32	R6K	carbenicillin	gentamicin	none	trc (no operator)	exsA1	CTGCTTTCGGCCAAGAGATT	araC	PBAD	Hsa Spy dcas9::3Xmyc	exsA knockdown control strain
pJQ33	R6K	carbenicillin	gentamicin	none	trc (no operator)	exsA2	GACAAGACGTTATCTGCTTT	araC	PBAD	Hsa Spy dcas9::3Xmyc	exsA knockdown control strain
pJQ47	R6K	carbenicillin	gentamicin	none	trc (no operator)	none	NA	none	Anderson BBa_J23117 (0.06 str)	Hsa Spy dcas9::3Xmyc	exsA knockdown control strain
pJQ48	R6K	carbenicillin	gentamicin	none	trc (no operator)	none	NA	none	Anderson BBa_J23114 (0.10 str)	Hsa Spy dcas9::3Xmyc	exsA knockdown control strain
pJQ49	R6K	carbenicillin	gentamicin	none	trc (no operator)	none	NA	none	Anderson BBa_J23115 (0.15 str)	Hsa Spy dcas9::3Xmyc	exsA knockdown control strain

Supplementary Table 2.3: Bacterial strains used in this study

Strain name	Organism	Genotype	Notes
PA14 WT	Pseudomonas aeruginosa UCBPP-PA14	wild-type	from J. Engel
PA14 WT + RFP	Pseudomonas aeruginosa UCBPP-PA14	attTn7::pJQ4_RR1_rfp (GentR)	WT + RFP positive control
dCas9$_{Sth}$-RFP-MCi-P$_{BAD}$	Pseudomonas aeruginosa UCBPP-PA14	attTn7::pJQ3 (GentR)	dCas9 protein toxicity "test" strain
dCas9$_{Spy}$-RFP-MCi-P$_{BAD}$	Pseudomonas aeruginosa UCBPP-PA14	attTn7::pJQ4 (GentR)	dCas9 protein toxicity "test" strain
dCas9$_{Sth}$-RFP-MCi-P$_{BAD}$-a*mRFP2*	Pseudomonas aeruginosa UCBPP-PA14	attTn7::pJQ3_Rock (GentR)	dCas9 protein toxicity "test" strain
dCas9$_{Spy}$-RFP-MCi-P$_{BAD}$-a*mRFP*	Pseudomonas aeruginosa UCBPP-PA14	attTn7::pJQ4_RR1 (GentR)	dCas9 protein toxicity "test" strain
dCas9$_{Spy}$-RFP-MCi-P1	Pseudomonas aeruginosa UCBPP-PA14	attTn7::pJQ11 (GentR)	dCas9 promoter strength "test" strain (no guide)
dCas9$_{Spy}$-RFP-MCi-P2	Pseudomonas aeruginosa UCBPP-PA14	attTn7::pJQ12 (GentR)	dCas9 promoter strength "test" strain (no guide)
dCas9$_{Spy}$-RFP-MCi-P3	Pseudomonas aeruginosa UCBPP-PA14	attTn7::pJQ13 (GentR)	dCas9 promoter strength "test" strain (no guide)
dCas9$_{Spy}$-RFP-MCi-P1-a*mRFP*	Pseudomonas aeruginosa UCBPP-PA14	attTn7::pJQ15 (GentR)	dCas9 promoter strength "test" strain (with guide)
dCas9$_{Spy}$-RFP-MCi-P2-a*mRFP*	Pseudomonas aeruginosa UCBPP-PA14	attTn7::pJQ16 (GentR)	dCas9 promoter strength "test" strain (with guide)
dCas9$_{Spy}$-RFP-MCi-P3-a*mRFP*	Pseudomonas aeruginosa UCBPP-PA14	attTn7::pJQ17 (GentR)	dCas9 promoter strength "test" strain (with guide)
dCas9$_{Spy}$-MCi-P1-a*exsA*1	Pseudomonas aeruginosa UCBPP-PA14	attTn7::pJQ23 (GentR)	exsA knockdown strain
dCas9$_{Spy}$-MCi-P1-a*exsA*2	Pseudomonas aeruginosa UCBPP-PA14	attTn7::pJQ24 (GentR)	exsA knockdown strain
dCas9$_{Spy}$-MCi-P2-a*exsA*1	Pseudomonas aeruginosa UCBPP-PA14	attTn7::pJQ25 (GentR)	exsA knockdown strain
dCas9$_{Spy}$-MCi-P2-a*exsA*2	Pseudomonas aeruginosa UCBPP-PA14	attTn7::pJQ26 (GentR)	exsA knockdown strain
dCas9$_{Spy}$-MCi-P3-a*exsA*1	Pseudomonas aeruginosa UCBPP-PA14	attTn7::pJQ27 (GentR)	exsA knockdown strain
dCas9$_{Spy}$-MCi-P3-a*exsA*2	Pseudomonas aeruginosa UCBPP-PA14	attTn7::pJQ28 (GentR)	exsA knockdown strain
dCas9$_{Spy}$-MCi-P$_{BAD}$	Pseudomonas aeruginosa UCBPP-PA14	attTn7::pJQ31 (GentR)	non-targeting control
dCas9$_{Spy}$-MCi-P$_{BAD}$-a*exsA*1	Pseudomonas aeruginosa UCBPP-PA14	attTn7::pJQ32 (GentR)	exsA knockdown control strain
dCas9$_{Spy}$-MCi-P$_{BAD}$-a*exsA*2	Pseudomonas aeruginosa UCBPP-PA14	attTn7::pJQ33 (GentR)	exsA knockdown control strain
dCas9$_{Spy}$-MCi-P1	Pseudomonas aeruginosa UCBPP-PA14	attTn7::pJQ47 (GentR)	non-targeting control
dCas9$_{Spy}$-MCi-P2	Pseudomonas aeruginosa UCBPP-PA14	attTn7::pJQ48 (GentR)	non-targeting control
dCas9$_{Spy}$-MCi-P3	Pseudomonas aeruginosa UCBPP-PA14	attTn7::pJQ49 (GentR)	non-targeting control
exsA::Tn7	Pseudomonas aeruginosa UCBPP-PA14	exsA::Tn (CarbR GentR)	exsA functional knockout (Liberati, 2006)
MFD pir E.coli	Escherichia coli K-12 MFD pir	RP4-2-Tc::ΔMu1::aac(3)IV-ΔaphA-Δnic35-ΔMu2::zeo, ΔdapA::(erm-	DAP-dependent mating strain from KC Huang, PMID: 20935093
MFD pir E.coli/Mobile-CRISRPi1	Escherichia coli K-12 MFD pir	RP4-2-Tc::ΔMu1::aac(3)IV-ΔaphA-Δnic35-ΔMu2::zeo, ΔdapA::(erm-pir), ΔrecA, pJMP1039(AmpR, GenR)	tri-parental mating helper strain, expresses Tn7 transposase, nearly identical to pTNS3, from J. Peters PMID: 18156318
Pir E.coli	Escherichia coli K-12 BW25141	Δ(araD-araB)567, ΔlacZ4787(::rrnB-3), Δ(phoB-phoR)580, λ-, galU95,	Pir+ cloning strain from C. Gross

RNA extraction

PA14 Mobile-CRISPRi strains, *exsA*::Tn, and WT were streaked onto Vogel Bonner minimal medium (VBMM) or LB agar plates and incubated overnight at 37°C. One colony from each plate was grown in MinS (T3SS-inducing minimal medium supplemented with nitrotriacetic acid and lacking calcium medium) (50) or LB medium at 37°C for 16 hours with shaking at 250 rpm. Then, the strains were subcultured in 400 µL fresh MinS or LB medium until the OD_{600nm} reached 1.0. Total RNA was extracted from cell pellets using the RNeasy minikit (Qiagen) according to the manufacturer's instructions with on-column DNase I digestion (Qiagen). The RNA extracts were aliquoted and stored at –80°C.

Reverse transcriptase quantitative PCR

cDNA was synthesized using random hexamer primers and a RevertAid first-strand cDNA synthesis kit (Thermo Scientific, Waltham, MA). To check the amplification efficiency of the primers, a 1:50 dilution of WT PA14 cDNA was mixed with PowerUp SYBR green master mix (Thermo Scientific) and detected by the MX3000P qPCR System (Stratagene, La Jolla, CA). Primers for T3SS-related genes (**Supplementary Table 2.3**) had amplification efficiencies between 90% and 110%. A PA14 housekeeping gene, *nadB*, was used as an internal control for normalization of total RNA levels. (51) The relative efficiency of each primer pair was tested and compared with that of *nadB*, and the threshold cycle ($2^{\Delta\Delta CT}$) data analysis was used. (52) All reactions were performed in triplicates and repeated at least twice using independent cultures, with average values of biological replicates and error bars representing standard deviation of $\Delta\Delta CT$.

cDNA library preparation and RNA-seq

The RNA concentration for each sample was determined with a NanoDrop spectrophotometer (Thermo Fisher Scientific). A total of 10 ng of RNA of each sample was fragmented for 6 min, cDNA libraries were prepared using a NEBNext Ultra RNA library prep kit for Illumina (New England BioLabs [NEB] number E7770S). Libraries were sequenced in collaboration with the Chan Zuckerberg Biohub in San Francisco on an Illumina MiSeq instrument in 150-bp paired-end runs. Approximately 1,000,000 reads were collected for each of the two samples, with 94% alignment to PA14 WT by Bowtie2,

(53) and transcripts were counted with HTSeq. (54) Only genes with a nonnormalized read count greater than 1 in both samples were included in analysis, with a coverage of 1,286 genes (20% genome). All RNA-seq data have been deposited in the National Center for Biotechnology Information's GEO database (55) and are accessible through accession number GSE134771.

Type III secretion profile of *Pseudomonas aeruginosa* by immunoblotting

To knock down the *exsA* gene, two specific sgRNAs, *exsA*1 and *exsA*2, were designed. PA14 Mobile-CRISPRi mutants, *exsA*::Tn, and WT were streaked onto VBMM agar plates and incubated at 37°C overnight. One colony from each plate was grown at 37°C for 16 hours in a shaking incubator at 250 rpm in MinS medium. (50) Bacteria were removed by centrifugation at 6,000 *g* for 15 min. Then the supernatant was collected and the secreted proteins were precipitated by the addition of ammonium sulfate. The protein pellets were dissolved in sample buffer. After boiling, samples were loaded onto ExpressPlus 4% to 20% PAGE gels (Genscript, Piscataway, NJ) and run under denaturing conditions. PAGE gels were transferred to a polyvinylidene difluoride (PVDF) membrane and immunoblotted with polyclonal rabbit antiserum against ExoU, ExoT/ExoS, PopB, and PopD proteins, as previously described. (50)

Murine infection model

Pathogen-free male C57BL/6J mice, 8 weeks of age, were purchased from Jackson Laboratories. Animal experiments were conducted in accordance with the approval of the Institutional Animal Care and Use Committee (IACUC) at UCSF. A total of 29 mice were randomly assigned in the following 5 groups: G1, WT PA14, 6 mice; G2, P3 with *mRFP*-targeting sgRNA, 5 mice; G3, P3 with *exsA*1 targeting sgRNA, 10 mice; G4, *exsA*::Tn, 6 mice; and G5, saline control, 2 mice. Mice were anesthetized with isofluorane prior to intratracheal instillation with bacteria at a range of 1×10^5 to 1×10^7 CFU/animal in a volume of 50 µl, per an established protocol. (44) Animal weights and rectal temperatures were measured prior to euthanasia. The lungs were collected in 1 ml of sterile PBS and processed with a handheld homogenizer (Polytron PT1200E; Kinematica). A total of 50 µl of lung homogenate with appropriate dilutions were spread onto PIA plates with and without gentamicin to count output CFU. The bacterial recovery rate was calculated as the ratio of output CFU to input CFU. For whole-blood analysis, blood was collected by cardiac puncture into acid citrate dextrose (Sigma-Aldrich), and white blood cells (WBCs) were measured by a hematology analyzer (Genesis; Oxford Science).

Microscopy

An overnight culture was diluted 1:100 and grown to mid-log phase in LB medium. This culture was diluted to an OD_{600nm} of 0.1 before being added to an agar pad composed of 1% agarose and LB medium. No. 1 coverslips were used, and the slide was sealed with

Valap. Thereafter, 250 µl of LB medium was added to the agar pad to prevent desiccation. Sample slides were mounted in the stage top of a Nikon Ti microscope warmed to 37°C. All images were collected on a Nikon Ti-E inverted microscope equipped with a Plan Apo VC 100/1.4. Images were acquired with an Andor Zyla 4.2 sCMOS camera controlled with MicroManager. Multiple stage positions were collected using an ASI XYZ stage. Brightness and contrast were adjusted (identically for compared image sets) using Fiji software.

Statistical analysis

GraphPad Prism (v. 7.0) was used for the statistical analysis of all the data. For log-transformed bacterial recovery rate, temperature, WBC counts, and weight changes, all groups were analyzed by ordinary one-way analysis of variance (ANOVA) followed by Tukey's multiple-comparison test. For the transcription data, two-way ANOVA followed by Tukey's multiple-comparison test was implemented. To compare changes in fluorescence at 14 hours, data points associated with *mRFP*-targeting sgRNAs were normalized to median fluorescence of the respective strain without sgRNAs. One-way ANOVA followed by Tukey's multiple-comparison test was used to assess the significance of the knockdown levels.

Acknowledgements

I thank my co-authors (Dr. Jiuxin Qu, Dr. Michelle A. Yu, Shuyan Chen, Amy Lyden, Nadia Herrera, Melanie R. Silvis, Emily Crawford, Mark R. Looney, Jason Peters, and Oren S. Rosenberg), as well as S. Fortune for the dCas9$_{sth}$ plasmid, A. Hauser for the polyclonal rabbit antiserum for *exsA*-related proteins, and C. Gross and J. Engel for productive discussions and some strains. The sequencing team at the Chan Zuckerberg Biohub (N. Neff, B. Yu, R. Sit, and M. Tan) assisted with RNA-seq experiments. C. Mahendra and A. Borges in the lab of J. Bondy-Demony (UCSF) provided technical assistance during the fluorescence plate reader assay. Microscopy data were acquired at the Nikon Imaging Center at UCSF.

This work was supported by NIH 1K22AI137122 (to J.M.P.), NIAID R01 AI125445 (to M.R.L.), NSF-GRFP 1650113 (to N.K.P.), the National Natural Science Foundation of China 81400005/H0104 and Special Support Fund of Shenzhen for Introduced High-Level Medical Team and Translational medicine of Biochip in clinical laboratory SZSM201412005 (to J.Q.), and 5R01EB024014, Chan-Zuckerberg Biohub, CF Foundation Research Development Program, and Gilead Sciences Research Scholars Program in Cystic Fibrosis (to O.S.R.).

We declare no competing interests. Author contributions were as follows: conceptualization, J.M.P. and O.S.R.; methodology and investigation, J.Q., N.K.P., M.A.Y.,

S.C., N.H., A.L., E.C., and M.R.S.; supervision, E.C., M.R.L., and O.S.R.; draft writing and revision, J.Q., N.K.P., J.M.P., and O.S.R.; funding acquisition, O.S.R.

References

1. Wassenaar TM, Gaastra W. 2001. Bacterial virulence: can we draw theline? FEMS Microbiol Lett 201:1–7. https://doi.org/10.1111/j.1574-6968 .2001.tb10724.x.
2. Tufariello JM, Chapman JR, Kerantzas CA, Wong K-W, Vilchèze C, JonesCM, Cole LE, Tinaztepe E, Thompson V, Fenyö D, Niederweis M, Ueberheide B, Philips JA, Jacobs WR. 2016. Separable roles for *Mycobacterium tuberculosis* ESX-3 effectors in iron acquisition and virulence. Proc Natl Acad Sci U S A 113:E348–57. https://doi.org/10.1073/pnas.1523321113.
3. van Opijnen TK, Bodi L, Camilli A. 2009. Tn-seq: high-throughput parallelsequencing for fitness and genetic interaction studies in microorganisms. Nat Methods 6:767–772. https://doi.org/10.1038/nmeth.1377.
4. Goodman AL, Wu M, Gordon JI. 2011. Identifying microbial fitnessdeterminants by insertion sequencing using genome-wide transposon mutant libraries. Nat Protoc 6:1969–1980. https://doi.org/10.1038/nprot .2011.417.
5. Burrack LS, Higgins DE. 2007. Genomic approaches to understandingbacterial virulence. Curr Opin Microbiol 10:4–9. https://doi.org/10.1016/ j.mib.2006.11.004.
6. Bachman MA, Breen P, Deornellas V, Mu Q, Zhao L, Wu W, Cavalcoli JD,Mobley HLT. 2015. Genome-wide identification of *Klebsiella pneumoniae* fitness genes during lung infection. mBio 6:e00775-15. https://doi.org/ 10.1128/mBio.00775-15.

7. Fu YM, Waldor K, Mekalanos JJ. 2013. Tn-Seq analysis of *Vibrio cholerae* intestinal colonization reveals a role for T6SS-mediated antibacterial activity in the host. Cell Host Microbe 14:652–663. https://doi.org/10 .1016/j.chom.2013.11.001.

8. Gawronski JD, Wong SMS, Giannoukos GD, Ward V, Akerley BJ. 2009. Tracking insertion mutants within libraries by deep sequencing and a genome-wide screen for *Haemophilus* genes required in the lung. Proc Natl Acad Sci U S A 106:16422–16427. https://doi.org/10.1073/pnas .0906627106.

9. Kamp HD, Patimalla-Dipali B, Lazinski DW, Wallace-Gadsden F, Camilli A.2013. Gene fitness landscapes of *Vibrio cholerae* at important stages of its life cycle. PLoS Pathog 9:e1003800. https://doi.org/10.1371/journal .ppat.1003800.

10. Skurnik D, Roux D, Aschard H, Cattoir V, Yoder-Himes D, Lory S, Pier GB.2013. A comprehensive analysis of in vitro and in vivo genetic fitness of *Pseudomonas aeruginosa* using high-throughput sequencing of transposon libraries. PLoS Pathog 9:e1003582. https://doi.org/10.1371/ journal.ppat.1003582.

11. Turner KH, Wessel AK, Palmer GC, Murray JL, Whiteley M. 2015. Essential genome of *Pseudomonas aeruginosa* in cystic fibrosis sputum. Proc Natl Acad Sci U S A 112:4110–4115. https://doi.org/10.1073/ pnas.1419677112.

12. Verhagen LM, de Jonge MI, Burghout P, Schraa K, Spagnuolo L, MennensS, Eleveld MJ, van der Gaast-de Jongh CE, Zomer A, Hermans PWM, Bootsma HJ. 2014. Genome-wide identification of genes essential for the survival of *Streptococcus*

pneumoniae in human saliva. PLoS One. 9:e89541. https://doi.org/10.1371/journal.pone.0089541.

13. Wang N, Ozer EA, Mandel MJ, Hauser AR. 2014. Genome-wide identification of *Acinetobacter baumannii* genes necessary for persistence in the lung. mBio 5:e01163. https://doi.org/10.1128/mBio.01163-14.
14. Gutierrez MG, Yoder-Himes DR, Warawa JM. 2015. Comprehensive identification of virulence factors required for respiratory melioidosis using Tn-seq mutagenesis. Front Cell Infect Microbiol 5:78. https://doi.org/10 .3389/fcimb.2015.00078.
15. Moule MG, Spink N, Willcocks S, Lim J, Guerra-Assunção JA, Cia F,Champion OL, Senior NJ, Atkins HS, Clark T, Bancroft GJ, Cuccui J, Wren BW. 2016. Characterization of new virulence factors involved in the intracellular growth and survival of *Burkholderia pseudomallei*. Infect Immun 84:701–710. https://doi.org/10.1128/IAI.01102-15.
16. Perry BJ, Akter MS, Yost CK. 2016. The use of transposon insertionsequencing to interrogate the core functional genome of the legume symbiont *Rhizobium leguminosarum*. Front Microbiol 7:1873. https://doi .org/10.3389/fmicb.2016.01873.
17. Forsyth RA, Haselbeck RJ, Ohlsen KL, Yamamoto RT, Xu H, Trawick JD,Wall D, Wang L, Brown-Driver V, Froelich JM, C KG, King P, McCarthy M, Malone C, Misiner B, Robbins D, Tan Z, Zhu Zy Z, Carr G, Mosca DA, Zamudio C, Foulkes JG, Zyskind JW. 2002. A genome-wide strategy for the identification of essential genes in

Staphylococcus aureus. Mol Microbiol 43:1387–1400. https://doi.org/10.1046/j.1365-2958.2002.02832.x.

18. Ji Y, Zhang B, Van SF, Horn, Warren P, Woodnutt G, Burnham MK, Rosenberg M. 2001. Identification of critical staphylococcal genes using conditional phenotypes generated by antisense RNA. Science 293: 2266–2269. https://doi.org/10.1126/science.1063566.
19. Jackson AL, Bartz SR, Schelter J, Kobayashi SV, Burchard J, Mao M, Li B,Cavet G, Linsley PS. 2003. Expression profiling reveals off-target gene regulation by RNAi. Nat Biotechnol 21:635–637. https://doi.org/10.1038/ nbt831.
20. Doench JG, Petersen CP, Sharp PA. 2003. siRNAs can function as miRNAs.Genes Dev 17:438–442. https://doi.org/10.1101/gad.1064703.
21. Sigoillot FD, Lyman S, Huckins JF, Adamson B, Chung E, Quattrochi B,King RW. 2012. A bioinformatics method identifies prominent offtargeted transcripts in RNAi screens. Nat Methods 9:363–366. https://doi .org/10.1038/nmeth.1898.
22. Cho SH, Haning K, Contreras LM. 2015. Strain engineering via regulatorynoncoding RNAs: not a one-blueprint-fits-all. Curr Opin Chem Eng 10: 25–34. https://doi.org/10.1016/j.coche.2015.07.008.
23. de Lorenzo V, Eltis L, Kessler B, Timmis KN. 1993. Analysis of *Pseudomonas* gene products using lacIq/Ptrp-lac plasmids and transposons that confer conditional phenotypes. Gene 123:17–24. https://doi.org/10 .1016/0378-1119(93)90533-9.

24. Castang S, McManus HR, Turner KH, Dove SL. 2008. H-NS family members function coordinately in an opportunistic pathogen. Proc Natl Acad Sci U S A 105:18947–18952. https://doi.org/10.1073/pnas.0808215105.

25. Wei J-R, Krishnamoorthy V, Murphy K, Kim J-H, Schnappinger D, Alber T,Sassetti CM, Rhee KY, Rubin EJ. 2011. Depletion of antibiotic targets has widely varying effects on growth. Proc Natl Acad Sci U S A 108:4176–4181. https://doi.org/10.1073/pnas.1018301108.

26. Cameron DE, Collins JJ. 2014. Tunable protein degradation in bacteria.Nat Biotechnol 32:1276–1128. https://doi.org/10.1038/nbt.3053.

27. Meisner J, Goldberg JB. 2016. The Escherichia coli rhaSR-PrhaBAD inducible promoter system allows tightly controlled gene expression over a wide range in *Pseudomonas aeruginosa*. Appl Environ Microbiol 82: 6715–6727. https://doi.org/10.1128/AEM.02041-16.

28. Qi LS, Larson MH, Gilbert LA, Doudna JA, Weissman JS, Arkin AP, Lim WA.2013. Repurposing CRISPR as an RNA-guided platform for sequencespecific control of gene expression. Cell 152:1173–1183. https://doi.org/ 10.1016/j.cell.2013.02.022.

29. Peters JM, Colavin A, Shi H, Czarny TL, Larson MH, Wong S, Hawkins JS,Lu CHS, Koo B-M, Marta E, Shiver AL, Whitehead EH, Weissman JS, Brown ED, Qi LS, Huang KC, Gross CA. 2016. A comprehensive, CRISPR-based functional analysis of essential genes in bacteria. Cell 165:1493–1506. https://doi.org/10.1016/j.cell.2016.05.003.

30. Jinek M, Chylinski K, Fonfara I, Hauer M, Doudna JA, Charpentier E. 2012. A programmable dual-RNA-guided DNA endonuclease in adaptive bacterial immunity. Science 337:816–821. https://doi.org/10.1126/science .1225829.

31. Peters JM, Koo B-M, Patino R, Heussler GE, Hearne CC, Qu J, Inclan YF,Hawkins JS, Lu CHS, Silvis MR, Harden MM, Osadnik H, Peters JE, Engel JN, Dutton RJ, Grossman AD, Gross CA, Rosenberg OS. 2019. Enabling genetic analysis of diverse bacteria with Mobile-CRISPRi. Nat Microbiol 4:244–250. https://doi.org/10.1038/s41564-018-0327-z.

32. Zhang S, Voigt CA. 2018. Engineered dCas9 with reduced toxicity inbacteria: implications for genetic circuit design. Nucleic Acids Res 46: 11115–11125. https://doi.org/10.1093/nar/gky884.

33. Rock JM, Hopkins FF, Chavez A, Diallo M, Chase MR, Gerrick ER, PritchardJR, Church GM, Rubin EJ, Sassetti CM, Schnappinger D, Fortune SM. 2017. Programmable transcriptional repression in mycobacteria using an orthogonal CRISPR interference platform. Nat Microbiol 2:16274. https:// doi.org/10.1038/nmicrobiol.2016.274.

34. Khlebnikov A, Risa O, Skaug T, Carrier TA, Keasling JD. 2000. Regulatablearabinose-inducible gene expression system with consistent control in all cells of a culture. J Bacteriol 182:7029–7034. https://doi.org/10.1128/ jb.182.24.7029-7034.2000.

35. Jang S, Jang S, Jung GY. 2018. Toward tunable dynamic repressionusing CRISPRi. Biotechnol J 13:e1800152. https://doi.org/10.1002/biot .201800152.

36. Loessner H, Leschner S, Endmann A, Westphal K, Wolf K, Kochruebe K,Miloud T, Altenbuchner J, Weiss S. 2009. Drug-inducible remote control of gene expression by probiotic *Escherichia coli* Nissle 1917 in intestine, tumor and gall bladder of mice. Microbes Infect 11:1097–1105. https:// doi.org/10.1016/j.micinf.2009.08.002.

37. Loessner H, Endmann A, Leschner S, Westphal K, Rohde M, Miloud T, Hämmerling G, Neuhaus K, Weiss S. 2007. Remote control of tumourtargeted *Salmonella enterica* serovar Typhimurium by the use of L-arabinose as inducer of bacterial gene expression in vivo. Cell Microbiol 9:1529–1537. https://doi.org/10.1111/j.1462-5822.2007.00890.x.

38. Seri K, Sanai K, Matsuo N, Kawakubo K, Xue C, Inoue S. 1996. L-arabinose selectively inhibits intestinal sucrase in an uncompetitive manner and suppresses glycemic response after sucrose ingestion in animals. Metab Clin Exp 45:1368–1374. https://doi.org/10.1016/S0026-0495(96)90117-1.

39. Hovey AK, Frank DW. 1995. Analyses of the DNA-binding and transcriptional activation properties of ExsA, the transcriptional activator of the *Pseudomonas aeruginosa* exoenzyme S regulon. J Bacteriol 177: 4427–4436. https://doi.org/10.1128/jb.177.15.4427-4436.1995.

40. Liberati NT, Urbach JM, Miyata S, Lee DG, Drenkard E, Wu G, Villanueva J,Wei T, Ausubel FM. 2006. An ordered, nonredundant library of *Pseudomonas aeruginosa*

strain PA14 transposon insertion mutants. Proc Natl Acad Sci U S A 103:2833–2838. https://doi.org/10.1073/pnas.0511100103.

41. Marsden AE, Intile PJ, Schulmeyer KH, Simmons-Patterson ER, Urbanowski ML, Wolfgang MC, Yahr TL. 2016. Vfr directly activates exsA transcription to regulate expression of the *Pseudomonas aeruginosa* type III secretion system. J Bacteriol 198:1442–1450. https://doi.org/10.1128/ JB.00049-16.

42. Apodaca G, Bomsel M, Lindstedt R, Engel J, Frank D, Mostov KE, WienerKronish J. 1995. Characterization of *Pseudomonas aeruginosa*-induced MDCK cell injury: glycosylation-defective host cells are resistant to bacterial killing. Infect Immun 63:1541–1551.

43. Kudoh I, Wiener-Kronish JP, Hashimoto S, Pittet JF, Frank D. 1994. Exoproduct secretions of *Pseudomonas aeruginosa* strains influence severity of alveolar epithelial injury. Am J Physiol 267:L551–L556. https:// doi.org/10.1152/ajplung.1994.267.5.L551.

44. Ortiz-Muñoz G, Looney MR. 2015. Non-invasive intratracheal instillationin mice. Bio Protoc 5:e1504. https://doi.org/10.21769/BioProtoc.1504.

45. Murry JP, Sassetti CM, Lane JM, Xie Z, Rubin EJ. 2008. Transposon sitehybridization in *Mycobacterium tuberculosis*. Methods Mol Biol 416: 45–59. https://doi.org/10.1007/978-1-59745-321-9_4.

46. Hensel M, Shea JE, Gleeson C, Jones MD, Dalton E, Holden DW. 1995.

Simultaneous identification of bacterial virulence genes by negative selection. Science 269:400–403. https://doi.org/10.1126/science.7618105.

47. Zhao H, Sun Y, Peters JM, Gross CA, Garner EC, Helmann JD. 2016. Depletion of undecaprenyl pyrophosphate phosphatases disrupts cell envelope biogenesis in *Bacillus subtilis*. J Bacteriol 198:2925–2935. https://doi.org/10.1128/JB.00507-16.

48. Rousset F, Cui L, Siouve E, Becavin C, Depardieu F, Bikard D. 2018. Genome-wide CRISPR-dCas9 screens in *E. coli* identify essential genes and phage host factors. PLoS Genet 14:e1007749. https://doi.org/10 .1371/journal.pgen.1007749.

49. Rice LB. 2008. Federal funding for the study of antimicrobial resistancein nosocomial pathogens: no ESKAPE. J Infect Dis 197:1079–1108. https://doi.org/10.1086/533452.

50. El Solh AA, Akinnusi ME, Wiener-Kronish JP, Lynch SV, Pineda LA, SzarpaK. 2008. Persistent infection with *Pseudomonas aeruginosa* in ventilatorassociated pneumonia. Am J Respir Crit Care Med 178:513–519. https:// doi.org/10.1164/rccm.200802-239OC.

51. Lequette Y, Lee JH, Ledgham F, Lazdunski A, Greenberg EP. 2006. Adistinct QscR regulon in the *Pseudomonas aeruginosa* quorum-sensing circuit. J Bacteriol 188:3365–3370. https://doi.org/10.1128/JB.188.9.3365 -3370.2006.

52. Livak KJ, Schmittgen TD. 2001. Analysis of relative gene expression datausing real-time quantitative PCR and the 2(-Delta Delta C(T)) Method. Methods 25:402–408. https://doi.org/10.1006/meth.2001.1262.

53. Langmead B, Salzberg S. 2012. Fast gapped-read alignment with Bowtie 2. Nat Methods 9:357–359. https://doi.org/10.1038/nmeth.1923.

54. Anders S, Pyl PT, Huber W. 2015. HTSeq—a Python framework to workwith high-throughput sequencing data. Bioinformatics 31:166–169. https://doi.org/10.1093/bioinformatics/btu638.

55. Edgar R, Domrachev M, Lash AE. 2002. Gene Expression Omnibus: NCBIgene expression and hybridization array data repository. Nucleic Acids Res 30:207–210. https://doi.org/10.1093/nar/30.1.207.

Chapter 3

Tool Application: Profiling genetic vulnerabilities to host clearance mechanisms

Abstract

Multi-drug resistant *Pseudomonas aeruginosa* causes highly morbid infections that are challenging to treat. While antibiotics reduce bacterial populations during infection, host immunity plays a key role in elimination of pathogenic bacteria. Identifying genetic targets that create vulnerabilities to host clearance mechanisms may uncover strategies to potentiate host immunity against bacterial infections. We developed a pooled *in vivo* CRISPRi screen that revealed that partial genetic depletions of 197 individual *P. aeruginosa* genes generated fitness defects in a murine pneumonia model. *pgsA*, an essential gene uncovered in our screen known to be strongly upregulated in human infection, demonstrated significant vulnerability to host clearance despite limited *in vitro* fitness defects. The use of CRISPRi screening to uncover genetic vulnerabilities represents a promising strategy to prioritize antibacterial targets that interact with host immunity.

Introduction

Pseudomonas aeruginosa is an environmental bacterium that is a common causative agent of both acute and chronic infections. Due to its inherent resistance to antibiotics and increasing levels of acquired resistance, multi-drug resistant *P. aeruginosa* has been prioritized as a serious threat by the WHO. (1) While *P. aeruginosa* is estimated to have 321 core essential genes required for growth of multiple strains under multiple culturing conditions, (2) only a small fraction of these genes have been targeted for inhibition by small molecule antibiotics in clinical use and clinical development. (3)

While antibiotics are useful for reducing the bacterial burden during infection, their interactions and potential synergy with native host processes for bacterial clearance are underexploited. It is conceivable that the extent of target inhibition required for bacterial growth inhibition *in vitro* may exceed that which is needed *in vivo*, where the host immune system mediates clearance of the infection. For example, the synergy of beta-lactam antibiotics with host-produced antimicrobial peptides has been shown to reduce the burden of bacteria demonstrating *in vitro* resistance to the beta-lactam. (4–8)

Consequently, target-based whole-cell screens in antibiotic discovery efforts may neglect chemical matter with sufficient *in vivo* efficacy due to poor *in vitro* potency. Comparison of *in vitro* minimal inhibitory concentrations of antibiotics with their associated reduction of bacterial burden during *in vivo* infections is confounded by pharmacokinetic and pharmacodynamic properties of the antibiotic. Thus, a goal of

bacterial geneticists has been to substitute chemical inhibition with genetic inhibition, thereby eliminating this confounding effect and expanding the scope of potential antibacterial gene targets to include those without known chemical inhibitors.

For genes that are non-essential *in vitro*, large-scale genetic inhibition through transposon insertion sequencing has previously led to the classification of *in vivo* gene essentiality. (9) Transposon sequencing of *P. aeruginosa* under various infection conditions has revealed many virulence factors, where gene knockout leads to attenuated virulence of the mutant strain. (10) However, anti-virulence interventions have yet to demonstrate clinical efficacy and may not be suitable for people experiencing chronic *P. aeruginosa* lung infections associated with cystic fibrosis, often characterized by downregulation or loss-of-function mutations in virulence associated genes. (11) Given that complete genetic inhibition strategies cannot be used to probe potential antibiotic targets due to *in vitro* essentiality, a partial genetic perturbation strategy enables us to probe this valuable category of genes.

Importantly, the notion of essentiality implies a binary effect of genetic inhibition on bacterial fitness, even though intermediary inhibition with chemical drugs indicates that the effect of target inhibition on fitness is, instead, a continuous variable. This gradient is captured by gene vulnerability, (12) where partial genetic perturbation of essential genes can confer a quantifiable fitness defect. The significance and magnitude of gene vulnerability may vary based on culture conditions and can be measured by depletion of

the specific mutant from a pooled library. (12–16) Essential genes with large *in vivo* vulnerabilities may represent a promising new class of antibacterial targets, since antibiotics must often be administered at high dosages that are capped by dose-limiting adverse effects, and corresponding inhibitors with no *in vitro* efficacy may have been previously overlooked.

Essential genes have been historically difficult to manipulate precisely, as they are requisite for pathogen survival. CRISPR interference (CRISPRi), where a catalytically inactive variant of the Cas9 nuclease (dCas9) sterically hinders RNA polymerase elongation leading to reduced transcription, is a powerful tool for loss of function screens. We have previously developed Mobile-CRISPRi, a modular and scalable platform to construct knockdown strains in a variety of pathogens, (17–19) which enables us to detect gene vulnerability under *in vitro* and *in vivo* settings.

A recent pooled CRISPRi screen of the Gram-positive microorganism *Streptococcus pneumoniae* in a murine pneumonia model revealed new potential virulence factors and the *in vivo* non-essentiality of a potential antibiotic target that was essential *in vitro*. (20) 31 genes were identified with greater *in vivo* essentiality ($\log_2$FC >1, p_{adj}<0.05) than *in vitro* essentiality; however, due to severe infection-associated bottlenecks limiting screen robustness, the knockdown of only one non-essential gene (*purA*) was confirmed to yield attenuated virulence, with nearly 2 log reduction in bacterial burden. Co-infection with influenza A virus promoted *S. pneumoniae* growth, overcoming the infection bottleneck

and enabling the identification of several virulence-associated genes. The present study details a different protocol to surmount infection-associated bottlenecks in a *P. aeruginosa* lung infection model.

Conditional induction or repression of genes during infection are presumably associated with adaptations required for maintaining fitness in various environments. As such, elevated gene expression during infection provides circumstantial evidence for the gene's role in bacterial processes important for establishing and/or maintaining infection. In our partial genetic inhibition studies, we gather gene vulnerability insights and explore the implications of gene upregulation during infection.

Results

Mobile-CRISPRi Enables Pooled Construction of an Essential Gene Knockdown Library

Due to concerns pertaining to the titratability and uniformity of gene knockdown when using an inducible CRISPRi promoter in an *in vivo* model, we previously characterized the efficacy of constitutive promoters (17) to drive CRISPR interference. Repression of *mrfp* in PA14 using three different constitutive promoters (P1, P2, P3) driving dCas9 activity generated a range of 88% decrease of fluorescence by P1 to 94% by P3 when paired with the same *mrfp*-targeting sgRNA. (17) Comparing the fluorescence-based *mrfp* knockdown ratios (non-targeting sgRNA: targeting sgRNA), P3 is less than double the

strength of P1. To identify highly vulnerable genes during infection, where slight genetic perturbation confers a large *in vivo* fitness defect despite limited *in vitro* deficiencies, we employed a weak promoter (P1) in construction of a pooled PA14 essential gene knockdown library.

Targeted genes in the PA14 essential gene knockdown library were chosen from a transposon sequencing study that identified the "core" essential genome for *Pseudomonas*. (2) Genes that were deemed essential in atleast one of the lab or infection-related growth media were included in our library design (**Supplementary Table 3.1**). For each gene targeted, four sgRNAs were synthesized with complementarity to the gene at varied distances from the transcription start site. (18) To assess bottlenecks and control for the effects of CRISPRi knockdown during *in vivo* experiments, 1,000 non-targeting sgRNAs were included in the pooled sgRNA library as negative controls. After insertion of the pooled sgRNA library into the Mobile-CRISPRi plasmids, the constructs were chromosomally integrated into PA14 through triparental mating (**Figure 3.1**).

Supplementary Table 3.1: PA14 Essential Gene Knockdown Library

Gene ID, name, and essentiality in 9 different *Pseudomonas* strains in 5 different conditions (as reported by Poulsen et. al.). Genes that are essential in all 9 strains across all tested conditions (LB, M9, Fetal Bovine Serum, Synthetic Cystic Fibrosis Medium, and urine) are deemed "Core" essential genes, whereas genes that are essential in only a subset of those conditions are deemed "Conditional".

PA14_ID	Gene Name	# strains essential (LB)	# strains essential (M9)	# strains essential (FBS)	# strains essential (SCFM)	# strains essential (Urine)	Essential Category
PA14_00010	dnaA	9	9	9	9	9	Core
PA14_00020	dnaN	9	9	9	9	9	Core
PA14_00050	gyrB	9	9	9	9	9	Core
PA14_00060	plsC	9	0	9	9	1	Conditional
PA14_00070	gmhB	9	9	9	9	9	Core
PA14_00090	glyS	9	9	9	9	9	Core
PA14_00100	glyQ	9	9	9	9	9	Core
PA14_00190	fmt	9	9	9	9	9	Core
PA14_00200	def	9	7	9	9	9	Conditional
PA14_00240	tsaC	9	9	9	9	9	Core
PA14_00280	hemF	9	9	0	9	9	Conditional
PA14_00290	aroE	9	9	8	9	9	Conditional
PA14_00440	trpA	0	9	3	9	2	Conditional
PA14_00450	trpB	0	9	6	9	1	Conditional
PA14_04110	serA	8	9	9	9	0	Conditional
PA14_04310	rpiA	9	9	9	9	9	Core
PA14_04380		0	9	0	0	0	Conditional
PA14_04460	lgt	9	9	9	9	9	Core
PA14_04480	thyA	9	9	9	9	9	Core
PA14_04580	folA	9	9	9	9	9	Core
PA14_04630	ilvD	0	9	0	0	9	Conditional
PA14_04750	fdx1	9	9	9	9	9	Core
PA14_04760	coaD	9	9	9	9	9	Core
PA14_04900	ftsY	9	9	9	9	9	Core
PA14_04930	rpoH	9	9	9	9	9	Core
PA14_04980	thiG	0	9	0	9	0	Conditional
PA14_05070	metW	0	9	8	0	9	Conditional
PA14_05080	metX	0	9	8	0	9	Conditional
PA14_05150	proC	0	9	0	0	0	Conditional
PA14_05250	pyrC	0	9	9	9	9	Conditional

PA14_ID	Gene Name	# strains essential (LB)	# strains essential (M9)	# strains essential (FBS)	# strains essential (SCFM)	# strains essential (Urine)	Essential Category
PA14_05260	pyrB	0	8	9	9	9	Conditional
PA14_05280	yqgF	9	9	9	9	9	Core
PA14_05460	bioA	9	9	0	9	9	Conditional
PA14_05550	oprM	9	0	2	0	9	Conditional
PA14_05590	metF	0	9	9	0	9	Conditional
PA14_05620	sahH	9	9	9	9	9	Core
PA14_06500	bioB	9	9	0	9	9	Conditional
PA14_06510	bioF	9	9	0	9	9	Conditional
PA14_06540	bioC	9	9	1	9	8	Conditional
PA14_06570	bioD	9	9	0	9	9	Conditional
PA14_07090	metK	9	9	9	9	9	Core
PA14_07130	tktA	9	9	9	9	9	Core
PA14_07170	epd	9	1	0	9	0	Conditional
PA14_07190	pgk	9	0	0	9	0	Conditional
PA14_07230	fda	9	9	9	9	9	Core
PA14_07520	rpoD	9	9	9	9	9	Core
PA14_07530	dnaG	9	9	9	9	9	Core
PA14_07560	rpsU	9	9	9	9	9	Core
PA14_07570	gcp	9	9	9	9	9	Core
PA14_07590	folB	9	9	9	9	9	Core
PA14_07620	cca	9	9	9	9	1	Conditional
PA14_07740	pdxA	9	9	0	9	8	Conditional
PA14_07760	surA	9	9	9	9	9	Core
PA14_07770	ostA	9	9	9	9	9	Core
PA14_07910	rpe	9	9	9	9	9	Core
PA14_07940	trpE	0	9	0	0	0	Conditional
PA14_08350	trpD	0	9	0	8	0	Conditional
PA14_08360	trpC	0	9	0	9	1	Conditional
PA14_08400	COQ7	9	9	9	9	9	Core
PA14_08470	hemJ	9	9	0	9	9	Conditional
PA14_08480	argC	0	9	9	1	9	Conditional
PA14_08510	yadR	9	9	9	9	9	Core
PA14_08620	birA	9	9	9	9	9	Core
PA14_08630	coaX	9	9	9	9	9	Core
PA14_08710	nusG	9	9	9	9	9	Core
PA14_08720	rplK	9	9	9	9	9	Core
PA14_08730	rplA	9	9	9	9	9	Core

PA14_ID	Gene Name	# strains essential (LB)	# strains essential (M9)	# strains essential (FBS)	# strains essential (SCFM)	# strains essential (Urine)	Essential Category
PA14_08740	rplJ	9	9	9	9	9	Core
PA14_08760	rpoB	9	9	9	9	9	Core
PA14_08780	rpoC	9	9	9	9	9	Core
PA14_08790	rpsL	9	9	9	9	9	Core
PA14_08810	rpsG	9	9	9	9	9	Core
PA14_08820	fusA1	9	9	9	9	9	Core
PA14_08840	rpsJ	9	9	9	9	9	Core
PA14_08850	rplC	9	9	9	9	9	Core
PA14_08860	rplD	9	9	9	9	9	Core
PA14_08870	rplW	9	9	9	9	9	Core
PA14_08880	rplB	9	9	9	9	9	Core
PA14_08890	rpsS	9	9	9	9	9	Core
PA14_08910	rpsC	9	9	9	9	9	Core
PA14_08920	rplP	9	9	9	9	9	Core
PA14_08940	rpsQ	9	9	9	9	9	Core
PA14_08950	rplN	9	9	9	9	9	Core
PA14_08960	rplX	9	9	9	9	9	Core
PA14_08970	rplE	9	9	9	9	9	Core
PA14_08980	rpsN	9	9	9	9	9	Core
PA14_08990	rpsH	9	9	9	9	9	Core
PA14_09000	rplF	9	9	9	9	9	Core
PA14_09010	rplR	9	9	9	9	9	Core
PA14_09020	rpsE	9	9	9	9	9	Core
PA14_09040	rplO	9	1	6	9	1	Conditional
PA14_09050	secY	9	9	9	9	9	Core
PA14_09080	rpsM	9	9	9	9	9	Core
PA14_09090	rpsK	9	9	9	9	9	Core
PA14_09100	rpsD	9	9	9	9	9	Core
PA14_09115	rpoA	9	9	9	9	9	Core
PA14_09130	rplQ	9	9	9	9	9	Core
PA14_11090	cupB4	1	8	5	9	5	Conditional
PA14_11400	ribD	9	9	9	9	9	Core
PA14_11410	ribC	9	9	9	9	9	Core
PA14_11450	nusB	9	9	9	9	9	Core
PA14_11460	thiL	9	9	9	9	9	Core
PA14_11510	ribA	9	9	9	9	9	Core
PA14_11550	dxs	9	9	9	9	9	Core

PA14_ID	Gene Name	# strains essential (LB)	# strains essential (M9)	# strains essential (FBS)	# strains essential (SCFM)	# strains essential (Urine)	Essential Category
PA14_11560	ispA	3	1	9	9	1	Conditional
PA14_11690	ppa	9	9	9	9	9	Core
PA14_11845	mpl	7	2	2	9	5	Conditional
PA14_11860	ubiX	9	8	9	9	9	Conditional
PA14_12010	proA	0	9	0	0	0	Conditional
PA14_12060	pbpA	9	9	9	9	9	Core
PA14_12070	rodA	9	9	9	9	9	Core
PA14_12120	lipB	9	9	9	9	9	Core
PA14_12130	lis	9	9	9	9	9	Core
PA14_12200	holA	9	9	9	9	9	Core
PA14_12210	lptE	9	9	9	9	9	Core
PA14_12230	leuS	9	9	9	9	9	Core
PA14_12280	cutE	9	9	9	9	9	Core
PA14_12310	ybeY	9	9	9	9	9	Core
PA14_12390	hemL	9	9	0	9	9	Conditional
PA14_12400	thiE	0	9	0	9	0	Conditional
PA14_12410	thiD	0	9	0	9	0	Conditional
PA14_14440	valS	9	9	9	9	9	Core
PA14_14500	yjgP	9	9	9	9	9	Core
PA14_14510	yjgQ	9	9	9	9	9	Core
PA14_14630	secD	9	9	9	9	9	Core
PA14_14650	secF	9	9	9	9	9	Core
PA14_14680	suhB	9	9	9	9	9	Core
PA14_14730	iscS	9	9	9	9	9	Core
PA14_14750	iscA	9	9	9	9	9	Core
PA14_14770	hscB	9	9	9	9	9	Core
PA14_14780	hscA	9	9	9	9	9	Core
PA14_14800	fdx2	9	9	9	9	9	Core
PA14_14820	ndk	9	9	9	9	6	Conditional
PA14_14880	gcpE	9	9	9	9	9	Core
PA14_14890	hisS	9	9	9	9	9	Core
PA14_14930	engA	9	9	9	9	9	Core
PA14_15030	leuA	0	9	0	0	2	Conditional
PA14_15310	guaB	9	9	9	9	9	Core
PA14_15340	guaA	9	9	9	9	9	Core
PA14_15680	cumB	9	9	9	9	9	Core
PA14_15740	purL	0	9	9	9	7	Conditional

PA14_ID	Gene Name	# strains essential (LB)	# strains essential (M9)	# strains essential (FBS)	# strains essential (SCFM)	# strains essential (Urine)	Essential Category
PA14_15960	ffh	9	9	9	9	9	Core
PA14_15970	rpsP	9	8	9	8	8	Conditional
PA14_15980	rimM	9	9	9	9	9	Core
PA14_15990	trmD	9	1	9	9	2	Conditional
PA14_16070	hom	0	9	9	0	9	Conditional
PA14_16090	thrC	0	9	8	0	7	Conditional
PA14_16480	wspF	8	9	4	9	9	Conditional
PA14_16510	prfB	9	9	9	9	9	Core
PA14_16530	lysS	9	9	9	9	9	Core
PA14_16700	adk	9	9	9	9	9	Core
PA14_16710	yeaZ	9	9	9	9	9	Core
PA14_16950	dapD	9	9	9	9	9	Core
PA14_17060	rpsB	9	9	9	9	9	Core
PA14_17070	tsf	9	9	9	9	9	Core
PA14_17080	pyrH	9	9	9	9	9	Core
PA14_17100	frr	9	9	9	9	9	Core
PA14_17110	uppS	9	9	9	9	9	Core
PA14_17120	cdsA	9	9	9	9	9	Core
PA14_17130	dxr	9	9	9	9	9	Core
PA14_17150	bamA	9	9	9	9	9	Core
PA14_17180	lpxD	9	9	9	9	9	Core
PA14_17190	fabZ	9	9	9	9	9	Core
PA14_17210	lpxA	9	9	9	9	9	Core
PA14_17220	lpxB	9	9	9	9	9	Core
PA14_17260	dnaE	9	9	9	9	9	Core
PA14_17270	accA	9	9	9	9	9	Core
PA14_17280	mesJ	9	9	9	9	9	Core
PA14_17290	pyrG	9	9	9	9	9	Core
PA14_17310	kdsA	9	9	9	9	9	Core
PA14_17320	eno	9	9	8	9	9	Conditional
PA14_17340	ispD	9	9	9	9	9	Core
PA14_17420	ispF	9	9	9	9	9	Core
PA14_17930	glpD	9	1	9	9	1	Conditional
PA14_18610	argF	0	9	2	0	9	Conditional
PA14_18700	rnt	9	3	6	9	5	Conditional
PA14_18710	pyrC	9	9	9	9	9	Core
PA14_18740	argG	0	9	9	2	9	Conditional

PA14_ID	Gene Name	# strains essential (LB)	# strains essential (M9)	# strains essential (FBS)	# strains essential (SCFM)	# strains essential (Urine)	Essential Category
PA14_19050	metG	9	9	9	9	9	Core
PA14_19065	mrp	9	9	9	9	9	Core
PA14_19090	dcd	9	1	9	9	9	Conditional
PA14_20140	fpr	9	9	9	9	9	Core
PA14_22010	minE	9	1	9	1	2	Conditional
PA14_22020	minD	9	0	1	1	0	Conditional
PA14_22040	minC	9	0	0	1	0	Conditional
PA14_23070	zwf	0	9	0	0	0	Conditional
PA14_23080	pgl	0	9	0	4	2	Conditional
PA14_23090	eda	0	9	0	0	0	Conditional
PA14_23220	ubiG	9	9	9	9	9	Core
PA14_23260	gyrA	9	9	9	9	9	Core
PA14_23270	serC	9	9	9	9	8	Conditional
PA14_23280	pheA	9	9	4	0	0	Conditional
PA14_23290	hisC2	9	0	1	1	0	Conditional
PA14_23310		9	6	9	9	2	Conditional
PA14_23320	cmk	9	9	9	9	9	Core
PA14_23330	rpsA	9	9	9	9	9	Core
PA14_23460	orfN	9	6	9	9	9	Conditional
PA14_23500	tyrB	1	9	8	1	9	Conditional
PA14_23560	gltx	9	9	9	9	9	Core
PA14_23750	leuC	0	9	0	0	9	Conditional
PA14_23760	leuD	0	9	0	0	9	Conditional
PA14_23790	leuB	0	9	0	0	9	Conditional
PA14_23800	asd	9	9	9	9	9	Core
PA14_23850	trpF	0	9	0	0	0	Conditional
PA14_23860	accD	9	9	9	9	9	Core
PA14_23880	folC	9	9	9	9	9	Core
PA14_23920	purF	0	9	9	9	3	Conditional
PA14_23930	metZ	0	9	8	0	9	Conditional
PA14_24220	ppnK	9	9	9	9	9	Core
PA14_24640	pyrD	9	9	9	9	9	Core
PA14_24710	evgA	3	1	9	3	1	Conditional
PA14_25080	fadB	9	1	0	1	1	Conditional
PA14_25090	foaB	9	0	0	1	0	Conditional
PA14_25110	topA	9	9	9	9	9	Core
PA14_25250	gapA	9	0	9	9	4	Conditional

PA14_ID	Gene Name	# strains essential (LB)	# strains essential (M9)	# strains essential (FBS)	# strains essential (SCFM)	# strains essential (Urine)	Essential Category
PA14_25390	sth	9	0	0	1	0	Conditional
PA14_25430	lolC	9	9	9	9	9	Core
PA14_25440	lolD	9	9	9	9	9	Core
PA14_25450	lolE	9	9	9	9	9	Core
PA14_25500	exbD	9	0	4	8	9	Conditional
PA14_25510	lpxK	9	9	9	9	9	Core
PA14_25530	kdsB	9	9	9	9	9	Core
PA14_25550	murB	9	9	9	9	9	Core
PA14_25560	rne	9	9	9	9	9	Core
PA14_25650	fabD	9	9	9	9	9	Core
PA14_25660	fabG	9	9	9	9	9	Core
PA14_25690	fabF1	8	1	9	4	1	Conditional
PA14_25740	tmk	9	9	9	9	9	Core
PA14_25760	holB	9	9	9	9	9	Core
PA14_25840	ETFDH	9	9	9	9	9	Core
PA14_25860	etfB	9	9	9	9	9	Core
PA14_25880	etfA	9	9	9	9	9	Core
PA14_25900	fabV	9	9	9	9	9	Core
PA14_26890	pyrF	2	8	9	9	9	Conditional
PA14_27210	efp	9	1	9	9	9	Conditional
PA14_27940	rsbU	9	1	9	9	1	Conditional
PA14_27950	rsbW	9	1	9	9	1	Conditional
PA14_28650	thrS	9	9	9	9	9	Core
PA14_28660	infC	9	9	9	9	9	Core
PA14_28680	rplT	9	9	9	9	9	Core
PA14_28690	pheS	9	9	9	9	9	Core
PA14_28710	pheT	9	9	9	9	9	Core
PA14_30110	purB	9	9	9	9	9	Core
PA14_30150	trmU	9	9	9	9	9	Core
PA14_30290	ftsK	9	9	9	9	9	Core
PA14_30310	lolA	9	9	9	9	9	Core
PA14_30330	serS	9	9	9	9	9	Core
PA14_30340	cysG	0	9	0	0	0	Conditional
PA14_30370	tusE	9	9	9	9	9	Core
PA14_30380	tusB	9	9	9	9	9	Core
PA14_30390	tusC	9	9	9	9	9	Core
PA14_30400	dsrE	9	9	9	9	9	Core

PA14_ID	Gene Name	# strains essential (LB)	# strains essential (M9)	# strains essential (FBS)	# strains essential (SCFM)	# strains essential (Urine)	Essential Category
PA14_30670	pgsA	9	9	9	9	9	Core
PA14_31290	pa1L	9	8	9	9	1	Conditional
PA14_31580	ACADM	1	9	1	4	8	Conditional
PA14_32130	xylL	7	9	9	7	6	Conditional
PA14_32420		9	0	0	5	1	Conditional
PA14_33270	pvdG	9	2	3	6	1	Conditional
PA14_33530		9	7	8	6	3	Conditional
PA14_33690	pvdE	9	9	9	9	9	Core
PA14_34600	gapB	5	9	3	2	0	Conditional
PA14_36780	mgtC	9	7	6	6	7	Conditional
PA14_38395	mexX	9	0	9	8	9	Conditional
PA14_38410	amrB	9	0	9	8	9	Conditional
PA14_39980	qscR	9	3	9	4	1	Conditional
PA14_41050	dnaQ	9	9	9	9	9	Core
PA14_41060	rnhA	9	1	3	2	2	Conditional
PA14_41350	folD	9	9	9	9	9	Core
PA14_41360	cysS	9	9	9	9	9	Core
PA14_41380	glnS	9	9	9	9	9	Core
PA14_41400	lpxH	9	9	9	9	9	Core
PA14_41470	acnB	9	9	9	9	9	Core
PA14_41575	sigX	9	1	9	9	6	Conditional
PA14_41840	cysH	0	9	2	0	0	Conditional
PA14_41870	cysB	0	9	0	0	0	Conditional
PA14_42720	masA	1	1	9	9	0	Conditional
PA14_42760	aroC	9	9	9	9	9	Core
PA14_43680	fabA	9	9	9	9	3	Conditional
PA14_43690	fabB	9	9	9	9	9	Core
PA14_43940	sucD	8	0	9	9	1	Conditional
PA14_43950	sucC	9	1	9	9	1	Conditional
PA14_43970	lpdG	9	9	9	9	9	Core
PA14_44000	sucB	9	9	9	9	9	Core
PA14_44010	sucA	9	9	9	9	9	Core
PA14_44020	sdhB	9	1	9	9	9	Conditional
PA14_44030	sdhA	9	1	9	9	9	Conditional
PA14_44050	sdhD	9	1	9	9	9	Conditional
PA14_44060	sdhC	9	1	9	9	9	Conditional
PA14_44070	gltA	9	9	9	9	2	Conditional

PA14_ID	Gene Name	# strains essential (LB)	# strains essential (M9)	# strains essential (FBS)	# strains essential (SCFM)	# strains essential (Urine)	Essential Category
PA14_44370	ccoN	0	1	9	0	0	Conditional
PA14_44440	fixI	1	1	9	9	1	Conditional
PA14_44630	dnaX	9	9	9	9	9	Core
PA14_44660	lig	9	9	9	9	9	Core
PA14_44910		8	3	9	7	3	Conditional
PA14_44920		9	9	9	9	6	Conditional
PA14_45290	ccmH	1	0	9	7	1	Conditional
PA14_45350	ccmC	8	1	9	9	1	Conditional
PA14_46020	yfiP	9	1	0	0	6	Conditional
PA14_46470	pdxB	9	9	0	9	0	Conditional
PA14_49340	pcpS	9	9	9	9	9	Core
PA14_49380	dapE	9	9	9	9	9	Core
PA14_49460	nrdA	9	9	9	9	9	Core
PA14_49470	nrdB	9	9	9	9	9	Core
PA14_50800	pdxH	9	9	0	9	8	Conditional
PA14_51270	dapA	9	8	6	9	1	Conditional
PA14_51710	oprL	9	9	9	9	9	Core
PA14_51720	tolB	9	9	9	9	9	Core
PA14_51730	tolA	9	9	9	9	9	Core
PA14_51740	tolR	9	9	9	9	9	Core
PA14_51750	tolQ	9	9	9	9	9	Core
PA14_51820	aspS	9	9	9	9	9	Core
PA14_51900	proS	9	9	9	9	9	Core
PA14_52010	hda	9	9	9	9	9	Core
PA14_52040	purM	0	9	9	9	2	Conditional
PA14_52050	purN	0	9	1	9	0	Conditional
PA14_52580	lysC	9	9	9	9	9	Core
PA14_52600	alaS	9	9	9	9	9	Core
PA14_52850		6	8	4	1	9	Conditional
PA14_54290	pdxJ	9	9	0	9	2	Conditional
PA14_54320	era	9	9	9	9	9	Core
PA14_54330	rnc	9	0	0	2	0	Conditional
PA14_54350	lepB	9	9	9	9	9	Core
PA14_54390	mucD	9	0	8	0	7	Conditional
PA14_54420	mucA	9	1	8	3	2	Conditional
PA14_54480	ygfZ	9	9	9	9	9	Core
PA14_55390		9	6	9	9	8	Conditional

PA14_ID	Gene Name	# strains essential (LB)	# strains essential (M9)	# strains essential (FBS)	# strains essential (SCFM)	# strains essential (Urine)	Essential Category
PA14_55660	recD	9	9	9	9	9	Core
PA14_55670	recB	9	9	9	9	9	Core
PA14_55690	recC	9	9	9	9	9	Core
PA14_55770	pitA	9	1	9	9	0	Conditional
PA14_55800	cpaA	9	9	9	9	7	Conditional
PA14_56300	fumA	9	1	5	9	1	Conditional
PA14_56780	sodB	9	9	9	9	9	Core
PA14_57010	groEL	9	9	9	9	9	Core
PA14_57020	groES	9	9	9	9	9	Core
PA14_57190	mutT	0	9	0	9	0	Conditional
PA14_57220	secA	9	9	9	9	9	Core
PA14_57250		9	9	9	9	9	Core
PA14_57260	lpxC	9	9	9	9	9	Core
PA14_57275	ftsZ	9	9	9	9	9	Core
PA14_57290	ftsA	9	9	9	9	9	Core
PA14_57300	ftsQ	9	9	9	9	9	Core
PA14_57330	murC	9	9	9	9	9	Core
PA14_57340	murG	9	9	9	9	9	Core
PA14_57360	ftsW	9	9	9	9	9	Core
PA14_57370	murD	9	9	9	9	9	Core
PA14_57380	mraY	9	9	9	9	9	Core
PA14_57390	murF	9	9	9	9	9	Core
PA14_57410	murE	9	9	9	9	9	Core
PA14_57425	ftsI	9	9	9	9	9	Core
PA14_57440	ftsL	9	9	9	9	9	Core
PA14_57450	mraW	9	9	9	9	9	Core
PA14_57460	mraZ	1	9	9	9	9	Conditional
PA14_57500	diaA	9	9	9	9	9	Core
PA14_57540	CYC1	0	1	9	8	1	Conditional
PA14_57560	CYTB	1	1	9	9	1	Conditional
PA14_57570	UQCRFS1	0	1	9	2	0	Conditional
PA14_57580	rpsI	9	9	9	9	9	Core
PA14_57590	rplM	9	9	9	9	9	Core
PA14_57670	trpS	9	9	9	9	9	Core
PA14_57770	hisC1	0	9	0	0	0	Conditional
PA14_57780	hisD	0	9	0	0	0	Conditional
PA14_57800	hisG	0	9	0	0	0	Conditional

PA14_ID	Gene Name	# strains essential (LB)	# strains essential (M9)	# strains essential (FBS)	# strains essential (SCFM)	# strains essential (Urine)	Essential Category
PA14_57810	murA	9	9	9	9	9	Core
PA14_57890	yrbH	9	9	9	9	9	Core
PA14_57910	lptC	9	9	9	9	9	Core
PA14_57920	lptA	9	9	9	9	9	Core
PA14_57930	lptB	9	9	9	9	9	Core
PA14_57940	rpoN	9	9	9	9	9	Core
PA14_57960	ptsN	9	1	9	9	1	Conditional
PA14_58120	mreD	9	9	9	9	9	Core
PA14_58130	mreC	9	9	9	9	9	Core
PA14_58150	mreB	9	9	9	9	9	Core
PA14_58180	gatA	9	9	9	9	9	Core
PA14_58190	gatB	9	9	9	9	9	Core
PA14_58700	nadC	0	9	0	8	0	Conditional
PA14_58780	coaE	9	9	9	9	9	Core
PA14_60230	comL	9	9	9	9	9	Core
PA14_60330	lytB	9	9	9	9	9	Core
PA14_60360	lspA	9	8	9	9	9	Conditional
PA14_60370	ileS	9	9	9	9	9	Core
PA14_60380	ribF	9	9	9	9	9	Core
PA14_60390	mviN	9	9	9	9	9	Core
PA14_60400	rpsT	9	9	9	9	9	Core
PA14_60420	proB	1	9	7	1	0	Conditional
PA14_60445	obg	9	9	9	9	9	Core
PA14_60450	rpmA	9	2	9	9	0	Conditional
PA14_60470	ispB	9	9	9	9	9	Core
PA14_60890	glyA	9	9	9	9	0	Conditional
PA14_61360		9	9	9	9	9	Core
PA14_61400	mqoB	9	2	9	9	2	Conditional
PA14_61580	hemH	9	9	0	9	9	Conditional
PA14_61660	murI	9	9	9	9	9	Core
PA14_61670	moeB	9	9	9	9	9	Core
PA14_61700	prfA	9	9	9	9	9	Core
PA14_61710	hemA	9	9	0	9	9	Conditional
PA14_61740	lolB	9	9	9	9	9	Core
PA14_61750	ipk	9	9	9	9	9	Core
PA14_61770	prs	9	6	9	9	7	Conditional
PA14_61790	pth	9	9	9	9	9	Core

PA14_ID	Gene Name	# strains essential (LB)	# strains essential (M9)	# strains essential (FBS)	# strains essential (SCFM)	# strains essential (Urine)	Essential Category
PA14_61840	vapI	4	3	9	4	5	Conditional
PA14_61890		9	9	9	9	9	Core
PA14_62120	pssA	9	9	9	9	9	Core
PA14_62130	ilvC	0	9	0	0	9	Conditional
PA14_62150	ilvH	0	9	0	5	9	Conditional
PA14_62160	ilvI	2	9	0	9	9	Conditional
PA14_62570	folK	9	9	9	9	9	Core
PA14_62580	panB	9	1	1	9	8	Conditional
PA14_62620	pgi	9	0	1	9	3	Conditional
PA14_62710	pnp	9	9	9	9	9	Core
PA14_62720	rpsO	9	9	9	9	9	Core
PA14_62760	infB	9	9	9	9	9	Core
PA14_62770	nusA	9	9	9	9	9	Core
PA14_62780	yhbC	9	9	9	9	9	Core
PA14_62830	tpiA	0	3	9	9	1	Conditional
PA14_62840	glmM	9	9	9	9	9	Core
PA14_62850	folP	9	9	9	9	9	Core
PA14_62860	ftsH	9	1	9	9	3	Conditional
PA14_62870	rrmJ	9	0	9	9	1	Conditional
PA14_62910	carB	8	9	9	9	9	Conditional
PA14_62930	carA	8	9	9	9	9	Conditional
PA14_62940	dapB	9	9	9	9	9	Core
PA14_62960	dnaJ	9	9	9	9	9	Core
PA14_62970	dnaK	9	1	9	9	1	Conditional
PA14_62990	grpE	9	9	9	9	9	Core
PA14_63020	fur	9	9	9	9	9	Core
PA14_63030	omlA	9	9	9	9	9	Core
PA14_64090	aroQ1	9	9	8	9	9	Conditional
PA14_64100	accB	9	9	9	9	9	Core
PA14_64110	accC	9	9	9	9	9	Core
PA14_64190	fis	9	9	9	9	9	Core
PA14_64200	purH	0	9	9	9	9	Conditional
PA14_64220	purD	2	9	9	9	9	Conditional
PA14_64980	nadE	9	9	9	9	9	Core
PA14_65130	dnaB	9	9	9	9	9	Core
PA14_65170	rpsR	9	9	9	9	9	Core
PA14_65180	rpsF	9	9	9	9	9	Core

PA14_ID	Gene Name	# strains essential (LB)	# strains essential (M9)	# strains essential (FBS)	# strains essential (SCFM)	# strains essential (Urine)	Essential Category
PA14_65230	purA	9	9	9	9	9	Core
PA14_65250	hisX	0	9	0	0	0	Conditional
PA14_65310	hfq	9	9	9	1	1	Conditional
PA14_65380	tsaE	9	9	9	9	9	Core
PA14_65410	orn	5	1	9	8	1	Conditional
PA14_65560	serB	8	9	8	7	0	Conditional
PA14_65570		9	9	9	9	9	Core
PA14_65605	parC	9	9	9	9	9	Core
PA14_65660	parE	9	9	9	9	9	Core
PA14_65740	thiC	0	9	0	9	0	Conditional
PA14_65960	kdtA	9	9	9	9	9	Core
PA14_66000		9	9	9	9	9	Core
PA14_66010		9	9	9	9	9	Core
PA14_66060	waaE	9	9	9	9	9	Core
PA14_66080	msbA	9	9	9	9	9	Core
PA14_66090		9	9	9	9	9	Core
PA14_66170		9	0	9	9	1	Conditional
PA14_66190		9	9	9	9	9	Core
PA14_66210	waaX	9	9	9	9	9	Core
PA14_66220	waaP	9	9	9	9	9	Core
PA14_66230	waaG	9	9	9	9	9	Core
PA14_66240	waaC	9	9	9	9	9	Core
PA14_66250	waaF	9	9	9	9	9	Core
PA14_66290	aceA	8	1	8	9	1	Conditional
PA14_66550	hemE	9	9	0	9	9	Conditional
PA14_66600	aroB	9	9	9	9	9	Core
PA14_66610	aroK	9	9	8	9	9	Conditional
PA14_66720	priA	9	9	9	9	8	Conditional
PA14_66750	argS	9	9	9	9	9	Core
PA14_66760		9	9	9	9	9	Core
PA14_66800		3	1	9	5	3	Conditional
PA14_66900	ubiE	9	9	9	9	9	Core
PA14_66910	ubiJ	9	9	9	9	9	Core
PA14_66920	ubiB	9	9	9	9	9	Core
PA14_66940	hisI	0	9	0	0	0	Conditional
PA14_66950	hisE	0	9	0	0	0	Conditional
PA14_66980	tatC	1	1	9	9	1	Conditional

PA14_ID	Gene Name	# strains essential (LB)	# strains essential (M9)	# strains essential (FBS)	# strains essential (SCFM)	# strains essential (Urine)	Essential Category
PA14_67490	fbp	9	9	9	9	9	Core
PA14_67600	glnA	9	9	9	9	9	Core
PA14_67770	pgm	9	9	8	9	9	Conditional
PA14_67880	hisF1	0	9	1	1	0	Conditional
PA14_67890	hisA	0	9	0	0	0	Conditional
PA14_67930	hisB	0	9	0	0	0	Conditional
PA14_68170	rmlB	9	2	9	9	4	Conditional
PA14_68190	rmlD	9	2	6	9	2	Conditional
PA14_68210	rmlC	9	2	9	9	7	Conditional
PA14_68360	fabY	9	9	9	9	9	Core
PA14_68670	ldcA	8	0	1	0	9	Conditional
PA14_68740	argA	0	9	9	0	9	Conditional
PA14_68955	ubiI	9	9	9	9	9	Core
PA14_68980	ubiH	9	9	9	9	9	Core
PA14_69150	ubiD	9	9	9	9	9	Core
PA14_69190	rho	9	9	9	9	9	Core
PA14_69200	trxA	9	1	9	9	8	Conditional
PA14_69240	hemB	9	9	0	9	9	Conditional
PA14_69440	hemD	9	9	0	9	9	Conditional
PA14_69450	hemC	9	9	0	9	9	Conditional
PA14_69500	argH	0	9	9	9	9	Conditional
PA14_69670	lysA	0	9	5	0	9	Conditional
PA14_69690	dapF	9	9	9	9	9	Core
PA14_69810	glnK	8	9	9	9	9	Conditional
PA14_69910	rep	9	1	9	9	9	Conditional
PA14_70190	rpmB	9	1	9	9	9	Conditional
PA14_70240	coaBC	9	9	9	9	9	Core
PA14_70260	dut	9	5	8	9	8	Conditional
PA14_70280	argB	0	9	0	0	9	Conditional
PA14_70370	pyrE	0	7	3	9	6	Conditional
PA14_70440	gmk	9	9	9	9	9	Core
PA14_70730	ubiA	9	9	9	9	9	Core
PA14_70800	phoU	8	9	8	9	6	Conditional
PA14_70810	pstB	9	0	0	2	0	Conditional
PA14_71600	purK	0	9	8	9	9	Conditional
PA14_71620	purE	0	9	9	9	9	Conditional
PA14_71720	oadA	0	9	0	0	0	Conditional

PA14_ID	Gene Name	# strains essential (LB)	# strains essential (M9)	# strains essential (FBS)	# strains essential (SCFM)	# strains essential (Urine)	Essential Category
PA14_71740	accC	0	9	1	0	0	Conditional
PA14_71750	pycR	0	9	0	0	0	Conditional
PA14_72480	engB	9	9	9	9	9	Core
PA14_72490	polA	3	1	9	7	1	Conditional
PA14_72970	tonB	9	9	9	9	9	Core
PA14_73170	glmS	9	9	9	9	9	Core
PA14_73220	glmU	9	9	9	9	9	Core
PA14_73240	atpD	9	9	9	9	9	Core
PA14_73250	atpG	9	9	9	9	9	Core
PA14_73260	atpA	9	9	9	9	9	Core
PA14_73280	atpH	9	9	9	9	9	Core
PA14_73310	atpB	9	9	9	9	9	Core
PA14_73320	atpI	9	1	9	9	9	Conditional
PA14_73370	gidA	9	9	9	9	9	Core
PA14_73400	thdF	9	9	9	9	9	Core
PA14_73410	yidC	9	9	9	9	9	Core

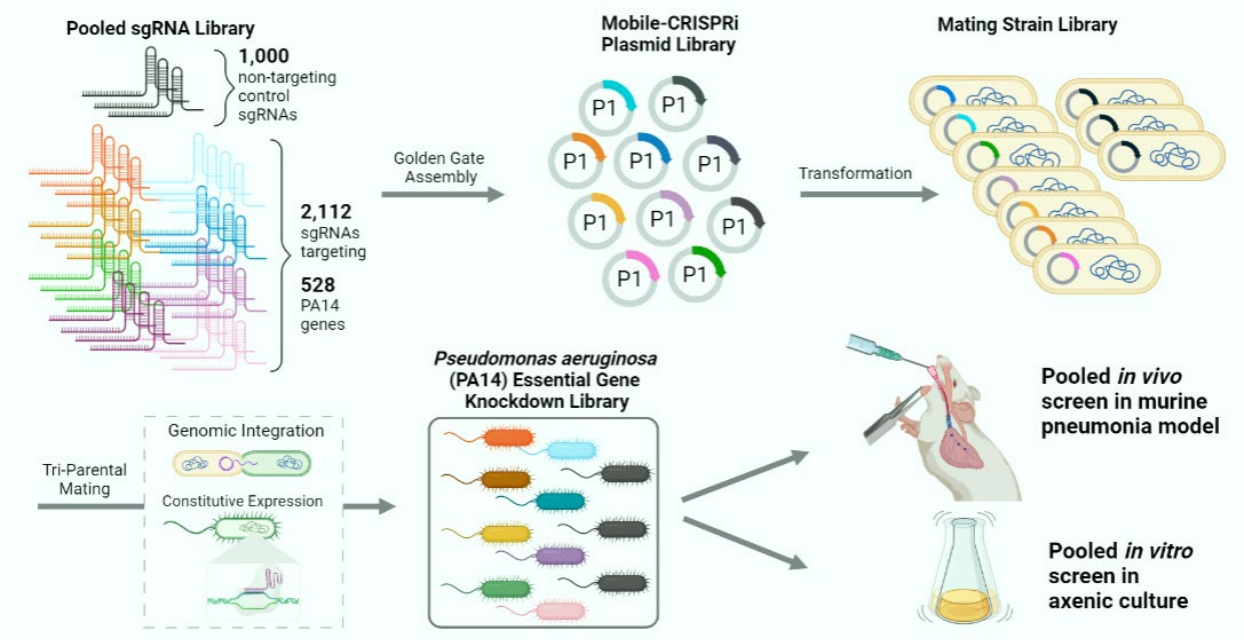

Figure 3.1: Construction of a *Pseudomonas* essential gene knockdown library
An sgRNA library of 3,112 oligonucleotides represents 528 PA14 genes demonstrating essentiality in LB or infection-related media targeted by 4 sgRNAs per gene as well as 1,000 non-targeting sgRNA controls. The pooled sgRNA library was inserted into restriction digested Mobile-CRISPRi plasmids containing a constitutive promoter driving dCas9 activity. The pooled Mobile-CRISPRi constructs were transferred into an *E. coli* mating strain and chromosomally integrated into PA14 through triparental mating to generate a pooled knockdown library.

The representation of the 1,000 non-targeting sgRNAs followed a normal distribution in the pooled mating strain library and in the pooled PA14 knockdown library (**Supplementary Fig. 3.1**), suggesting that there were no significant technical bottlenecks in construction of the mating strain library. However, next-generation sequencing revealed that ~12% of targeted genes were not detected in the PA14 knockdown library inoculum (**Supplementary Fig. 3.1**). Ultimately, the PA14 knockdown library consists of 466 genes represented by at least one sgRNA.

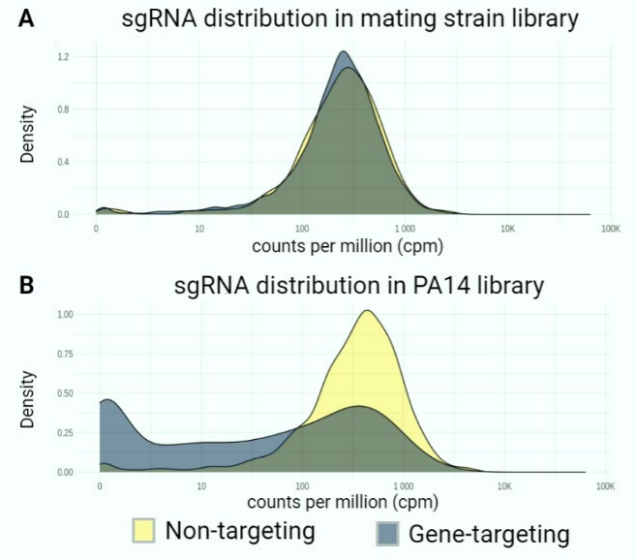

Supplementary Figure 3.1: sgRNA distributions in pooled mating strain library and pooled PA14 knockdown library
(A) Histogram of targeting (blue-grey) and non-targeting (yellow) sgRNAs present in the mating strain knockdown library. (B) Histogram of targeting (blue-grey) and non-targeting (yellow) sgRNAs present in PA14 knockdown library.

An *in vivo* CRISPRi screen in *P. aeruginosa* murine pneumonia model overcomes infection-associated bottlenecks

Pooled library infections are affected by bottlenecks that can confound the effects of genetic inhibition on measurement of strain loss after infection. (21) Bottlenecks can arise from several mechanisms such as: physical barriers to infection, strain loss during inoculation, host clearance pathways as the bacteria transition to invasive disease, or stochastic depletion of mutant strains. Other technical issues with experimental infection models in animals include induction of fatal septic shock with too high of a bacterial inoculum, underrepresentation of the library at time of inoculation or sacrifice, and

insufficient duration of infection resulting in too few bacterial doublings, all of which disallow robust detection of strain depletion.

Our experimental protocol addressed these pitfalls. Direct intratracheal instillation (22) was preferred to other indirect delivery methods, such as intranasal instillation, which may generate an additional physical barrier and subsequent strain loss. To minimize the loss of knockdown strains targeting highly vulnerable genes in our inoculum, mice were inoculated with a dilution from a thawed glycerol stock, rather than allowing the pooled libraries to grow in axenic culture before inoculation (**Fig. 3.2A**). Inefficient PCR amplification from gDNA isolated directly from the lung homogenates created a technical bottleneck that was surmounted by plating the lung homogenates on agar plates prior to gDNA extraction (**Fig. 3.2B**). As a strategy to distinguish unique vulnerabilities associated with the infection environment from general growth defects conferred by repression of an essential gene, an *in vitro* screen was carried out in parallel to the *in vivo* screen (**Fig. 3.2C**).

Two groups of five mice were intratracheally instilled with approximately 4.6E11 CFU/animal and 4.6E10 CFU/animal of the PA14 knockdown library (**Fig. 3.2A**). This 1-log variation in the bacterial inoculum drastically affected the ability of mice to clear the infection. In the 4.6E10 CFU/animal group, the recovery of animal temperature and weights by the 24-hour time point indicated drastic clearance of infection (**Fig. 3.2D**). Indeed, the population of negative control sgRNAs is skewed in the lung homogenate

samples recovered from this group, suggesting stochastic depletion independent of genetic perturbation. Next-generation sequencing accordingly exposed bottlenecks in the samples recovered from mice infected with the diluted inoculum that prohibited downstream assessment of gene vulnerability.

Within the group of mice infected with the more concentrated inoculum of 4.6E11 CFU/animal, two mice succumbed to the infection during the 24-hour period. The relatively low weight loss coupled with large temperature change in the three surviving mice suggest this was likely due to septic shock (**Fig. 3.2D**). In the lung homogenates from the three surviving mice, normal distributions of non-targeting controls are recovered, suggesting that the infection bottleneck issue was subdued (**Fig. 3.2E**). Evaluation of the bottleneck size revealed that the population complexity of the library was similar between gene-targeting and non-targeting strains in both the *in vitro* and *in vivo* samples (**Fig. 3.2F**). The similarity of the distributions between the inoculum and *in vitro* samples suggests that the strains in the PA14 knockdown library have already adapted to growth in LB during the library construction process (**Fig. 3.2E**). In contrast, the distribution of gene-targeting sgRNAs is skewed in the *in vivo* sample, implying that the fitness of the knockdown strains changes in the infection environment (**Fig. 3.2E**).

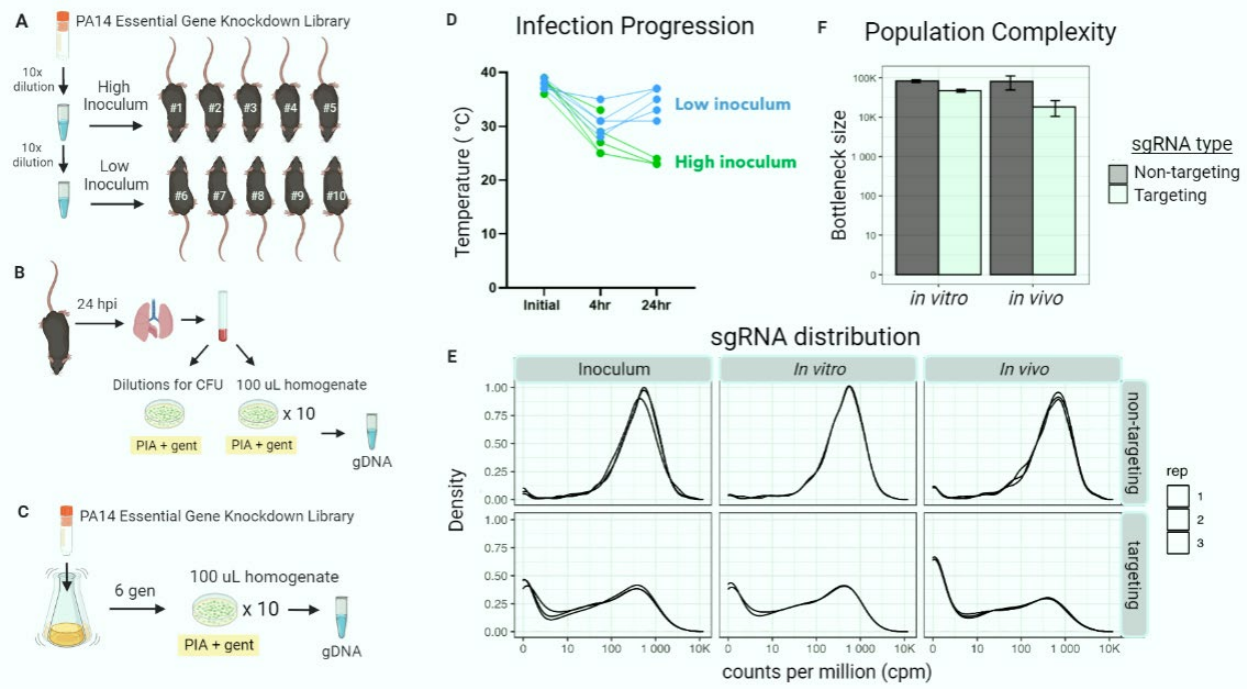

Figure 3.2: Murine pneumonia infection with PA14 Essential Gene Knockdown Library

(A) Two groups of five mice were intratracheally instilled with approximately 4.6E11 CFU/animal and 4.6E10 CFU/animal of the PA14 knockdown library. (B) Following 24 hours of infection, lung homogenates were plated on PIA + 30 µg/mL gentamicin. Colonies were scraped from plates after 24 hours of growth, followed by gDNA extraction, amplicon library preparation, and NGS. (C) Simultaneously, inoculum was added to 25 mL LB and grown for 6 generations before plating on PIA + 30 µg/mL gentamicin. (D) Change in mice's rectal temperatures and weights following 24 hours of infection. (E) Distribution of gene-targeting and non-targeting sgRNAs recovered from the plated samples representing inoculum, *in vitro* growth, and lung homogenates. (F) Bottleneck size estimates from *in vitro* samples and *in vivo* samples corresponding to the 4.6E11 CFU/animal infection

An *in vivo* CRISPRi Screen Reveals Gene Vulnerability during Murine Pneumonia

In probing the importance of PA14 genes during murine pneumonia infection, we sought to identify hypomorphs with heightened vulnerability to clearance by the host. Of the 466 genes represented in the PA14 essential gene knockdown library, strains corresponding to 187 genes were depleted (LFC < -1, FDR < 0.05) after 24 hours of growth in the mouse lung (**Fig. 3A**). The complete set of depleted genes was not associated with a single biological pathway, suggesting that perturbation of essential genes from a variety of processes generates *in vivo* vulnerabilities (**Fig. 3B**). Notably, knockdown strains associated with lipopolysaccharide and lipoprotein transport, purine biosynthesis, ubiquinone biosynthesis, DNA replication, and translation were associated with significant *in vivo* vulnerabilities. Of note, virulence pathways mediated by secreted products, like siderophore production, or community dynamics may not be captured in this pooled CRISPRi screen if such deficiencies in one member of the library can be compensated for by other co-infected members of the library. (23)

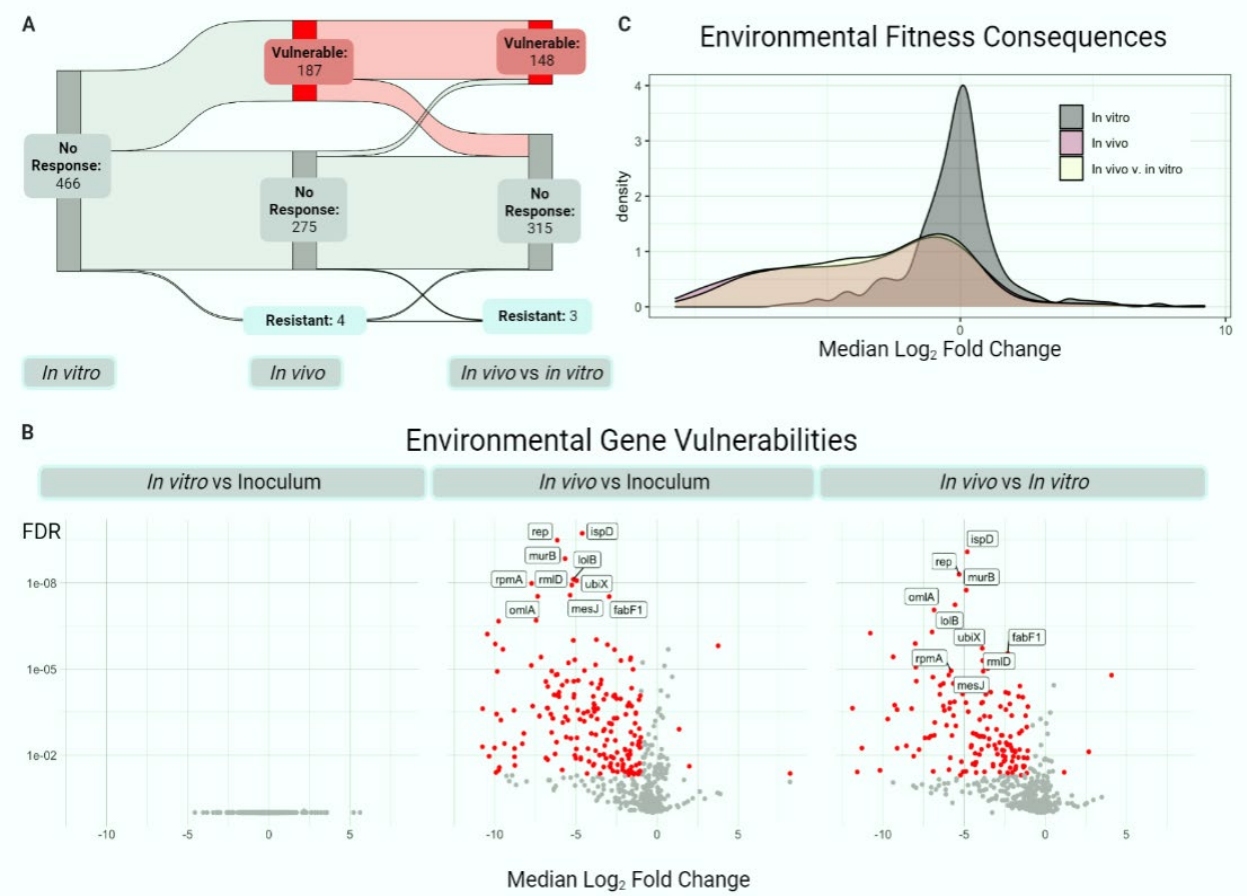

Figure 3.3: PA14 essential gene vulnerabilities in *in vitro* and *in vivo* screens

(A) Volcano plots of average strain depletion corresponding to each targeted gene after 6 generations of growth in LB, 24 of murine pneumonia infection, and *in vivo* vulnerability normalized to *in vitro* vulnerability. Data used to generate this graph is presented in **Supplementary Table 3.2**. (B) Sankey diagram depicting number of genes where knockdown led to *in vivo* vulnerability, *in vitro* vulnerability, and/or greater *in vivo* vulnerability than *in vitro* vulnerability. (C) Median log2 fold change for each sgRNA (gene-targeting and non-targeting) in the listed condition compared to the inoculum.

Supplementary Table 3.2: Data from screens normalized to inoculum

Log2 fold change and false discovery rates for all detected and the statistical comparison of the two conditions

		In vitro		In vivo		In vivo v. in vitro	
locus_tag	**gene**	**L2FC**	**FDR**	**L2FC**	**FDR**	**L2FC**	**FDR**
PA14_65740	thiC	0.86	8.38E-01	-0.41	8.12E-01	-1.49	4.75E-03
PA14_33270	pvdG	-0.04	1.00E+00	0.04	9.03E-05	0.06	3.13E-04
PA14_00440	trpA	-0.36	1.00E+00	-0.13	5.22E-01	0.00	7.03E-01
PA14_11460	thiL	-0.21	1.00E+00	-0.87	1.64E-03	-0.31	2.97E-03
PA14_66940	hisI	-0.46	1.00E+00	-1.10	2.73E-04	-0.16	4.54E-02
PA14_08470	hemJ	0.31	1.00E+00	-0.32	3.71E-05	-1.29	3.27E-03
PA14_14800	fdx2	-0.64	1.00E+00	-1.93	1.80E-10	-1.88	2.63E-05
PA14_62840	glmM	-0.20	1.00E+00	-6.14	9.24E-22	-5.96	4.51E-21
PA14_25660	fabG	-0.20	1.00E+00	-2.61	4.77E-17	-2.43	5.30E-12
PA14_67880	hisF1	-0.02	1.00E+00	-0.32	9.90E-01	-0.22	5.68E-01
PA14_61670	moeB	0.20	1.00E+00	-3.45	1.10E-15	-3.66	8.29E-16
PA14_61740	lolB	0.21	1.00E+00	-5.16	3.63E-28	-5.56	1.49E-26
PA14_12390	hemL	0.03	1.00E+00	0.15	3.40E-02	0.10	1.74E-01
PA14_05280	ruvX	-0.13	1.00E+00	-2.63	8.68E-21	-2.45	9.00E-15
PA14_41870	cysB	0.20	1.00E+00	-0.08	5.72E-01	-0.08	8.15E-01
PA14_62990	grpE	0.28	1.00E+00	0.61	4.83E-03	0.16	6.25E-01
PA14_18700	rnt	-0.41	1.00E+00	-1.65	1.80E-11	-1.45	1.08E-04
PA14_67890	hisA	0.42	1.00E+00	-0.33	1.16E-02	-0.59	8.85E-02
PA14_16950	dapD	0.08	1.00E+00	-2.47	6.27E-14	-2.15	8.35E-13
PA14_12280	lnt	0.03	1.00E+00	0.51	4.57E-02	0.33	1.60E-01
PA14_55800	cpaA	-0.07	1.00E+00	-0.35	6.98E-01	-0.30	9.70E-01
PA14_31290	lecA	0.04	1.00E+00	0.09	4.16E-02	0.05	3.37E-01
PA14_15960	ffh	0.39	9.98E-01	-0.93	3.85E-02	-1.33	1.36E-03
PA14_46020	yfiP	-0.08	1.00E+00	0.13	1.98E-02	0.19	4.16E-02
PA14_52850		0.05	1.00E+00	-0.13	8.56E-01	-0.10	7.96E-01
PA14_36780	mgtC	0.14	1.00E+00	-1.53	1.27E-04	-1.15	1.79E-02
PA14_23460	orfN	-0.80	6.75E-01	-3.06	3.91E-30	-2.27	3.00E-13
PA14_57670	trpS	-0.03	1.00E+00	-2.57	1.16E-01	-2.56	3.20E-02
PA14_12310	ybeY	0.15	1.00E+00	-0.31	3.83E-01	-0.31	9.05E-01
PA14_44920		-0.08	1.00E+00	0.02	2.57E-01	0.06	3.33E-01
PA14_41060	rnhA	-0.23	1.00E+00	-6.48	1.61E-23	-6.26	1.77E-21
PA14_25760	holB	0.10	1.00E+00	0.25	1.34E-05	-0.07	3.92E-03
PA14_04630	ilvD	0.17	1.00E+00	-0.86	2.99E-02	-1.66	3.62E-04
PA14_61660	murI	-0.09	1.00E+00	-4.04	1.30E-15	-3.96	6.32E-16
PA14_62940	dapB	0.15	1.00E+00	0.11	2.46E-01	0.06	3.47E-01

		In vitro		In vivo		In vivo v. in vitro	
locus_tag	**gene**	**L2FC**	**FDR**	**L2FC**	**FDR**	**L2FC**	**FDR**
PA14_69440	hemD	0.09	1.00E+00	-0.33	5.86E-01	-0.22	1.53E-01
PA14_05070	metW	0.12	1.00E+00	-0.43	8.03E-01	-0.64	5.53E-01
PA14_68210	rmlC	-1.54	9.93E-01	-2.50	1.19E-10	-0.98	9.08E-02
PA14_51730	tolA	0.15	1.00E+00	-0.94	1.22E-01	-0.97	2.61E-01
PA14_11410	ribC	-0.07	1.00E+00	-0.08	7.54E-01	-0.15	8.51E-01
PA14_30330	serS	-0.32	1.00E+00	-0.06	7.35E-01	0.25	3.57E-01
PA14_71750	pycR	0.12	1.00E+00	0.21	3.32E-02	0.13	8.91E-02
PA14_04460	lgt	0.18	1.00E+00	-1.38	7.86E-01	-1.58	4.13E-01
PA14_17120	cdsA	0.03	1.00E+00	-0.73	1.04E-01	-0.67	4.67E-01
PA14_70280	argB	-0.07	1.00E+00	0.45	1.43E-07	0.53	1.65E-06
PA14_23850	trpF	0.15	1.00E+00	-0.09	6.54E-01	-0.17	6.22E-01
PA14_66240	waaC	0.16	1.00E+00	-2.25	1.92E-08	-2.76	4.75E-08
PA14_62620	pgi	-0.43	1.00E+00	-3.13	1.48E-17	-2.72	1.81E-12
PA14_55390		-0.17	1.00E+00	-0.11	3.61E-12	-0.07	7.41E-08
PA14_61890		0.35	1.00E+00	0.23	2.71E-11	-0.14	1.25E-07
PA14_44910		0.08	1.00E+00	-0.10	6.66E-01	0.03	6.29E-01
PA14_24710	evgA	0.16	1.00E+00	0.24	1.94E-01	0.09	4.51E-01
PA14_70370	pyrE	0.04	1.00E+00	-0.69	2.76E-01	-0.75	1.50E-01
PA14_66600	aroB	0.25	1.00E+00	-3.25	5.57E-06	-3.51	3.84E-05
PA14_71620	purE	2.19	1.00E+00	-0.13	8.96E-01	-2.33	1.88E-01
PA14_73170	glmS	-0.17	1.00E+00	-2.23	1.70E-13	-2.07	6.29E-09
PA14_68170	rmlB	-1.71	6.94E-01	-3.87	1.39E-15	-2.18	5.69E-04
PA14_17100	frr	-0.76	9.76E-01	-1.03	3.41E-22	-0.29	2.30E-14
PA14_62720	rpsO	0.46	1.00E+00	-0.89	7.94E-12	-1.39	3.04E-10
PA14_16070	hom	0.58	9.99E-01	-0.12	4.63E-01	-0.97	1.73E-01
PA14_18610	argF	-0.21	1.00E+00	-0.16	8.40E-01	0.03	5.03E-01
PA14_23790	leuB	-0.04	1.00E+00	-1.15	1.14E-04	-1.15	3.82E-05
PA14_66230	waaG	0.12	1.00E+00	0.04	8.28E-03	-0.10	2.41E-03
PA14_08360	trpC	0.11	1.00E+00	-0.01	4.69E-01	-0.15	9.48E-01
PA14_39980	qscR	-0.33	1.00E+00	-0.51	7.81E-06	-0.15	5.63E-03
PA14_69690	dapF	-0.21	1.00E+00	0.03	4.82E-02	0.07	3.75E-01
PA14_17080	pyrH	-0.42	9.99E-01	-1.48	5.03E-15	-1.08	1.53E-08
PA14_71600	purK	0.06	1.00E+00	0.06	1.69E-01	-0.27	8.09E-01
PA14_17420	ispF	0.05	1.00E+00	-0.86	1.98E-02	-0.66	2.21E-01
PA14_07940	trpE	-0.04	1.00E+00	-0.62	2.04E-01	-0.50	5.30E-01
PA14_11510	ribA	-0.35	9.98E-01	-6.42	7.82E-15	-6.09	5.05E-13
PA14_46470	pdxB	-0.53	1.00E+00	-1.49	1.47E-01	-1.22	1.48E-01
PA14_15030	leuA	-0.03	1.00E+00	-0.34	2.28E-02	-0.56	1.86E-02

		In vitro		In vivo		In vivo v. in vitro	
locus_tag	**gene**	**L2FC**	**FDR**	**L2FC**	**FDR**	**L2FC**	**FDR**
PA14_60390	mviN	-0.64	1.00E+00	-1.16	5.87E-03	-0.54	2.17E-01
PA14_55670	recB	-0.41	1.00E+00	-1.11	5.43E-07	-0.54	6.96E-02
PA14_49470	nrdB	-0.45	1.00E+00	-3.80	1.45E-19	-3.36	7.17E-14
PA14_23760	leuD	0.06	1.00E+00	-0.51	3.15E-01	-0.53	7.57E-01
PA14_08480	argC	-0.01	1.00E+00	-0.20	8.35E-01	-0.42	8.61E-01
PA14_30150	trmU	-1.23	1.00E+00	-5.07	4.50E-16	-3.86	2.19E-10
PA14_25690	fabF1	-0.56	1.00E+00	-2.96	1.39E-30	-2.31	3.66E-18
PA14_23090	eda	-0.08	9.99E-01	0.26	9.45E-03	0.08	5.33E-01
PA14_68360	fabY	0.20	1.00E+00	-1.70	1.50E-01	-1.86	2.42E-01
PA14_07130	tktA	-0.07	9.98E-01	-0.65	1.82E-01	-0.59	3.75E-01
PA14_08350	trpD	-0.01	1.00E+00	-0.78	6.48E-02	-0.85	1.14E-01
PA14_68740	argA	-0.12	1.00E+00	0.28	4.60E-03	0.39	1.11E-02
PA14_23070	zwf	0.23	1.00E+00	-1.01	9.95E-05	-1.07	2.14E-02
PA14_57190	mutT	-0.09	1.00E+00	0.23	1.06E-06	0.30	9.70E-06
PA14_54480	ygfZ	-0.43	1.00E+00	-7.45	5.07E-63	-4.89	7.49E-43
PA14_17340	ispD	0.05	1.00E+00	-4.61	1.29E-40	-4.81	6.79E-36
PA14_57560	CYTB	-1.08	1.00E+00	-0.62	5.96E-01	0.11	6.65E-01
PA14_62930	carA	0.89	1.00E+00	0.35	2.28E-02	-0.46	5.02E-01
PA14_57800	hisG	0.03	1.00E+00	-0.69	2.62E-01	-0.71	5.72E-01
PA14_08510	erpA	-0.10	1.00E+00	-0.77	3.95E-01	-0.69	5.45E-01
PA14_05590	metF	-0.06	1.00E+00	-0.42	7.86E-01	-0.38	4.89E-01
PA14_04380		0.25	1.00E+00	-0.67	6.73E-02	-0.85	6.05E-02
PA14_05150	proC	-0.58	1.00E+00	-0.54	6.54E-02	-0.79	1.32E-01
PA14_52580	lysC	0.23	1.00E+00	-1.82	8.45E-13	-2.17	1.02E-09
PA14_60470	ispB	-0.09	1.00E+00	-0.71	2.25E-01	-0.63	5.62E-01
PA14_06540	bioC	-0.40	1.00E+00	-1.31	1.00E-08	-0.93	4.22E-04
PA14_60360	lspA	1.44	1.00E+00	-5.60	7.14E-08	-7.06	5.30E-09
PA14_23800	asd	-0.28	1.00E+00	-0.42	3.26E-02	-0.16	8.36E-02
PA14_07590	folB	0.14	1.00E+00	-2.80	2.39E-12	-2.95	4.38E-11
PA14_69240	hemB	-0.01	1.00E+00	-1.36	2.04E-05	-1.08	7.99E-04
PA14_54330	rnc	-0.31	1.00E+00	-0.71	1.28E-03	-0.42	6.29E-02
PA14_70810	pstB	0.15	1.00E+00	-0.05	5.31E-01	-0.06	7.17E-01
PA14_65180	rpsF	0.45	1.00E+00	-8.83	3.90E-12	-9.29	3.01E-13
PA14_71720	oadA	0.54	1.00E+00	0.69	1.22E-09	0.08	3.06E-01
PA14_00240	tsaC	0.12	9.97E-01	-1.08	5.55E-03	-2.10	2.79E-05
PA14_60420	proB	0.09	1.00E+00	0.15	5.53E-09	0.14	8.82E-07
PA14_17280	mesJ	-1.39	1.00E+00	-5.36	3.73E-24	-3.82	2.55E-12
PA14_66610	aroK	-0.13	1.00E+00	-0.92	9.33E-02	-0.88	6.05E-01

		In vitro		In vivo		In vivo v. in vitro	
locus_tag	**gene**	**L2FC**	**FDR**	**L2FC**	**FDR**	**L2FC**	**FDR**
PA14_15680	cumB	-0.07	1.00E+00	-0.78	9.47E-03	-0.75	2.67E-01
PA14_12120	lipB	0.00	1.00E+00	-0.81	5.97E-04	-0.82	6.37E-03
PA14_69910	rep	-0.43	1.00E+00	-6.16	5.13E-41	-5.31	2.38E-32
PA14_17070	tsf	-1.11	9.97E-01	-8.13	1.96E-50	-7.04	6.38E-38
PA14_30380	tusB	-0.05	1.00E+00	-2.66	1.05E-07	-2.47	2.27E-05
PA14_71740	accC	0.03	1.00E+00	-0.20	1.98E-05	-0.24	1.09E-01
PA14_55770	pitA	-0.50	1.00E+00	-0.98	2.46E-09	-0.78	1.12E-06
PA14_62160	ilvI	0.36	1.00E+00	-0.95	1.08E-05	-1.21	1.09E-08
PA14_70730	ubiA	-0.33	1.00E+00	-6.06	3.40E-10	-5.76	1.63E-07
PA14_06570	bioD	0.16	1.00E+00	-0.42	4.19E-01	-0.52	5.83E-01
PA14_11090	cupB4	0.10	1.00E+00	-0.35	9.63E-01	-0.46	9.48E-01
PA14_45290	ccmH	0.27	1.00E+00	-0.30	7.12E-02	-0.14	7.98E-01
PA14_44370	ccoN	-0.32	1.00E+00	-0.60	2.98E-01	-0.23	7.53E-01
PA14_57770	hisC1	-0.02	1.00E+00	-1.38	4.93E-07	-1.33	8.43E-03
PA14_30290	ftsK	-0.09	9.98E-01	-1.17	3.20E-04	-1.10	3.82E-03
PA14_61750	ipk	-0.22	1.00E+00	-0.44	1.80E-03	-0.11	5.83E-02
PA14_07190	pgk	0.20	1.00E+00	-0.69	1.13E-03	-0.77	2.33E-02
PA14_67930	hisB	0.48	1.00E+00	-0.11	8.32E-04	-0.60	2.51E-03
PA14_57250		-0.13	1.00E+00	-0.43	7.90E-05	-0.26	2.23E-03
PA14_08730	rplA	0.29	1.00E+00	0.35	1.10E-06	0.05	7.10E-02
PA14_00280	hemF	-0.50	1.00E+00	-0.76	3.75E-01	-0.28	8.19E-01
PA14_62970	dnaK	1.12	9.40E-01	0.93	3.72E-11	0.23	3.19E-02
PA14_57780	hisD	0.14	1.00E+00	-0.35	4.95E-01	-0.51	9.04E-01
PA14_25390	sth	0.01	1.00E+00	-0.05	4.72E-01	-0.02	8.82E-01
PA14_61790	pth	-0.43	1.00E+00	-1.72	2.84E-08	-1.34	5.25E-03
PA14_69810	glnK	-0.43	1.00E+00	-2.69	3.35E-04	-2.27	8.35E-03
PA14_11560	ispA	-0.20	1.00E+00	-3.28	2.70E-06	-3.04	4.23E-06
PA14_62130	ilvC	0.44	1.00E+00	0.19	6.90E-01	-0.47	7.60E-01
PA14_22040	minC	-0.20	1.00E+00	-1.07	3.17E-04	-0.88	5.69E-02
PA14_61400	mqoB	0.01	1.00E+00	-3.48	1.74E-17	-3.62	9.94E-15
PA14_54290	pdxJ	0.02	1.00E+00	-1.31	2.33E-05	-1.36	1.28E-02
PA14_31580	ACADM	0.11	1.00E+00	0.22	1.14E-03	0.10	1.28E-01
PA14_62150	ilvH	0.43	1.00E+00	0.58	2.36E-02	-0.85	2.00E-01
PA14_16480	wspF	0.45	1.00E+00	-1.65	1.95E-03	-1.60	1.99E-05
PA14_50800	pdxH	-0.08	1.00E+00	-2.69	5.56E-10	-2.73	1.20E-05
PA14_25250	gapA	-0.10	1.00E+00	-3.66	5.26E-15	-3.58	1.42E-11
PA14_07740	pdxA	-0.35	1.00E+00	-2.57	5.37E-05	-1.86	7.70E-03
PA14_60330	lytB	0.00	1.00E+00	-1.97	1.24E-12	-1.99	4.52E-09

		In vitro		In vivo		In vivo v. in vitro	
locus_tag	**gene**	**L2FC**	**FDR**	**L2FC**	**FDR**	**L2FC**	**FDR**
PA14_41050	dnaQ	-0.33	9.98E-01	-6.20	1.18E-27	-5.88	3.84E-24
PA14_14880	ispG	-0.71	1.00E+00	-5.85	4.74E-15	-3.81	5.66E-10
PA14_17110	uppS	-1.41	1.00E+00	-3.88	8.35E-06	-2.48	1.97E-03
PA14_65380	tsaE	-0.07	1.00E+00	-3.31	7.13E-06	-2.54	8.19E-05
PA14_17180	lpxD	0.18	9.98E-01	0.38	1.83E-02	0.19	2.06E-01
PA14_19050	metG	0.29	9.98E-01	-3.77	8.61E-09	-4.07	3.52E-09
PA14_14650	secF	0.18	1.00E+00	-0.51	6.52E-01	-0.30	9.61E-01
PA14_05260	pyrB	0.47	1.00E+00	0.06	6.03E-02	-0.43	4.59E-01
PA14_05080	metX	-0.17	1.00E+00	-0.69	1.48E-01	-0.75	1.35E-01
PA14_23500	tyrB	0.19	1.00E+00	-0.51	1.01E-01	-0.74	2.66E-02
PA14_66760		0.29	1.00E+00	-1.19	3.33E-01	-1.49	1.12E-01
PA14_04310	rpiA	-0.11	1.00E+00	-2.12	8.33E-09	-2.03	2.01E-07
PA14_24220	ppnK	0.27	1.00E+00	0.02	7.74E-03	-0.56	4.17E-01
PA14_70800	phoU	0.09	1.00E+00	-2.80	3.18E-02	-2.66	1.23E-02
PA14_57570	UQCRFS1	-0.29	1.00E+00	-0.62	7.90E-01	-0.26	9.88E-01
PA14_25650	fabD	-0.01	1.00E+00	-3.93	1.56E-10	-3.94	6.54E-10
PA14_65605	parC	-0.04	1.00E+00	-0.50	2.98E-06	-0.45	7.44E-05
PA14_07770	lptD	1.08	1.00E+00	-6.86	3.94E-25	-7.95	5.07E-28
PA14_00450	trpB	0.18	1.00E+00	-0.16	3.35E-04	-0.14	4.42E-03
PA14_65230	purA	-0.28	1.00E+00	-5.12	1.44E-09	-3.41	1.61E-07
PA14_23220	ubiG	0.06	1.00E+00	-1.57	6.92E-09	-1.65	2.71E-08
PA14_00050	gyrB	-0.16	1.00E+00	-0.70	5.91E-01	-0.55	6.17E-01
PA14_44070	gltA	-0.44	1.00E+00	-1.50	1.96E-02	-1.07	1.22E-01
PA14_05250	pyrC	-0.08	9.99E-01	-0.57	5.71E-06	-2.18	6.37E-09
PA14_41840	cysH	0.34	1.00E+00	0.22	5.38E-01	0.02	8.65E-01
PA14_58780	coaE	0.12	1.00E+00	-0.92	2.68E-01	-1.30	2.30E-01
PA14_68980	ubiH	-0.65	1.00E+00	-8.77	3.36E-05	-8.14	1.43E-03
PA14_66920	ubiB	0.11	1.00E+00	-0.06	1.86E-02	-0.19	2.20E-01
PA14_66980	tatC	-0.60	1.00E+00	-5.15	3.41E-12	-4.57	9.50E-08
PA14_44440	fixI	-0.30	1.00E+00	-0.18	9.59E-01	0.05	4.31E-01
PA14_73400	thdF	-0.70	1.00E+00	-1.12	1.75E-02	-0.10	8.16E-01
PA14_14770	hscB	-0.38	9.98E-01	-1.05	1.81E-02	-0.68	3.65E-01
PA14_57540	CYC1	-0.67	1.00E+00	-0.63	4.67E-01	-0.12	8.69E-01
PA14_30670	pgsA	-1.74	9.81E-01	-4.07	5.45E-14	-2.62	8.15E-05
PA14_68670	ldcA	0.38	1.00E+00	-0.42	1.44E-01	-1.01	4.56E-01
PA14_17130	ispC	-0.68	1.00E+00	-7.15	5.89E-30	-6.49	3.56E-22
PA14_07620	cca	-0.09	1.00E+00	-1.62	4.74E-17	-1.56	1.49E-12
PA14_08620	birA	-0.07	1.00E+00	-3.74	9.53E-18	-3.86	1.56E-15

		In vitro		In vivo		In vivo v. in vitro	
locus_tag	**gene**	**L2FC**	**FDR**	**L2FC**	**FDR**	**L2FC**	**FDR**
PA14_62760	infB	-0.53	1.00E+00	-0.34	1.12E-01	0.51	1.45E-01
PA14_25560	rne	-0.21	1.00E+00	-1.75	9.43E-03	-1.14	1.20E-01
PA14_28650	thrS	0.76	1.00E+00	-1.27	1.16E-01	-2.04	1.31E-03
PA14_00200	def	0.19	1.00E+00	-2.45	8.31E-05	-2.66	6.98E-08
PA14_56300	fumA	-1.12	1.00E+00	-1.33	2.63E-01	-0.12	7.30E-01
PA14_65130	dnaB	0.05	9.98E-01	-2.95	1.09E-09	-3.01	4.92E-09
PA14_14750	icsA	-1.58	1.00E+00	-3.62	6.18E-15	-2.04	6.35E-06
PA14_41400	lpxH	0.42	1.00E+00	-1.75	2.39E-05	-2.65	8.13E-09
PA14_30370	tusE	0.05	1.00E+00	0.25	1.26E-06	0.00	5.85E-04
PA14_51720	tolB	0.38	1.00E+00	-0.59	3.26E-01	-1.04	6.63E-02
PA14_57360	ftsW	0.05	9.98E-01	-4.26	2.69E-06	-4.32	6.52E-06
PA14_66010		0.10	1.00E+00	-3.97	5.86E-03	-4.08	2.21E-02
PA14_32130	xylL	0.06	1.00E+00	-0.38	7.15E-01	-0.47	6.81E-02
PA14_05460	bioA	-0.14	1.00E+00	-0.68	8.98E-01	-0.35	8.92E-01
PA14_23930	metZ	-0.08	1.00E+00	-0.01	3.41E-01	-0.03	6.34E-01
PA14_20140	fpr	0.06	1.00E+00	-0.13	2.28E-06	-0.36	1.81E-04
PA14_62580	panB	1.01	1.00E+00	-3.87	2.61E-10	-5.41	2.08E-13
PA14_70240	coaBC	-0.78	1.00E+00	0.07	1.44E-01	0.83	2.44E-01
PA14_65170	rpsR	0.30	1.00E+00	-7.23	3.88E-09	-7.15	1.11E-07
PA14_55660	recD	-0.05	1.00E+00	-1.62	2.28E-04	-1.59	1.04E-03
PA14_18740	argG	0.32	1.00E+00	0.66	4.49E-07	0.10	4.41E-02
PA14_69670	lysA	0.09	1.00E+00	0.31	4.49E-03	0.47	1.96E-02
PA14_14500	lptF	-1.05	9.98E-01	-6.56	1.11E-16	-5.52	3.30E-12
PA14_23330	rpsA	0.22	9.98E-01	-7.75	2.01E-54	-7.99	7.82E-55
PA14_66220	waaP	0.12	1.00E+00	-4.86	1.47E-24	-5.60	3.92E-23
PA14_41470	acnB	-0.10	1.00E+00	-2.06	1.33E-02	-1.97	8.13E-02
PA14_17270	accA	0.29	1.00E+00	-0.20	5.36E-01	-0.58	6.28E-01
PA14_66210	waaX	0.39	1.00E+00	-0.51	7.65E-01	-0.91	2.21E-01
PA14_70260	dut	-0.34	1.00E+00	-1.04	5.20E-05	-0.73	2.00E-02
PA14_07090	metK	-0.77	1.00E+00	-5.84	1.30E-13	-5.09	4.77E-11
PA14_66800		-0.12	1.00E+00	-0.79	1.00E-03	-0.64	2.88E-02
PA14_52050	purN	-0.03	1.00E+00	-4.48	2.05E-12	-5.42	4.12E-12
PA14_27210	efp	-0.63	1.00E+00	-3.23	3.86E-06	-1.84	4.73E-03
PA14_06510	bioF	-0.45	1.00E+00	0.05	1.21E-01	0.20	4.06E-01
PA14_62710	pnp	-0.15	1.00E+00	-4.88	1.08E-09	-4.75	1.76E-09
PA14_54320	era	0.12	1.00E+00	-1.12	6.60E-05	-1.25	6.72E-03
PA14_72970	tonB1	-0.53	1.00E+00	-0.30	4.09E-01	0.26	7.54E-02
PA14_11860	ubiX	-0.63	1.00E+00	-4.96	1.53E-23	-3.89	5.20E-14

		In vitro		In vivo		In vivo v. in vitro	
locus_tag	**gene**	**L2FC**	**FDR**	**L2FC**	**FDR**	**L2FC**	**FDR**
PA14_23080	pgl	0.28	1.00E+00	-0.51	3.21E-02	-0.92	2.38E-01
PA14_11400	ribD	0.64	1.00E+00	-2.47	4.39E-05	-3.12	2.89E-06
PA14_43680	fabA	0.13	1.00E+00	-0.04	6.84E-01	-0.19	9.90E-01
PA14_69500	argH	0.47	1.00E+00	0.69	2.56E-02	0.10	6.83E-01
PA14_66950	hisE	-0.69	1.00E+00	-1.57	1.12E-06	-1.25	7.03E-02
PA14_51710	oprL	0.42	1.00E+00	-2.13	1.49E-02	-2.48	1.75E-03
PA14_61360		-0.97	1.00E+00	0.40	7.77E-01	1.36	4.68E-01
PA14_24640	pyrD	0.13	1.00E+00	-0.16	4.71E-02	-0.26	4.25E-01
PA14_12410	thiD	0.70	1.00E+00	-2.36	2.78E-01	-3.07	2.15E-01
PA14_00290	aroE	0.25	1.00E+00	-1.75	3.39E-03	-1.86	1.28E-03
PA14_04750	fdx1	0.19	9.98E-01	-0.86	2.70E-01	-1.07	1.89E-01
PA14_25550	murB	-0.33	1.00E+00	-5.67	6.20E-58	-4.87	9.03E-52
PA14_00070	gmhB	0.34	9.98E-01	-1.99	1.83E-04	-2.34	2.85E-05
PA14_62570	folK	0.05	1.00E+00	0.15	1.38E-03	0.16	4.20E-02
PA14_25080	fadB	-0.44	1.00E+00	-2.17	4.80E-03	-1.75	6.24E-02
PA14_66190		0.31	9.98E-01	-10.45	1.83E-67	-10.77	1.17E-68
PA14_04760	coaD	0.15	1.00E+00	-0.48	8.87E-01	-0.33	9.40E-01
PA14_30310	lolA	0.21	1.00E+00	-6.24	3.59E-15	-6.47	1.11E-14
PA14_00060	plsC	-1.27	1.00E+00	0.38	6.81E-01	1.63	2.16E-01
PA14_34600	gapB	0.60	1.00E+00	-0.40	1.59E-02	-0.56	1.17E-02
PA14_62870	rlmE	-1.76	1.00E+00	-3.28	5.42E-09	-1.29	1.02E-01
PA14_33530	fpvF	0.04	1.00E+00	-0.23	3.65E-01	0.00	5.30E-01
PA14_30340	cysG	0.18	1.00E+00	-0.18	1.11E-03	-0.25	7.74E-02
PA14_72480	engB	-1.37	1.00E+00	-3.90	4.58E-13	-2.55	7.92E-06
PA14_68955	ubiI	0.01	1.00E+00	-0.27	9.74E-01	-0.29	7.99E-01
PA14_12400	thiE	0.09	1.00E+00	-1.26	1.44E-02	-2.91	5.51E-03
PA14_69150	ubiD	-0.69	1.00E+00	-2.85	1.93E-03	-2.15	4.43E-02
PA14_14510	lptG	-0.10	1.00E+00	-4.28	2.09E-09	-3.94	3.47E-06
PA14_43950	sucC	-0.23	1.00E+00	0.17	3.48E-01	-0.08	8.69E-01
PA14_60230	comL	0.90	1.00E+00	-4.75	1.20E-08	-5.66	3.60E-11
PA14_16090	thrC	0.13	1.00E+00	-0.97	2.00E-01	-0.76	6.97E-01
PA14_73370	gidA	-0.24	1.00E+00	-0.29	2.07E-01	-0.50	3.88E-01
PA14_17310	kdsA	0.50	1.00E+00	-3.79	3.09E-10	-4.31	4.49E-09
PA14_41350	folD	0.44	9.98E-01	-1.96	3.73E-04	-2.41	2.56E-05
PA14_66170		-0.47	1.00E+00	-6.77	6.46E-13	-6.32	1.30E-11
PA14_58130	mreC	-0.03	1.00E+00	-2.84	1.20E-06	-2.82	1.23E-05
PA14_63030	omlA	-0.30	1.00E+00	-7.37	5.07E-33	-6.87	7.99E-31
PA14_49380	dapE	0.83	1.00E+00	-0.72	3.94E-02	-1.92	1.65E-01

		In vitro		In vivo		In vivo v. in vitro	
locus_tag	**gene**	**L2FC**	**FDR**	**L2FC**	**FDR**	**L2FC**	**FDR**
PA14_08630	coaX	-0.54	1.00E+00	-0.46	9.15E-01	0.07	9.00E-01
PA14_09000	rplF	-2.39	9.81E-01	-5.59	4.51E-09	-3.22	4.19E-03
PA14_04980	thiG	2.21	9.96E-01	0.43	3.60E-01	-1.79	5.59E-01
PA14_66750	argS	0.21	9.98E-01	-1.58	9.54E-03	-1.81	5.38E-03
PA14_23260	gyrA	-0.64	1.00E+00	-0.77	1.23E-01	-0.14	5.27E-01
PA14_12010	proA	-0.35	1.00E+00	-1.52	3.47E-02	-1.19	5.84E-01
PA14_11845	mpl	-3.30	1.00E+00	-2.58	3.69E-02	0.71	4.60E-01
PA14_51270	dapA	-0.26	1.00E+00	-4.52	3.19E-10	-4.28	8.91E-08
PA14_28660	infC	-1.91	1.00E+00	-6.36	1.62E-14	-4.46	3.04E-08
PA14_72490	polA	-0.18	1.00E+00	-0.39	2.19E-03	-1.01	2.30E-02
PA14_07170	epd	0.33	1.00E+00	-3.69	1.62E-07	-4.04	5.93E-08
PA14_23280	pheA	-0.39	9.98E-01	-1.67	6.03E-04	-1.29	3.73E-02
PA14_12130	lis	-0.52	1.00E+00	-1.40	7.69E-03	-0.90	8.07E-01
PA14_08760	rpoB	-0.25	1.00E+00	0.49	1.93E-04	0.73	4.51E-02
PA14_64220	purD	0.27	1.00E+00	-2.87	4.87E-03	-2.81	6.91E-03
PA14_04930	rpoH	0.58	1.00E+00	-1.97	1.30E-01	-2.57	1.96E-02
PA14_43690	fabB	-0.23	9.98E-01	-0.10	7.22E-01	0.12	5.32E-01
PA14_14890	hisS	-1.11	1.00E+00	-3.15	9.27E-04	-2.06	3.49E-02
PA14_51900	proS	0.16	1.00E+00	-0.40	2.80E-01	-0.57	8.70E-01
PA14_64090	aroQ1	0.62	1.00E+00	-0.53	3.08E-04	-1.16	8.85E-02
PA14_73220	glmU	-0.52	1.00E+00	-0.80	4.69E-01	-0.29	6.23E-01
PA14_62850	folP	0.17	1.00E+00	-3.09	2.07E-07	-3.46	1.37E-07
PA14_49340	pcpS	0.20	1.00E+00	-1.44	7.22E-02	-1.65	9.60E-02
PA14_12200	holA	-0.12	1.00E+00	-5.15	3.41E-22	-5.04	1.22E-20
PA14_69190	rho	-0.85	1.00E+00	-1.99	7.09E-03	-1.16	4.15E-01
PA14_32420	mexS	0.37	1.00E+00	-3.04	1.79E-01	-3.65	3.36E-02
PA14_64980	nadE	0.10	1.00E+00	-5.55	1.23E-15	-5.67	2.16E-15
PA14_17930	glpD	1.44	1.00E+00	-1.61	2.86E-02	-2.49	3.90E-02
PA14_56780	sodB	0.10	1.00E+00	-1.42	2.02E-02	-1.38	2.76E-02
PA14_25090	foaB	-0.33	1.00E+00	-2.08	7.92E-03	-1.21	3.72E-01
PA14_43940	sucD	-0.05	1.00E+00	-0.70	7.27E-01	-0.82	5.84E-01
PA14_58700	nadC	2.17	2.89E-02	1.36	4.76E-07	-0.64	8.31E-01
PA14_58180	gatA	-0.16	1.00E+00	-9.72	2.39E-27	-7.96	4.75E-23
PA14_07230	fda	-0.18	9.98E-01	-3.92	1.87E-13	-3.76	2.06E-11
PA14_25110	topA	-0.56	1.00E+00	-2.82	5.88E-04	-2.28	2.71E-02
PA14_44660	lig	-0.18	1.00E+00	-3.55	4.93E-07	-3.22	4.81E-06
PA14_44000	sucB	-0.64	9.98E-01	-0.25	9.68E-01	0.38	5.63E-01
PA14_42760	aroC	0.64	1.00E+00	-1.62	4.31E-01	-2.28	1.97E-01

		In vitro		In vivo		In vivo v. in vitro	
locus_tag	**gene**	**L2FC**	**FDR**	**L2FC**	**FDR**	**L2FC**	**FDR**
PA14_42720	masA	-0.85	1.00E+00	-1.29	1.98E-02	-0.20	4.79E-01
PA14_33690	pvdE	0.12	1.00E+00	-6.03	5.96E-12	-6.24	3.63E-11
PA14_54350	lepB	-1.31	1.00E+00	-9.98	1.05E-24	-6.91	1.05E-17
PA14_57960	ptsN	-0.19	1.00E+00	-0.80	3.17E-02	-0.71	9.09E-02
PA14_64200	purH	0.11	9.98E-01	-0.71	4.21E-01	-0.83	3.90E-01
PA14_66080	msbA	-0.07	9.98E-01	0.01	5.75E-01	0.06	6.12E-01
PA14_07760	surA	0.35	1.00E+00	-2.20	5.75E-02	-2.56	6.37E-02
PA14_25740	tmk	-0.60	9.95E-01	-5.65	3.14E-13	-5.06	1.62E-08
PA14_65570		0.28	1.00E+00	0.30	7.03E-01	-0.01	8.85E-01
PA14_25840	ETFDH	-0.15	1.00E+00	-1.14	5.26E-01	-0.36	8.22E-01
PA14_15990	trmD	0.14	9.98E-01	-1.82	1.58E-03	-1.98	1.47E-03
PA14_23880	folC	-0.33	1.00E+00	-3.94	1.26E-05	-4.58	2.72E-07
PA14_66290	aceA	-0.63	1.00E+00	0.56	3.85E-03	1.17	4.65E-03
PA14_23310		0.02	9.98E-01	-0.78	3.60E-01	-0.81	4.23E-01
PA14_69200	trxA	-0.09	1.00E+00	-5.17	8.61E-20	-6.32	2.71E-18
PA14_23920	purF	-0.47	1.00E+00	-4.71	1.69E-04	-4.25	1.98E-03
PA14_62770	nusA	0.01	1.00E+00	-8.05	9.99E-04	-6.75	2.80E-03
PA14_65410	orn	1.58	1.00E+00	-4.04	1.40E-07	-4.22	5.38E-09
PA14_00100	glyQ	0.51	1.00E+00	-0.90	4.27E-01	-1.42	4.63E-01
PA14_67770	pgm	0.70	1.00E+00	0.06	9.09E-01	-0.66	8.35E-01
PA14_23270	serC	-0.64	1.00E+00	-0.72	9.24E-01	-0.10	7.81E-01
PA14_05620	sahH	0.00	1.00E+00	-0.86	6.43E-01	-1.09	4.25E-01
PA14_09100	rpsD	-0.57	9.98E-01	-4.49	3.32E-10	-3.93	1.47E-07
PA14_57920	lptA	0.75	9.97E-01	-1.55	1.39E-02	-2.32	4.66E-01
PA14_04580	folA	1.29	1.00E+00	0.36	1.28E-03	-0.95	2.35E-02
PA14_18710	pyrC	-0.25	1.00E+00	-3.39	1.55E-01	-3.16	8.30E-02
PA14_62960	dnaJ	0.29	1.00E+00	-1.56	7.51E-01	-0.98	7.85E-01
PA14_58190	gatB	0.10	1.00E+00	-3.64	1.31E-02	-3.76	2.19E-03
PA14_19090	dcd	0.69	1.00E+00	-2.92	3.37E-05	-4.06	1.02E-06
PA14_06500	bioB	-0.11	1.00E+00	0.24	7.75E-01	0.32	8.46E-01
PA14_07910	rpe	0.06	1.00E+00	-0.42	7.51E-01	-0.50	8.67E-01
PA14_25880	etfA	0.39	1.00E+00	-0.85	5.35E-01	-1.70	5.49E-01
PA14_69450	hemC	0.23	9.98E-01	-3.39	1.81E-02	-3.63	1.96E-02
PA14_57010	groEL	-0.75	1.00E+00	-9.85	2.50E-16	-9.14	1.67E-11
PA14_30390	tusC	-0.33	1.00E+00	-4.19	1.56E-05	-3.87	1.92E-03
PA14_68190	rmlD	-1.30	9.97E-01	-5.27	2.39E-32	-3.55	3.64E-19
PA14_11450	nusB	-2.24	9.95E-01	-6.79	1.22E-10	-3.29	1.00E+00
PA14_66720	priA	0.80	1.00E+00	-1.51	2.89E-02	-2.32	1.65E-03

		In vitro		In vivo		In vivo v. in vitro	
locus_tag	**gene**	**L2FC**	**FDR**	**L2FC**	**FDR**	**L2FC**	**FDR**
PA14_16530	lysS	0.15	9.98E-01	-5.00	1.51E-04	-5.17	1.98E-04
PA14_58120	mreD	0.06	1.00E+00	-2.10	1.50E-03	-1.80	8.51E-03
PA14_60450	rpmA	-2.25	1.00E+00	-7.73	3.04E-31	-5.80	2.78E-15
PA14_23560	gltX	-0.45	9.98E-01	-7.25	6.59E-13	-6.81	2.69E-11
PA14_08710	nusG	-0.54	1.00E+00	-1.43	7.33E-03	-0.90	5.13E-01
PA14_17260	dnaE	-0.14	1.00E+00	-9.47	5.11E-33	-9.34	5.48E-31
PA14_57930	lptB	-1.03	9.98E-01	-0.58	7.70E-01	0.44	5.60E-01
PA14_15310	guaB	-0.48	1.00E+00	-2.43	3.35E-03	-1.97	7.62E-02
PA14_19065	mrp	0.63	1.00E+00	-0.39	1.37E-02	-1.04	1.28E-02
PA14_12210	lptE	-0.18	1.00E+00	-0.20	2.74E-01	-0.77	1.79E-01
PA14_57940	rpoN	-0.06	1.00E+00	3.76	1.99E-27	4.09	5.68E-20
PA14_17210	lpxA	1.07	9.98E-01	0.25	7.68E-01	-0.84	8.09E-01
PA14_25860	etfB	0.67	1.00E+00	-1.90	4.57E-01	-2.35	2.42E-01
PA14_65660	parE	0.39	1.00E+00	-5.53	1.31E-11	-5.94	3.14E-13
PA14_44050	sdhD	-1.22	1.00E+00	-2.16	6.88E-02	-0.77	6.98E-01
PA14_49460	nrdA	-0.29	9.98E-01	-9.31	1.91E-07	-9.04	6.86E-07
PA14_60380	ribF	-0.33	1.00E+00	-5.08	1.54E-06	-5.85	4.87E-06
PA14_57220	secA	0.32	9.98E-01	-6.51	5.11E-09	-6.85	3.49E-09
PA14_44020	sdhB	-1.43	1.00E+00	-3.30	5.05E-03	-1.72	7.70E-02
PA14_52010	hda	0.17	1.00E+00	-4.71	9.19E-07	-4.90	9.64E-06
PA14_57370	murD	0.58	9.98E-01	-0.73	7.01E-01	-1.33	4.24E-01
PA14_14680	suhB	-4.05	8.90E-01	-5.47	1.78E-17	-2.35	4.11E-03
PA14_66910	ubiJ	-0.78	1.00E+00	-6.74	4.81E-05	-5.97	2.97E-03
PA14_65310	hfq	0.26	1.00E+00	-4.94	2.96E-03	-5.22	1.97E-03
PA14_04480	thyA	0.24	9.98E-01	-8.30	8.84E-08	-8.56	8.87E-08
PA14_44630	dnaX	1.12	1.00E+00	-10.75	1.93E-14	-11.89	2.71E-16
PA14_08720	rplK	-1.13	1.00E+00	-3.29	1.73E-03	-2.17	1.22E-03
PA14_17220	lpxB	0.09	1.00E+00	-0.21	6.78E-01	-0.32	9.56E-01
PA14_07570	gcp	-0.30	1.00E+00	-2.38	2.78E-01	-2.10	4.11E-01
PA14_57410	murE	0.00	9.98E-01	-2.72	4.82E-03	-2.74	9.62E-03
PA14_12060	pbpA	0.79	1.00E+00	-2.37	4.56E-02	-3.17	1.07E-02
PA14_57890	kdsD	-0.20	9.98E-01	-9.87	2.74E-16	-9.69	2.69E-15
PA14_66550	hemE	-1.60	1.00E+00	-2.30	1.11E-01	-0.78	5.75E-01
PA14_09090	rpsK	-0.31	9.98E-01	-0.87	4.89E-01	-0.57	7.98E-01
PA14_43970	lpd	-0.81	1.00E+00	-5.06	4.16E-03	-4.14	7.25E-03
PA14_55690	recC	-0.40	1.00E+00	-1.54	2.66E-02	-1.48	3.22E-01
PA14_61840	vapI	0.11	1.00E+00	0.80	6.34E-01	0.68	7.24E-01
PA14_16710	tsaB	-0.84	1.00E+00	-2.07	1.79E-01	-1.25	7.06E-01

		In vitro		In vivo		In vivo v. in vitro	
locus_tag	**gene**	**L2FC**	**FDR**	**L2FC**	**FDR**	**L2FC**	**FDR**
PA14_28690	pheS	-0.26	1.00E+00	-3.72	1.61E-01	-3.48	1.84E-01
PA14_12070	rodA	-0.45	1.00E+00	-8.21	1.63E-08	-7.78	4.26E-07
PA14_14820	ndk	-0.74	9.98E-01	-4.98	1.08E-05	-4.26	3.58E-04
PA14_61700	prfA	-1.58	1.00E+00	-5.31	2.88E-07	-3.75	1.69E-03
PA14_15340	guaA	2.64	9.98E-01	-8.94	1.34E-03	-11.59	1.44E-04
PA14_66090		-0.80	9.98E-01	-0.20	9.35E-01	0.59	4.77E-01
PA14_62780	rimP	0.93	1.00E+00	1.95	3.05E-04	-2.65	5.25E-02
PA14_57450	mraW	0.49	9.98E-01	-0.20	9.68E-01	-0.71	8.68E-01
PA14_11690	ppa	0.35	1.00E+00	-3.64	2.07E-03	-4.01	1.59E-02
PA14_00020	dnaN	0.56	9.98E-01	-2.45	2.46E-01	-3.02	1.98E-01
PA14_63020	fur	-0.48	1.00E+00	-4.95	1.46E-10	-4.49	9.47E-07
PA14_25500	exbD	-0.84	1.00E+00	-0.73	5.76E-01	0.09	5.43E-01
PA14_38395	mexX	-0.23	1.00E+00	-1.95	3.09E-01	-1.83	3.06E-01
PA14_08920	rplP	0.22	1.00E+00	-0.25	9.70E-01	-0.49	9.96E-01
PA14_62910	carB	3.61	1.00E+00	0.67	1.25E-01	-0.80	2.52E-01
PA14_57020	groES	-2.48	9.01E-01	-6.85	3.01E-07	-4.39	2.54E-03
PA14_57260	lpxC	-0.19	1.00E+00	0.18	5.74E-01	0.36	8.20E-01
PA14_27950	rsbW	3.44	9.86E-01	3.90	5.90E-02	0.45	9.06E-01
PA14_09040	rplO	-2.19	9.98E-01	-4.64	2.13E-02	-2.47	3.33E-01
PA14_64100	accB	0.77	1.00E+00	1.66	3.21E-02	0.87	4.49E-01
PA14_65250	hisX	0.53	9.98E-01	-10.77	2.73E-09	-11.31	1.29E-09
PA14_08810	rpsG	-1.44	1.00E+00	-6.19	4.59E-06	-4.77	7.98E-03
PA14_04110	serA	0.15	1.00E+00	-5.35	2.61E-05	-5.52	4.24E-05
PA14_57910	lptC	0.51	1.00E+00	-7.67	2.94E-12	-8.25	9.51E-13
PA14_61710	hemA	-1.70	9.98E-01	-0.30	1.13E-01	2.68	1.49E-04
PA14_09080	rpsM	0.59	1.00E+00	-3.61	1.81E-02	-4.21	4.02E-03
PA14_23750	leuC	-0.10	1.00E+00	-2.84	2.15E-03	-2.76	1.51E-02
PA14_23290	hisC2	2.04	1.00E+00	-0.60	1.77E-01	-2.66	2.44E-01
PA14_25450	lolE	-3.23	1.00E+00	-10.36	2.48E-06	-6.59	2.27E-03
PA14_08940	rpsQ	1.23	9.98E-01	-0.53	9.08E-01	-1.78	5.06E-01
PA14_17150	bamA	-1.01	9.98E-01	-1.21	4.73E-01	-0.22	9.76E-01
PA14_30400	dsrE	0.63	1.00E+00	-2.38	3.36E-02	-3.02	7.29E-02
PA14_15980	rimM	-2.22	8.87E-01	-9.67	1.69E-12	-7.46	2.82E-08
PA14_08820	fusA1	-0.81	1.00E+00	-1.00	2.32E-01	-0.21	8.74E-01
PA14_17190	fabZ	-0.81	9.98E-01	-1.45	3.42E-01	-0.65	8.29E-01
PA14_54390	mucD	0.70	1.00E+00	2.19	1.24E-01	-0.58	9.01E-01
PA14_25900	fabV	2.59	1.00E+00	-3.36	4.85E-02	-5.97	1.02E-03
PA14_45350	ccmC	-1.61	1.00E+00	-3.51	9.28E-03	-1.92	4.30E-01

		In vitro		In vivo		In vivo v. in vitro	
locus_tag	**gene**	**L2FC**	**FDR**	**L2FC**	**FDR**	**L2FC**	**FDR**
PA14_70190	rpmB	-0.26	9.98E-01	-2.17	8.60E-02	-1.92	2.14E-01
PA14_17060	rpsB	-2.61	1.00E+00	-6.73	1.65E-12	-4.29	6.87E-06
PA14_05550	oprM	0.26	1.00E+00	0.23	8.91E-01	-0.05	9.84E-01
PA14_57810	murA	0.13	9.98E-01	-1.04	7.15E-01	-1.19	7.27E-01
PA14_66900	ubiE	0.45	9.98E-01	-9.72	5.28E-05	-10.19	4.41E-05
PA14_44030	sdhA	-1.50	1.00E+00	-1.67	7.38E-01	-0.19	6.27E-01
PA14_14440	valS	-1.41	9.98E-01	-1.40	4.38E-01	-0.01	8.93E-01
PA14_51750	tolQ	1.12	9.98E-01	-0.94	7.92E-01	-2.08	5.31E-01
PA14_14730	iscS	-0.93	1.00E+00	-3.96	2.01E-03	-3.04	9.07E-02
PA14_22020	minD	-0.52	9.98E-01	-1.81	4.03E-01	-1.31	6.67E-01
PA14_15740	purL	-0.63	1.00E+00	-6.60	3.74E-03	-5.75	1.99E-01
PA14_64110	accC	-0.29	9.98E-01	-0.27	9.94E-01	0.00	9.12E-01
PA14_73240	atpD	-0.37	1.00E+00	0.25	1.71E-01	0.60	4.28E-01
PA14_09010	rplR	3.20	1.00E+00	3.73	1.10E-01	0.52	9.34E-01
PA14_14930	engA	-0.69	9.88E-01	-4.46	3.77E-04	-3.78	1.29E-02
PA14_07530	dnaG	2.95	9.98E-01	-6.41	2.88E-02	-9.38	4.38E-03
PA14_60370	ileS	-0.69	9.98E-01	-8.73	1.63E-07	-8.05	2.05E-06
PA14_60445	obg	-2.51	1.00E+00	-5.85	3.08E-04	-3.36	8.48E-03
PA14_70440	gmk	1.69	9.98E-01	1.89	3.17E-01	0.18	8.78E-01
PA14_08400	COQ7	2.32	9.98E-01	-3.91	8.71E-02	-6.24	9.90E-03
PA14_73280	atpH	1.27	9.98E-01	1.23	5.02E-01	-0.06	9.48E-01
PA14_65560	serB	-1.00	9.98E-01	-2.59	3.51E-01	-1.60	6.86E-01
PA14_07520	rpoD	0.29	1.00E+00	-4.33	3.92E-05	-4.64	2.63E-03
PA14_08870	rplW	-1.37	9.98E-01	-2.20	4.19E-01	-0.85	8.58E-01
PA14_00190	fmt	2.81	9.98E-01	0.58	7.38E-01	-2.25	4.94E-01
PA14_41380	glnS	5.30	8.57E-01	8.29	5.09E-03	2.98	3.47E-01
PA14_51820	aspS	0.96	9.98E-01	-0.60	9.13E-01	-1.58	7.04E-01
PA14_41360	cysS	-2.49	9.65E-01	-5.77	1.38E-04	-3.31	1.24E-01
PA14_65960	waaA	1.33	9.98E-01	-6.24	7.77E-03	-7.59	1.88E-03
PA14_44060	sdhC	-1.29	9.98E-01	-0.56	9.13E-01	0.72	7.54E-01
PA14_60890	glyA	-0.39	9.98E-01	-4.25	6.66E-02	-3.87	1.44E-01
PA14_61770	prs	0.98	9.98E-01	2.64	7.45E-02	1.65	3.82E-01
PA14_41575	sigX	-0.44	9.98E-01	-2.36	2.79E-01	-1.94	4.87E-01
PA14_04900	ftsY	-0.25	1.00E+00	-2.28	5.45E-01	-2.04	6.14E-01
PA14_23860	accD	0.51	9.98E-01	2.97	2.49E-01	2.45	4.74E-01
PA14_08850	rplC	-3.15	9.98E-01	0.35	7.88E-01	3.48	1.90E-01
PA14_30110	purB	-2.22	9.97E-01	-6.26	3.48E-06	-4.06	1.73E-02
PA14_22010	minE	1.55	9.98E-01	-6.42	2.95E-02	-7.98	1.33E-02

		In vitro		In vivo		In vivo v. in vitro	
locus_tag	**gene**	**L2FC**	**FDR**	**L2FC**	**FDR**	**L2FC**	**FDR**
PA14_57380	mraY	5.60	8.51E-01	8.20	5.14E-03	2.58	3.57E-01
PA14_67600	glnA	-1.59	9.98E-01	-6.69	1.01E-02	-5.12	6.92E-02
PA14_60400	rpsT	-0.11	9.98E-01	1.68	4.05E-01	1.77	5.15E-01
PA14_25510	lpxK	-1.91	9.98E-01	-8.76	9.62E-06	-6.87	6.97E-04
PA14_09050	secY	-3.22	9.98E-01	-9.76	7.81E-05	-6.56	8.90E-03
PA14_64190	fis	-3.80	9.98E-01	-9.93	2.94E-04	-6.15	2.50E-02
PA14_57300	ftsQ	-0.01	9.98E-01	0.61	7.17E-01	0.60	7.89E-01
PA14_09020	rpsE	-4.56	4.78E-01	-10.01	1.16E-06	-5.47	8.06E-03
PA14_54420	mucA	-0.64	9.98E-01	1.31	6.20E-01	1.93	6.15E-01
PA14_44010	sucA	-2.94	9.98E-01	-9.10	7.53E-03	-6.18	6.92E-02
PA14_08740	rplJ	-2.25	9.98E-01	-9.29	8.26E-04	-7.05	1.21E-02
PA14_23320	cmk	-1.65	9.98E-01	-8.70	1.53E-02	-7.07	5.42E-02

In contrast, no significant *in vitro* vulnerability was detected for all strains in the PA14 knockdown library, implying that genetic perturbation had limited impact on fitness during growth in axenic culture (**Fig. 3.3A** and **B**). A statistical comparison of differential *in vivo* vulnerability compared to baseline *in vitro* vulnerability revealed 148 genes that are significantly more vulnerable in the lung infection environment than in axenic culture. The lack of detectable genetic vulnerabilities during *in vitro* growth supports the notion that strains in the library inoculum are fit to begin with and strain loss during infection is likely not due to inherent weaknesses related to perturbing essential genes.

Of the genes that exhibited greater *in vivo* vulnerability than *in vitro* vulnerability, *ispD* stands out as the most confident hit. *IspD* is involved in the non-mevalonate pathway of isoprenoid precursor biosynthesis–also called the MEP (2C-methyl-D-erythritol 4-phosphate) pathway—which is conserved among many microbial pathogens and absent

from animals, making it a suitable drug target. In preliminary results, knockdown of *ispD* in PA14 using P1 generated no detectable fitness defects when the mutant was grown in rich media, and mice infected with *ispD*-P1 clear the bacterial burden 99.99%.

The purine biosynthesis pathway is enriched among genes exhibiting significant *in vivo* vulnerability. Transposon insertion sequencing shows that multiple purine biosynthesis genes (*purD*, *purE*, *purF*, *purH*, *purK, purL*, *purN*) are dispensable for growth in rich media but are required in Synthetic Cystic Fibrosis Medium (SCFM), whereas *purA* and *purB* are essential in both medias. (2) A previous study also revealed the essentiality of *purA* in a *S. pneumoniae* murine pneumonia model. (20) In our screen, significant *in vivo* vulnerability was detected for all mentioned genes except *purE*, *purH*, *purK*. For these genes, the extent of knockdown may not have been strong enough to elicit *in vivo* fitness defects. Given that complete genetic inhibition of *purD*, *purF*, *purL*, and *purN* does not drastically impede bacterial growth *in vitro*, chemical inhibitors that exploit this vulnerability in purine biosynthesis may not exhibit *in vitro* activity. Thus, the *in vivo* vulnerability and essentiality of *purA* and *purB* in PA14 offers support for their prioritization as targets in antibacterial development.

In another example, all seven genes of the lipopolysaccharide transport pathway (*lptB, lptC, lptD, lptE, lptF, lptG, lptH*) are essential both in rich media and SCFM. (2) Mobile-CRISPRi mediated perturbation of these genes generates significant vulnerability *in vivo* without detectable *in vitro* vulnerability—with the exception of *lptB* and *lptE,* for which

no significant *in vivo* vulnerability is detected. This implies that this extent of knockdown of these genes is tolerated by PA14 when grown in rich media but not in the lung infection environment. In agreement with these findings, a conditional deletion of *lptH* in PA01 has previously been shown to have attenuated virulence in a murine pneumonia model. (24) Partial genetic perturbation allows us to build upon such observations and identify other genes with heightened *in vivo* vulnerability.

Table 3.1: Comparison of essentiality and vulnerability in the purine biosynthesis and lipopolysaccharide transport pathways.
SCFM is an abbreviation for synthetic cystic fibrosis medium.

	Essential in LB (Poulsen et al.)	Essential in SCFM (Poulsen et al.)	Vulnerable *in vivo* (this study)
purA	Yes	Yes	Yes
purB	Yes	Yes	Yes
purD	No	Yes	Yes
purE	No	Yes	No
purF	No	Yes	Yes
purH	No	Yes	No
purK	No	Yes	No
purL	No	Yes	Yes
purN	No	Yes	Yes
lptA/lptH	Yes	Yes	Yes
lptB	Yes	Yes	No
lptC	Yes	Yes	Yes

	Essential in LB (Poulsen et al.)	Essential in SCFM (Poulsen et al.)	Vulnerable *in vivo* (this study)
lptD	Yes	Yes	Yes
lptE	Yes	Yes	No
lptF	Yes	Yes	Yes
lptG	Yes	Yes	Yes

The alternative sigma factor *rpoN* is the rare example of a gene where perturbation decreases *in vivo* vulnerability. RpoN regulates many virulence pathways and blocks the transcription of over 700 RpoN-regulated genes has previously been shown to attenuate virulence. (25) *P. aeruginosa* commonly evolves *rpoN* loss-of-function mutations during chronic infection of cystic fibrosis patients, suggesting that repression of this gene may improve *in vivo* fitness of the strain. (11, 26, 27) Modifications of pathogen-associated molecular patterns (PAMPs), such as those linked to RpoN regulation, enable immune evasion and survival in the infection environment through hindering immune recognition and activation. (28, 29) Supplementation of the virulence-related gene activity by other co-infected members of the library may allow the *rpoN*-deficient mutant to escape host clearance mechanisms.

Upregulated Genes in Human Infections Exhibit Vulnerability in Murine Pneumonia Model

In order to further explore our screen's ability to uncover genetic vulnerability during a mammalian infection we compared our genetically vulnerable genes to genes known to be strongly upregulated during human infection. Previous studies revealed little overall correlation across the entire genome between transcriptionally important genes, whose expression is affected by a change in the environment, and phenotypically important genes, whose fitness is affected by a change in the environment. (30) However, phenotypically and transcriptionally important genes overlap when probing the effects of nutritional stress on metabolic genes. (30) We hypothesize that core essential genes that are upregulated during infection will be vulnerable in the host if they cannot be upregulated due to genetic or chemical inhibition and thus may represent promising antibiotic targets.

Comparing the PA14 core essential gene list (2) with a dataset of transcriptionally upregulated PA14 genes during human infections (31) converged in 4 core essential PA14 genes that are upregulated during human infection: *lptG, lptH, pgsA, cysS* (**Fig. 3.4A**). Two genes, *lptG* and *lptH*, are part of the lipopolysaccharide transport system. As previously mentioned, a conditional deletion of *lptH* in PA01 has previously been shown to have attenuated virulence in a murine pneumonia model. (24) The remaining two genes, *pgsA* and *cysS*, are involved in phospholipid biosynthesis and tRNA

aminoacylation, respectively. For all four genes, insignificant *in vitro* vulnerability and significant *in vivo* vulnerability was detected, suggesting that the fitness consequences of inhibiting these genes may be more evident *in vivo* than *in vitro*.

Using the three constitutive promoters of increasing strength characterized in our prior work, (17) we generated three knockdown mutants corresponding to *pgsA: pgsA*-P1, *pgsA*-P2, *pgsA*-P3. Growth of these strains in culture was not substantially different from WT PA14 and a rfp-targeting Mobile-CRISPRi mutant (**Fig. 3.4B** and **C**) suggesting that genetic inhibition did not confer genotoxicity or gene-related fitness defects. When planktonic cultures of the *pgsA* knockdown strains and WT PA14 were used in murine pneumonia mono-infections at 1E4 CFU/animal, *pgsA*-P2 demonstrated statistically significant >99% reduction in bacterial burden following 18 hours of infection (**Fig. 3.4D**). Next, we pursued murine pneumonia single strain-infections at a higher bacterial inoculum to capture the full extent of bacterial load reduction enabled by the repression of pgsA. While three of the four mice succumbed to the 1E8 CFU/animal infection with WT PA14, mice infected with a similar inoculum of *pgsA*-P2 knockdown mutants were able to clear >99.9% of the bacterial burden. These findings suggest that subtle inhibition of the core essential gene *pgsA* significantly enhances infection clearance *in vivo* despite not producing noticeable phenotypic effects *in vitro.*

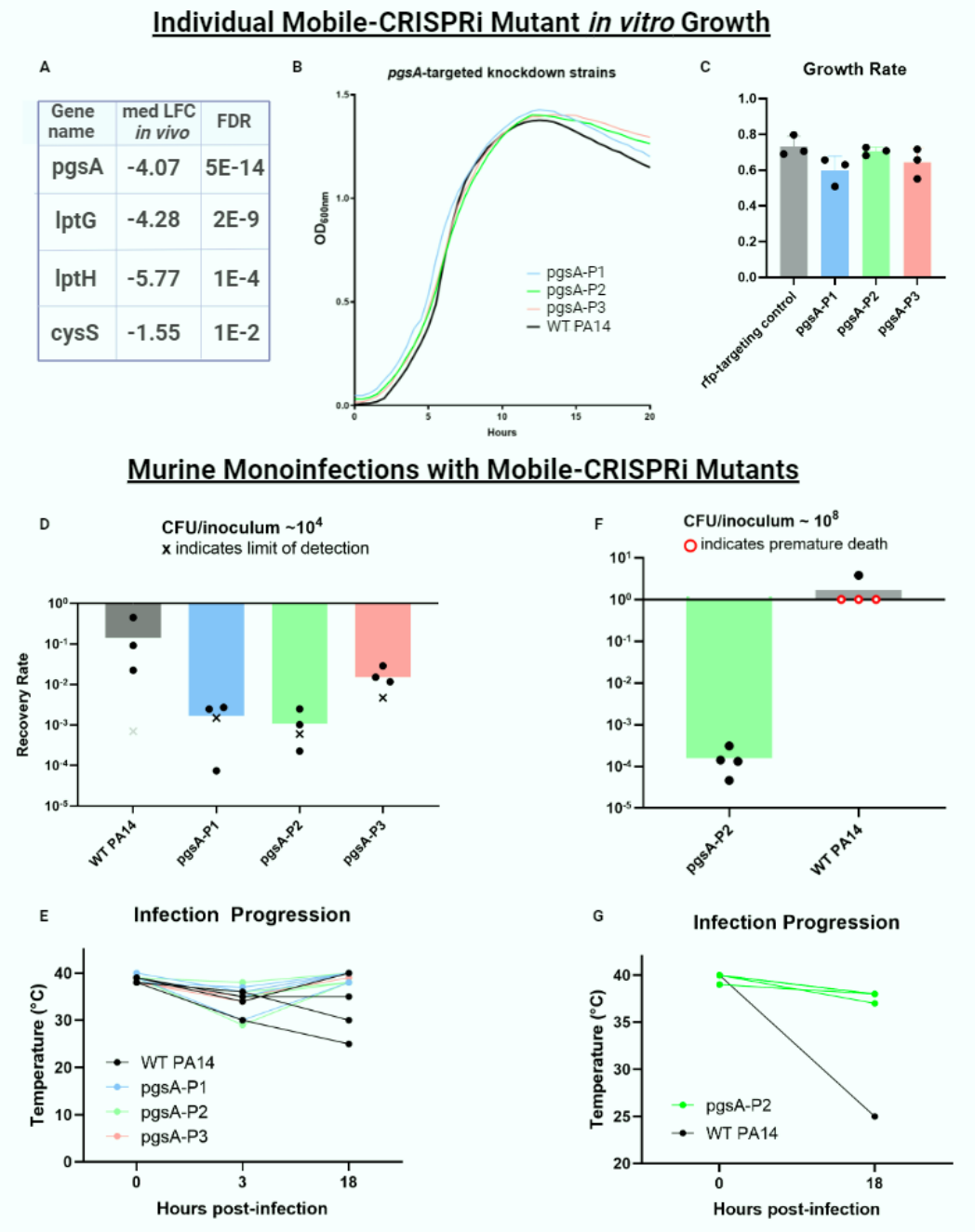

Figure 3.4: Murine pneumonia infection with individual *pgsA* knockdown mutants
(A) Of the four PA14 genes that are essential and transcriptionally upregulated during human infection, *pgsA* is the most confident hit in our screen for *in vivo* vulnerability. (B) Growth curves of WT PA14, and *pgsA* knockdown mutants using P1, P2, and P3 constitutive promoters. (C) Growth rates of *pgsA* knockdown mutants compared to a control rfp-targeting knockdown mutant. (D) Change in bacterial burden from time of inoculation to 18 hours post-infection and (E) temperature change during a low burden of infection. (F) CFU reduction and (G) temperature change in a high burden infection. Recovery rate = recovered CFU/ inoculum CFU.

Discussion

The pooled *in vivo* CRISPRi screen conducted in this study reveals a heightened vulnerability to host immunity processes for 187 PA14 genes. In particular, genetic perturbation of the essential genes *pgsA* and *ispD* did not significantly affect the growth of PA14 in axenic culture, but the same perturbation *in vivo* impeded productive host infection by these mutants. Given that these bacterial genes are required for growth in a mammalian host and are not conserved in humans, they may serve as promising antibacterial targets. Furthermore, partial genetic depletion for a set of 148 PA14 genes results in greater vulnerability to host clearance in a murine pneumonia model than to competition within the pooled library during growth in axenic culture. Specific genes (*pgsA*, *cysS*, *lptH*, *lptG*) known to be strongly upregulated, and presumably required for pathogenic adaptation during infection, were found to be differentially vulnerable *in vivo*.

These vulnerability profiles are dependent on the extent of knockdown elicited by the P1 promoter and variability of efficacy among the four sgRNAs per gene. Stronger inhibition may reveal vulnerabilities for other genes that were not significantly sensitive to repression driven by P1 in either *in vitro* or *in vivo* conditions. Conversely, weaker inhibition may alleviate growth-hampering fitness defects that may have led to underrepresentation of essential gene knockdown mutants in the inoculum. Another

reason these strains may be missing is potentially insufficient coverage of the library obtained following triparental mating into PA14.

Comparison of *in vitro* fitness defects to *in vivo* fitness defects is inherently affected by the number of doublings that proceed under both conditions. Since the depletion of an unfit strain is expected to increase in magnitude over time, the fitness defect may not be detected if too few doubling times are captured. The *in vitro* 6-generation time point (OD_{600nm} 0.01 to 0.64) was chosen to mimic antibacterial discovery platforms, which typically track bacterial growth from a log-phase culture diluted to 1E5–1E6 CFU/mL until stationary phase. However, *in vivo* generation time may not necessarily match *in vitro* generation time, further complicating the comparison. Similarly, the extent of knockdown effect on gene expression may not be conserved *in vivo*. For example, knockdown of genes that are upregulated during infection may yield a larger extent of repression *in vivo* compared to *in vitro*. In this case, a chemical inhibitor that matches the partial genetic inhibition level driven by Mobile-CRISPRi may not achieve the same level of bacterial clearance as exhibited by the genetically inhibited strain.

The genetic vulnerability insights gleaned in this study may not entirely elucidate chemical vulnerability. For example, for targets such as enzymes that have a natural substrate, the genetic mode of inhibition corresponds only to non-competitive chemical inhibition, as target depletion is equivalent to reducing V_{max} while leaving K_m unchanged. (32) However, emerging therapeutic modalities such as CRISPR systems, targeted protein

degradation, or antisense technology could closely mimic the results of our partial genetic inhibition approach. Furthermore, just as targeting virulence pathways as an antibacterial strategy has proven challenging due to the lack of *in vitro* MICs, inhibitors of genes with enhanced *in vivo* vulnerability may face similar barriers to drug development. Developing *in vitro* assays or identifying non-mammalian model organisms that are predictive of exploiting *in vivo* vulnerabilities (33) is critical for capitalizing on this paradigm of target prioritization.

The phenomenon where greater vulnerability is observed *in vivo* than *in vitro* for certain genes suggests that *in vitro* growth inhibitory measurements may undervalue the therapeutic potential of inhibiting these genes *in vivo*. Considering that many small molecule antibiotics have dose-limiting toxicities that have stymied their clinical development, (3) the concept of achieving high efficacy of bacterial clearance with a reduced drug dose is especially pertinent. LptD-targeting murepavadin (34) recently failed phase 3 clinical trials due to nephrotoxicity issues; however, lipopolysaccharide transport system components, including *lptD*, exhibit heightened *in vivo* vulnerability, suggesting that chemical inhibition of these gene targets to a level with indiscernible effects *in vitro* may be sufficient to clear the infection *in vivo*. Interestingly, a lower dose of murepavadin was sufficient to achieve the same level of antibacterial activity in the mouse lung compared to the mouse thigh. (35) This discrepancy was equivocally attributed to unpublished data on higher penetrance of the drug into epithelial lining

fluid compared to other tissues by the study authors; another explanation could be greater vulnerability of *lptD* in the lung than in the thigh.

Methods

Construction of PA14 individual knockdown strains

A top and bottom oligo corresponding to the desired sgRNA with the appropriate overhangs to mediate Golden Gate Assembly was ordered. Separate reactions with T4 polynucleotide kinase were run prior to annealing the top and bottom oligos. The annealed mixture was ligated with a Bsa1-HFv2 digested Mobile-CRISPRi plasmid and transformed into the *E. coli* pir+ strain via electroporation. Plasmids were isolated from the recovered colonies and sgRNA insertion was verified by PCR and sequencing. Plasmids were electroporated into the *E. coli* mfdpir+ strain in preparation for mating. Incubation of the generated mfdpir+ strain combined with a strain containing a transposase and WT PA14 yielded PA14 mutants with a chromosomally integrated Mobile-CRISPRi system.

Construction of PA14 knockdown mutant library

A pooled sgRNA library covering genes in **Supplementary Table 1** was ordered as a single-stranded DNA oligonucleotides (Twist Bioscience) and cloned into Mobile-CRISPRi plasmids containing the P1 constitutive promoter driving dCas9 activity through Golden Gate Assembly. This library was transferred into a mating strain (mfdpir+) before

chromosomal integration into PA14. As the library contains 3,112 unique sgRNAs (gene-targeting and non-targeting), at least 30x representation (>9,300 colonies) was needed to achieve sufficient coverage of the library following mating. The colonies were scraped from the plates and aliquoted into glycerol stocks for long-term storage.

Preparation of the pooled library inoculum & *in vitro* screen

One glycerol stock of the PA14 knockdown library was thawed out, centrifuged, and resuspended in 1 mL PBS. Based on the OD_{600nm} measurement of this suspension, a flask with 25 mL LB was inoculated at a starting OD_{600nm} of 0.01 and incubated at 37 °C with shaking at 225 rpm. When the culture reached OD_{600nm} of 0.64, 800 µL of the culture was plated on a large, square *Pseudomonas* Isolation Agar (PIA) plates with and without 30 µg/mL gentamicin. The plates were incubated for 48 hours prior to harvest. 3-6 mL of LB was used to scrape colonies off the plates with an L-shaped spreader. These cell suspensions were centrifuged and stored at -80 °C prior to gDNA extraction.

Mouse infection with pooled library

Starting with the resuspension of the glycerol stock in PBS, the inocula were prepared with two serial ten-fold dilutions. The more concentrated of the two inocula was diluted and spread on PIA and PIA + 30 µg/mL gentamicin plates for CFU enumeration. The remaining contents of the glycerol tube were centrifuged, and the pellet was frozen for gDNA extraction.

Pathogen-free male C57BL/6J mice, 8 weeks of age, were purchased from Jackson Laboratories. Animal experiments were conducted in accordance with the approval of the Institutional Animal Care and Use Committee (IACUC) at UCSF. A total of 10 mice were anesthetized with isofluorane prior to intratracheal instillation with 50 µl of the *Pseudomonas* knockdown library per an established protocol (22). Animal weights and rectal temperatures were measured at multiple timepoints to monitor the course of the infection.

Mice were sacrificed 24 hours post-infection. Lungs were collected in 3 ml of sterile PBS and homogenized by grinding the lung tissue against a cell strainer with the back of a syringe plunger. 100 µL of lung homogenates were directly plated on 10 PIA + 30 µg/mL gentamicin plates. Then the homogenates were diluted to various degrees in LB media and the same dilution was plated on both PIA and PIA + 30 µg/mL gentamicin plates for CFU enumeration. The plates were incubated for 48 hours prior to harvest. 3-6 mL of LB was used to scrape colonies off PIA + 30 ug/mL gent plates with an L-shaped spreader, and the 10 plates were combined to generate each mouse sample. These cell suspensions were centrifuged and stored at -80 °C prior to gDNA extraction.

Mouse infection with single strain

In separate experiments, 5 mL ON cultures in LB +/- 30 µg/mL gentamicin were grown from glycerol stocks of pgsA-P1, pgsA-P2, pgsA-P3, ispD-P1, mrfp-P1, and WT PA14. After 16 hours, cultures were diluted 1:100 in 3 mL LB +/- 30 µg/mL gentamicin and allowed to grow for 3 hours with shaking at 225 rpm. 1 mL of the sub-culture was washed and resuspended in 1 mL PBS. The suspensions were diluted according to calculations based on OD_{600nm} measurements to yield the final inocula. The mouse infection protocol as detailed above was followed. Mice were sacrificed 18 hours post infection, and lungs were manually homogenized as detailed above. Various dilutions of the lung homogenates were plated on PIA and PIA + 30 µg/mL gentamicin plates for CFU enumeration. Recovery rate was determined as the ratio of total CFU recovered from the animal after infection to total CFU instilled in the animal.

Amplicon library preparation & analysis

Qiagen DNeasy Blood & Tissue kit was used to extract gDNA from samples, and NEBNext Ultra II Q5® Master Mix was used for amplicon library preparation. Custom-made TruSeq primers extend the amplicon to incorporate the i5 and i7 ends, which are recognized by DualSeq primers procured from the Chan-Zuckerburg Biohub. The DualSeq primers are indexed to indicate sample identity and were demultiplexed after NGS. To determine number of reads needed from NGS, the number of unique barcodes was multiplied by a factor of 1,500 (3,112 * 1,500 = ~5,000,000) for robust detection of strain depletion.

Growth Curves

3 mL LB + 30 µg/mL gentamicin cultures were inoculated with each PA14 strain and incubated at 37 °C with shaking at 225 rpm for 16 hours. Cultures were diluted 1:100 into fresh LB media and 200 µL of the respective cultures was added to each well in a 96-well plate. This plate was covered with an optically clear seal, and a needle was used to poke holes in each of the wells. OD_{600nm} were monitored during incubation in a microplate reader (Synergy H1; BioTek Instruments, VT) with continuous, fast, double orbital shaking. Samples were blanked with a well containing LB media. Results are representative of at least two biological replicates.

Acknowledgements

I acknowledge Dr. Michelle Yu, MD, PhD and Michael Kwon for their expertise and assistance in performing murine pneumonia model experiments, as well as Dr. Jason Peters, PhD and Ryan Ward for their expertise assistance in analyzing next-generation sequencing data with a custom-built computational pipeline.

References

1. Tacconelli, Magrini, Kahlmeter, Singh. Global priority list of antibiotic-resistant bacteria to guide research, discovery, and development of new antibiotics. WHO AIDS Tech Bull.

2. Poulsen BE, Yang R, Clatworthy AE, White T, Osmulski SJ, Li L, Penaranda C, Lander ES, Shoresh N, Hung DT. 2019. Defining the core essential genome of Pseudomonas aeruginosa. Proc Natl Acad Sci U S A 116:10072–10080.

3. Prasad NK, Seiple IB, Cirz RT, Rosenberg OS. 2022. Leaks in the Pipeline: a Failure Analysis of Gram-Negative Antibiotic Development from 2010 to 2020. Antimicrob Agents Chemother 66:e0005422.

4. Kristian SA, Timmer AM, Liu GY, Lauth X, Sal-Man N, Rosenfeld Y, Shai Y, Gallo RL, Nizet V. 2007. Impairment of innate immune killing mechanisms by bacteriostatic antibiotics. FASEB J 21:1107–1116.

5. Dhand A, Bayer AS, Pogliano J, Yang S-J, Bolaris M, Nizet V, Wang G, Sakoulas G. 2011. Use of Antistaphylococcal -Lactams to Increase Daptomycin Activity in Eradicating Persistent Bacteremia Due to Methicillin-Resistant Staphylococcus aureus: Role of Enhanced Daptomycin Binding. Clinical Infectious Diseases https://doi.org/10.1093/cid/cir340.

6. Sakoulas G, Bayer AS, Pogliano J, Tsuji BT, Yang S-J, Mishra NN, Nizet V, Yeaman MR, Moise PA. 2012. Ampicillin enhances daptomycin- and cationic host defense peptide-mediated killing of ampicillin- and vancomycin-resistant Enterococcus faecium. Antimicrob Agents Chemother 56:838–844.

7. Dhand A, Sakoulas G. 2014. Daptomycin in combination with other antibiotics for the treatment of complicated methicillin-resistant Staphylococcus aureus bacteremia. Clin Ther 36:1303–1316.

8. Sakoulas G, Nonejuie P, Kullar R, Pogliano J, Rybak MJ, Nizet V. 2015. Examining the use of ceftaroline in the treatment of Streptococcus pneumoniae meningitis with reference to human cathelicidin LL-37. Antimicrob Agents Chemother 59:2428–2431.

9. van Opijnen T, Camilli A. 2012. A fine scale phenotype-genotype virulence map of a bacterial pathogen. Genome Res 22:2541–2551.

10. Skurnik D, Roux D, Aschard H, Cattoir V, Yoder-Himes D, Lory S, Pier GB. 2013. A comprehensive analysis of in vitro and in vivo genetic fitness of Pseudomonas aeruginosa using high-throughput sequencing of transposon libraries. PLoS Pathog 9:e1003582.

11. Smith EE, Buckley DG, Wu Z, Saenphimmachak C, Hoffman LR, D'Argenio DA, Miller SI, Ramsey BW, Speert DP, Moskowitz SM, Burns JL, Kaul R, Olson MV. 2006. Genetic

adaptation by Pseudomonas aeruginosa to the airways of cystic fibrosis patients. Proc Natl Acad Sci U S A 103:8487–8492.

12. Wei J-R, Krishnamoorthy V, Murphy K, Kim J-H, Schnappinger D, Alber T, Sassetti CM, Rhee KY, Rubin EJ. 2011. Depletion of antibiotic targets has widely varying effects on growth. Proc Natl Acad Sci U S A 108:4176–4181.

13. Hawkins JS, Silvis MR, Koo B-M, Peters JM, Osadnik H, Jost M, Hearne CC, Weissman JS, Todor H, Gross CA. 2020. Mismatch-CRISPRi Reveals the Co-varying Expression-Fitness Relationships of Essential Genes in Escherichia coli and Bacillus subtilis. Cell Syst 11:523–535.e9.

14. Jost M, Santos DA, Saunders RA, Horlbeck MA, Hawkins JS, Scaria SM, Norman TM, Hussmann JA, Liem CR, Gross CA, Weissman JS. 2020. Titrating gene expression using libraries of systematically attenuated CRISPR guide RNAs. Nat Biotechnol 38:355–364.

15. Keren L, Hausser J, Lotan-Pompan M, Vainberg Slutskin I, Alisar H, Kaminski S, Weinberger A, Alon U, Milo R, Segal E. 2016. Massively Parallel Interrogation of the Effects of Gene Expression Levels on Fitness. Cell 166:1282–1294.e18.

16. Bosch B, DeJesus MA, Poulton NC, Zhang W, Engelhart CA, Zaveri A, Lavalette S, Ruecker N, Trujillo C, Wallach JB, Li S, Ehrt S, Chait BT, Schnappinger D, Rock JM.

2021. Genome-wide gene expression tuning reveals diverse vulnerabilities of M. tuberculosis. Cell 184:4579–4592.e24.

17. Qu J, Prasad NK, Yu MA, Chen S, Lyden A, Herrera N, Silvis MR, Crawford E, Looney MR, Peters JM, Rosenberg OS. 2019. Modulating pathogenesis with Mobile-CRISPRi. J Bacteriol 201.

18. Banta AB, Ward RD, Tran JS, Bacon EE, Peters JM. 2020. Programmable Gene Knockdown in Diverse Bacteria Using Mobile-CRISPRi. Curr Protoc Microbiol 59:e130.

19. Peters JM, Koo B-M, Patino R, Heussler GE, Hearne CC, Qu J, Inclan YF, Hawkins JS, Lu CHS, Silvis MR, Harden MM, Osadnik H, Peters JE, Engel JN, Dutton RJ, Grossman AD, Gross CA, Rosenberg OS. 2019. Enabling genetic analysis of diverse bacteria with Mobile-CRISPRi. Nat Microbiol 4:244–250.

20. Liu X, Kimmey JM, Matarazzo L, de Bakker V, Van Maele L, Sirard J-C, Nizet V, Veening J-W. 2021. Exploration of Bacterial Bottlenecks and Streptococcus pneumoniae Pathogenesis by CRISPRi-Seq. Cell Host Microbe 29:107–120.e6.

21. Abel S, Abel zur Wiesch P, Chang H-H, Davis BM, Lipsitch M, Waldor MK. 2015. Sequence tag-based analysis of microbial population dynamics. Nat Methods 12:223–6, 3 p following 226.

22. Ortiz-Muñoz G, Looney MR. 2015. Non-invasive Intratracheal Instillation in Mice. Bio Protoc 5.

23. Griffin AS, West SA, Buckling A. 2004. Cooperation and competition in pathogenic bacteria. Nature 430:1024–1027.

24. Fernández-Piñar R, Lo Sciuto A, Rossi A, Ranucci S, Bragonzi A, Imperi F. 2015. In vitro and in vivo screening for novel essential cell-envelope proteins in Pseudomonas aeruginosa. Sci Rep 5:17593.

25. Lloyd MG, Lundgren BR, Hall CW, Gagnon LB-P, Mah T-F, Moffat JF, Nomura CT. 2017. Targeting the alternative sigma factor RpoN to combat virulence in Pseudomonas aeruginosa. Scientific Reports https://doi.org/10.1038/s41598-017-12667-y.

26. Jeukens J, Boyle B, Kukavica-Ibrulj I, Ouellet MM, Aaron SD, Charette SJ, Fothergill JL, Tucker NP, Winstanley C, Levesque RC. 2014. Comparative genomics of isolates of a Pseudomonas aeruginosa epidemic strain associated with chronic lung infections of cystic fibrosis patients. PLoS One 9:e87611.

27. Marvig RL, Dolce D, Sommer LM, Petersen B, Ciofu O, Campana S, Molin S, Taccetti G, Johansen HK. 2015. Within-host microevolution of Pseudomonas aeruginosa in Italian cystic fibrosis patients. BMC Microbiol 15:218.

28. Cigana C, Curcurù L, Leone MR, Ieranò T, Lorè NI, Bianconi I, Silipo A, Cozzolino F, Lanzetta R, Molinaro A, Bernardini ML, Bragonzi A. 2009. Pseudomonas aeruginosa exploits lipid A and muropeptides modification as a strategy to lower innate immunity during cystic fibrosis lung infection. PLoS One 4:e8439.

29. Amiel E, Lovewell RR, O'Toole GA, Hogan DA, Berwin B. 2010. Pseudomonas aeruginosa evasion of phagocytosis is mediated by loss of swimming motility and is independent of flagellum expression. Infect Immun 78:2937–2945.

30. Jensen PA, Zhu Z, van Opijnen T. 2017. Antibiotics Disrupt Coordination between Transcriptional and Phenotypic Stress Responses in Pathogenic Bacteria. Cell Rep 20:1705–1716.

31. Cornforth DM, Dees JL, Ibberson CB, Huse HK, Mathiesen IH, Kirketerp-Møller K, Wolcott RD, Rumbaugh KP, Bjarnsholt T, Whiteley M. 2018. Pseudomonas aeruginosa transcriptome during human infection. Proc Natl Acad Sci U S A 115:E5125–E5134.

32. Ramachandran V, Ramachandran V, Singh R, Yang S, Ragadeepthi T, Mohapatra S, Khandelwal S, Patel S. 2013. Genetic and chemical knockdown: a complementary strategy for evaluating an anti-infective target. Advances and Applications in Bioinformatics and Chemistry https://doi.org/10.2147/aabc.s39198.

33. Benghezal M, Adam E, Lucas A, Burn C, Orchard MG, Deuschel C, Valentino E, Braillard S, Paccaud J-P, Cosson P. 2007. Inhibitors of bacterial virulence identified in a surrogate host model. Cell Microbiol 9:1336–1342.

34. Srinivas N, Jetter P, Ueberbacher BJ, Werneburg M, Zerbe K, Steinmann J, Van der Meijden B, Bernardini F, Lederer A, Dias RLA, Misson PE, Henze H, Zumbrunn J, Gombert FO, Obrecht D, Hunziker P, Schauer S, Ziegler U, Käch A, Eberl L, Riedel K, DeMarco SJ, Robinson JA. 2010. Peptidomimetic antibiotics target outer-membrane biogenesis in Pseudomonas aeruginosa. Science 327:1010–1013.

35. Melchers MJ, Teague J, Warn P, Hansen J, Bernardini F, Wach A, Obrecht D, Dale GE, Mouton JW. 2019. Pharmacokinetics and Pharmacodynamics of Murepavadin in Neutropenic Mouse Models. Antimicrob Agents Chemother 63.

Chapter 4

Tool Application: Profiling genetic vulnerabilities to phage predation

Abstract

Existing antibiotics have lost reliability in curing bacterial infections, threatening the very foundations of modern medicine. Capturing interest as a novel modality for infection control, bacteriophages (phages) are naturally potent killers of bacteria and omnipresent in our environment. Since the 20th century, phage therapy has been considered a promising alternative to traditional small molecule antibiotics, but its utility has been severely restricted by intrinsic anti-phage mechanisms that protect bacteria from phage predation. A better understanding of these mechanisms could inform phage therapy development. In this work, we use genetic and proteomic approaches to identify vulnerabilities associated with *Pseudomonas aeruginosa* essential genes, which can be translated into small molecule inhibitors for co-administration with phage therapy. In this foundational work, we show some enhancement of DMS3 phage family activity against PA14 through genetic inhibition of essential genes *pyrC*, *lptH*, *lpxD*, and non-essential genes *trmH*, *xcpP*, and *algP*.

Introduction

Small molecule antibiotic drugs historically have not kept pace with continually evolving pathogens, resulting in antibacterial resistance. Bacteriophage (phage) are natural predators of bacteria, and both have co-evolved offensive and defensive mechanisms against each other. Among these anti-phage mechanisms used by bacteria for protection against phage predation is the CRISPR system, which has been exploited by researchers as a powerful genetic tool. Investigating such phage-host interactions has the potential to yield more tools for research and therapeutic development.

Phage therapy development has shown promise as an alternative to failing small molecule antibiotics, but anti-phage mechanisms represent a major hurdle. In the modern era, our ability to isolate, sequence, analyze, modify, and deliver phage therapies has improved dramatically. (1,2) To enhance the potency of phage as therapeutics, a deeper, molecular-level understanding of phage-host interactions is needed, as bacteria harbor many innate and acquired mechanisms to resist phage predation.

Efforts to create an exhaustive list of anti-phage mechanisms has been pursued mostly through probing non-essential bacterial genes where knockout enhances phage predation. (3–5) However, due to technological limitations, these studies have largely overlooked highly conserved bacterial essential genes. While all known bacterial anti-phage mechanisms are non-essential under standard laboratory conditions, many

phages alter host metabolism, and all phages rely on essential host processes like transcription and translation—suggesting that essential genes may be involved in anti-phage resistance mechanisms.

A groundbreaking study by Bikard and colleagues (6) recently explored the feasibility of using CRISPRi to reveal phage-host interactions in *E. coli*, including bacterial essential genes. The focus of the study was on bacterial strains where gene knockdown led to abrogation of phage activity. Genes where knockdown led to sensitization to phage predation were difficult to identify since phage-resistant mutants dominated the post-infection library population, drowning out mutants with either neutral or negative fitness levels.

While most studies in the area involve phages that are inherently successful in lysing bacteria, the potential to enhance a weakly lytic phage through inhibition of bacterial resistance mechanisms has not been as thoroughly investigated. We sought to design an experiment that would capture instances where knockdown of bacterial essential genes involved in anti-phage mechanisms renders the bacteria more susceptible to phage predation, thereby potentiating the productivity of phage infection. Such a study would not only reveal anti-phage resistance mechanisms, but also could guide the development of small molecule adjuvants to phage therapy.

To complement the genetic screening approach, we use an unbiased proteomic analysis to identify interactions between phage and bacterial proteins that mediate anti-phage resistance mechanisms. The abundance (7) and dynamics (8) of protein complexes can be determined through size-exclusion chromatography coupled with mass-spectrometry using a data-independent acquisition mode. This method enables mining of the phage accessory genome, revealing not only host processes that can be antagonized by phage, but also phage engineering strategies to overcome intrinsic resistance.

To demonstrate the utility of this dual-pronged approach, we sought to identify resistance mechanisms against engineered variants of the DMS3 model phage, part of the Mu-like phage family. DMS3 contains a wide repertoire of largely uncharacterized accessory proteins that are enriched for anti-host interactions. While it is a temperate phage, it can be easily locked into the lytic cycle by deletion of the c-repressor. (9,10) These lytic variants escape common superinfection exclusion mediated by the immunity protein expressed by endogenous prophages (10) and is non-immunogenic (11) in comparison to other phages.

As part of a manufactured system of checks and balances, we use both wildtype *Pseudomonas aeruginosa* and an engineered variant fortified with extra spacers targeting DMS3 phage to probe resistance mechanisms against DMS3 phage relatives, including those containing anti-CRISPR proteins. By arming bacteria with strong weapons and phage with similarly matched armor enables phage to use proteins in its accessory

genome to kill bacteria that display the slightest weakness in the form of a genetic vulnerability. Importantly, this precarious balance allows us to detect these small windows of opportunity created by perturbation of bacterial essential genes.

Results

Mobile-CRISPRi Enables Modulation of Phage Productivity

The phage DMS3mvir is a lytic phage unable to replicate in PA14 because it is targeted by a natural spacer in the Type I-F CRISPR system of PA14, while phage DMS3vir can replicate in PA14 due to protospacer mismatches (**Fig. 4.1A**). (9) Knockdown of two distinct *cas* gene operons in the PA14 CRISPR-cas locus (*csy1-2-3-4 and cas1-2-3*) using Mobile-CRISPRi makes DMS3mvir replication possible but does not affect DMS3vir infection. Notably, the knockdown strains enable the same extent of phage replication that is observed in both complete CRISPR knock-out strains and phage possessing the CRISPR-inhibiting anti-CRISPR protein AcrIF1 (**Fig. 4.1A)**.

As another example, knockdown of *pilA*, which encodes the major subunit of the type IV pilus, inhibits the replication of the pilus-dependent DMS3-like phage JBD30 in PA14 **(Fig. 4.1B)**. These results demonstrate that Mobile-CRISPRi can be used to discover bacterial sensitizing and protective factors against a variety of phages.

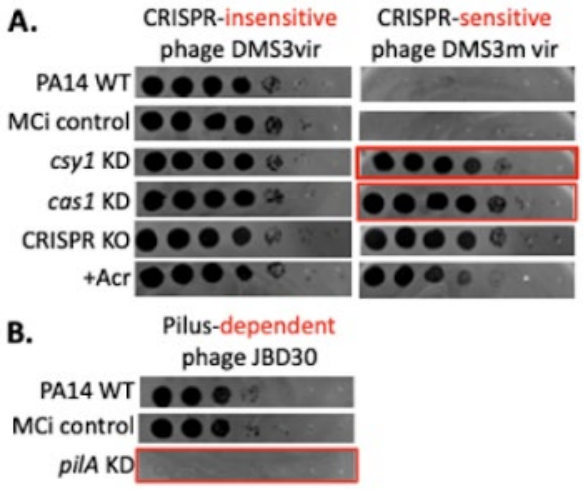

Figure 4.1: Gain and loss of phage infectivity in response to targeted CRISPRi depletion of protective and phage-sensitizing factors.
10-fold serial dilutions of the CRISPR-sensitive phage DMS3mvir or CRISPR-resistant phage DMS3vir spotted on indicated PA14 host strains. (A) Mobile-CRISPRi knockdown of the PA14 CRISPR-cas locus (cas1 KD, cys1 KD) makes DMS3mvir replication possible. (B) Depletion of the pilus (pilA KD), a phage receptor required for adsorption of the phage JBD30, leads to loss of viral entry and infectivity.

A Pooled CRISPRi Screen to Probe PA14 Protective Factors Against DMS3 Phage

Since phage and bacteria have co-evolved multiple offensive and defensive mechanisms, we chose to artificially introduce some of these known stressors (bacterial CRISPR systems and phage anti-CRISPR systems) while probing for bacterial vulnerabilities to phage predation. Previous work of the Bondy-Denomy lab revealed that PA14 carries a Type I-F CRISPR system, for which efficacy depends on the number of protospacers matching the target phage (9). Through laboratory evolution, a PA14 strain with 5

protospacers (PA14-5sp) that are a perfect match to DMS3mvir demonstrated resistance to lysis.

We have engineered a library of PA14-5sp mutants that are transcriptionally repressed in 528 individual essential genes via Mobile-CRISPRi. The genes were chosen according to essentiality in atleast one media, including infection-related conditions, as determined in a transposon screen. (12) The extent of gene knockdown was varied by 1) using a series of three constitutive promoters within a small gradation of strengths in driving *dcas9* expression (13) and 2) by designing four sgRNAs at various regions along the gene, since distance from the transcription start site decreases knockdown levels. (14–16) The knockdown strains in this library (PA14-5sp KD Lib) represent combinations of the 3 constitutive promoters and the sgRNA library, including 1,000 non-targeting negative controls (**Fig. 4.2A**).

This PA14-5sp essential gene knockdown library was used to search for essential genes with protective properties against phage, expanding the known repertoire of non-essential genes that interact with phage (**Fig. 4.2B**). To this end, the library was exposed to the model phage DMS3mvir and engineered variants containing anti-CRISPR proteins. The interactions between PA14-5sp and a lytic phage expressing a strong (*acrIF1*) or weak (*acrIF4*) anti-CRISPR creates a delicate equilibrium between host and phage, which can be perturbed with knockdowns of bacterial essential genes.

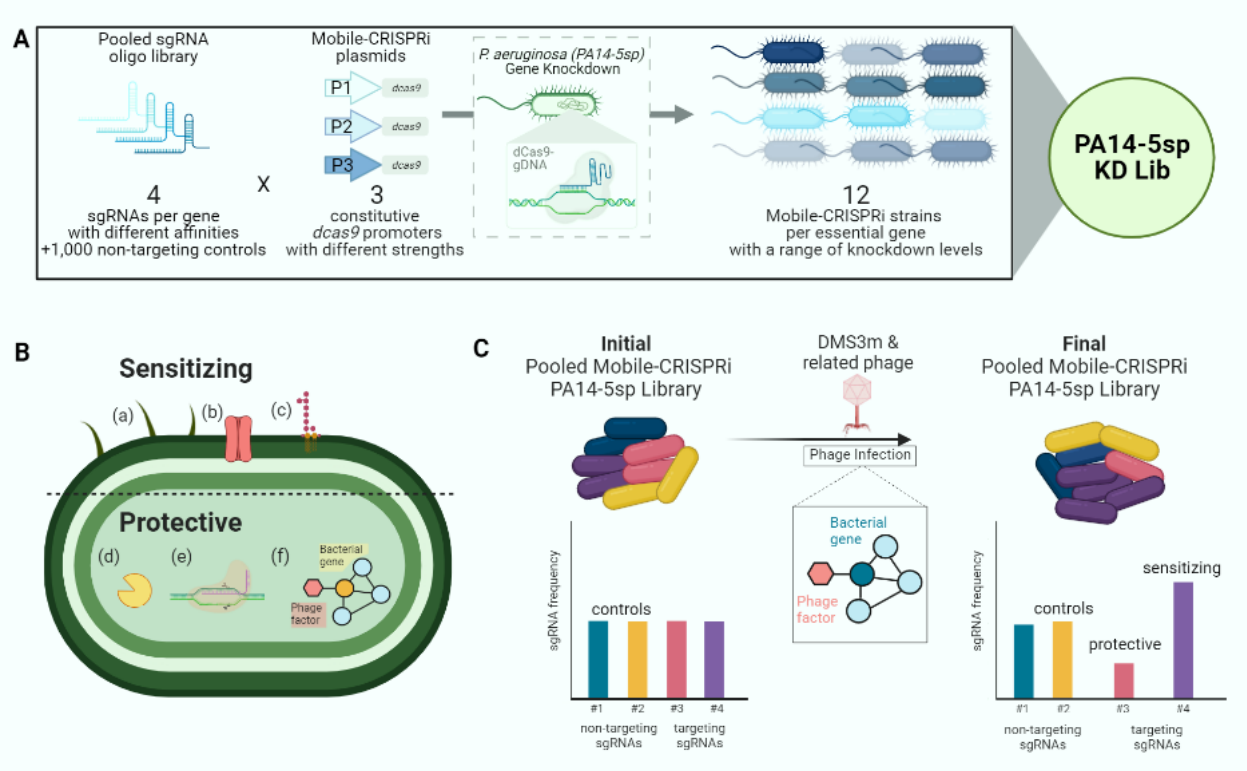

Figure 4.2: Mobile-CRISPRi library and screen design

(A) A pooled sgRNA library was designed to contain 3,112 sgRNAs, representing 528 PA14 genes demonstrating essentiality in LB or infection-related media targeted by 4 sgRNAs per gene as well as 1,000 non-targeting sgRNA controls. The pooled sgRNA library was inserted into restriction digested Mobile-CRISPRi plasmids containing one of three constitutive promoter driving dCas9 activity. The pooled Mobile-CRISPRi constructs were chromosomally integrated into the PA14-5sp strain through mating to generate a pooled knockdown library. The knockdown libraries associated with each promoter (PA14-5sp P1 Lib, PA14-5sp P2 Lib, PA14-5sp P3 Lib) were combined in equivalent proportions to generate PA14-5sp KD Lib. (B) Examples of sensitizing and protective gene products that we seek to find in this screen. ***Sensitizing:*** (a) pilli, (b) porins, (c) LPS, O-antigen; ***Protective:*** (d) restriction enzymes, (e) CRISPR, (f) putative bacterial essential genes that resist phage infection that we aim to uncover in this screen. (C) Visual representation of genetic screen, in which the PA14-5sp KD Lib is exposed to phage. Knockdown strains that are depleted in the final population are considered "hits", as they demonstrate heightened vulnerability to phage predation compared to non-targeting negative control strains and may play a protective role.

In the screen, PA14-5sp KD Lib was infected with two different doses of three phages (DMS3mvir, DMS3mvir+AcrIF1, or DMS3mvir+AcrIF4), and samples were taken at 3 different time points (5, 11, and 24 hours). These conditions were chosen based on preliminary growth curves using PA14-5sp P1 Lib (**Supplementary Fig. 4.1**). After gDNA extraction, amplicon library preparation, and next-generation sequencing of the samples, we identified knockdown strains that were exceptionally depleted in each condition relative to the distribution of non-targeting control strains (**Fig. 4.2C**).

	OD600		
	5.5 h	11 h	24h
Uninfected-1	1.575	3.125	7.3
Uninfected-2	1.65	3.475	7.04
DMS3m vir 1	0.755	5.725	7.26
DMS3m vir 2	1.4	5.1	6.1
acrIF4 Low dose -1	1.22	5.825	4.08
acrIF4 Low dose -2	0.915	5.55	4.6
acrIF4 High dose 1	0.865	4.225	2.36
acrIF4 High dose 2	0.88	4.525	2.06
acrIF1 Low dose 1	1.345	3.45	3.94
acrIF1 Low dose 2	1.305	5.55	4.2
acrIF1 High dose 1	1.015	0.6*	1.12
acrIF1 High dose 2	1.005	0.565*	1.38

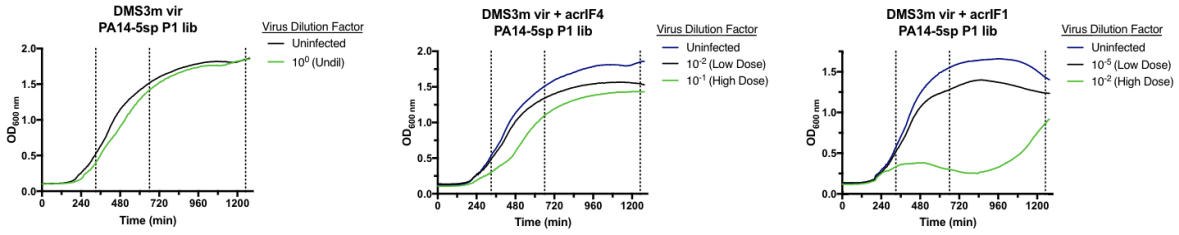

Supplementary Figure 4.1: Growth curves corresponding to PA14-5sp P1 Lib exposed to DMS3mvir phage and variants at multiple time points
The chart shows manually taken data with spectrophotomer for PA14-5sp growth under different phage infection conditions. Graphs show data collected by a plate reader for the infection of the PA14-5sp P1 library with various concentrations of DMS3mvir phages.

To begin analysis of next-generation sequencing results, several quality control metrics were assessed. In comparing the library populations of duplicate samples, the low correlation of population distributions in several samples suggested technical issues concerning reproducibility or noisiness of data. Samples with correlation values (r) > 0.7 of fractional composition of non-targeting controls between duplicate samples were DMS3mvir 11 hr, DMS3mvir 24 hr, DMS3mvir acrF4 high dilution 11 hr, DMS3mvir acrF4 low dilution 24 hr, uninfected 11 hr, and uninfected 24 hr. Corroborating the lack of reproducibility in the 5 hour samples, the population of 1,000 non-targeting controls exhibited skewed distributions in all the 5 hr samples, including the uninfected bacterial cultures, indicating a bottleneck effect (**Supplementary Fig. 4.2**). To resolve this matter, only the samples with high reproducibility were carried forward in the analysis pipeline, and Z-scores were calculated for every strain in the library based on the distribution of the non-targeting controls in the libraries associated with each of the 3 promoters.

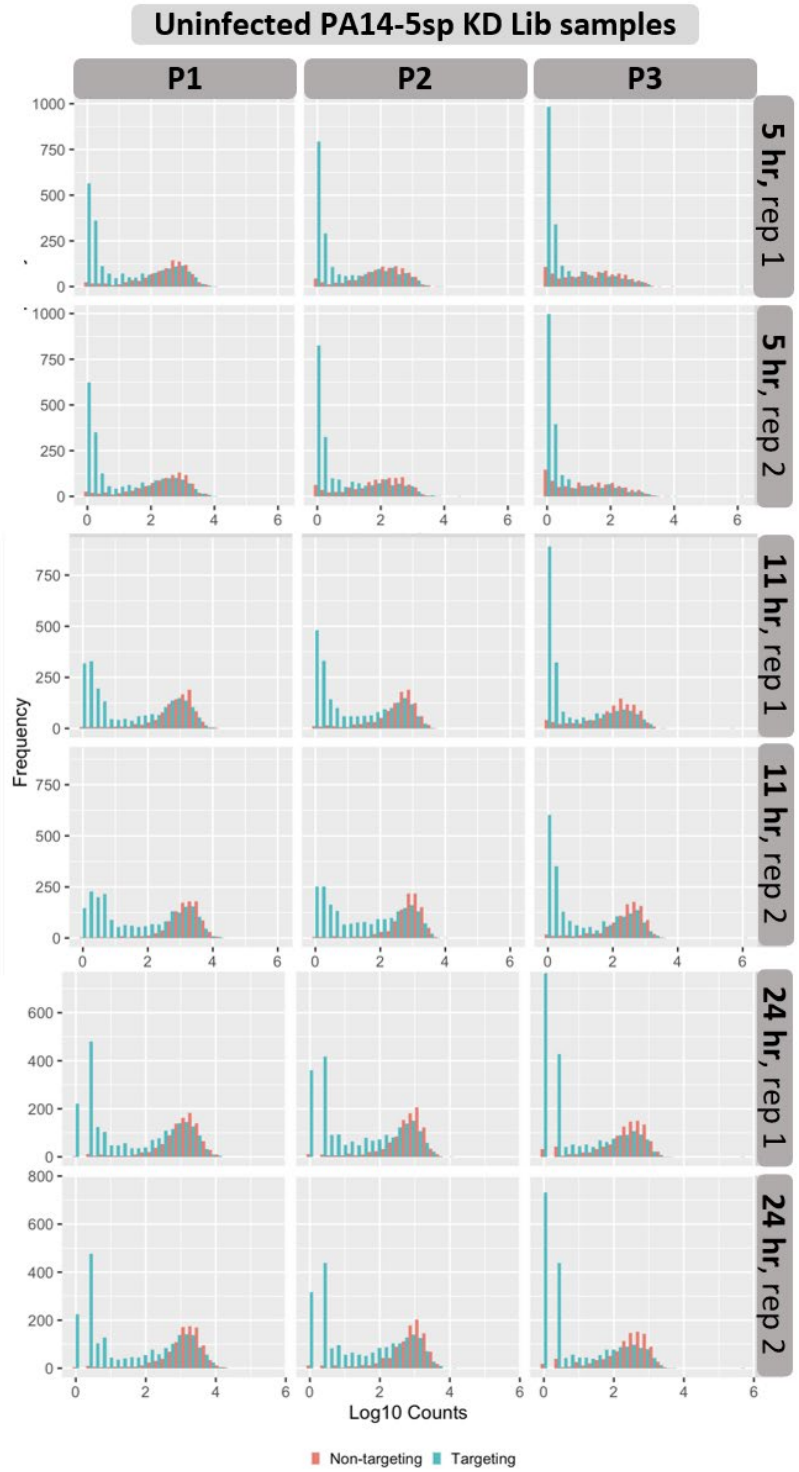

Supplementary Figure 4.2: Histograms for PA14-5sp KD Lib sgRNA distributions in uninfected samples over time

Next-generation sequencing analysis generated a count matrix for all detected sgRNA-promoter pairings. sgRNA distributions are depicted for each duplicate taken at 5 hours, 11 hours, and 24 hours post-infection and separated according to promoter number.

Moreover, individual mutants in the uninfected PA14-5sp KD Lib cultures were expected to maintain their fractional composition over the course of time, based on the lack of *in vitro* fitness defects observed for the PA14-P1 library used in Chapter 3. However, the distribution of mutants with gene-targeting sgRNAs shifts from 5 hours to 11 hours and 24 hours. This dynamic suggests that there may be underlying competition among the PA14-5sp P1, PA14-5sp P2, and PA14-5sp P3 libraries, and strain depletion in the phage-infection conditions may not be entirely attributable to bacteria-phage interactions. To account for time-dependent depletion of strains in the absence of phage, biologically relevant depletions were determined based on the difference in Z-scores of strains representing each targeted gene in the uninfected and infected conditions.

Accordingly, "hits" in our screen correspond to strains exhibiting lower fitness in the phage-infected condition compared to the uninfected condition, resulting in positive Z-score differences (**Fig. 4.3**). The threshold of >3 Z-score difference to be considered a hit is consistent with the lack of negative control strain appearing in that region (**Supplementary Fig. 4.3**). Small subsets of strains, defined by unique combinations of sgRNAs and promoters, are classified as hits in each of the four infection conditions that met the duplicate correlation threshold of $r > 0.7$. With few exceptions, these hits are largely non-overlapping among the different phage infection conditions, suggesting that bacterial vulnerabilities may depend on the phage's extent of protection against CRISPR and stage of infection.

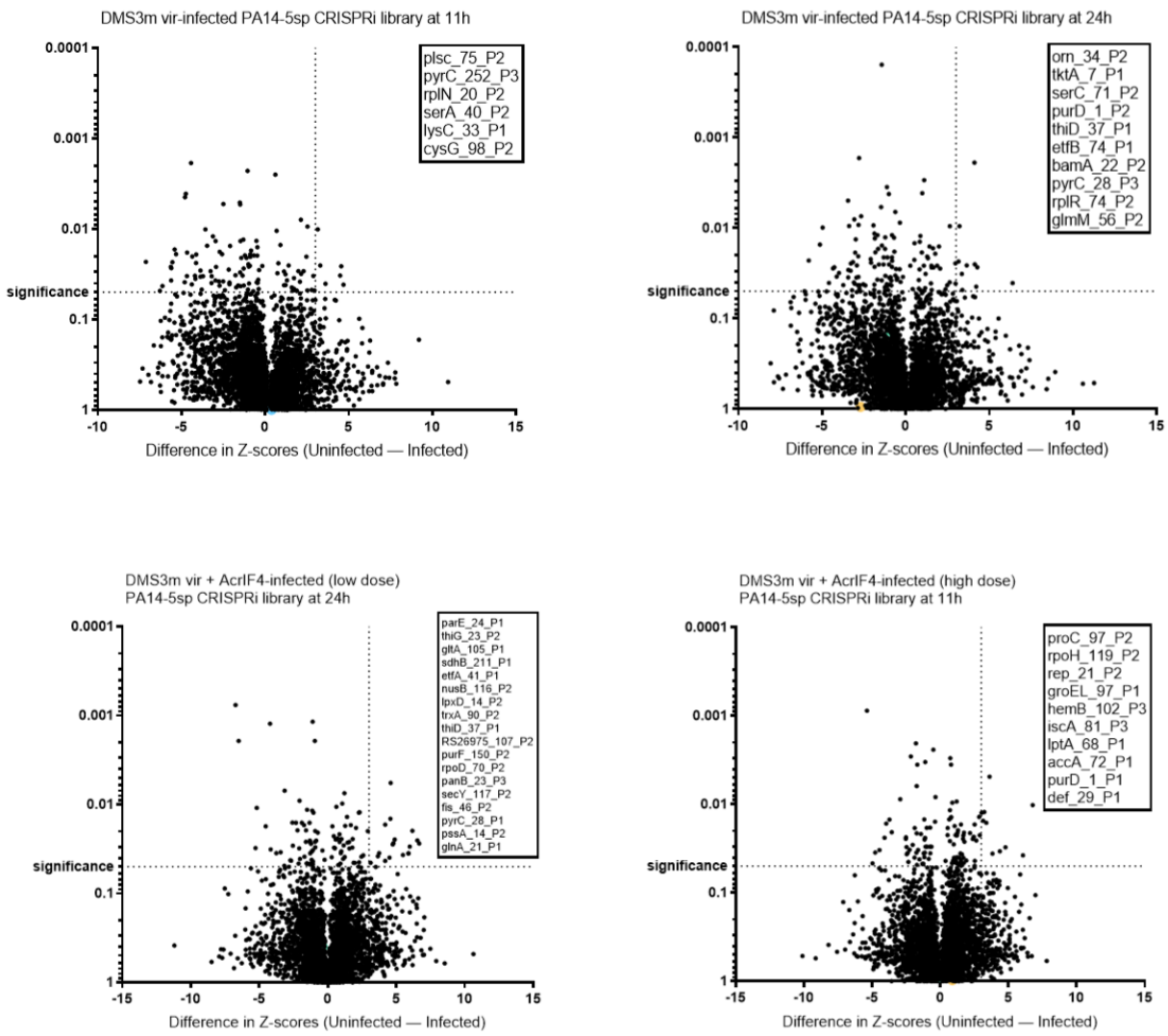

Figure 4.3: Volcano plots from the genetic screen

The log percent read metric was determined for each sgRNA-promoter pairing to normalize counts across samples, and Z-scores were calculated in relation to the distribution of 1,000 non-targeting sgRNA negative control strains. P values were calculated according to the subtraction of the Z-score associated with the infected sample from that of the uninfected sample for each gene. The upper right quadrant of the volcano plot represents Mobile-CRISPRi mutants (with unique sgRNA and promoter combinations) exhibiting reduced fitness specifically during phage infection. Mutants with a Z-score difference >3 and p val <.05 are listed in the box and represented as dots in the upper right quadrant of the graph.

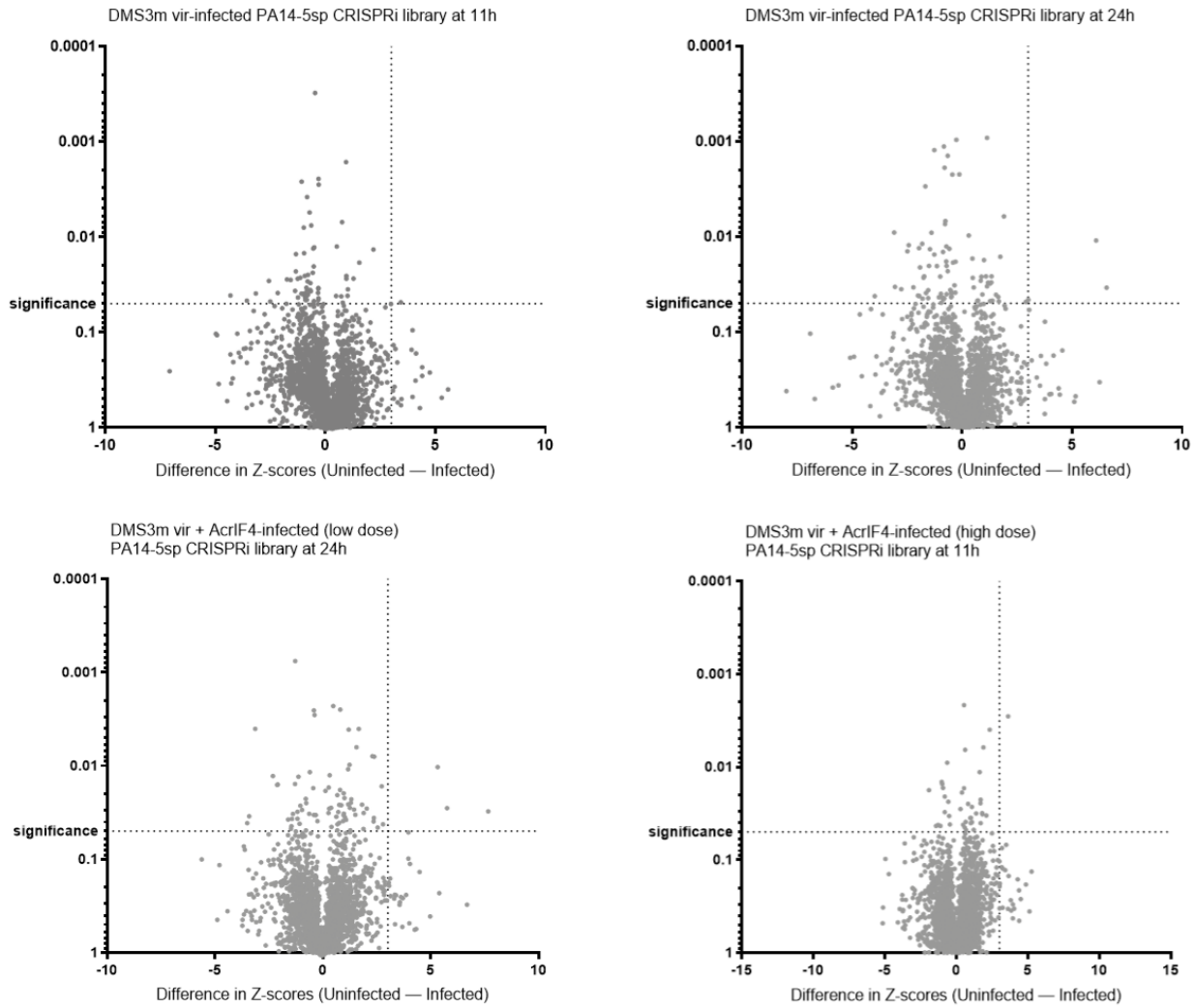

Supplementary Figure 4.3: Volcano plots of negative control strains from the genetic screen

The log percent read metric was determined for each of the 3,000 non-targeting sgRNA-promoter pairings to normalize counts across samples, and Z-scores were calculated in relation to the distribution of 1,000 non-targeting sgRNA negative control strains. P values were calculated according to the subtraction of the Z-score associated with the infected sample from that of the uninfected sample for each gene. The upper right quadrant of the volcano plot represents negative control strains (with unique sgRNA and promoter combinations) with reduced fitness specifically during phage infection. A limited number of negative control strains are present in the region defined by a Z-score difference >3 and p val <0.05.

Essential gene knockdown-mediated sensitization to phage predation has limited generalizability

To validate the results of our screen, we returned to our hypothesis that perturbation of PA14 genes to an extent with unnoticeable growth defects may generate a vulnerability that DMS3mvir can exploit, despite the phage's weak lytic activity in the wildtype PA14 strain. Universal, time-independent, and phage-independent genetic vulnerabilities that can be exploited to enhance phage predation are attractive as target candidates for adjuvant therapy. As such, we chose to validate the susceptibility of several Mobile-CRISPRi mutants based on conserved depletion (not necessarily significant) in multiple infection conditions (**Fig. 4.4**). This commonality suggests that the targeted genes are involved in general resistance to phage infection, rather than a phage-specific response.

PA14 Mobile-CRISPRi mutants corresponding to the selected hits were created individually using previously developed procedures and assessed in plaque assays. Downregulation of *nusB* in *E. coli* has been reported to increase strain fitness during lambda phage infection (17–18) but Mobile-CRISPRi mutants targeting *nusB* did not exhibit differential susceptibility to DMS3mvir infection in the validation assay (**Fig. 4.5**). Of all the Mobile-CRISPRi mutants tested, slight enhancement in plaquing efficiency of DMS3mvir + AcrIF4 was observed against PA14 knockdowns of *lptH, pyrC*, and *lpxD* (**Fig. 4.5A** and **B**). Notably, the *pyrC* knockdown mutant demonstrated heightened vulnerability to the DMS3mvir phage without the anti-CRISPR systems (**Fig. 4.5A** and **C**).

A

		DMS3mvir at 11 hr		DMS3mvir at 24 hr		DMS3mvir + AcrIF4 (low dose) at 24 hr		DMS3mvir + AcrIF4 (high dose) at 11 hr	
Target and TSS Offset	Promoter	Z-score diff (uninfected-infected)	pval	Z-score diff (uninfected-infected)	pval	Z-score diff (uninfected-infected)	pval	Z-score diff (uninfected-infected)	pval
amrB_109	P1	4.234326571	0.770	8.93247467	0.388	6.816198853	0.434	1.692782559	0.979
dnaA_101	P2	2.828059347	0.529	4.910710689	0.180	6.490492498	0.145	3.045943718	0.438
nusA_60	P2	7.836149536	0.513	3.062939524	0.377	3.178995488	0.287	5.695846244	0.582
nusB_116	P2	-1.234370984	0.432	4.530624405	0.142	6.659725889	0.027	-1.092248054	0.706
nusB_59	P3	7.054630719	0.510	0.307387165	0.800	-0.213934641	0.736	6.392155833	0.475
lptA_68	P1	2.654430675	0.195	-2.981045647	0.377	-0.804495807	0.684	3.824744735	0.036
lptA_68	P2	9.197402481	0.168	6.91609704	0.246	5.663986419	0.278	6.549800767	0.193
trmD_43	P1	2.686195345	0.086	8.423094949	0.603	7.908728086	0.574	3.403311835	0.087
lpxD_82	P1	4.846226487	0.367	5.665526651	0.358	3.733520305	0.479	2.957912449	0.451
pyrC_28	P1	4.92190126	0.172	0.013586259	0.844	4.735710767	0.028	-0.332774923	0.741
pyrC_28	P2	5.806432924	0.124	0.030054304	0.746	-0.49869143	0.903	4.798451625	0.176
serA_40	P2	4.483285995	0.033	0.508514315	0.879	2.008461179	0.603	3.531752036	0.076

B

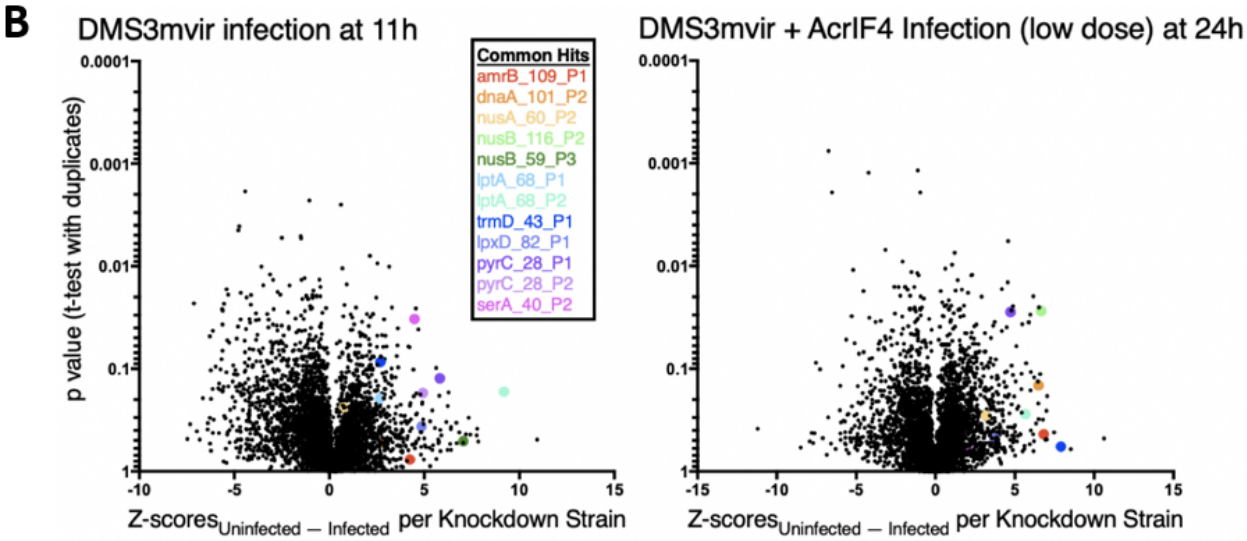

Figure 4.4: Generalizability as a prioritization metric for hit validation

Knockdown PA14-5sp strains sensitized to phage infection should have Z-score differences of atleast 1. (A) A list of Mobile-CRISPRi mutants that are depleted across multiple phage infection conditions that were chosen for further validation. We only analyzed conditions with fair reproducibility, and the Z-score and p value for each strain (defined by targeted gene, transcription start site offset of the sgRNA, and dCas9 promoter) are displayed. (B) Volcano plots from two example conditions are shown to highlight strains that are depleted in all infection conditions, which are color-coded to represent hits for further validation.

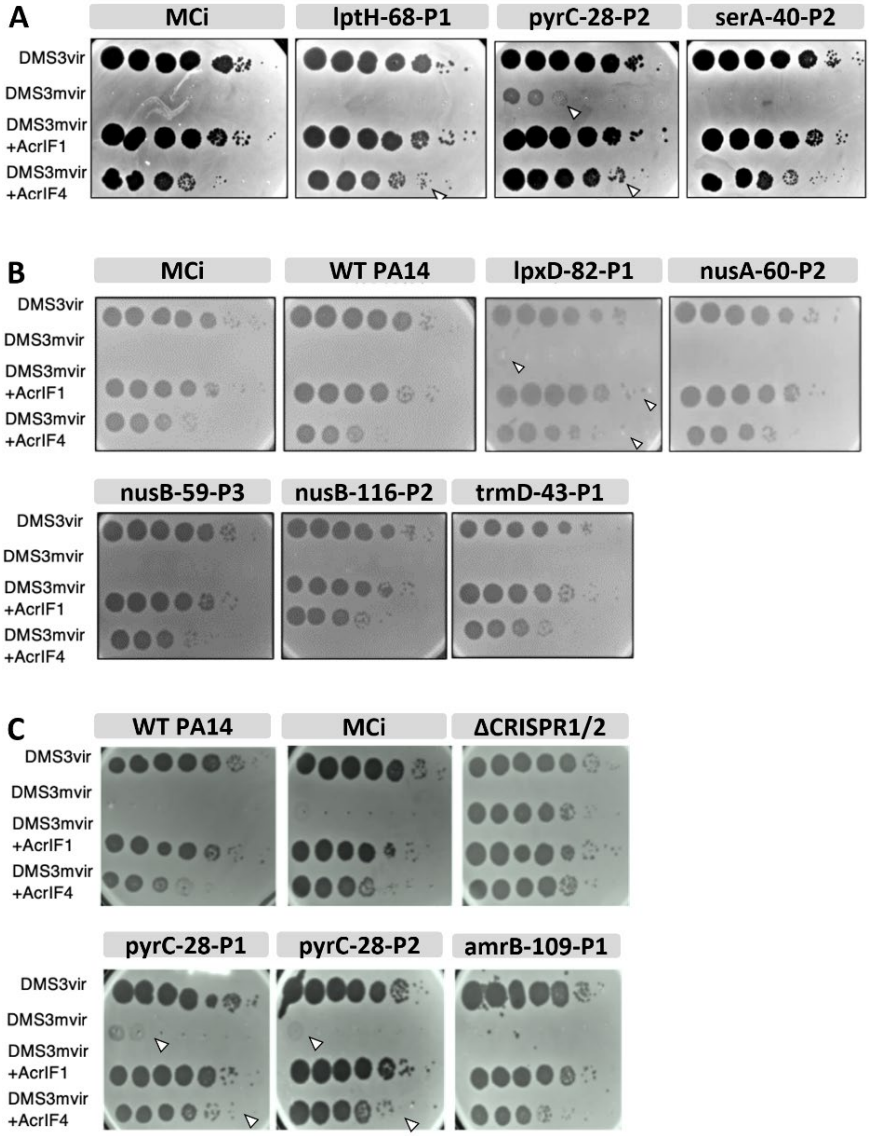

Figure 4.5: Validation of PA14 Mobile-CRISPRi hypersensitivity to phage lysis

Spot-titration assays are shown for the DMS3mvir panel of phages used in the genetic screen against various Mobile-CRISPRi mutants in 3 separate experiments (A, B and C), where phage concentration decreases left-to-right. A CRISPRi control strain (MCi) with a non-targeting sgRNA is used for comparison. Arrowheads point to qualitative evidence of heightened vulnerability to phage-mediated lysis.

Phage sensitization phenotype of *pyrC* knockdown in solid phase is not recapitulated in liquid growth

As pyrC knockdown enhances the productivity of phage possessing no anti-CRISPR systems, we sought to characterize this interaction further. There are two copies of pyrC in the PA14 genome: one copy of *pyrC* is a dihydroorotase enzyme in the pyrimidine biosynthesis pathway and is conditionally essential in a systemic murine infection model. (12) Recently, a family of bacterial pyrimidine cyclase enzymes were discovered that specifically synthesize cCMP and cUMP following phage infection, which activate immune effectors that execute an antiviral response. (19)

Our *pyrC* hit is PA3527 (aka PA14_RS07500, PA14_18710), which is co-operonic with a ribonuclease T (*rnt*) gene and distinct from the *pyrRBS* operon involved in pyrimidine biosynthesis. Ribonuclease T is involved in tRNA biosynthesis and is responsible for the end-turnover of tRNA by removing the terminal AMP residue from uncharged tRNA. The involvement of this *pyrC* gene or *rnt* in phage defense has not been previously described.

Given the enhanced phage plaquing efficiency observed in *pyrC* knockdown strains, we expected to recapitulate similar phenotypic effects during growth in liquid media. As efficiency of plaquing was greatest for phage DMS3mvir + AcrIF4, we measured growth curves of PA14 strains exposed to this phage. We found that, despite the potentiation phenotype in solid media, infection of *pyrC* knockdown mutants with DMS3mvir + AcrIF4

phage yielded similar dynamics as infection of WT PA14 (**Fig. 4.6**). Yet enhanced, dose-dependent bacterial killing was observed in the inactivated CRISPR positive control bacterial strain, suggesting that the phage was indeed exerting lytic activity (**Fig. 4.6**). In contrast, preliminary growth curves involving *lptH* knockdown mutants demonstrate bacterial growth inhibition beginning at 10 hours post-exposure using similar titers of DMS3mvir + AcIF4 phage.

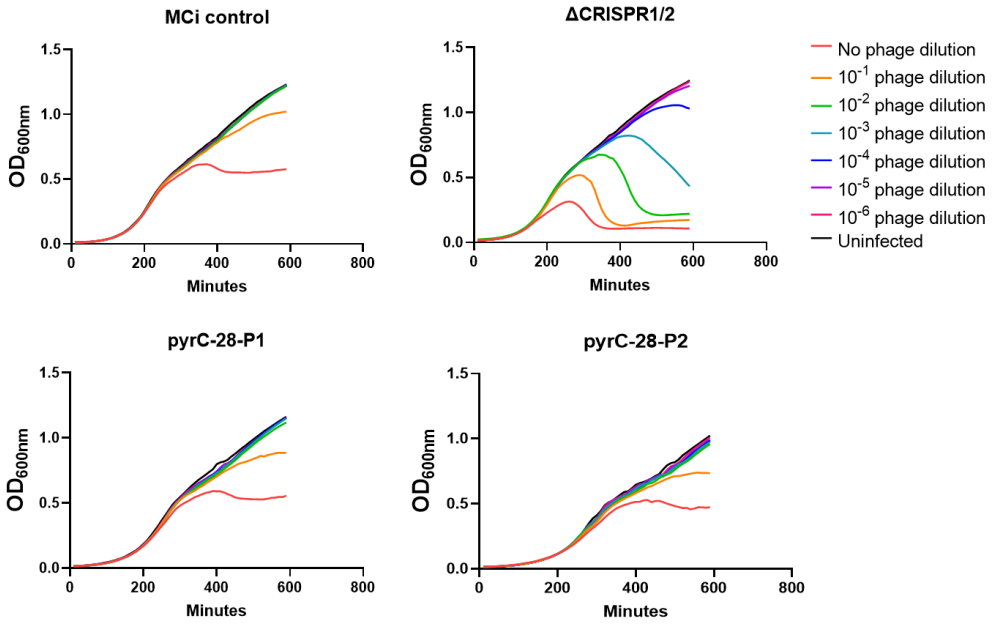

Figure 4.6: Liquid growth curves of *pyrC* knockdown mutants exposed to DMS3mvir + AcrIF4 phage

Growth curves of various bacterial strain (2 *pyrC* knockdowns, non-targeting sgRNA control, and inactivated CRISPR control) exposed to phage DMS3mvir + AcrIF4, as measured by a microplate reader.

While DMS3mvir + AcrIF4 had the greatest efficiency of plaquing on PA14, the DMS3mvir phage unarmed with anti-CRISPR protein also captured our interest: *pyrC* knockdown made PA14 more vulnerable to lysis by this phage despite the lack of intrinsic activity in wildtype PA14. When we attempted to recapitulate this potentiation in liquid growth curves, we once again were not able to distinguish the lytic activity of DMS3mvir against WT PA14 and *pyrC* knockdown mutants. We hypothesized that using a higher concentration of phage may allow us to observe the differential phenotype in liquid media. Plaque assays demonstrated that the PEG-concentrated phage stock was indeed more concentrated than the originally used stock, as lytic activity was observed in many more dilutions (**Fig. 4.7A**). However, the enhanced activity seen in solid growth conditions was abrogated in liquid growth conditions even when using this higher titer of the DMS3mvir phage against the *pyrC* knockdown mutants (**Fig. 4.7B**). Again, inactivation of CRISPR enabled dose-dependent productivity of phage infection. These results may be reflecting the differences in drivers of phage infection dynamics in solid phase growth (phage latent period, burst size, diffusion rate, and growth rate of the host) compared to liquid phase growth (adsorption rate, latent period, and burst size), and the solid phase determinants play a more critical role in the sensitization of *pyrC* mutants to DMS3mvir. This difference in performance between the liquid condition and solid condition may also have implications on the clinical utility of exploiting this vulnerability with DMS3mvir phage.

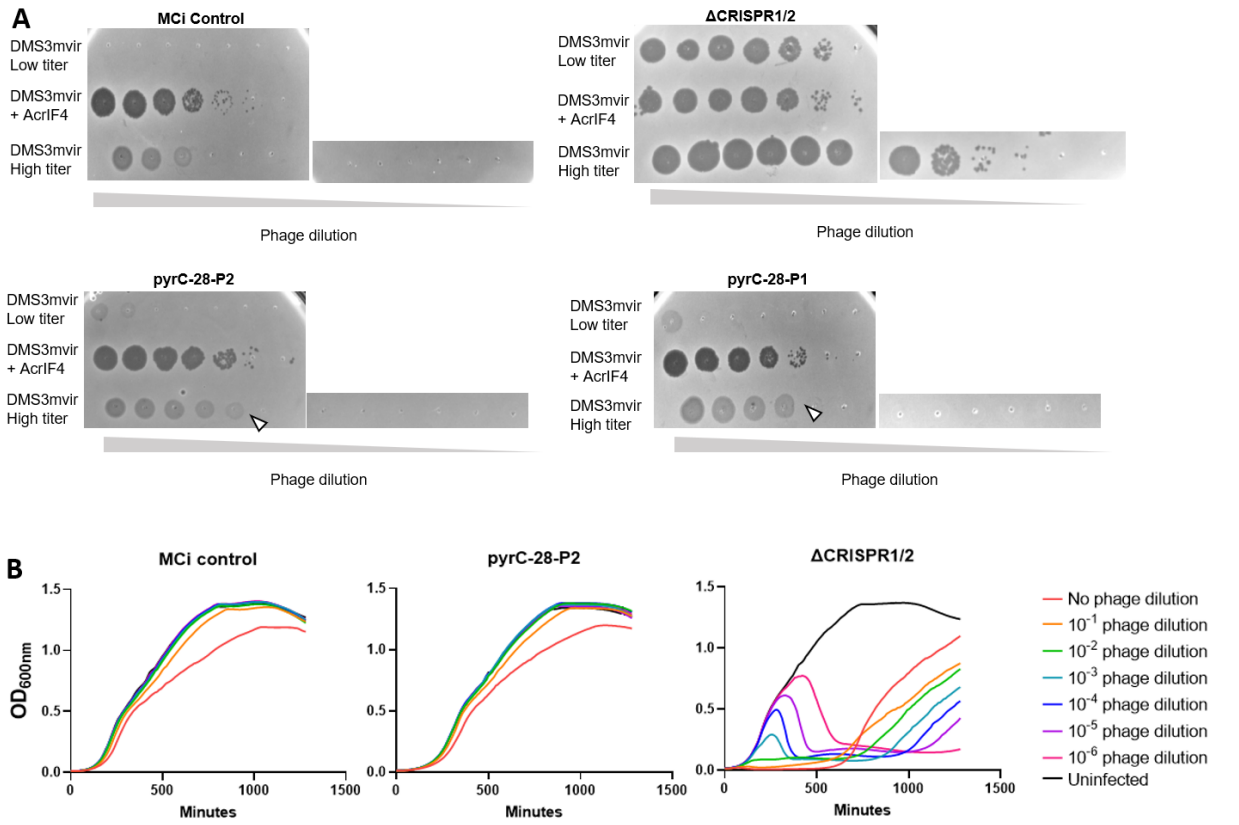

Figure 4.7: Plaque assays and growth curves with higher titers of DMS3mvir phage against *pyrC* knockdown mutants

A higher titer of DMS3mvir phage was purified through PEG precipitation. This phage stock was evaluated in (A) plaque assays and (B) liquid growth curves measured by a microplate reader. Arrowheads highlight increased efficiency of plaquing.

Next, we evaluated the generalizability of this *pyrC*-mediated vulnerability by challenging the Mobile-CRISPRi mutant strains with phages from different families in the Bond-Denomy lab's collection. We noted that the potentiation effect in *pyrC* knockdown mutants only applied to the DMS3 family, and the activity of KMV-like phage was actually diminished in the *pyrC* knockdown strains (**Supplementary Fig. 4.4**). This small screen suggests that the interaction between *pyrC* and phage predation factors is not a general mechanism for exploitation, as is the case for many non-essential defense mechanisms.

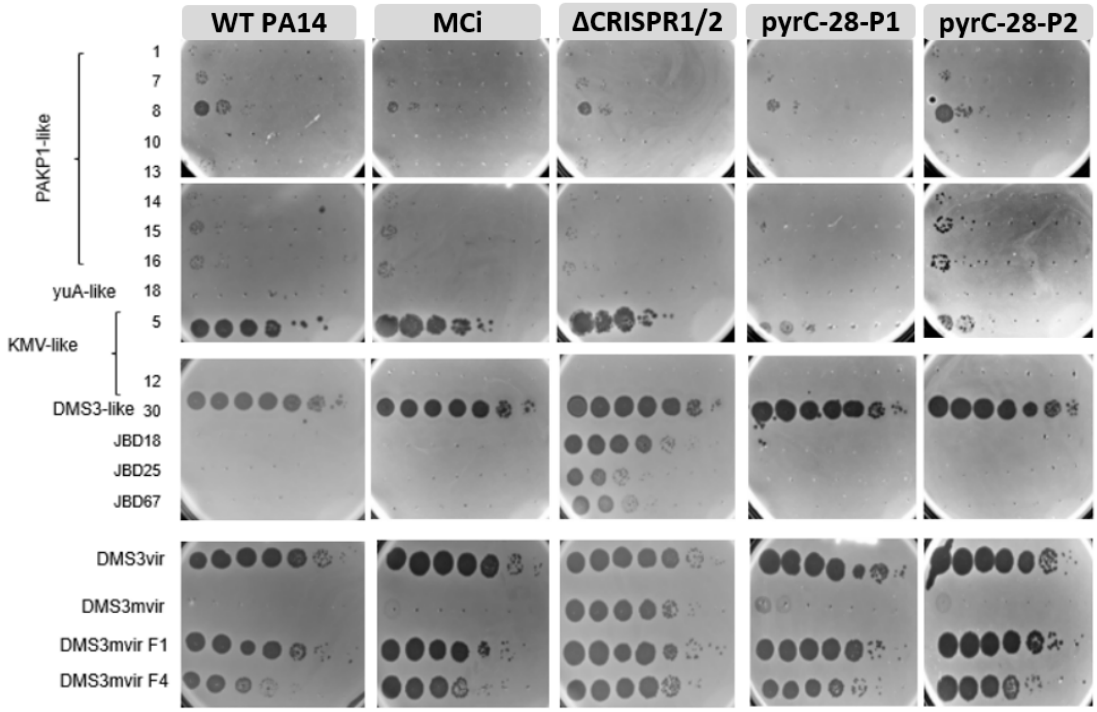

Supplementary Figure 4.4: Generalizability of *pyrC*-mediated vulnerability to phage predation

Plaque assays corresponding to a panel of phages from various families (10x serial dilutions from left to right) used to infect the indicated bacterial strains.

Investigation of knockdown strains with high confidence and low commonality yields hits with inconsistent sensitization to phage

Of the eight genes pursued in validation studies due to their commonality as "hits" in multiple screening conditions, only *pyrC*, *lptH*, and *lpxD* showed slight enhancement of phage infection, with limited evidence of recapitulation in liquid media. To interrogate whether the power of the screen is in detecting specific vulnerabilities at particular points in time, we probed several genes that demonstrated high-confidence and unique depletions in the individual conditions (**Fig. 4.8A**). Two separate plaque assays performed on different days using the same phage stocks exhibited disparate plaquing efficiency

results (**Fig. 4.8B** and **C**). We also observed a decrease in plaquing efficiency for several of the chosen strains. Due to these inconsistencies, results from this endeavor are inconclusive.

A

		DMS3mvir at 11 hr		DMS3mvir at 24 hr		DMS3mvir + AcrIF4 (low dose) at 24 hr		DMS3mvir + AcrIF4 (high dose) at 11 hr	
Target and TSS Offset	Promoter	Z-score diff (uninfected-infected)	pval	Z-score diff (uninfected-infected)	pval	Z-score diff (uninfected-infected)	pval	Z-score diff (uninfected-infected)	pval
etfA_41	P1	3.161241747	0.284	2.837080256	0.061	6.526287717	0.025	3.62901256	0.100
def_29	P1	2.766168674	0.401	4.324412636	0.368	0.718896994	0.822	6.068223376	0.038
accA_72	P1	0.2473358	0.722	0.620918071	0.755	0.847683547	0.833	4.368158446	0.034
serC_71	P2	-1.446222862	0.331	3.159370359	0.023	3.10736231	0.156	0.923827649	0.701
lysC_33	P1	3.602927468	0.040	6.470987466	0.377	7.479899063	0.418	-1.078861395	0.950
purD_1	P1	-4.670475643	0.033	-1.403323653	0.377	0.777923506	0.298	4.772814685	0.031
etfB_74	P1	-1.585033815	0.428	3.354418752	0.032	-0.400752769	0.907	-0.107473686	0.906

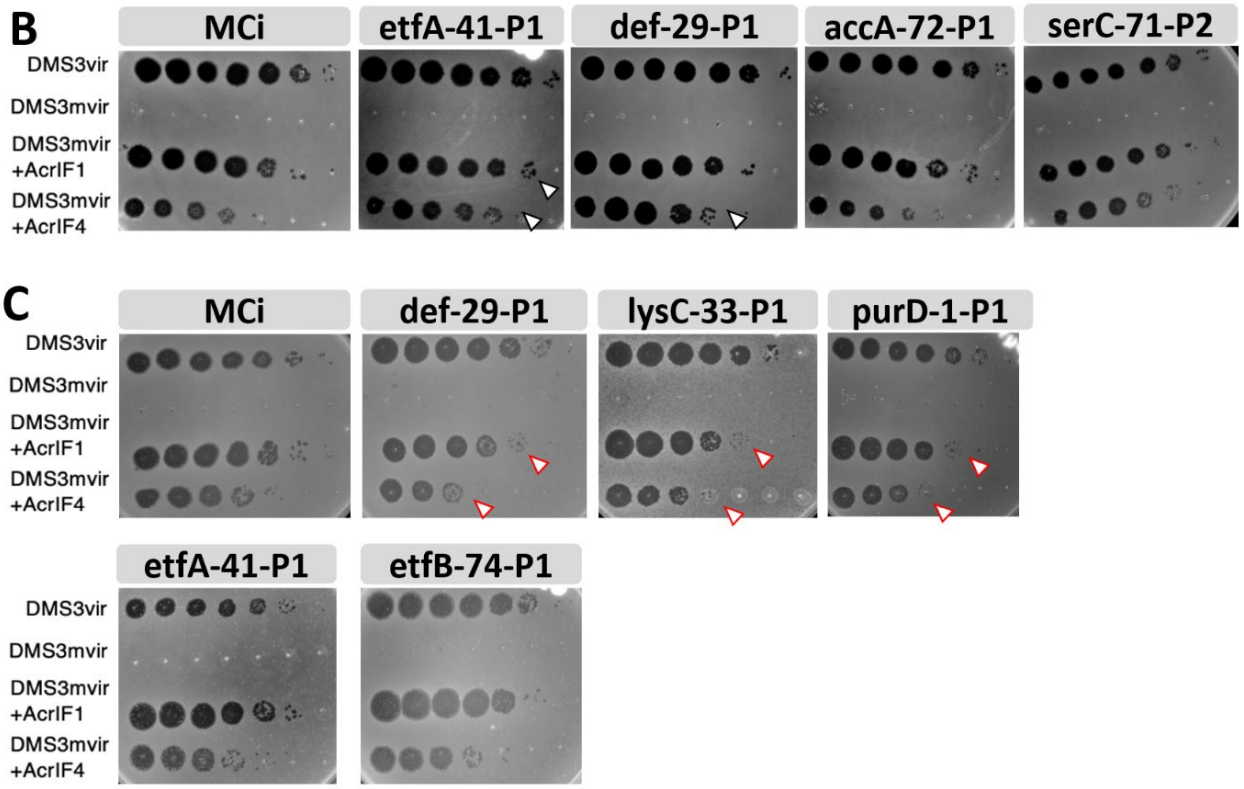

Figure 4.8: Validation of non-overlapping hits with significance in single conditions
(A) The most significant hits from each of the 4 screening conditions considered were selected. (B and C) Two rounds of plaque assays were performed using the same phage stocks and separate bacterial cultures. White arrowheads represent enhancement of plaquing efficiency, and red arrowheads represent diminished plaquing efficiency as compared to the MCi control strain.

An unbiased proteomic screen reveals non-essential bacterial proteins involved in protective and sensitizing interactions with phage

In parallel to the genetic screen, we sought to capture phage proteins that physically interact with host complexes to counter host resistance. The PA14-5sp infection with DMS3mvir + AcrIF4 from the genetic screen was scaled-up to enable proteomic analysis from both the whole cell lysate and the cell membrane. As this approach is not biased for essential bacterial genes or conferral of susceptibility to phage, we expected to see minimal overlap between the genetic and proteomic screens.

We utilized emerging proteomics technologies to detect these interactions between bacteria and phage during native infection. This was achieved in a proteome-wide and high-throughput manner using co-elution correlation profiling mass spectrometry and data-independent acquisition approaches. A list of putative complexes that differ from the infected and uninfected conditions were generated computationally and verified by manual inspection. These hits were chosen based on the following criteria: shift in elution according to size exclusion chromatography profile, reproducibility between the two replicates, having greater than 3 peptides supporting protein identification, and scoring under the 1% FDR threshold. Changes in abundance and molecular weight—indicating association or dissociation— of the complexes may be related to functional roles during phage infection.

Hits from the proteomic screen largely corresponded to PA14 genes that are non-essential in rich media. As such, transposon mutants associated with the hit genes were utilized to probe the susceptibility of strains lacking these proteins to phage predation. Several of these strains, representing *algP*, *trmH*, and *xcpP*, exhibited heightened susceptibility to DMS3mvir + AcrIF1 phage predation (**Fig. 4.9A**). Preliminary growth curves in liquid media showed increased susceptibility of *algP* transposon mutants to killing by the DMS3mvir + AcrIF4 phage. For other transposon mutants, representing PA14_10830, PA14_26540, and *narJ*, the plaquing efficiency of DMS3mvir + AcrIF4 phage is hindered (**Fig. 4.9B**).

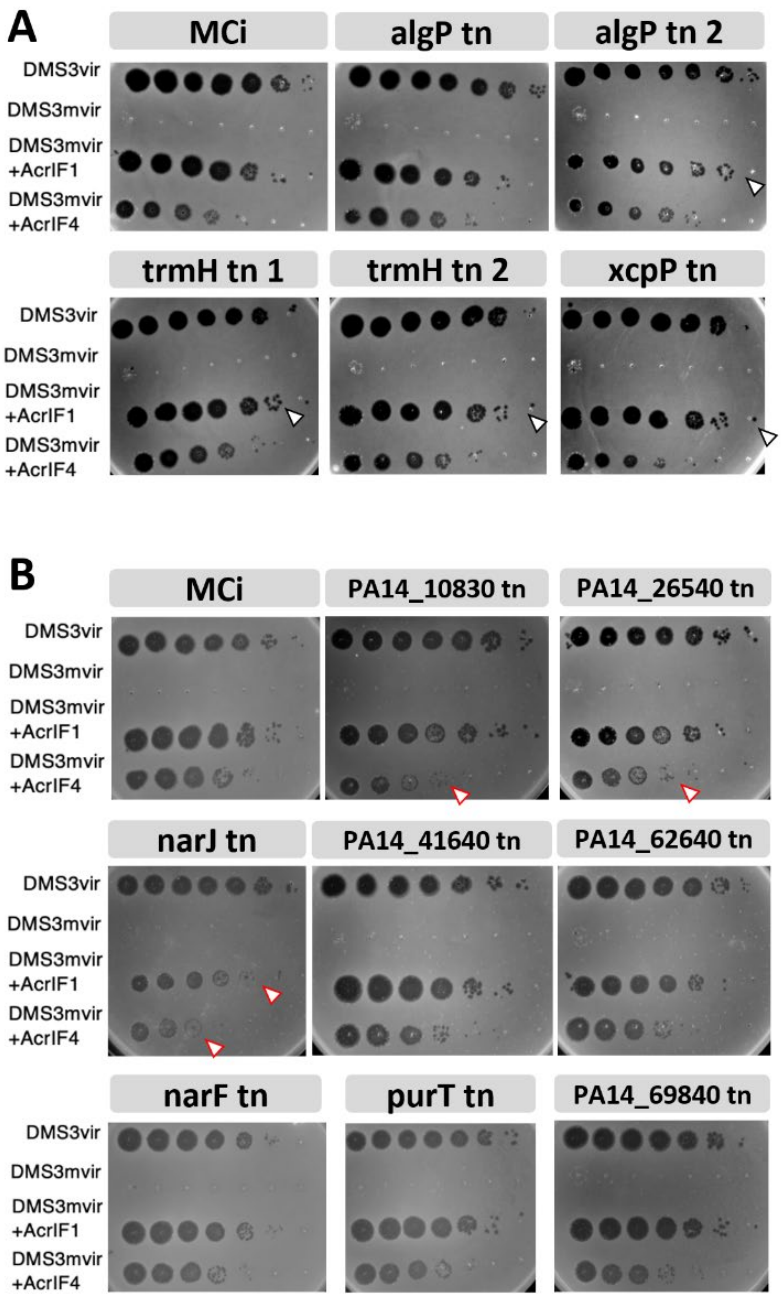

Figure 4.9: Plaque assays with transposon mutants for proteomic screen validation
PA14 transposon mutants corresponding to several proteomic screen hits were cultivated and exposed to phage in the DMS3 family. (A and B) Two rounds of plaque assays were performed using the same phage stocks. Concentration of phage titer decreases right to left. White arrowheads show enhancement of plaquing efficiency & red arrowheads show diminished plaquing efficiency as compared to MCi control.

Discussion

Our goal was to inform future phage therapy development by identifying essential pathways and complexes in the bacterial host that can be inhibited with small molecules or circumvented by phage engineering to boost lysis and retard the emergence of resistant bacteria during phage therapy. We used a dual-pronged approach involving a CRISPRi-based genetic screen and an unbiased proteomic screen to identify intrinsic bacterial resistance mechanisms to phage predation. We hypothesized that perturbing conserved essential genes would provide an opportunity to sensitize a wide variety of bacteria to phages that utilize those specific vulnerabilities.

We designed the screens in anticipation of encountering the challenged reported by other pooled screens studying bacteria-phage interactions. As noted by Bikard *et. al* (6) trains resistant to a very effective phage are anticipated to have strong positive fitness values, which can obfuscate the distinction between a strain with neutral fitness or low fitness. Conversely, our genetic screen utilized a very ineffective phage with low selective pressure, such that strains with increased susceptibility to lysis are anticipated to become selectively depleted from the library. We additionally engineered a delicate equilibrium between phage and bacterial defenses using anti-CRISPR proteins and an enhanced phage-targeting spacer, respectively.

However, the resolution of library composition after next-generation sequencing suffered from reproducibility issues, possibly due to computational errors in

demultiplexing the large library complexity. While we found ways to mitigate these issues (discarding datasets with poor quality control, setting the "hit" thresholds to exclude non-targeting controls, etc.), we were ultimately unable to identify strong genetic drivers of phage resistance that matched the phenotypic effect of knocking out the CRISPR defense machinery.

Investigations into phage-antibiotic interactions have demonstrated the ability of antibiotics to both synergize with phage as well as limit phage replication, dependent on the particular phage and antibiotic combination. (22) This insight opens exploration into rationalizing drug-phage synergies based on mutual targeting of the same essential processes. Overlaps in genetic vulnerabilities imply that inhibition of those essential genes may sensitize the bacteria to phage infection and antibiotic therapy.

Phages used in these experiments were unable to achieve robust lysis when infecting the wild-type strain, however some enhancement in phage infection was noted with the genetic inhibition of *pyrC*, *lptH*, *lpxD*, *trmH*, *algP*, and *xcpP*. The reported synergies between phage therapy and antibiotics or the innate immune system offer promising research avenues to develop combination therapies for clearing bacterial infections. By exploiting the fitness vulnerabilities experienced by bacteria that evolve resistance to lytic phages through surface modifications, it may be possible to simultaneously reduce bacterial virulence as well as re-sensitize bacteria to antibiotic or immune killing.

Methods

Genetic Screen

Thawed glycerol stocks of the P1, P2, and P3 PA14-5sp libraries were combined in equal proportions to form PA14-5sp KD Lib. This inoculum was added to multiple flasks containing 20 mL of LB + 30 µg/mL Gent + 10 mM $MgSO_4$ at an OD_{600nm} of 0.01. 200 µL of the following dilutions of phages were added to the cultures in duplicate: DMS3mvir + AcrIF1 at 10^{-2} and 10^{-5} dilutions, DMS3mvir + AcrIF4 at 10^{-1} and 10^{-2} dilutions, DMS3mvir undiluted, and no added phage. Samples were taken from each culture at 5.5 hr, 11 hr, and 24 hr.

For each CRISPRi phage infection experiment, sequencing data from the duplicates were combined for statistical analysis. For each sgRNA, experimental errors were estimated using frequency differences among two control replicates without phage exposure. P-values (one-sided) were then calculated to evaluate whether sgRNA frequencies with phage exposure are significantly different from the ones without phage exposure. A Z-score was calculated for every gene in each condition as shown below to normalize against the non-targeting control distribution.

$$Guide\ Z\ score = \frac{log_{10}(Counts + 1) - Avg(log_{10}(Ctrl\ guide\ counts + 1)}{Stdev(Ctrl\ guide\ counts)}$$

$$Gene\ Z\ score = \frac{\sum Guide\ Z\ scores}{\sqrt{Number\ of\ guides}}$$

Proteomics Screen

3 replicates of PA14-5sp overnight cultures were diluted 1:100 in 100 mL of LB + 10 mM $MgSO_4$ media. The same 10^{-1} dilution of DMS3mvir + AcrIF4 used in the genetic screen was used in this larger scale culture. The cultures were grown to an OD_{600nm} of 1, at which time both the native soluble and membrane protein compartments were collected and fractionated by SEC. Each fraction was analyzed by mass spectrometry to determine the identity of the PA14 proteins that co-elute.

Peptides from each fraction were injected into a Bruker timsTOF Pro mass spectrometer to detect phage and PA14 proteins that are present in each fraction. For mass spectrometry data collection, a data-independent acquisition (DIA) approach was implemented. The open source PCprophet package (20) was used to look for PA14 protein complexes that co-elute with each individual phage protein.

Transposon mutants from the PA14 Non-Redundant Transposon Insertion Mutant Set (PA14NR Set) were obtained from the Bondy-Denomy lab. (21) Details are shown in **Supplementary Table 4.1**.

Supplementary Table 4.1: Transposon mutants used in this study
Transposon information can be found at the following web address:
http://ausubellab.mgh.harvard.edu/cgi-bin/pa14/home.cgi

Gene name	Transposon mutants
PA14_10830	Mutant ID: 37082 PAMr_nr_mas_07_4:C5
PA14_62640	Mutant ID: 37765 PAMr_nr_mas_08_1:D8
narJ, PA14_13810	Mutant ID: 24921 PAMr_nr_mas_01_4:E3
purT, PA14_15890	Mutant ID: 23328 PAMr_nr_mas_01_1:E2
PA14_69840	Mutant ID: 28356 PAMr_nr_mas_03_3:C2
nqrF, PA14_25350	Mutant ID: 40917 PAMr_nr_mas_09_3:E3
PA14_26540	Mutant ID: 26754 PAMr_nr_mas_02_4:B5
PA14_41640	Mutant ID: 47145 PAMr_nr_mas_12_1:H4
PA14_66160	Mutant ID: 31546 PAMr_nr_mas_05_1:G10
algP, PA14_69370	(1) Mutant ID: 23357 PAMr_nr_mas_01_1:E4 (2) Mutant ID: 35005 PAMr_nr_mas_06_4:B9
trmH, PA14_65190	(1) Mutant ID: 32692 PAMr_nr_mas_05_4:B1 (2) Mutant ID: 28433 PAMr_nr_mas_14_4:G9
xcpP, PA14_23980	Mutant ID: 47432 PAMr_nr_mas_12_2:B8

Plaque Assays

150 µL of overnight bacterial cultures was added to 4 mL molten top agar containing LB plus 0.7% bacto agar and 10 mM $MgSO_4$. This was poured over solidified LB agar plates containing 1.5% bactoagar and 10 mM $MgSO_4$. Ten-fold serial dilutions of phages were made in SM phage buffer and 2 µL of each dilution was spotted on the top agar. The plates were incubated overnight at 30 ˚C and photos were taken with Bio-Rad Gel Doc EZ System, with lighting corrections to improve visibility of plaques.

Growth Curves

2 mL overnight bacterial cultures were diluted 1:100 into LB + 10 mM $MgSO_4$ media. 140 µL of the diluted cultures were added into the appropriate wells of a 96-well plate. In parallel, 10-fold dilutions of the desired phages were made in SM phage buffer in a separate 96-well plate, and 10 µL of the appropriate phage dilution was added to each well. All plates included no phage controls and a blank media plus SM buffer control. OD_{600nm} measurements were taken every 10 minutes using a microplate reader (Synergy H1; BioTek Instruments, VT) with continuous, fast, double orbital shaking.

Acknowledgements

I thank Dr. Adolfo Cuesta, PhD, Dr. Andrea Fossati, PhD, Dr. Shweta Karambelkar, PhD, and Natalie Whitis for sharing their expertise and assisting in collecting much of the data. Dr. Joseph Bondy-Denomy, PhD, Dr. Danielle Swaney, PhD, and Dr. Oren Rosenberg provided generous guidance to facilitate the early stages of this interdisciplinary project.

References

1. Gordillo Altamirano FL, Barr JJ. Phage Therapy in the Postantibiotic Era. Clin Microbiol Rev. 2019 Jan 16;32(2):e00066-18.
2. Kortright KE, Chan BK, Koff JL, Turner PE. Phage Therapy: A Renewed Approach to Combat Antibiotic-Resistant Bacteria. Cell Host Microbe. 2019 Feb 13;25(2):219-232.
3. Qimron U, Marintcheva B, Tabor S, Richardson CC. Genomewide screens for Escherichia coli genes affecting growth of T7 bacteriophage. Proc Natl Acad Sci U S A. 2006 Dec 12;103(50):19039-44.
4. Maynard ND, Birch EW, Sanghvi JC, Chen L, Gutschow MV, Covert MW. A forward-genetic screen and dynamic analysis of lambda phage host-dependencies reveals an extensive interaction network and a new anti-viral strategy. PLoS Genet. 2010 Jul 8;6(7):e1001017.
5. Kortright KE, Chan BK, Turner PE. High-throughput discovery of phage receptors using transposon insertion sequencing of bacteria. *Proc Natl Acad Sci U S A*. 2020;117(31):18670-18679.
6. Rousset F, Cui L, Siouve E, Becavin C, Depardieu F, Bikard D. Genome-wide CRISPR-dCas9 screens in E. coli identify essential genes and phage host factors. *PLoS Genet*. 2018;14(11):e1007749.

7. Heusel M, Bludau I, Rosenberger G, Hafen R, Frank M, Banaei-Esfahani A, van Drogen A, Collins BC, Gstaiger M, Aebersold R. Complex-centric proteome profiling by SEC-SWATH-MS. Mol Syst Biol. 2019 Jan 14;15(1):e8438.

8. Heusel M, Frank M, Köhler M, Amon S, Frommelt F, Rosenberger G, Bludau I, Aulakh S, Linder MI, Liu Y, Collins BC, Gstaiger M, Kutay U, Aebersold R. A Global Screen for Assembly State Changes of the Mitotic Proteome by SEC-SWATH-MS. Cell Syst. 2020 Feb 26;10(2):133-155.e6.

9. Cady KC, Bondy-Denomy J, Heussler GE, Davidson AR, O'Toole GA. The CRISPR/Cas adaptive immune system of Pseudomonas aeruginosa mediates resistance to naturally occurring and engineered phages. J Bacteriol. 2012 Nov;194(21):5728-38.

10. Borges AL, Zhang JY, Rollins MF, Osuna BA, Wiedenheft B, Bondy-Denomy J. Bacteriophage Cooperation Suppresses CRISPR-Cas3 and Cas9 Immunity. Cell. 2018 Aug 9;174(4):917-925.e10.

11. Shiley JR, Comfort KK, Robinson JB. Immunogenicity and antimicrobial effectiveness of Pseudomonas aeruginosa specific bacteriophage in a human lung in vitro model. Appl Microbiol Biotechnol. 2017 Nov;101(21):7977-7985.

12. Poulsen BE, Yang R, Clatworthy AE, White T, Osmulski SJ, Li L, Penaranda C, Lander ES, Shoresh N, Hung DT. 2019. Defining the core essential genome of Pseudomonas aeruginosa. Proc Natl Acad Sci U S A 116:10072–10080.

13. Qu J, Prasad NK, Yu MA, Chen S, Lyden A, Herrera N, Silvis MR, Crawford E, Looney MR, Peters JM, Rosenberg OS. Modulating Pathogenesis with Mobile-CRISPRi. J Bacteriol. 2019 Oct 21;201(22):e00304-19.

14. Qi LS, Larson MH, Gilbert LA, Doudna JA, Weissman JS, Arkin AP, Lim WA. Repurposing CRISPR as an RNA-guided platform for sequence-specific control of gene expression. Cell. 2013 Feb 28;152(5):1173-83.

15. Jost M, Santos DA, Saunders RA, Horlbeck MA, Hawkins JS, Scaria SM, Norman TM, Hussmann JA, Liem CR, Gross CA, Weissman JS. Titrating gene expression using libraries of systematically attenuated CRISPR guide RNAs. Nat Biotechnol. 2020 Mar;38(3):355-364.

16. Hawkins JS, Silvis MR, Koo BM, Peters JM, Osadnik H, Jost M, Hearne CC, Weissman JS, Todor H, Gross CA. Mismatch-CRISPRi Reveals the Co-varying Expression-Fitness Relationships of Essential Genes in Escherichia coli and Bacillus subtilis. Cell Syst. 2020 Nov 18;11(5):523-535.e9.

17. Mutalik VK, Adler BA, Rishi HS, Piya D, Zhong C, Koskella B, Kutter EM, Calendar R, Novichkov PS, Price MN, Deutschbauer AM, Arkin AP. High-throughput mapping of the phage resistance landscape in E. coli. PLoS Biol. 2020 Oct 13;18(10):e3000877.

18. Ghosh B, Das A. nusB: a protein factor necessary for transcription antitermination in vitro by phage lambda N gene product. Proc Natl Acad Sci U S A. 1984 Oct;81(20):6305-9.

19. Tal N, Morehouse BR, Millman A, Stokar-Avihail A, Avraham C, Fedorenko T, Yirmiya E, Herbst E, Brandis A, Mehlman T, Oppenheimer-Shaanan Y, Keszei AFA, Shao S, Amitai G, Kranzusch PJ, Sorek R. Cyclic CMP and cyclic UMP mediate bacterial immunity against phages. Cell. 2021 Nov 11;184(23):5728-5739.e16.

20. Hu LZ, Goebels F, Tan JH, Wolf E, Kuzmanov U, Wan C, Phanse S, Xu C, Schertzberg M, Fraser AG, Bader GD, Emili A. EPIC: software toolkit for elution profile-based inference of protein complexes. Nat Methods. 2019 Aug;16(8):737-742.

21. Liberati NT, Urbach JM, Miyata S, Lee DG, Drenkard E, Wu G, Villanueva J, Wei T, Ausubel FM. An ordered, nonredundant library of Pseudomonas aeruginosa strain PA14 transposon insertion mutants. Proc Natl Acad Sci U S A. 2006 Feb 21;103(8):2833-8.

22. Kever L, Hardy A, Luthe T, Hünnefeld M, Gätgens C, Milke L, Wiechert J, Wittmann J, Moraru C, Marienhagen J, Frunzke J. Aminoglycoside Antibiotics Inhibit Phage Infection by Blocking an Early Step of the Infection Cycle. mBio. 2022 Jun 28;13(3):e0078322.

Conclusion

Given that the rise of antimicrobial resistance globally threatens the foundations of modern medicine, it is imperative to bring new antibacterial agents with low rates of resistance to the clinic. Existing antibiotics used to treat Gram-negative bacterial infections belong to a limited set of chemical classes, targeting less than a dozen essential bacterial genes. However, hundreds of bacterial genes have been identified as essential through transposon sequencing and comparative genomics studies, implying that inhibition of their gene products may lead to cell death.

This framework for antibacterial discovery was pursued by many to no avail in the late 1990s–2000s: During a seven-year effort at GlaxoSmithKline, three hundred genes were identified as potential drug targets, based on their conservation among bacterial species, lack of a human homolog, and essentiality for bacterial survival in lab cultivation media (Payne 2007). The company conducted seventy target-based high-throughput screening campaigns, producing sixteen hits that resulted in five leads—two of which were optimized and none of which progressed to human clinical trials. Similarly, 65 high-throughput screens were carried out by AstraZeneca, generating 19 hits that advanced to exploratory chemistry efforts, though none possessed Gram-negative activity. The failure of these endeavors underscores the importance of choosing chemical libraries with

appropriate physicochemical properties and mitigating risks associated with permeability, efflux, resistance emergence, and genetic dependencies.

With the disclosure of these narratives, clinically unvalidated antibacterial targets have become associated with a long history of failure and financial risks that are unbearable for the small-sized companies that are primarily driving antibacterial development today. This reputation has deterred antibacterial developers from pursuing these potential targets, in favor of established targets and chemical classes. This body of work serves to identify a major barrier in antibacterial clinical development and to develop and apply CRISPR-based technology towards de-risking novel antibacterial targets.

Chapter 1 examines the clinical development pipeline for antibiotic candidates with activity against Gram-negative bacteria between 2010–2020. This analysis revealed that most development efforts focused on well-established targets and chemical classes, particularly beta-lactams. The latest advances in beta-lactam development include a novel class of beta lactamase inhibitors and approval of a siderophore-conjugated beta-lactam that exploits a novel mode of entry. However, recent reports confirm the emergence of resistance to the siderophore-conjugated antibiotic, cefiderocol, suggesting that these innovations may soon lose clinical relevance. In the last decade, only 6 Gram-negative antibiotic candidates, representing 5 clinically unprecedented targets, were advanced to clinical trials. 4 of these were discontinued, further diminishing antibiotic developers' optimism for going after these novel targets. Thus, a strategy to

de-risk and prioritize underexploited antibiotic targets is required to encourage antibiotic developers to pursue them in clinical trials.

Despite limitations in company disclosures, the analysis pinpoints toxicity in phase 1 clinical trials as the major pitfall of Gram-negative antibiotic development over the last decade. Retrospective analysis of preclinical data associated with discontinued candidates reveals non-predictive toxicological and resistance-related findings. Poor safety profiles lead to post-approval issues for antibiotics as well: several fluoroquinolones have been withdrawn from clinical use due to adverse effects.

This safety-related bottleneck in antibiotic development contrasts sharply with other therapeutic pipelines, where the lowest success rate is in the transition from phase 2 to phase 3 trials. As the adage goes, the dose makes the poison: anecdotal evidence reveals that antibiotics are typically administered at a much higher dosage than drugs for other ailments. This has been attributed to the low cellular potency of antibiotics, where micromolar concentrations are required to kill the bacterial cell, whereas nanomolar concentrations are typical for achieving therapeutic efficacy in treating other medical conditions. Thus, the safety issues associated with antibiotics may be addressed by selecting targets that require little inhibition (less chemical matter) to impede bacterial growth during infection.

While antibiotics are often developed as standalone chemical weapons against pathogens, host immunity mechanisms play important roles in clearing the bacterial burden. These processes include nutritional immunity, where the nutrient-restrictive microenvironment impedes the growth of auxotrophic pathogens, and macrophage autophagy, which is the innate immune system's first line of defense. It is conceivable that the extent of target inhibition required for bacterial growth inhibition *in vitro* may exceed that which is needed *in vivo*, where the host immune system mediates clearance of the infection. Since the impact of host immunity effectors are not captured in axenic cultures where antibiotic action is assessed, we theorized that potential synergistic interactions between antibiotics and the host immune response may be underexplored. Exploiting such a synergism would provide an opportunity to lower the requisite antibiotic dose, such that it potentiates host immunity mechanisms in clearing the infection.

As a scalable proxy for chemical inhibition, we use genetic perturbation to probe for fundamental drivers of bacterial growth in the context of the host immune response. Of these genetic drivers, we are most interested in scenarios where partial inhibition leads to large fitness consequences in the infection microenvironment, despite limited growth defects when grown in axenic culture. Historically, these genetic drivers have been difficult to manipulate precisely, as they are requisite for pathogen survival. In chapter 2,

we develop a CRISPR-based technology that allows us to modulate gene expression in a murine pneumonia model.

Chapter 2 details the construction and characterization of *P. aeruginosa* knockdown strains using a modular and scalable genetic tool called Mobile-CRISPRi. Through triparental mating, the Mobile-CRISPRi construct was chromosomally integrated into *P. aeruginosa* strain PA14. Keeping our ultimate goal of assessing gene vulnerability in a murine infection model in mind, we replaced the inducible promoter driving dCas9 activity with constitutive promoters to avoid potential issues with non-homogenous distribution of inducer molecules in the murine lung tissue. We characterized the strength of these promoters by targeting a chromosomally integrated *mrfp* gene for CRISPRi-mediated repression and measuring the resultant fluorescence of these strains compared to *mrfp*-integrated control strains containing non-targeting sgRNAs. To demonstrate the utility of this system in a murine pneumonia model, we chose to recapitulate a known phenotype: knockout of the transcriptional activator *exsA* associated with the type 3 secretion system has previously been shown to attenuate *P. aeruginosa* virulence. Altogether, we provide the first application of CRISPRi to study conditionally essential virulence genes in mouse models of lung infection through partial gene perturbation.

While the design of a constitutive knockdown system and implementation of CRISPRi in a bacterial pathogenesis model were major milestones, one main question remained: since

this study did not include genes that are essential for *in vitro* growth, will our Mobile-CRISPRi system afford sufficient knockdown of *in vitro* essential genes to observe *in vivo* phenotypes without incurring *in vitro* fitness defects? In preliminary studies, dozens of Mobile-CRISPRi strains targeting *in vitro* essential genes were individually constructed using the three different constitutive promoters, and growth curves revealed very limited deviations from wildtype PA14 growth. Attempts to use qRT-PCR to assess the expression of the targeted genes were unsuccessful, and optimization of a reliable assay to robustly quantify each promoter-sgRNA pairing's on-target efficacy would benefit further studies. Having demonstrated the success of our constitutive knockdown system in an *in vivo* model, we sought to investigate the vulnerabilities of all *P. aeruginosa* essential genes in the murine pneumonia model.

Chapter 3 describes the construction of a pooled library of PA14 knockdown strains using Mobile-CRISPRi and its application in a murine pneumonia model towards uncovering *in vivo* gene vulnerabilities. We chose our library of 528 essential genes to target according to recent transposon sequencing studies carried out in multiple infection-related growth media. 4 sgRNAs were designed per gene and 1,000 non-targeting sgRNAs were included as negative controls. Next-generation sequencing revealed that the final library represents knockdowns of 466 genes (88% of the genes targeted), where missing strains may be attributable to either a small technical

bottleneck in library construction or significant fitness defects conferred by gene knockdown.

This library was used as inoculum to initiate a 24-hour murine pneumonia infection and an *in vitro* culture grown for 6 generations. We found that none of the strains exhibited significant fitness defects when grown *in vitro*—likely due to our constitutive knockdown method—implying that the fitness of the strains in the inoculum is at a "steady-state". On the other hand, partial genetic depletion of a diverse set of 197 *P. aeruginosa* genes results in a fitness defect in a murine pneumonia model. We validate the most promising hit by showing that partial genetic inhibition of *ispD* in the isoprenoid biosynthesis pathway results in hypersensitization to host clearance of bacterial infection. Additionally, of the four *P. aeruginosa* essential genes found to be transcriptionally upregulated during human infections (*lptG*, *lptH*, *pgsA*, *cysS*), *pgsA* was the most confident hit in our genetic screen. We show that despite limited fitness consequences on growth in rich media, *pgsA* knockdown mutants demonstrate significant vulnerability to host clearance mechanisms in our murine pneumonia model.

The genetic vulnerabilities presented in chapter 3 represent a novel paradigm for the prioritization of antibacterial targets that potentiate host immunity mechanisms. The Mobile-CRISPRi strains corresponding to these *in vivo* vulnerable genes can be used in a whole-cell target-based screening approach to find chemical matter that exhibits a synthetic lethality phenotype. Under this strategy, repression of the selected essential

gene and sub-MIC chemical inhibition of the same gene do not individually produce a noticeable fitness defect, however the combination of the two pressures significantly reduces fitness of the strain. Chemical inhibitors that elicit such a fitness defect in the knockdown strain but not in non-targeting negative control strains may specifically interact with the targeted gene. Such a screen would also select for chemical matter than can permeate the bacterial cell. As the antibiotic targets were prioritized on the basis of their *in vivo* vulnerability, chemical inhibitors that cause even mild fitness defects in the knockdown strains may be worth investigating in murine models of infection.

While chemical inhibitors have been the lynchpin of antibacterial therapeutics since their inception in the 1940s, phage therapy has emerged as another promising modality to combat bacterial infections. The low rates of cross-resistance with antibiotics and the ample evidence for synergy between phage and antibiotics suggests that co-administration of phage and antibiotics may have clinical utility in the treatment of multi-drug resistant bacterial infections. One major limitation of phage therapy is their narrow spectrum of activity, even within each bacterial species. Strategies to expand their host range can be developed through understanding bacterial mechanisms that confer intrinsic resistance to phage. All known defense mechanisms involve non-essential bacterial genes, and the role of essential bacterial genes as protective factors against phage predation remains unexplored. The Mobile-CRISPRi library enables us to probe

PA14 essential gene vulnerabilities under various conditions, providing the opportunity to investigate essential host processes driving intrinsic phage resistance.

Chapter 4 delineates a dual-pronged genetic and proteomic approach to identifying bacterial defense mechanisms against phage predation. The genetic screen utilizes the Mobile-CRISPRi library to selectively probe the involvement of PA14 essential genes as protective factors, whereas the proteomic screen represents an unbiased method of profiling protein interactions related to protection against phage predation. To bolster the sensitivity of these screens, we engineered a delicate equilibrium between phage and bacterial defenses using anti-CRISPR proteins and precisive CRISPR-targeting.

Exposing the Mobile-CRISPRi library to various phages and collecting samples at multiple time points revealed genetic vulnerabilities. Examples of genes where knockdown led to some qualitative enhancement of DMS3mvir + AcrIF4 phage predation in PA14 include *pyrC*, *lptH*, *lpxD*, and, less robustly, *etfA*, and *def*. These may represent protective factors that mediate bacterial resistance to phage, though inconsistencies between solid and liquid bacterial growth and lack of generalizability to other phage families have been observed.

Before conclusions can be made regarding the weak contributions of essential genes towards phage resistance, this screen should be repeated using only the P1 essential gene knockdown library (as was done in chapter 3 murine pneumonia experiment). The

genetic screen in chapter 4 utilized the combination of P1, P2, and P3- based Mobile-CRISPRi libraries, and reducing the complexity of the library may enable higher reproducibility and sgRNA identification accuracy. The low significance scores from the genetic screen in chapter 4 compared to that of chapter 3 indicates that the performed screen was not robust, though several hits were ultimately validated.

From the proteomic screen, several protein complexes were noted to change in abundance or interacting partners during PA14-5sp infection with DMS3mvir + AcrIF4 phage. These proteins largely corresponded to non-essential genes, which could be probed with transposon mutants. In validating the role of these proteins during phage infection, we found that knockout of *narJ* and a LysR family transcriptional regulator PA14_10830 obstructs phage infection. These genes fall under the classification of sensitizing factors, as phage likely utilize those proteins to carry out a productive infection. We also found transposon mutants corresponding to *trmH*, *xcpP*, and *algP* to exhibit higher sensitivity to phage infection. A major barrier to analyzing the results from this screen was the lack of a bioinformatic tool to prioritize the significance of the changes in the protein interaction networks between the uninfected and infected conditions.

It is notable that many outer membrane proteins described as phage receptors in Gram-negative bacteria are also important for pathogen survival in hosts. Outer membrane proteins also represent favorable antibiotic targets, as cell permeability and efflux

susceptibility are moot. Exploring synergistic strategies to inhibit these outer membrane proteins while rendering the bacterial cell more vulnerable to host immunity and/or phage predation is a promising direction for future antibacterial development. Developing antibacterial agents that sensitize bacteria to other modes of killing (host immunity and clearance processes or phage-mediated lysis) by interfering with essential processes may overcome existing resistance mechanisms and toxicity issues. Establishing preclinical and clinical development pathways and resistance surveillance procedures for antibacterial agents with sensitization properties rather than traditional *in vitro* activity will be crucial for translating these innovations into drugs with clinical utility.

Publishing Agreement

It is the policy of the University to encourage open access and broad distribution of all theses, dissertations, and manuscripts. The Graduate Division will facilitate the distribution of UCSF theses, dissertations, and manuscripts to the UCSF Library for open access and distribution. UCSF will make such theses, dissertations, and manuscripts accessible to the public and will take reasonable steps to preserve these works in perpetuity.

I hereby grant the non-exclusive, perpetual right to The Regents of the University of California to reproduce, publicly display, distribute, preserve, and publish copies of my thesis, dissertation, or manuscript in any form or media, now existing or later derived, including access online for teaching, research, and public service purposes.

DocuSigned by:
Neha Prasad
2CFD4E15DC3349E...
Author Signature

8/28/2022
Date